Methods in Molecular Biology 1682

Springer Protocols

Scott E. McNeil *Editor*

Characterization of Nanoparticles Intended for Drug Delivery

Second Edition

Humana Press

METHODS IN MOLECULAR BIOLOGY

Series Editor
John M. Walker
School of Life and Medical Sciences
University of Hertfordshire
Hatfield, Hertfordshire, AL10 9AB, UK

For further volumes:
http://www.springer.com/series/7651

Characterization of Nanoparticles Intended for Drug Delivery

Second Edition

Edited by

Scott E. McNeil

Nanotechnology Characterization Laboratory, Leidos Biomedical Research, Inc.
Frederick National Laboratory for Cancer Research, Frederick, MD, USA

Humana Press

Editor
Scott E. McNeil
Nanotechnology Characterization Laboratory, Leidos Biomedical Research, Inc.
Frederick National Laboratory for Cancer Research
Frederick, MD, USA

ISSN 1064-3745 ISSN 1940-6029 (electronic)
Methods in Molecular Biology
ISBN 978-1-4939-7350-7 ISBN 978-1-4939-7352-1 (eBook)
DOI 10.1007/978-1-4939-7352-1

Library of Congress Control Number: 2017953275

Printed on acid-free paper

This Humana Press imprint is published by Springer Nature
The registered company is Springer Science+Business Media LLC
The registered company address is: 233 Spring Street, New York, NY 10013, U.S.A.

Preface

It has been 6 years since the first edition of this book introduced methods for the characterization of nanoparticles intended for drug delivery. Since that time, basic and translational research considerably advanced the field of nanotechnology, leading to the clinical development of nanomedicines with greater sophistication and characterization requirements. In response to the growing needs of the nanotechnology community, this second edition book provides up-to-date protocols to characterize nanomaterials intended as drug delivery agents. These new and updated protocols are designed as tools for researchers and pharmaceutical and biotechnology developers to evaluate the clinical potential of nanomedicines in preclinical development. Specifically, they can be used to assess the nanomedicine's physicochemical parameters, toxicity, and safety concerns.

Progress in nanotechnology and biology continues to expand nanomedicine development, while simultaneously introduces new characterization challenges. Chapter 1 discusses the advances in nanomedicine and the obstacles in its evaluation. The remainder of the book contains new or updated protocols for nanomaterial characterization, including methods to test sterility and endotoxin (Chapters 2 and 3), physicochemical features (Chapters 4–8), immunological effects (Chapters 9–18), drug release (Chapter 19), and in vivo efficacy (Chapter 20). While protocols that characterize the physicochemical properties can be applied to nanomedicines intended for all routes of administration, most of the other in vitro protocols in this book are meant to evaluate nanoparticles that are administered intravenously. Most reported nano-based drug delivery agents are designed for intravenous route of administration. Although the methods in this book can be applied to a variety of nanoplatforms, certain assays may need to be individually tailored to the specific technology. Many of these methods have been devised, updated, and validated by scientists at the National Cancer Institute's Nanotechnology Characterization Laboratory (NCL) (https://ncl.cancer.gov) in order to accelerate the development of promising nano-based therapies and diagnostics. NCL continually optimizes and designs new characterization methods to meet the evolving requirements of nanomedicine developers.

There is a significant amount of effort and time put in by NCL and other groups at the Frederick National Laboratory to produce the protocols included in this volume. I would like to thank all the authors who have contributed to this work and made this second edition possible. Distinct recognition goes to the key scientists who developed the methods included in this book and those that serve as scientific leaders at NCL: Drs. Stephan Stern, Marina Dobrovolskaia, Jeff Clogston, and Pavan Adiseshaiah. Supporting their expertise is the dedicated, hands-on work by Edward Cedrone, Alpana Dongargaonkar, Matthew Hansen, Dr. Anna Ilinskaya, Chris McLeland, Barry Neun, Tim Potter, Jamie Rodriguez, Dr. Bhawna Sharma, and Sarah Skoczen. Collaborators, namely Dr. Krishna

Kota and Mackensie Smith, are appreciated for their time to enhance these chapters. Special thanks go out to Dr. Ulrich Baxa and Kunio Nagashima of the Electron Microscopy Lab at the Frederick National Laboratory and their former colleagues, Sarah Anderson and David Parmiter, for their development of advanced microscopy techniques for nanoparticle characterization. Also, I express gratitude to Drs. Maggie Swierczewska Scully and Rachael Crist for their contribution to Chapter 1 and hard work in assembling this book.

Frederick, MD, USA *Scott E. McNeil*

Acknowledgment

This project has been funded in whole or in part with Federal funds from the National Cancer Institute, National Institutes of Health, under Contract No. HHSN261200800001E. The content of this publication does not necessarily reflect the views or policies of the Department of Health and Human Services, nor does mention of trade names, commercial products, or organizations imply endorsement by the U.S. Government.

Contents

Contributors

Pavan P. Adiseshaiah • *Cancer Research Technology Program, Nanotechnology Characterization Laboratory, Leidos Biomedical Research, Inc., Frederick National Laboratory for Cancer Research, Frederick, MD, USA*

Sarah R. Anderson • *Microscopic Imaging Lab, Global Pathology, Drug Safety Research and Development, Pfizer, Inc., Groton, CT, USA*

Ulrich Baxa • *Cancer Research Technology Program, Electron Microscopy Laboratory, Leidos Biomedical Research, Inc., Frederick National Laboratory for Cancer Research, Frederick, MD, USA*

Edward Cedrone • *Cancer Research Technology Program, Nanotechnology Characterization Laboratory, Leidos Biomedical Research, Inc., Frederick National Laboratory for Cancer Research, Frederick, MD, USA*

Jeffrey D. Clogston • *Cancer Research Technology Program, Nanotechnology Characterization Laboratory, Leidos Biomedical Research, Inc., Frederick National Laboratory for Cancer Research, Frederick, MD, USA*

Rachael M. Crist • *Cancer Research Technology Program, Nanotechnology Characterization Laboratory, Leidos Biomedical Research, Inc., Frederick National Laboratory for Cancer Research, Frederick, MD, USA*

Marina A. Dobrovolskaia • *Cancer Research Technology Program, Nanotechnology Characterization Laboratory, Leidos Biomedical Research, Inc., Frederick National Laboratory for Cancer Research, Frederick, MD, USA*

Alpana A. Dongargaonkar • *Cancer Research Technology Program, Nanotechnology Characterization Laboratory, Leidos Biomedical Research, Inc., Frederick National Laboratory for Cancer Research, Frederick, MD, USA*

Matthew N. Hansen • *Cancer Research Technology Program, Nanotechnology Characterization Laboratory, Leidos Biomedical Research, Inc., Frederick National Laboratory for Cancer Research, Frederick, MD, USA*

Anna N. Ilinskaya • *Cancer Research Technology Program, Nanotechnology Characterization Laboratory, Leidos Biomedical Research, Inc., Frederick National Laboratory for Cancer Research, Frederick, MD, USA*

Krishna Kota • *Perkin Elmer, Inc., Waltham, MA, USA*

Christopher B. McLeland • *Cancer Research Technology Program, Nanotechnology Characterization Laboratory, Leidos Biomedical Research, Inc., Frederick National Laboratory for Cancer Research, Frederick, MD, USA*

Scott E. McNeil • *Nanotechnology Characterization Laboratory, Leidos Biomedical Research, Inc., Frederick National Laboratory for Cancer Research, Frederick, MD, USA*

Kunio Nagashima • *Cancer Research Technology Program, Electron Microscopy Laboratory, Leidos Biomedical Research, Inc., Frederick National Laboratory for Cancer Research, Frederick, MD, USA*

Barry W. Neun • *Cancer Research Technology Program, Nanotechnology Characterization Laboratory, Leidos Biomedical Research, Inc., Frederick National Laboratory for Cancer Research, Frederick, MD, USA*

David Parmiter • *Cancer Research Technology Program, Electron Microscopy Laboratory, Leidos Biomedical Research, Inc., Frederick National Laboratory for Cancer Research, Frederick, MD, USA*

Timothy M. Potter • *Cancer Research Technology Program, Nanotechnology Characterization Laboratory, Leidos Biomedical Research, Inc., Frederick National Laboratory for Cancer Research, Frederick, MD, USA*

Jamie C. Rodriguez • *Cancer Research Technology Program, Nanotechnology Characterization Laboratory, Leidos Biomedical Research, Inc., Frederick National Laboratory for Cancer Research, Frederick, MD, USA*

Bhawna Sharma • *Cancer Research Technology Program, Nanotechnology Characterization Laboratory, Leidos Biomedical Research, Inc., Frederick National Laboratory for Cancer Research, Frederick, MD, USA*

Sarah L. Skoczen • *Cancer Research Technology Program, Nanotechnology Characterization Laboratory, Leidos Biomedical Research, Inc., Frederick National Laboratory for Cancer Research, Frederick, MD, USA*

Mackensie C. Smith • *Cancer Research Technology Program, Nanotechnology Characterization Laboratory, Leidos Biomedical Research, Inc., Frederick National Laboratory for Cancer Research, Frederick, MD, USA*

Stephan T. Stern • *Cancer Research Technology Program, Nanotechnology Characterization Laboratory, Leidos Biomedical Research, Inc., Frederick National Laboratory for Cancer Research, Frederick, MD, USA*

Magdalena Swierczewska • *Cancer Research Technology Program, Nanotechnology Characterization Laboratory, Leidos Biomedical Research, Inc., Frederick National Laboratory for Cancer Research, Frederick, MD, USA*

Part I

Introduction

Chapter 1

Evaluating Nanomedicines: Obstacles and Advancements

Magdalena Swierczewska, Rachael M. Crist, and Scott E. McNeil

Abstract

Continued advancements in nanotechnology are expanding the boundaries of medical research, most notably as drug delivery agents for treatment against cancer. Drug delivery with nanotechnology can offer greater control over the biodistribution of therapeutic agents to improve the therapeutic index. In the last 20 years, a number of nanomedicines have transitioned into the clinic. As nanomedicines evolve, techniques to properly evaluate their safety and efficacy must also evolve. Characterization methods for nano-based materials must be adapted to the demands of nanomedicine developers and regulators. This second edition book provides updated characterization protocols designed to address the clinical potential of nanomedicines during their preclinical development. In this chapter, the characterization challenges of nanoparticles intended for drug delivery will be discussed, along with examples of advancements and improvements in nanomedicine characterization.

Key words Nanoparticles, Nanomedicine, Therapy, Efficacy, Toxicity, Active targeting, Passive targeting

1 Introduction

The nanometer is the functional scale in biology. Proteins, for example, are natural nanomaterials that play essential roles in cells, such as in cellular communication and motility. Therefore, controlling materials on the nanoscale offers the opportunity to develop medicines with precisely engineered functions in the body. Because nanoparticles can exhibit high surface to volume ratios, unique optical signals, tunable shapes, and/or modifiable surfaces, they provide a mechanism for controlling transport of various therapeutic cargo within the body both temporally and spatially. The application of nanoscale materials in medicine, generally termed nanomedicine, has become mainstream. Some of the first examples of novel nanomedicines that entered the clinic are exemplified in Fig. 1. In the last 22 years, the US Food and Drug Administration (FDA) has approved over 20 nanomedicine products [1–3]. In this time, information about nanomedicine cellular uptake, toxicity profiles, or how nanoformulations can alter the

Scott E. McNeil (ed.), *Characterization of Nanoparticles Intended for Drug Delivery*, Methods in Molecular Biology, Vol. 1682, DOI 10.1007/978-1-4939-7352-1_1,

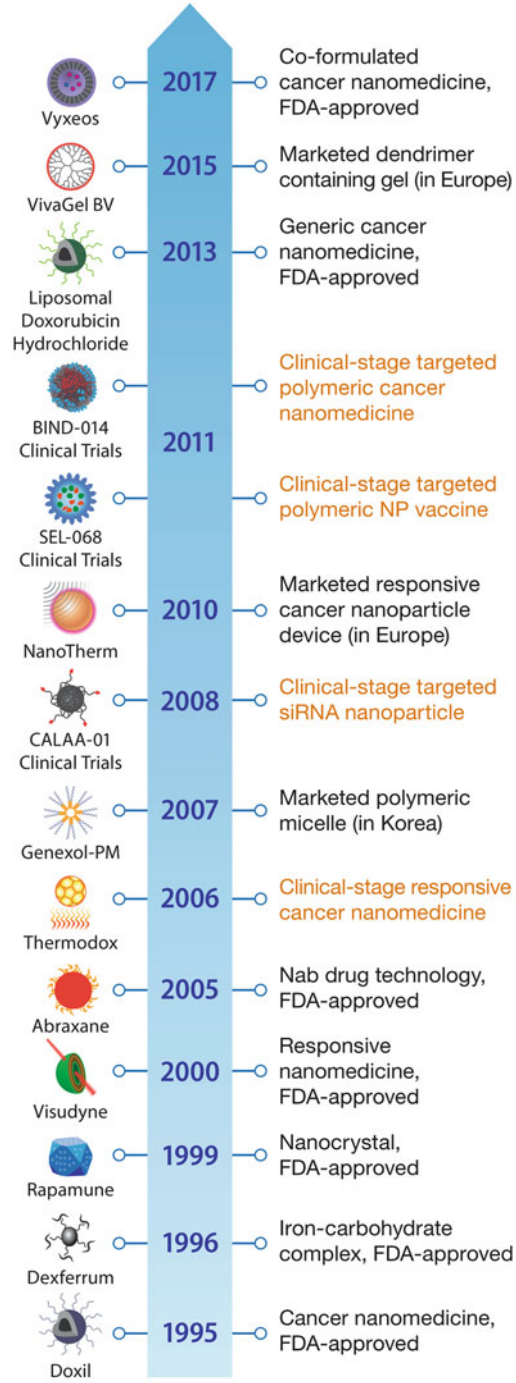

Fig. 1 Timeline of milestone nanomedicines entering the clinical stage. The evolution of nanotechnology in drug delivery is demonstrated, with an emphasis on when pioneering nanomedicines first entered clinical trials (*orange text*) or reached the commercial market (*black text*). The nanomedicine formulations have been previously reviewed [1–3, 5]. *Nab*: nanoparticle albumin-bound

pharmacokinetic properties of drugs has greatly advanced, and the complexity of novel nanomedicines entering early clinical development has increased. Correspondingly, the approaches used to characterize these complex and heterogeneous formulations must adapt. This second edition book introduces both new and updated protocols for the preclinical characterization of nanoparticles intended for drug delivery. The techniques are aimed at evaluating the formulation's physicochemical parameters, toxicity and safety concerns, and potential clinical benefit of nanomedicines early in their development process.

The goal of most nano-based strategies for drug delivery is to improve the therapeutic effectiveness of the active pharmaceutical ingredient (API) and/or reduce adverse effects. APIs that were previously considered ineffective because they may have suffered from poor pharmacokinetic profiles, inadequate stability, low solubility, or ones with dose-limiting toxicity could become viable therapies with a nano-based delivery strategy. For example, the antifungal drug amphotericin B induces dose-limiting nephrotoxicity that constrains its therapeutic efficacy [4]. However, AmBisome, a liposomal formulation of amphotericin B, decreases the principle toxicity of the traditional formulation and prolongs its systemic transport [4]. Consequently, the nanoformulation of amphotericin B can be safely administered at higher doses. This is just one example of how nanoplatforms have the potential to influence the pharmacokinetic profile and improve drug solubility and stability in order to provide a greater therapeutic index of the API. There are many others as well, including Doxil, DaunoXome, and Abraxane, that are reviewed elsewhere [5, 6].

Nanomedicines approved to date generally provide improvements in the delivery of APIs that were already in clinical use. Diprivan, an injectable emulsion of propofol in soybean oil, glycerol and egg lecithin used as an anesthetic, and Doxil, a PEGylated doxorubicin liposome first approved for Kaposi's sarcoma, are among the first nanomedicines in the clinic. Between the time these first nanomedicines were used clinically and 2005, most nanomedicines that entered the market were for non-cancer indications, such as one of the first approved nanocrystals, Rapamune, to prevent organ rejection after kidney transplantation and Visudyne, a light-activated liposomal drug for the photodynamic treatment of wet age-related macular degeneration [3]. Approved formulations in this time consisted of lipid complexes, liposomes, micelles, and nanocrystals with varied routes of administration from intravenous injections to oral and topical delivery. Since 2005, cancer nanomedicines have dominated the field [1–3, 5]. Most cancer nanomedicines are developed as systemically delivered nanoparticles so they can reach the tumor through passive means. By engineering nanocarriers using specific chemical compositions, shapes, and surfaces,

permeability into solid tumors may be tuned; thus, controlled drug delivery to its intended site of action may be attained.

To enable clinical translation of nanomedicines, adequate characterization in early development is needed to identify the nanoparticle's critical attributes and predict clinical success (or failure). This book introduces updated protocols geared at characterizing nano-based drug delivery strategies in early development that can be used to enable an Investigational New Drug (IND) or Investigational Device Exemption (IDE) application with the FDA. The Nanotechnology Characterization Laboratory (NCL; https://ncl.cancer.gov), which is a part of the National Cancer Institute's Alliance for Nanotechnology in Cancer, has optimized these assays to work for a variety of nano-based technologies intended for the delivery of cancer therapeutic and imaging agents. The NCL has examined several hundred different nanomedicines submitted from universities and companies worldwide and has helped several companies advance into or through clinical trials. As a result, NCL scientists have insight into the research and developmental needs of the nanotech community. With input from the FDA, NCL develops analytical protocols aimed at bridging the translational gap between discovery and clinical application of nanomedicine.

2 Evolving Complexity of Nanomedicines

Nanomedicines have gone through several incarnations over the years, each increasing in sophistication. As new formulations enter clinical trials, they build on the success of earlier versions, and introduce new characterization and development challenges. For example, nanoparticles intended for cancer therapy have evolved in their tumor-targeting strategies. Recent reviews highlight the progress of cancer nanomedicine and its challenges in clinical development [5, 7], much of which is related to the growing sophistication in the field.

First-generation cancer nanoparticles utilize passive targeting to the tumor [8, 9]. Doxil is one of the first approved cancer nanomedicines that demonstrated passive targeting in humans [6, 10]. Liposomal doxorubicin (Doxil) may be considered a "simple" first-generation strategy consisting of a liposome loaded with a previously FDA-approved small molecule; yet, its design features are far from straightforward [6]. Each component of Doxil has an important contribution to the nanomedicine's performance in vivo. Doxil consists of: (1) a well-controlled ratio of three different lipids in a specific physical state forming the lipid bilayer; (2) a specific drug-to-lipid ratio; (3) a PEGylated surface with optimized PEG length to extend the formulation's circulation time; and (4) a number of physical properties (pH gradient, permeability coefficients, solubility of drug, etc.) that enable active loading of the drug

into the liposome. Combined, these physicochemical parameters contribute to Doxil's advantages over doxorubicin—a longer in vivo half-life and greater accumulation of drug in the tumor. As a result, Doxil greatly reduces cardiotoxicity associated with the legacy drug [6]. Doxil was first FDA-approved in 1995, but new liposomal nanomedicines are still entering the clinic. Onivyde, an irinotecan liposome injection indicated in combination with fluorouracil and leucovorin for pancreatic cancer, was approved by the FDA in 2015. Vyxeos, a liposomal combination therapy, was also approved by the FDA in 2017. This next-generation formulation delivers two different cytotoxic drugs at a synergistic ratio. In Phase III clinical studies, Vyxeos revealed a 31% reduction in the risk of death compared to the standard of care regimen for the two drugs in patients with high-risk acute myeloid leukemia [11]. Many first-generation cancer nanomedicines are liposomes, but nanotechnology platforms such as albumin bound nanoparticles and polymeric nanoparticles have also been utilized to deliver chemotherapeutics passively to the tumor region [5].

Although passive targeting has become the cornerstone of first-generation cancer nanomedicines, it is now becoming clear that nanoparticle distribution varies between and within patient populations and tumor types [12]. With greater understanding in cancer biology, efforts are being made at defining biomarkers to afford better nanoparticle distribution and penetration into tumors, and to identify patients who can benefit the most from these nanomedicines. As a result, a number of novel, next-generation nanomedicine strategies have emerged. For example, nanotechnologies are being developed to actively target these newly identified biomarkers, as well as making use of additional drugs that reduce tumor microenvironment barriers to maximize tumor penetration. Other nanomedicine strategies utilize companion or simultaneous imaging strategies to monitor tumor permeability (ClinicalTrials.gov Identifier: NCT01770353), while others optimize drug release at the site of the tumor using stimuli-responsive nanoparticles [13, 14]. These and other complex nanomedicine strategies in development require a thorough understanding of the attributes that play critical roles in their intended functionality.

Cancer nanomedicines that target, or steer, the nanomedicine toward specific tumor biomarkers have additional challenges in development and characterization. Most nanoparticles are amenable to surface modifications. Therefore, complex targeting ligands such as antibodies, peptides, and proteins can be readily incorporated to aid in tumor targeting and increase drug accumulation. Many of these second-generation particles are currently undergoing clinical evaluation. For example, a targeted polymeric nanoparticle carrying docetaxel completed Phase II trials in patients with advanced solid tumors; however, these studies have demonstrated varied efficacy results depending on cancer type (ClinicalTrials.gov Identifiers:

NCT01300533, NCT01792479, NCT01812746) [15]. Preclinical data of a novel docetaxel prodrug loaded within a liposomal formulation and directed toward a receptor tyrosine kinase has demonstrated promising antitumor efficacy. The first-in-human clinical trial of this targeted nanomedicine, Merrimack's MM-310, started in early 2017 [16, 17]. Targeted nanoparticles are also being investigated in the clinic to carry new anticancer agents, such as therapeutic siRNA to solid tumors (ClinicalTrials.gov Identifiers: NCT02191878, NCT01159028, NCT02340156, NCT01517464) [2, 18], which may set the stage for the delivery of genome editing systems like CRISPR/Cas and TALEN.

Nanoparticles intended for cancer drug delivery are also evolving based on the type of therapeutic agent being delivered and the anticancer strategy being tested. Early cancer nanomedicines in the clinic predominately delivered chemotherapeutic agents that were previously FDA-approved. But now, nanoparticles are becoming attractive tools in the field of cancer immunotherapy to serve as carriers for potent antigens or adjuvants and to access key areas in the body to induce an immune response [19, 20]. Such complex nanoformulations have been extensively reported, but their translation into the clinic has been limited, possibly due to their challenging characterization questions. The development of nanomedicines toward these new therapeutic strategies warrants increased efforts into developing novel characterization methodologies.

Nanocarriers are also being engineered to simultaneously deliver multiple therapeutic agents, as demonstrated by the recently approved Vyxeos, or a combination of therapeutic and diagnostic agents [21]. Combinatorial delivery of multiple therapeutic agents, not limited to chemotherapeutic agents, could potentially provide a strategy to combat drug resistance exhibited in many aggressive tumors. Theranostics, the coupling of therapeutic products with diagnostic agents, can provide feedback via imaging results or other diagnostic probes about the efficacy of treatment, which may help in optimization and personalization of treatment in a more efficient manner than the current standard of care. Preclinical examples of these combination therapies have been summarized elsewhere in the literature [5].

In addition to passively and actively targeted nanoparticles, targeting the intended disease site can also be achieved with stimuli-responsive drug delivery nanoparticles [22, 23]. Responsive nanoparticles are designed to deliver their cargo in reaction to some intrinsic or external stimulus. The payload is released to the site of action only after the stimulus is detected and the nanoparticle undergoes a transition state. An intrinsic stimulus can be the pH, enzyme concentration, or temperature of the tumor microenvironment. An external stimulus can consist of magnetic or electrical fields, ultrasound, or radiation. Responsive drug delivery for cancer therapy can utilize passively or actively targeted nanoparticles for

transport to the tumor microenvironment upon which the stimulus is sensed or directly applied. For example, Visudyne is an FDA-approved, stimuli-responsive nanomedicine using photodynamic therapy [24]. ThermoDox is a clinical-stage example of heat-responsive doxorubicin delivery. This technology consists of thermally sensitive liposomes, which change structure when heated to a temperature range of 40–45 °C, allowing for doxorubicin drug release [25]. The external stimulus is applied by tumor-directed radiofrequency. Clinical studies are underway to investigate ThermoDox in combination with optimized radiofrequency ablation for patients with non-resectable liver cancer (ClinicalTrials.gov Identifier: NCT02112656). The goal of these dynamic particles is aimed at improving drug accumulation at the site of action; however, assessing drug kinetics in this type of system requires additional understanding of the particle's mechanism of physical transition, the level of stimulation required, and drug release profiles before and after stimulation. Also, externally stimulated nanoparticles have the added complexity of potentially being a drug-device combination, which requires additional know-how and may complicate translation and adoption by physicians.

Many of the first cancer nanomedicines to the clinic are beginning to go off-patent, that is they are losing their market exclusivity, permitting the development of affordable, generic nanomedicines. Generic drugs are copies of brand-name drugs that have the same dosage form, safety, strength, route of administration, quality, performance characteristics, and intended used. Liposomal Doxorubicin Hydrochloride is the first cancer nanodrug approved through an Abbreviated New Drug Application (ANDA) pathway. This generic, or follow-on product, is considered to be a copy of Doxil. Yet, many questions arise whether sameness can be established on such a complex formulation that depends on several critical parameters. Unlike generic drugs of conventional small molecules, determining sameness between two nanodrugs is a more complex process. There are usually several parameters that contribute to their safety, quality, and performance characteristics, and those parameters are generally sensitive to minor changes. This highlights the importance of appropriate characterization. Many critical properties and tests tend to be overlooked during the development of all types of nanoparticles, not just follow-on versions [26]. With greater intricacy of nanoplatforms comes greater characterization challenges, requiring sophisticated methods that can best predict clinical success early in the development path [7].

3 Characterization Challenges and Advancements

Complexity is an innate part of nanoparticles. Many properties not generally considered for small molecule medicines need to be thoroughly understood for nanoparticles. Multidisciplinary expertise and testing is essential to grasp a complete understanding of the design features that contribute to a safer and more effective therapy. Importantly, physicochemical properties of the nanoformulation need to be linked to their performance characteristics such as pharmacokinetic, biodistribution, efficacy, and toxicity profiles. Because of the demanding characterization needs, a clear advantage of the nanomedicine over existing formulations should be established early on in the development stage, along with a feasible manufacturing strategy to prevent expensive failures later on [7]. Important properties to investigate for all nanotech drug delivery formulations include sterility and endotoxin testing (Chapters 2 and 3), physicochemical properties (Chapters 4–8), in vitro immunological activity (Chapters 9–18), drug release kinetics in biological matrix (Chapter 19), and efficacy in predictive animal models of the intended disease indication (Chapter 20). These are the topics covered in this second edition book. Importantly though, nanomedicine characterization depends on many factors, including the drug, platform, and intended use. This book cannot capture all testing requirements for all nanodrugs in development. Rather, the protocols included here are meant to serve as a basis for the early evaluation of nanomedicine products in development.

Endotoxin is a major contaminant in early nanomedicine formulations [26]. If endotoxin levels are above certain thresholds, many immunotoxicity assays could give false-positive readings [27]. Taking precautions early in the development process to reduce endotoxin contamination will allow for a more accurate assessment of the toxicity profile of the nanomedicine and its components. However, some nanomaterials can interfere with commonly used assays that assess contaminants and they may exaggerate inflammatory properties of endotoxin [28]. Updated protocols for the detection of bacterial contamination and practical considerations to overcome endotoxin contamination are included in Chapters 2 and 3. Controlling bacterial and endotoxin contamination is highly recommended before conducting toxicity or immunology assays.

The particle's physicochemical properties, including size, size distribution, composition, surface characteristics, purity, and stability, are critical parameters to define because they can directly affect in vivo activity of the nanomedicine. New and updated protocols that assess physicochemical characteristics of the nanoparticle are found in Chapters 4–8. All nanoparticles rely on control at the nanoscale, meaning small variations may cause significant changes

to the nanoformulation. However, not all techniques are sensitive enough to detect small changes in physicochemical properties, so orthogonal techniques are recommended for a more thorough evaluation.

Surface characteristics, such as coating density, surface charge, surface area, and surface chemistry, need to be adequately described to make reproducible batches. Despite the importance of surface evaluation, it remains one of the most challenging physicochemical tests. There are only a few widely applicable assays for surface characterization. Most assays must be individually tailored for the specific surface ligand–nanoparticle combination being evaluated. Chapters 5 and 6 are protocols aimed at quantitating surface coatings of nanoparticles using reverse-phase high-performance liquid chromatography (RP-HPLC) and thermogravimetric analysis (TGA), respectively. While these too will require some optimization, the overall techniques can be used to quantitate various surface coatings on a variety of nanoplatforms. Imaging by immunoelectron microscopy, such as that described in Chapter 7, can also serve as a qualitative method to illustrate nanoparticle surfaces where appropriate antibodies are available. Some biological surface moieties have the added complexity of needing structure/shape evaluation, not simply quantification, to ensure it remains biologically active to fulfill its targeting function. Targeting ligands may not be attached in sufficient quantity or in the correct configuration to bind to the receptor. Therefore, a combination of different surface characterization techniques along with biological assays may be required for molecularly targeted nanomedicines.

Multiple protocols for nanoparticle size analysis were published in the first edition of this book, including dynamic light scattering (DLS), transmission electron microscopy (TEM), and atomic force microscopy (AFM) [29]. This second edition book highlights advances in TEM to specifically image liposomes, one of the most popular delivery strategies for cancer nanomedicines. Liposomes can be particularly challenging to image by TEM due to the soft nature of the particle, making it prone to imaging artifacts such as disruption of the bilayer, folding, or other distortion of the particle. Chapter 8 discusses negative staining and cryo-TEM techniques and tips for imaging these soft structures.

About a fifth of all drugs in clinical use from the 1970s to early 2000s were removed from the clinic due to adverse effects on the immune system [30, 31]. In vivo administration of new and combinatorial nanoproducts poses additional questions about possible adverse effects in vivo, including how the human immune system will respond [32]. Adverse immune reactions may include anaphylaxis, allergy, hypersensitivity, idiosyncratic reactions, and immunosuppression [30, 31, 33, 34]. Examining how the nanomedicine and its components interact with blood and immune cells in vitro can help prevent serious and potentially lethal reactions during

clinical evaluation [35, 36]. Updated immunological assays for nanomedicines are included in Chapters 9–18. Chapter 9 is an updated in vitro protocol to investigate nanomedicine-mediated hemolysis, particularly relevant for nanomedicines that contain cationic species or degradation products. Certain systemically administered nanoparticles can induce thrombosis or blood coagulation, which could become trapped in the lungs and cause embolisms. In vitro protocols, like that described in Chapter 10 to examine blood coagulation, can be predictive of in vivo thrombogenic reactions. Complement activation-related pseudoallergy (CARPA) is a life-threatening condition in humans. Nanoparticles delivering nucleic acids and ones made up of certain lipids are particularly susceptible to inducing CARPA [37]. In vitro assays to assess complement activation with human or non-human primate blood, as described in Chapter 13, can be good indicators of CARPA in vivo. These and other updated immunology assays included in this book provide knowledge about a nanoformulation's potential immunotoxicity. This information, if discovered early, can inform the development and optimization process before the initiation of costly in vivo studies and clinical trials.

In general, nanomedicines are designed to increase the half-life of the drug, enabling delivery of the API to its intended site of action. If the drug releases too quickly, it can produce off-target toxicities. On the other hand, if the formulation is too stable, the API will not be delivered in appropriate concentrations making it therapeutically ineffective. Drug release is therefore an important measure of nanoparticle stability. However, determining drug release in vivo is challenging because drug binding can equilibrate between the nanoparticle and abundant proteins in the blood. The method described in Chapter 19 is a simple approach to evaluate drug release in biological matrix. The only requirement for the method is that a stable isotope-labeled version of the drug be available. This method is unique from other drug release methods in that it uses biological matrix (e.g., whole blood or plasma versus buffered solutions), and can differentiate between free/unbound, protein bound, and nanoparticle bound drug fractions. It can be utilized as an in vitro tool to predict nanomaterial stability in vivo or to evaluate pharmacokinetic parameters from an in vivo study. In addition, the method can be used to evaluate bioequivalence between an innovator nanomedicine and a follow-on product looking to enter the market through an ANDA [40].

Preclinical efficacy and safety are essential evaluation criteria for all nanoformulations in early development. The design of a preclinical animal study is most predictive if the clinical indication for the nanomedicine is known and the disease model, route of administration, and dosing volume closely resemble the parameters that will be used clinically. Chapter 20 provides a comprehensive protocol and recommendations on how to devise and analyze in vivo preclinical efficacy studies in rodent models. Appropriate drug and

nanoformulation controls should be carefully selected, especially for nanomedicines that require molecular targeting and/or internal or external stimuli to be effective. No in vitro animal model is completely predictive of clinical results. This is due in part to the heterogeneous make-up of the patient population that cannot be adequately captured in a controlled animal setting. Testing in multiple relevant models affords the best glimpse of clinical outcomes. For cancer nanomedicines, understanding how the physicochemical features of the nanoparticle relate to tumor biology is critical to achieve meaningful results [5, 39]. For this reason, it is imperative to gain a thorough understanding of the nanoparticle's properties through rigorous characterization.

4 Importance of Updated Nanoparticle Characterization

Many characterization assays used during the development of first-generation nanomedicines leveraged methods used to study conventional, small molecule drugs. But with advancements in nanotechnology, new characterization tools and methods have been developed that can better account for the unique properties of nanomaterials. In addition, nanomedicines continue to evolve with increasingly more complex features that require greater multidisciplinary scrutiny. Many new nanoplatforms, such as virus platforms and exosomes have been introduced in the literature but have yet to enter the United States market [40]. Nanoparticles are also emerging in the field of cancer immunotherapy, prompting the development of nanocarriers for antigens and adjuvants for the design of synthetic vaccines. With such advancements, there are vast opportunities for new therapeutic agents. As a result, there is a clear need to address this progressive nano-landscape by advancing characterization techniques that can answer critical regulatory questions and best predict clinical outcomes.

This second edition book consists of new and updated protocols that are aimed at evaluating the clinical potential of nanomedicine products in preclinical development. The protocols are meant for use by the research community and pharmaceutical and biotechnology developers of nano-based products intended for drug delivery. Most in vitro protocols in this book are designed to evaluate nanoparticles that are administered intravenously, while protocols that characterize the physicochemical properties can be applied to nanomedicines intended for all routes of administration. Although it is envisioned that many of these optimized methods can be applied to a variety of nanoplatforms, there may be limitations to their application for novel therapeutic platforms. This second edition book offers up-to-date nanomedicine characterization protocols in order to address the growing needs of the nanotechnology community. Optimized characterization techniques,

like those introduced in this book, can drive the next generation of innovative cancer therapeutics from discovery to the clinic.

Acknowledgment

This project has been funded in whole or in part with Federal funds from the National Cancer Institute, National Institutes of Health, under Contract No. HHSN261200800001E. The content of this publication does not necessarily reflect the views or policies of the Department of Health and Human Services, nor does mention of trade names, commercial products, or organizations imply endorsement by the U.S. Government.

References

1. Weissig V, Pettinger TK, Murdock N (2014) Nanopharmaceuticals (part 1): products on the market. Int J Nanomedicine 9:4357–4373. https://doi.org/10.2147/IJN.S46900
2. Anselmo AC, Mitragotri S (2016) Nanoparticles in the clinic. Bioeng Transl Med 1 (1):10–29. https://doi.org/10.1002/btm2.10003
3. Havel HA (2016) Where are the nanodrugs? An industry perspective on development of drug products containing nanomaterials. AAPS J 18(6):1351–1353. https://doi.org/10.1208/s12248-016-9970-6
4. Boswell GW, Buell D, Bekersky I (1998) AmBisome (Liposomal Amphotericin B): a comparative review. J Clin Pharmacol 38 (7):583–592. https://doi.org/10.1002/j.1552-4604.1998.tb04464.x
5. Shi J, Kantoff PW, Wooster R, Farokhzad OC (2017) Cancer nanomedicine: progress, challenges and opportunities. Nat Rev Cancer 17 (1):20–37. https://doi.org/10.1038/nrc.2016.108
6. Barenholz Y (2012) Doxil®—the first FDA-approved nano-drug: lessons learned. J Control Release 160(2):117–134. https://doi.org/10.1016/j.jconrel.2012.03.020
7. Grossman JH, Crist RM, Clogston JD (2017) Early development challenges for drug products containing nanomaterials. AAPS J 19 (1):92–102. https://doi.org/10.1208/s12248-016-9980-4
8. Matsumura Y, Maeda H (1986) A new concept for macromolecular therapeutics in cancer chemotherapy: mechanism of tumoritropic accumulation of proteins and the antitumor agent smancs. Cancer Res 46(12 Part 1):6387–6392
9. Maeda H, Wu J, Sawa T, Matsumura Y, Hori K (2000) Tumor vascular permeability and the EPR effect in macromolecular therapeutics: a review. J Control Release 65(1–2):271–284. https://doi.org/10.1016/S0168-3659(99)00248-5
10. Gabizon A, Catane R, Uziely B, Kaufman B, Safra T, Cohen R, Martin F, Huang A, Barenholz Y (1994) Prolonged circulation time and enhanced accumulation in malignant exudates of doxorubicin encapsulated in polyethyleneglycol coated liposomes. Cancer Res 54 (4):987–992
11. (2016) Celator Pharmaceuticals® presented phase 3 trial results in patients with high-risk acute myeloid leukemia demonstrating VYXEOS™ (CPX-351) significantly improved overall survival. Ewing, NJ. http://www.prnewswire.com/news-releases/celator-announces-phase-3-trial-for-vyxeos-cpx-351-in-patients-with-high-risk-acute-myeloid-leukemia-demonstrates-statistically-significant-improvement-in-overall-survival-300235620.html
12. Prabhakar U, Maeda H, Jain RK, Sevick-Muraca EM, Zamboni W, Farokhzad OC, Barry ST, Gabizon A, Grodzinski P, Blakey DC (2013) Challenges and key considerations of the enhanced permeability and retention effect for nanomedicine drug delivery in oncology. Cancer Res 73(8):2412–2417. https://doi.org/10.1158/0008-5472.can-12-4561
13. Adiseshaiah PP, Crist RM, Hook SS, McNeil SE (2016) Nanomedicine strategies to overcome the pathophysiological barriers of pancreatic cancer. Nat Rev Clin Oncol 13 (12):750–765. https://doi.org/10.1038/nrclinonc.2016.119

14. Chauhan VP, Jain RK (2013) Strategies for advancing cancer nanomedicine. Nat Mater 12(11):958–962. https://doi.org/10.1038/nmat3792
15. Hrkach J, Von Hoff D, Mukkaram Ali M, Andrianova E, Auer J, Campbell T, De Witt D, Figa M, Figueiredo M, Horhota A, Low S, McDonnell K, Peeke E, Retnarajan B, Sabnis A, Schnipper E, Song JJ, Song YH, Summa J, Tompsett D, Troiano G, Van Geen HT, Wright J, LoRusso P, Kantoff PW, Bander NH, Sweeney C, Farokhzad OC, Langer R, Zale S (2012) Preclinical development and clinical translation of a PSMA-targeted docetaxel nanoparticle with a differentiated pharmacological profile. Sci. Transl. Med 4(128):128ra139. https://doi.org/10.1126/scitranslmed.3003651
16. Kamoun WS, Luus L, Pien C, Kornaga T, Oyama S, Huang ZR, Tipparaju S, Kirpotin DB, Marks JD, Koshkaryev A, Geddie M, Xu L, Lugovosky A, Drummond DC (2016) Abstract 871: nanoliposomal targeting of ephrin receptor A2 (EphA2): preclinical in vitro and in vivo rationale. Cancer Res 76(14 Supplement):871–871. https://doi.org/10.1158/1538-7445.am2016-871
17. Kirpotin DB, Tipparaju S, Huang ZR, Kamoun WS, Pien C, Kornaga T, Oyama S, Olivier K, Marks JD, Koshkaryev A, Schihl SS, Fetterly G, Schoeberl B, Noble C, Hayes M, Drummond DC (2016) Abstract 3912: MM-310, a novel EphA2-targeted docetaxel nanoliposome. Cancer Res 76(14 Supplement):3912–3912. https://doi.org/10.1158/1538-7445.am2016-3912
18. Davis ME, Zuckerman JE, Choi CHJ, Seligson D, Tolcher A, Alabi CA, Yen Y, Heidel JD, Ribas A (2010) Evidence of RNAi in humans from systemically administered siRNA via targeted nanoparticles. Nature 464 (7291):1067–1070. https://doi.org/10.1038/nature08956
19. Smith DM, Simon JK, Baker JR Jr (2013) Applications of nanotechnology for immunology. Nat Rev Immunol 13(8):592–605. https://doi.org/10.1038/nri3488
20. Swartz MA, Hirosue S, Hubbell JA (2012) Engineering approaches to immunotherapy. Sci Transl Med 4(148):148rv9. https://doi.org/10.1126/scitranslmed.3003763
21. Bao G, Mitragotri S, Tong S (2013) Multifunctional nanoparticles for drug delivery and molecular imaging. Annu Rev Biomed Eng 15 (1):253–282. https://doi.org/10.1146/annurev-bioeng-071812-152409
22. Mura S, Nicolas J, Couvreur P (2013) Stimuli-responsive nanocarriers for drug delivery. Nat Mater 12(11):991–1003. https://doi.org/10.1038/nmat3776
23. van Elk M, Murphy BP, Eufrásio-da-Silva T, O'Reilly DP, Vermonden T, Hennink WE, Duffy GP, Ruiz-Hernández E (2016) Nanomedicines for advanced cancer treatments: transitioning towards responsive systems. Int J Pharm 515(1–2):132–164. https://doi.org/10.1016/j.ijpharm.2016.10.013
24. Bressler NM, Bressler SB (2000) Photodynamic therapy with verteporfin (visudyne): impact on ophthalmology and visual sciences. Invest Ophthalmol Vis Sci 41(3):624–628
25. Landon CD, Park JY, Needham D, Dewhirst MW (2011) Nanoscale drug delivery and hyperthermia: the materials design and preclinical and clinical testing of low temperature-sensitive liposomes used in combination with mild hyperthermia in the treatment of local cancer. Open Nanomed J 3:38–64. https://doi.org/10.2174/1875933501103010038
26. Crist RM, Grossman JH, Patri AK, Stern ST, Dobrovolskaia MA, Adiseshaiah PP, Clogston JD, McNeil SE (2013) Common pitfalls in nanotechnology: lessons learned from NCI's nanotechnology characterization laboratory. Integr Biol (Camb) 5(1):66–73. https://doi.org/10.1039/c2ib20117h
27. Dobrovolskaia MA, Neun BW, Clogston JD, Grossman JH, McNeil SE (2014) Choice of method for endotoxin detection depends on nanoformulation. Nanomedicine (Lond) 9 (12):1847–1856. https://doi.org/10.2217/nnm.13.157
28. Dobrovolskaia MA, Patri AK, Potter TM, Rodriguez JC, Hall JB, McNeil SE (2012) Dendrimer-induced leukocyte procoagulant activity depends on particle size and surface charge. Nanomedicine (Lond) 7(2):245–256. https://doi.org/10.2217/nnm.11.105
29. McNeil SE (ed) (2011) Characterization of nanoparticles intended for drug delivery, Methods in molecular biology, vol 697. Humana Press, New York. https://doi.org/10.1007/978-1-60327-198-1
30. Smith DA, Schmid EF (2006) Drug withdrawals and the lessons within. Curr Opin Drug Discov Devel 9(1):38–46
31. Wysowski DK, Nourjah P (2004) Analyzing prescription drugs as causes of death on death certificates. Public Health Rep 119(6):520. https://doi.org/10.1016/j.phr.2004.09.001
32. Dobrovolskaia MA, McNeil SE (2007) Immunological properties of engineered nanomaterials. Nat Nanotechnol 2(8):469–478
33. Wilke RA, Lin DW, Roden DM, Watkins PB, Flockhart D, Zineh I, Giacomini KM, Krauss

RM (2007) Identifying genetic risk factors for serious adverse drug reactions: current progress and challenges. Nat Rev Drug Discov 6 (11):904–916. https://doi.org/10.1038/nrd2423

34. Wysowski DK, Swartz L (2005) Adverse drug event surveillance and drug withdrawals in the United States, 1969-2002: the importance of reporting suspected reactions. Arch Intern Med 165(12):1363–1369. https://doi.org/10.1001/archinte.165.12.1363
35. Dobrovolskaia MA, McNeil SE (2013) Understanding the correlation between in vitro and in vivo immunotoxicity tests for nanomedicines. J Control Release 172(2):456–466. https://doi.org/10.1016/j.jconrel.2013.05.025
36. Dobrovolskaia MA (2015) Pre-clinical immunotoxicity studies of nanotechnology-formulated drugs: challenges, considerations and strategy. J Control Release 220(Pt B):571–583. https://doi.org/10.1016/j.jconrel.2015.08.056
37. Szebeni J, Muggia F, Gabizon A, Barenholz Y (2011) Activation of complement by therapeutic liposomes and other lipid excipient-based therapeutic products: prediction and prevention. Adv Drug Deliv Rev 63 (12):1020–1030. https://doi.org/10.1016/j.addr.2011.06.017
38. Skoczen S, McNeil SE, Stern ST (2015) Stable isotope method to measure drug release from nanomedicines. J Control Release 220:169–174
39. Adiseshaiah PP, Hall JB, McNeil SE (2010) Nanomaterial standards for efficacy and toxicity assessment. Wiley Interdiscip Rev Nanomed Nanobiotechnol 2(1):99–112. https://doi.org/10.1002/wnan.66
40. Batrakova EV, Kim MS (2015) Using exosomes, naturally-equipped nanocarriers, for drug delivery. J Control Release 219:396–405. https://doi.org/10.1016/j.jconrel.2015.07.030

Part II

Sterility and Endotoxin Testing

Chapter 2

Detection of Bacterial Contamination in Nanoparticle Formulations by Agar Plate Test

Timothy M. Potter, Barry W. Neun, Anna N. Ilinskaya, and Marina A. Dobrovolskaia

Abstract

Bacterial contamination can confound the results of in vitro and in vivo preclinical tests. This protocol describes a procedure for detection of microbial contamination in nanotechnology-based formulations. Nanoparticle samples and controls are spread on the surface of agar and growth of bacterial colonies is monitored after 72 h of incubation. The intended purpose of this assay is to avoid introduction of microbial contamination into in vitro cell cultures and in vivo animal studies utilizing the test nanomaterial. This assay is not intended to certify the material as sterile.

Key words Nanoparticles, Contamination, Bacteria, Yeast, Mold

1 Introduction

This protocol describes a procedure for detection of bacterial contamination in a nanoparticle formulation. The assay requires 0.5 mL of the test nanomaterial in its final formulation. The concentration of nanoparticles in this formulation is case-specific. When such information is not available, for example when a test nanomaterial is received from a commercial supplier in a form not intended for biomedical applications, the concentration of the stock is 1 mg/mL. The weight information can refer to either active pharmaceutical ingredient or total construct; it can also represent total metal content or other units. Such information is specific to each nanoparticle and should be recorded to aid result interpretation. This test detects bacterial contamination and is mainly intended to avoid contamination of cell cultures or transmitting microbial contaminants to animals in preclinical studies of efficacy, biodistribution, and toxicity. This method is not applicable to test nanoparticle antimicrobial activity, microbial resistance, validation of the sterilization procedure, or lot release. If this is your aim,

Scott E. McNeil (ed.), *Characterization of Nanoparticles Intended for Drug Delivery*, Methods in Molecular Biology, Vol. 1682, DOI 10.1007/978-1-4939-7352-1_2,

in-depth analysis of sterility parameters can be performed according to the United States Pharmacopeia standards USP30-51, 30-61, and 30-71 [1–3]. Safety precautions for working with engineered nanomaterials are summarized in **Note 1**.

2 Materials

1. Sterile PBS.
2. Luria-Bertani (LB) Broth: LB Broth composition is 10 g/L Tryptone, 5.0 g/L Yeast Extract, and 0.5 g/L NaCl. It is supplied as a liquid, but can also be purchased as a powder. If you use liquid media, it does not require any additional manipulation. Powdered media has to be reconstituted in water. In this case, please follow the instruction from the manufacturer of the powdered media. Sterilize the media you prepare from powdered formula for 15 min at 121 °C. Cool to room temperature and either use fresh or store in the refrigerator.
3. LB Agar Plates. The composition of the LB agar is 10 g/L Tryptone, 5.0 g/L Yeast Extract, 0.5 g/L NaCl, 15 g/L Agar. It can be prepared by dissolving 15 g of agar in 1 L of LB media or from the commercial powdered formula containing all components in a dry form. For example, the commercial LB agar (Sigma, L3272) is supplied as a powder. When prepared according to the manufacturer's instructions, 30.5 g of powder is dissolved in 1 L of water, then heated to boiling until complete dissolution and autoclaved for 15 min at 121 °C to sterilize. The media should be cooled and poured into petri dishes to solidify. The plates can be used freshly prepared or stored at 4 °C (Fig. 1).
4. Negative control: Sterile PBS or water. The negative control is acceptable if no colony forming units (CFU) are observed upon completion of the test.
5. Positive control: Bacterial cultures (e.g. ATCC #25254) at a dilution which will allow at least 10 CFU/mL.

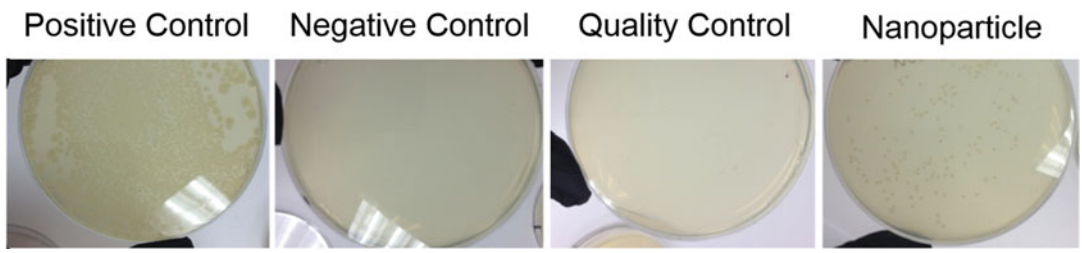

Fig. 1 Sample of agar plate test results. Positive results from agar plate test of a silica-based nanoparticle formulation

6. 0.1 N Hydrochloric acid (HCl). Prepare by diluting commercial stock reagents in sterile water.
7. 0.1 N Sodium Hydroxide (NaOH). Prepare by diluting commercial stock reagents in sterile water.
8. Buffer used to reconstitute test nanomaterial.
9. Test nanoparticles reconstituted in sterile PBS, water, or in appropriate vehicle. If the vehicle is a buffer or media other than water and PBS, the vehicle control should be included in the test. The nanoparticle samples are tested directly from stock and at several serial 10-fold dilutions: no dilution, 10-fold, 100-fold, 1000-fold. The pH of the study sample should be checked using a pH microelectrode and adjusted with either sterile NaOH or HCl as necessary to be within the pH range 6–8. If NaOH or HCl are not compatible with a given nanoparticle formulation, adjust pH using a procedure recommended by the nanomaterial manufacturer. To avoid sample contamination from the microelectrode, always remove a small aliquot of the sample for use in measuring the pH.
10. Sterile tubes, 5 mL.
11. Petri dishes.

3 Methods

1. Remove the LB plates from the refrigerator and allow them to warm up to room temperature. Prepare two plates for each sample and four plates for negative and positive controls. Plate one set of negative and positive controls before plating test samples, and plate the second set after plating test samples.
2. Using sterile conditions apply 50 μL of controls or nanoparticle preparation at each dilution onto the surface of the agar and evenly distribute the sample using a sterile disposable bacterial spreader. Allow liquid to absorb, then recap the Petri dish, turn it upside down to prevent condensation and place into the incubator.
3. Incubate for 72 h at a nominal temperature of 37 °C.
4. Remove dishes from the incubator and examine for appearance of colonies. Perform colony count.
5. Report results according to the following formula (*see* **Notes 2** and **3**):

   $$\#\text{Colonies} \times \text{Dilution Factor} \times \text{Sampling Factor} = \text{CFU/mL}$$

6. Review **Note 4** for additional details.

4 Notes

1. Always wear appropriate personal protective equipment and take appropriate precautions when handling your nanomaterial. Many occupational health and safety practitioners recommend wearing two layers of gloves when handling nanomaterials. Also, be sure to follow your facility's recommended disposal procedure for your specific nanomaterial.
2. To estimate sampling factor, consider what proportion of the test sample is represented by 50 μL of the test aliquot spread on the plate. For example, if the final formulation is supplied as a 1 mL aliquot, the sampling factor is 20; if it is 10 mL, the sampling factor is 200; if it is 0.5 mL, the sampling factor is 10, etc.
3. To assess whether nanoparticles can inhibit bacterial growth, a positive control sample at the same final dilution is spiked into the test nanoparticle sample. For example, when you spike 440 CFU per 2.2 mL of nanoparticle solution at a given dilution and 50 μL is plated on the surface of agar, the final inhibition control contains the same concentration of nanoparticles as the nanoparticle unspiked sample and the same concentration of bacteria as in the positive control (10 CFU/mL).
4. NCL does not endorse suppliers. However, we found that a new user benefits from knowing catalog information of reagents used in our assays. If you need ideas of what reagents are used at the NCL, please review NCL method STE 2.2 available at https://ncl.cancer.gov/resources/assay-cascade-protocols. When other reagents are used, the assay performance may change. When using reagents and instruments from sources other than that used in our protocols, assay performance qualification is needed to verify the assay functionality and validity.

Acknowledgment

This project has been funded in whole or in part with Federal funds from the National Cancer Institute, National Institutes of Health, under Contract No. HHSN261200800001E. The content of this publication does not necessarily reflect the views or policies of the Department of Health and Human Services, nor does mention of trade names, commercial products, or organizations imply endorsement by the U.S. Government.

References

1. USP standard 51 (2007) Antimicrobial effectiveness testing USP 30 NF 25 1
2. USP standard 61 (2007) Microbial limit tests USP 30 NF 25 1
3. USP standard 71 (2007) Sterility tests USP 30 NF 25 1

Chapter 3

Considerations and Some Practical Solutions to Overcome Nanoparticle Interference with LAL Assays and to Avoid Endotoxin Contamination in Nanoformulations

Barry W. Neun and Marina A. Dobrovolskaia

Abstract

Monitoring endotoxin contamination in drugs and medical devices is required to avoid pyrogenic response and septic shock in patients receiving these products. Endotoxin contamination of engineered nanomaterials and nanotechnology-based medical products represents a significant translational hurdle. Nanoparticles often interfere with an in vitro Limulus Amebocyte Lysate (LAL) assay commonly used in the pharmaceutical industry for the detection and quantification of endotoxin. Such interference challenges the preclinical development of nanotechnology-formulated drugs and medical devices containing engineered nanomaterials. Protocols for analysis of nanoparticles using LAL assays have been reported before. Here, we discuss considerations for selecting an LAL format and describe a few experimental approaches for overcoming nanoparticle interference with the LAL assays to obtain more accurate estimation of endotoxin contamination in nanotechnology-based products. The discussed approaches do not solve all types of nanoparticle interference with the LAL assays but could be used as a starting point to address the problem. This chapter also describes approaches to prevent endotoxin contamination in nanotechnology-formulated products.

Key words Endotoxin, LAL, Interference, Inhibition enhancement control

1 Introduction

Endotoxin is a building block of the gram-negative bacterial cell wall [1]. Many cell types have an endotoxin receptor complex and respond to this bacterial ligand. Mononuclear phagocytes are particularly sensitive and produce cytokines, chemokines, and other pro-inflammatory messengers in response to low (picogram) quantities of endotoxin [2]. These pro-inflammatory substances result in pathophysiological events leading to fever and hypotension and at high levels may also lead to severe tissue and organ damage [1]. Common life-threatening conditions observed in response to high endotoxin levels in humans are septic shock syndrome, toxic anterior segment syndrome, multiple organ failures (mainly kidney, lungs, and liver), and disseminated intravascular coagulation.

Scott E. McNeil (ed.), *Characterization of Nanoparticles Intended for Drug Delivery*, Methods in Molecular Biology, Vol. 1682, DOI 10.1007/978-1-4939-7352-1_3,

Endotoxin contamination is particularly problematic for pharmaceutical products and medical devices. If these products get contaminated with endotoxin, the results of preclinical toxicity and efficacy studies may be confounded and lead to wrong conclusions. In the clinical setting, they will lead to immunotoxicity in patients. Regulatory authorities recognize this problem and mandate endotoxin limits that depend on the type of product, the dose, and the route of administration of the given pharmaceutical product. The biological activity of endotoxin is measured in endotoxin units (EU). The endotoxin limit (EL), specific for each product, depends on the threshold pyrogenic dose (K) and the maximum dose (M) of the given product administered per kilogram of body weight per single hour. The EL for parenteral drugs is calculated according to the formula K/M. The K-value described in the United States Pharmacopeia is 5 EU/kg for all parenteral routes except for intrathecal route, for which the threshold pyrogenic dose is 0.2 EU/kg [3]. The EL for radiopharmaceuticals depends on the volume of the product in milliliters (V) and is equal to $175/V$ and $14/V$ for most parenteral routes and intrathecal route, respectively [3]. The allowable EL mandated for the surfaces of medical devices is 0.5 EU/mL (or 20 EU/device) and for products in contact with the cardiovascular and lymphatic systems and cerebrospinal fluid is 0.06 EU/mL (or 2.15 EU/device) [4]. According to the new FDA guideline, the EL for intraocular fluids is 0.2 EU/mL and that for solid ocular devices is 0.2 EU/device [5].

Due to its presence virtually everywhere (air, water, many common laboratory reagents, equipment, and surfaces) and resistance to autoclaving, endotoxin is a common contaminant in engineered nanomaterials and nanotechnology-formulated drugs and devices produced in research laboratories [6, 7]. As much as one-third of nanotechnology formulations fail in preclinical phase due to excessive endotoxin contamination [8].

In addition to the concerns regarding endotoxin presence in pharmaceutical products and devices discussed above, nanotechnology products experience an additional challenge. Recent reports from our laboratory [9] and other investigators [10–14] demonstrated that some nanoparticles are not pro-inflammatory alone but exaggerate the inflammatory properties of low concentrations of endotoxin. This challenge complicates the estimation of the EL using formulas we discussed above and, in the absence of a specific regulatory guideline or standard, suggests that nanotechnology products possessing the endotoxin-exaggerating property should be virtually free from endotoxin.

The in vitro method traditionally used in the pharmaceutical industry to detect and quantify endotoxin contamination is the Limulus Amebocyte Lysate (LAL) test, which exists in three formats: turbidity, chromogenic, and gel-clot [15]. Both turbidity and chromogenic assays can be performed in an end-point and kinetic

mode. In addition, a newer version of an LAL derivative assay has been developed with recombinant factor C [16–18]. This assay utilizes a substrate that upon cleavage by endotoxin-activated lysate produces a fluorescent product and operates in the kinetic mode [16–18]. The kinetic assays, in general, have greater assay sensitivity (or lambda) than their end-point counterparts [15]. Understanding the difference in lambda of various LAL assays is necessary for both experimental design and inter-assay data comparison, because this value is used to calculate the maximum valid dilution (MVD). Many chemicals may interfere with the LAL assays, however, due to their complex composition and unique physicochemical properties. Nanotechnology-based products experience a greater spectrum of interference with the LAL [15, 19, 20].

In this chapter, we discuss factors one may consider when selecting an LAL assay suitable for the given nanoformulation and suggest several practical approaches, which may be used to overcome interference from certain nanomaterials. Although the proposed experimental steps do not completely solve the problem of nanoparticle interference with the LAL assays, they may serve as a starting point to analyze nanoparticles with physicochemical properties similar to those used in our case studies. We will also discuss approaches to prevent endotoxin contamination in nanotechnology-formulated products and to remove endotoxin from contaminated particles.

2 Choosing an LAL Format

Some of the nanoparticle interferences with the LAL can be predicted based on the nanomaterial's basic physicochemical properties such as absorbance spectrum at or about 405 nm because chromogenic LAL assay is performed at this wavelength. The decision tree presented in Fig. 1 may be helpful in making a choice about the LAL format.

3 Overcoming False-Positive Results Due to Contamination with Beta-Glucans

Despite its high sensitivity to endotoxin, traditional LAL assays also detect beta-glucans. The LAL proteins activated by endotoxin and beta-glucans are different. Factor C is activated by the endotoxin, while Factor G is triggered by beta-glucans [15]. Despite the difference in the sensing protein and pathway, the result (e.g., gelation or turbidity) of the LAL reaction triggered by endotoxin and beta-glucans is the same and often leads to overestimation of endotoxin in the sample containing beta-glucans. While monitoring the presence of beta-glucans is important to identify potential fungal contamination of pharmaceutical products, it should be

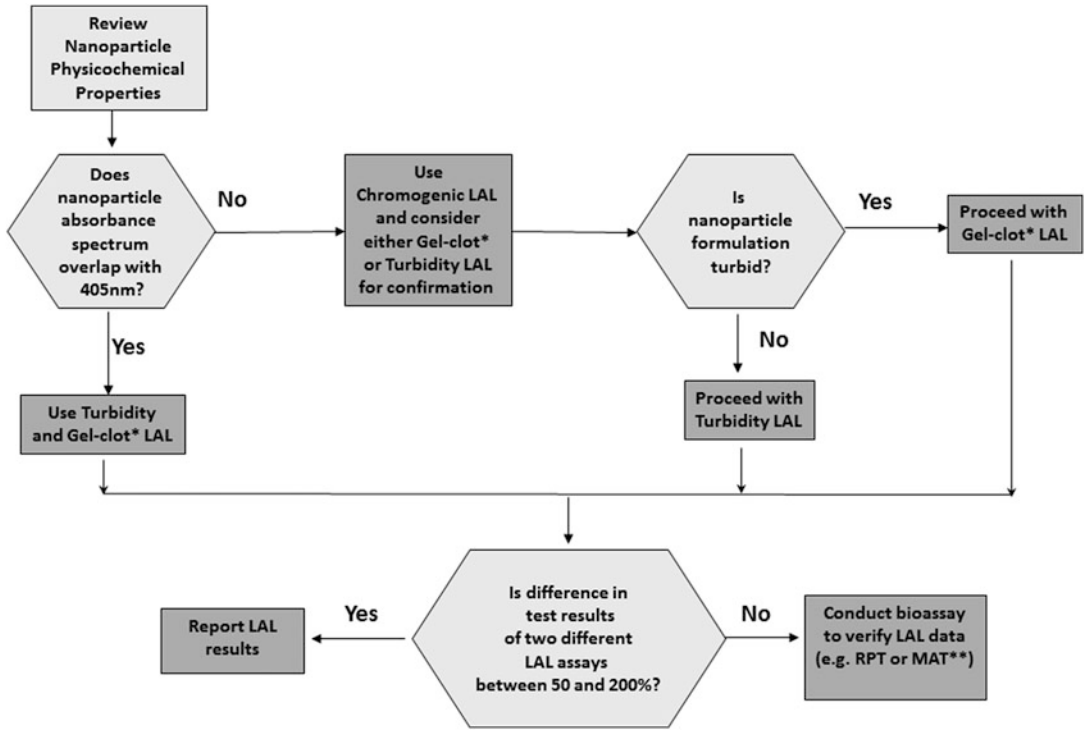

Fig. 1 Decision tree for selecting LAL format. Selection of the LAL format starts at evaluating the nanoparticle physicochemical properties. Two LAL formats are used to analyze the same formulation. If the results are in agreement, the LAL results are reported. If the results disagree, follow-up assessment is conducted using a biological assay. This decision tree was initially described in reference [35] and is presented here with modifications. *MAT* monocyte activation test; *RPT* rabbit pyrogen test; *asterisk* according to the USP and FDA guideline, in case of discrepancy between test results of different LAL methods, the decision is made by the Gel-Clot assay; *double asterisk* MAT application is limited when a test nanoformulation contains cytotoxic drug; other methods and controls can be used; apply scientific justification to result interpretation and preparation of appropriate controls

performed using specific assays, e.g., Fungitell [21, 22]. When present in the LAL reaction, beta-glucans activate Factor G pathway and result in inaccurate detection and quantification of endotoxin. Filtration through cellulose acetate filters commonly used during production of nanotechnology-based formulations is the common reason for nanoparticle contamination with beta-glucans. Cellulose-based filters are a known source of beta-glucans and increase the rate of false-positive LAL results [23]. The interference from beta-glucans can be overcome by performing sample analysis using recombinant Factor C assay [16–18], by reconstituting lysate in the Glucashield buffer or by diluting the test sample with β-G-Blocker reagent (*see* **Note 1**). In the case study presented in Fig. 2, the false-positive interference from beta glucan in several nanoparticle formulations was solved by using Glucashield Buffer for reconstitution of the lysate before proceeding with the LAL reaction.

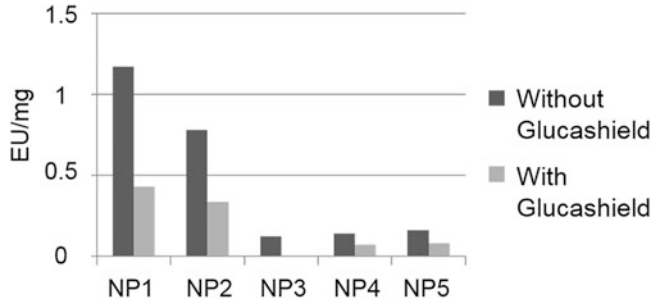

Fig. 2 Overcoming false-positive results caused by beta-glucan contamination. Five nanoparticle formulations (NP1-NP5) were tested by kinetic turbidity LAL procedure as described earlier [24]. The same nanoparticle sample was analyzed with and without GlucaShield buffer. A decrease in the assay result generated using GlucaShield buffer is indicative of beta-glucan contamination commonly arising from cellulose-based filters used during nanoparticle manufacturing. Shown is the mean response of two replicates (%CV < 20)

4 Overcoming False-Negative Results Due to the Presence of Cationic Charge

Endotoxin is the heterogeneous and chemically diverse entity. The central part of the endotoxin is lipopolysaccharide (LPS), which in turn has a complex chemical structure. The biologically active component of LPS is lipid A, composed of a disaccharide backbone, four to six fatty acids, and one or two phosphate groups [1]. Anionic phosphate groups of lipid A can react electrostatically with cationic materials. Such an interaction neutralizes LPS and makes it invisible to the LAL reaction. Therefore, inhibition of endotoxin detection is commonly observed with cationic nanoparticles (e.g., amine-terminated dendrimers and liposomes). This type of interference can be overcome by dilution not exceeding the MVD. However, dilution alone is often ineffective for many cationic nanomaterials. In some cases, adding sodium dodecyl sulfate (SDS) to such test samples may help to overcome the interference (Fig. 3; *see* **Note 2**).

5 Overcoming False-Negative Results Due to Endotoxin Entrapment

Endotoxin is lipophilic and can be entrapped in lipid-based, hollow nanoparticles such as liposomes [1]. The LAL assays detect only endotoxin present in solution and therefore can miss endotoxin entrapped in nanoparticles. The entrapment, therefore, may lead to the underestimation of endotoxin in the liposome formulations. Processing of a nanoparticle test sample before LAL analysis may be needed to release the entrapped endotoxin. Here, we describe a procedure which was developed and verified for liposomes with a composition identical to that of commercial Doxil formulation (Fig. 4). The method includes heat treatment. Place the test sample into a borosilicate tube, cover with parafilm, and incubate on a

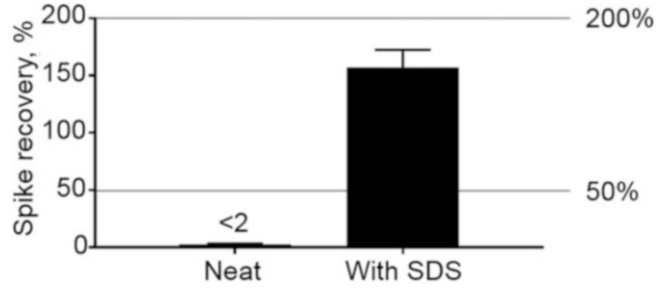

Fig. 3 Overcoming false-negative results due to the cationic charge. Cationic DOTAP liposomes were analyzed by kinetic turbidity LAL procedure as described earlier [24]. The cationic liposome sample (Neat) was analyzed at several dilutions within the assay MVD. The spike recovery of the untreated sample at all dilutions was below 2%. The same sample was also tested at the same dilutions after addition of 0.5% SDS and showed an acceptable spike recovery. Shown is the mean spike recovery ± SD ($N = 2$)

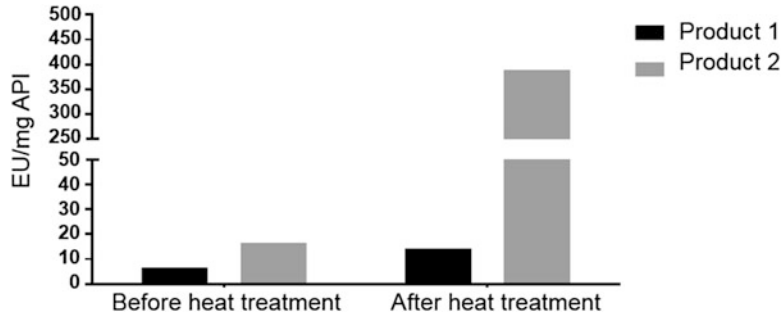

Fig. 4 Example of endotoxin release from liposomes after heat treatment. Two formulations of PEGylated liposomes (product 1 and product 2) were tested by kinetic turbidity LAL procedure as described earlier [24]. The composition of these liposomes was identical to that used in Doxil. The active pharmaceutical ingredients (APIs) were different in product 1 and product 2. The same nanoparticle sample was analyzed without heat treatment (Before heat treatment) and after 30 min of incubation at 96 °C (After heat treatment). Shown is the mean response of two replicates (%CV < 20)

heating block set at 96 °C for 15–30 min (*see* **Note 3**). Allow the sample to cool down to room temperature and centrifuge at 2500 × *g* for 5 min to bring all sample content down to the bottom of the test tube. After that proceed with preparing dilution and testing according to the standard LAL procedure, for example, like the procedure described in reference [24].

6 Some Experimental Approaches to Remove Endotoxin from Reagents, Equipment, Contaminated Nanoparticle Formulations, and Their Components

Endotoxin removal from equipment and reagents used for nanoparticle synthesis depends on the type of materials and their resistance to depyrogenation procedures. The easiest, reliable, and widely accessible depyrogenation method is baking at high

temperature (≥200 °C) for at least 30 min. This procedure can be used to depyrogenate glassware, spatulas, and other heat-resistant tools commonly used during synthesis of nanoparticles. The high temperature is damaging the most nanomaterials. However, some (e.g., carbon nanotubes and certain metallic particles) can tolerate it. The combination of high temperature and an acid or base is used to depyrogenate materials by acid or base hydrolysis, respectively. While different hydrolysis procedures are available, incubation in the presence of 0.05 M HCl for 30 min at 100 °C or in 0.5 M NaOH at 50 °C for 30 min are used most frequently [25]. Gamma-irradiation is another conventional sterilization and depyrogenation process [26]. Some nanoparticles (e.g., citrate-stabilized gold colloids) can tolerate it, while other materials (e.g., silver colloids) do not [27]. Since most cell culture grade disposable plasticware (e.g., serological pipets, tips, flasks, dishes, and tubes) are sterilized by gamma-irradiation, using these materials during nanoparticle synthesis can help reduce endotoxin in the final product. Both heat and gamma-irradiation procedures are not applicable to nanomaterials containing biological components (recombinant proteins and antibodies), nucleic acids, and peptides. Sterile filtration, autoclaving, ethylene oxide, high hydrostatic pressure, and UV light are additional methods commonly used to sterilize surfaces, medical devices, and some nanomaterials. Some of these procedures, such as ethylene oxide sterilization, are also efficient depyrogenation methods. Similar to gamma-irradiation discussed above, most of these approaches are too harsh for most nanomaterials, especially those containing proteins, peptide, and nucleic acids [26]. Endotoxin can be removed from these nanoparticles and their components using other methods including, but not limited to, ion exchange chromatography, Triton X-114 extraction, and affinity columns [28–33].

Different sensitivity of nanoparticle carriers, drugs, and targeting ligands to standard sterilization and depyrogenation procedures makes terminal sterilization approaches unfeasible for most nanoformulations [26]. However, applying suitable methods to clean individual formulation components followed by pyrogen-free assembly into a final product is often considered an efficient way of producing endotoxin-free nanoformulations. Cavicide, a quaternary ammonium containing disinfectant, is useful in both sterilizing surfaces and endotoxin removal. Cavicide can be used to clean laboratory surfaces and parts of the synthesis equipment intolerant to high temperatures. If Cavicide is used to clean plastic surfaces or tubings which come in contact with the nanoformulation during a synthetic procedure, rinsing these surfaces with an excess of pyrogen-free water is recommended to remove traces of Cavicide after depyrogenation.

7 Precautions to Avoid Endotoxin Contamination in Nanoformulations

Although various procedures are available for endotoxin removal [30–33], it is easier to prevent contamination than to clean up a contaminated product. The following steps are found useful for avoiding contamination of nanoparticles with endotoxin during synthetic procedures [15, 34]:

(a) Clean and disinfect working surfaces with Cavicide.

(b) Whenever possible, use disposable pyrogen-free materials. Depyrogenate all non-disposable materials (glassware, spatulas, stir-bars, etc.) necessary for the synthetic procedure.

(c) Depyrogenate or use disposable pyrogen-free parts of the equipment that will come in contact with the nanomaterial (columns, tubing, etc.).

(d) Select starting reagents and verify that all chemicals, components, and precursors used during synthesis are pyrogen-free (*see* **Note 4**).

(e) If possible, perform the synthetic procedure in a biological safety cabinet or a clean room facility.

(f) Wear gloves and clean them by spraying and rubbing in Cavicide before touching tubes, reagents and other materials and parts of equipment used during the synthesis. Change gloves frequently.

(g) Do not cough, sneeze, or breath directly to reaction tubes. Avoid touching non-sterile surfaces. Change tips and replace pipettes if they accidentally touched the side of the tube, reagent storage bottle, or another non-sterile surface.

8 Notes

1. Recombinant Factor C assay kit and β-G-blocker reagents are commercially available products produced by Lonza (catalog numbers 50-658U and N190, respectively). GlucaShield Buffer is a commercially available reagent provided by Associates of Cape Code (catalog number GB051-5). A test nanomaterial with excitation/emission wavelengths at or around 380/440 nm or light absorbance at or around 440 nm may interfere with Recombinant Factor C assay. This interference can be overcome by increasing sample dilution. The dilution of the test sample, however, should not exceed the MVD which is calculated according to the following formula:

$$(\mathrm{EL} \times \text{sample concentration})/\lambda$$

When performing Recombinant Factor C assay, one needs to consider using inhibition enhancement controls similar to those employed in the traditional LAL assay. β-G-blocker is combined with the test sample at a 1:1 volume ratio. It demonstrates good performance in the LAL kits from the same manufacturer. GlucaShield buffer is used to reconstitute the LAL lysate. Similar to β-G-blocker, this reagent exhibits excellent performance with kits and other LAL reagents produced by the same manufacturer that produces the buffer.

2. Prepare 1% SDS in LAL grade water. Prepare dilutions of the test nanomaterials according to the MVD. Combine equal volumes of the test sample and 1% SDS, and proceed with the analysis according to the standard LAL protocol. It is important to account for the 2-fold dilution during experiment planning and the result analysis. For example, if the MVD is 500 and the neat test sample is analyzed at dilutions 5, 50, and 500, you will need to dilute the test sample 2.5, 25, and 250-fold. When equal volumes of the nanoparticle at these dilutions are combined with 1% SDS solution, the final test sample dilutions are 5, 50, and 500, and the concentration of the SDS is 0.5%.
3. Performance verification of this procedure was conducted using control standard endotoxin (CSE), which is known to be less stable than naturally occurring endotoxin. Heat treatment for a period exceeding 30 min results in a decrease in the CSE spike recovery below 50%.
4. Most commercially available water for cell culture is pyrogen-free (e.g., Hyclone, catalog number SH30529.02) and is suitable for nanoparticle synthesis. Specialized LAL grade water such as that available from Lonza (catalog number W50–1000) and Associates of Cape Code (catalog number W100P) can also be used. In general, 18 MΩ per se is not indicative of pyrogen-free water. Bacteria can colonize in water pipes and filters commonly used in laboratory water purification systems. Autoclaving is appropriate for sterilization but does not eliminate endotoxin. Therefore, in-house produced, autoclaved 18 MΩ water can be used instead of commercial pyrogen-free water only after analysis by LAL assay demonstrating endotoxin levels below the assay sensitivity (ideally <0.001 EU/mL).

Acknowledgment

This project has been funded in whole or in part with Federal funds from the National Cancer Institute, National Institutes of Health, under Contract No. HHSN261200800001E. The content of this publication does not necessarily reflect the views or policies of the Department of Health and Human Services, nor does mention of trade names, commercial products, or organizations imply endorsement by the U.S. Government.

References

1. Brade H, Opal SM, Vogel SN, Morrison DC (eds) (1999) Endotoxin in health and disease. Marcel Dekker Inc., New York
2. Dobrovolskaia MA, Vogel SN (2002) Toll receptors, CD14, and macrophage activation and deactivation by LPS. Microbes Infect 4 (9):903–914. doi:10.1016/S1286-4579(02)01613-1
3. USP 30 NF 25 (2007) <85> Bacterial endotoxins test. vol 1
4. HHS, US FDA (2012) Guidance for industry. Pyrogen and endotoxins testing: questions and answers. https://www.fda.gov/downloads/drugs/guidances/ucm310098.pdf
5. HHS, US FDA (2015) .Guidance for Industry and Food and Drug Administration Staff. Endotoxin testing recommendations for single-use intraocular ophthalmic devices. https://www.fda.gov/downloads/medicaldevices/deviceregulationandguidance/guidancedocuments/ucm393376.pdf
6. Jones CF, Grainger DW (2009) In vitro assessments of nanomaterial toxicity. Adv Drug Deliv Rev 61(6):438–456. doi:10.1016/j.addr.2009.03.005
7. Sharma SK (1986) Endotoxin detection and elimination in biotechnology. Biotechnol Appl Biochem 8(1):5–22
8. Crist RM, Grossman JH, Patri AK, Stern ST, Dobrovolskaia MA, Adiseshaiah PP, Clogston JD, McNeil SE (2013) Common pitfalls in nanotechnology: lessons learned from NCI's Nanotechnology Characterization Laboratory. Integr Biol (Camb) 5(1):66–73. doi:10.1039/c2ib20117h
9. Dobrovolskaia MA, Patri AK, Potter TM, Rodriguez JC, Hall JB, McNeil SE (2012) Dendrimer-induced leukocyte procoagulant activity depends on particle size and surface charge. Nanomedicine (Lond) 7(2):245–256. doi:10.2217/nnm.11.105
10. Inoue K (2011) Promoting effects of nanoparticles/materials on sensitive lung inflammatory diseases. Environ Health Prev Med 16 (3):139–143. doi:10.1007/s12199-010-0177-7
11. Inoue K, Takano H (2011) Aggravating impact of nanoparticles on immune-mediated pulmonary inflammation. Scientific World J 11:382–390. doi:10.1100/tsw.2011.44
12. Inoue K, Takano H, Yanagisawa R, Hirano S, Kobayashi T, Fujitani Y, Shimada A, Yoshikawa T (2007) Effects of inhaled nanoparticles on acute lung injury induced by lipopolysaccharide in mice. Toxicology 238(2–3):99–110. doi:10.1016/j.tox.2007.05.022
13. Inoue K, Takano H, Yanagisawa R, Hirano S, Sakurai M, Shimada A, Yoshikawa T (2006) Effects of airway exposure to nanoparticles on lung inflammation induced by bacterial endotoxin in mice. Environ Health Perspect 114 (9):1325–1330. doi:10.1289/ehp.8903
14. Shi Y, Yadav S, Wang F, Wang H (2010) Endotoxin promotes adverse effects of amorphous silica nanoparticles on lung epithelial cells in vitro. J Toxicol Environ Health A 73 (11):748–756. doi:10.1080/15287391003614042
15. Dobrovolskaia MA, McNeil SE (2016) Nanoparticles and endotoxin. In: Dobrovolskaia MA, McNeil SE (eds) Handbook of immunological properties of engineered nanomaterials, vol 1. World Scientific Publishing, Singapore, pp 143–187
16. Alwis KU, Milton DK (2006) Recombinant factor C assay for measuring endotoxin in house dust: comparison with LAL, and (1 –> 3)-beta-D-glucans. Am J Ind Med 49 (4):296–300. doi:10.1002/ajim.20264
17. Ding JL, Ho B (2010) Endotoxin detection–from limulus amebocyte lysate to recombinant factor C. Subcell Biochem 53:187–208. doi:10.1007/978-90-481-9078-2_9

18. McKenzie JH, Alwis KU, Sordillo JE, Kalluri KS, Milton DK (2011) Evaluation of lot-to-lot repeatability and effect of assay media choice in the recombinant Factor C assay. J Environ Monit 13(6):1739–1745. doi:10.1039/c1em10035a
19. Fujita Y, Nabetani T (2014) Iron sulfate inhibits Limulus activity by induction of structural and qualitative changes in lipid A. J Appl Microbiol 116(1):89–99. doi:10.1111/jam.12349
20. Reich J, Lang P, Grallert H, Motschmann H (2016) Masking of endotoxin in surfactant samples: effects on Limulus-based detection systems. Biologicals 44(5):417–422. doi:10.1016/j.biologicals.2016.04.012
21. Lyons JL, Roos KL, Marr KA, Neumann H, Trivedi JB, Kimbrough DJ, Steiner L, Thakur KT, Harrison DM, Zhang SX (2013) Cerebrospinal fluid (1,3)-beta-D-glucan detection as an aid for diagnosis of iatrogenic fungal meningitis. J Clin Microbiol 51(4):1285–1287. doi:10.1128/jcm.00061-13
22. Tran T, Beal SG (2016) Application of the 1,3-beta-D-Glucan (Fungitell) assay in the diagnosis of invasive fungal infections. Arch Pathol Lab Med 140(2):181–185. doi:10.5858/arpa.2014-0230-RS
23. Henne W, Schulze H, Pelger M, Tretzel J, von Sengbusch G (1984) Hollow-fiber dialyzers and their pyrogenicity testing by Limulus amebocyte lysate. Artif Organs 8(3):299–305
24. Neun BW, Dobrovolskaia MA (2011) Detection and quantitative evaluation of endotoxin contamination in nanoparticle formulations by LAL-based assays. Methods Mol Biol 697:121–130. doi:10.1007/978-1-60327-198-1_12
25. Sandle T (2011) A practical approach to depyrogenation studies using bacterial endotoxin. J GxP Compliance 15(4):90–96
26. Subbarao N (2016) Nanoparticle sterility and sterilization of nanomaterials. In: Dobrovolskaia MA, McNeil SE (eds) Handbook of immunological properties of engineered nanomaterials, vol 1 and 6. World Scientific Publishing Ltd, Singapore, pp 53–75
27. Zheng J, Clogston JD, Patri AK, Dobrovolskaia MA, McNeil SE (2011) Sterilization of silver nanoparticles using standard gamma irradiation procedure affects particle integrity and biocompatibility. J Nanomed Nanotechnol 2011(Suppl 5):001. doi:10.4172/2157-7439.s5-001
28. Ragab AA, Van De Motter R, Lavish SA, Goldberg VM, Ninomiya JT, Carlin CR, Greenfield EM (1999) Measurement and removal of adherent endotoxin from titanium particles and implant surfaces. J Orthop Res 17(6):803–809. doi:10.1002/jor.1100170603
29. Dobrovolskaia MA, Neun BW, Clogston JD, Ding H, Ljubimova J, McNeil SE (2010) Ambiguities in applying traditional Limulus amebocyte lysate tests to quantify endotoxin in nanoparticle formulations. Nanomedicine (Lond) 5(4):555–562. doi:10.2217/nnm.10.29
30. London AS, Mackay K, Lihon M, He Y, Alabi BR (2014) Gel filtration chromatography as a method for removing bacterial endotoxin from antibody preparations. Biotechnol Prog 30(6):1497–1501. doi:10.1002/btpr.1961
31. Ma R, Zhao J, Du HC, Tian S, Li LW (2012) Removing endotoxin from plasmid samples by Triton X-114 isothermal extraction. Anal Biochem 424(2):124–126. doi:10.1016/j.ab.2012.02.015
32. Mack L, Brill B, Delis N, Groner B (2014) Endotoxin depletion of recombinant protein preparations through their preferential binding to histidine tags. Anal Biochem 466:83–88. doi:10.1016/j.ab.2014.08.020
33. Magalhaes PO, Lopes AM, Mazzola PG, Rangel-Yagui C, Penna TC, Pessoa A Jr (2007) Methods of endotoxin removal from biological preparations: a review. J Pharm Pharm Sci 10(3):388–404
34. Afonin KA, Grabow WW, Walker FM, Bindewald E, Dobrovolskaia MA, Shapiro BA, Jaeger L (2011) Design and self-assembly of siRNA-functionalized RNA nanoparticles for use in automated nanomedicine. Nat Protoc 6(12):2022–2034. doi:10.1038/nprot.2011.418
35. Dobrovolskaia MA, Germolec DR, Weaver JL (2009) Evaluation of nanoparticle immunotoxicity. Nat Nanotechnol 4(7):411–414. doi:10.1038/nnano.2009.175

Part III

Physicochemical Characterization

Chapter 4

Elemental Analysis in Biological Matrices Using ICP-MS

Matthew N. Hansen and Jeffrey D. Clogston

Abstract

The increasing exploration of metallic nanoparticles for use as cancer therapeutic agents necessitates a sensitive technique to track the clearance and distribution of the material once introduced into a living system. Inductively coupled plasma mass spectrometry (ICP-MS) provides a sensitive and selective tool for tracking the distribution of metal components from these nanotherapeutics. This chapter presents a standardized method for processing biological matrices, ensuring complete homogenization of tissues, and outlines the preparation of appropriate standards and controls. The method described herein utilized gold nanoparticle-treated samples; however, the method can easily be applied to the analysis of other metals.

Key words ICP-MS, Biological matrices, Nanoparticles, Blood, Biodistribution, Homogenization

1 Introduction

Inductively coupled plasma mass spectrometry (ICP-MS) is an elemental analysis technique based upon the theories of mass spectrometry [1]. Inductively coupled plasma is used as the ionization technique and it atomizes anything that passes through the plasma. Once atomized, the atoms in the solution are separated based on their m/z ratio. For ICP-MS, masses are scanned from 1 to 283 amu, and most elements can be analyzed [1]. To ensure efficient atomization, samples are often homogenized prior to introduction into the plasma. This is increasingly important for biological samples that contain solid matter (tissues) or other components (lipids, proteins, cells). Those components could stick to surfaces in the sample introduction system of the ICP-MS and adversely affect the accuracy of the results [2, 3]. To prevent this, biological samples are often digested in concentrated acids and heated to high temperatures in order to provide a timely and efficient break down of the biological material [2–5].

Herein we describe a basic method for processing biological samples and analyzing them for the presence of metals, more

Scott E. McNeil (ed.), *Characterization of Nanoparticles Intended for Drug Delivery*, Methods in Molecular Biology, Vol. 1682, DOI 10.1007/978-1-4939-7352-1_4,

specifically for the presence of gold nanoparticles in tissue samples. The first step in this process will be to ensure the complete dissolution of the biological material and the nanoparticles. Once a homogeneous liquid sample has been created, approximate concentrations of the elements of interest will be determined by a semi-quantitative analysis of the samples. The samples will then be diluted as needed and appropriate calibration standards will be prepared. Furthermore, the preparation of appropriate controls, standards, as well as additional methods for eliminating matrix effects when there are insufficient blank samples will be discussed.

2 Materials

1. Inductively coupled plasma mass spectrometer with autosampler.
2. 30 mL and 60 mL low-density polyethylene (LDPE) sample bottles.
3. 18 mL LDPE sample vials.
4. 250 mL high-density polyethylene (HDPE) sample bottle.
5. Ultra-pure (18 MΩ-cm resistance) water.
6. Trace element grade acids (HCl and HNO_3).
7. NIST standard reference materials (SRM) 2131 (Au), NIST SRM 3124a (In), NIST SRM 3129a (Li), NIST SRM 3131a (Mg), NIST 3134 (Mo), NIST SRM 3167a (Y), NIST SRM 3113 (Co), NIST SRM 3108 (Cd), NIST SRM 3110 (Ce), and NIST SRM 3158 (Tl).
8. MARS Xpress microwave digestion system (CEM Corp.).
9. Vessel capping station for MARS Xpress (CEM Corp.).
10. 10 mL perfluoroalkoxy alkane (PFA) microwave vessels (CEM corp.).
11. *1.5% HNO_3: 4% HCl Acid Solution:* In a 2 L LDPE container, add 1.74 L of ultra-pure water, 43 mL of concentrated HNO_3, 217 mL of concentrated HCl, and mix well.

3 Methods

3.1 Sample Homogenization

1. Allow tissue samples to equilibrate to room temperature.
2. Pre-weigh and record the weights of the microwave vessels (*see* **Note 1**).
3. Add the tissue samples to the microwave vessels.
4. Weigh and record the weight of the vessels containing the tissue.

Table 1
Microwave digestion program for tissues in small (10 mL) vessels

Step	Power (W)	Power setting (%)	Ramp time (min)	*T* (°C)	Hold time (min)
1	800	100	25:00	120	20:00
2	400	0	0	0	30:00
3	800	100	15:00	195	20:00
4	400	0	0	0	25:00

5. Add 1 mL of concentrated HNO_3 and 3 mL of concentrated HCl to the sample vials (*see* **Notes 2** and **3**).
6. Allow to sit uncapped for at least 15 min in a chemical fume hood. During this time gas will evolve from the sample, and it is important to allow the gas to completely dissipate prior to weighing.
7. After gas has dissipated, weight the vessel again and record the weight (*see* **Note 4**).
8. Cap the microwave vessel using the capping station.
9. Place the microwave vessels in the sample carousel and record the position of each microwave vessel.
10. Microwave the samples according to the parameters in Table 1.

3.2 Sample Dilution (First Dilution)

1. Allow the sample to cool.
2. Label and weigh 60 mL LDPE sample vials.
3. Transfer the complete contents of the microwave vessel to the appropriately labeled LDPE bottle.
4. Weigh and record the weight of the bottle plus the digested sample.
5. Dilute the samples to a total volume of 50 mL by adding 46 mL of ultra-pure water.
6. Record the final weight of the vial plus the solution.

3.3 Semi-Quantitative Standards

3.3.1 10 µg/g Semi-Quantitative Standard

1. Weigh an empty 250 mL HDPE sample bottle.
2. Add 250 µL each of NIST SRMs for Ce, Co, Y, Tl, Li, Mg, Mo, and Cd, recording the weight of the sample bottle after each SRM is added.
3. Dilute the standards to a total volume of 250 mL by adding 248 mL of the 1.5% HNO_3: 4% HCl solution.
4. Record the weight of the final solution.

3.3.2 50 ng/g Semi-Quantitative Standard

1. Record the weight of an 18 mL LDPE sample vial.
2. Add 50 µL of the 10 µg/g semi-quant standard solution to the sample vial.
3. Weigh and record the weight of the sample bottle plus the standard solution.
4. Dilute the standard to a total volume of 10 mL by adding 9.95 mL of the 1.5% HNO_3: 4% HCl solution.
5. Weigh and record the weight of the final solution and sample vial.

3.4 Semi-Quantitative Analysis

1. Perform the semi-quantitative analysis according to the procedures specified by your ICP-MS manufacturer. For the Agilent ICP-MS, transfer approximately 10 mL of sample to the 18 mL sample vials. Arrange the samples on the carousel such that the first sample is the semi-quantitative standard solution prepared in section 3.3.2.
2. Prepare a sequence with a minimum of 1 blank run between each sample acquisition. Blank runs consist of the 1.5% HNO_3: 4% HCl solution.
3. Once the acquisition is finished, use the recorded weights from sections 3.3.1 and 3.3.2 to determine the exact concentration of each standard contained in the semi-quantitative standard solution. Use these values to calibrate the semi-quantitative analysis and determine the approximate concentration of the analyte in each sample. This value should be within 30% of the actual value of the analyte in solution, and will provide a good estimate of the order samples should be run in, arranged from lowest concentration to greatest, and whether any additional dilutions should be performed.

3.5 Perform Necessary Dilutions

1. Because the target concentration range for the quantitative analysis will be from 0 to 50 ng/g, it may be necessary to dilute the samples further for them to fall within this concentration range. If additional serial dilutions are needed, follow the steps outlined in Subheading 3.2, adjusting the amount of sample being diluted accordingly to obtain the desired approximate concentration.
2. Perform all additional dilutions using the 1.5% HNO_3: 4% HCl solution. Samples may be made up to a total of 30 mL using the 30 mL LDPE sample bottles to save resources. In either instance, make sure to record all weights and retain any unused samples from prior dilutions, should samples need to be remade.

3.6 Calibration Standards

3.6.1 50 µg/g Au Standard Solution

1. Label a 30 mL LDPE sample bottle "50 µg/g Au SRM 3121." Weigh and record its weight (*see* **Note 5**).
2. Add 150 µL of the Stock NIST SRM 3121 Au standard solution to the bottle. Weigh and record the weight of the standard plus the bottle.
3. Dilute to a total volume of 30 mL by adding 29.850 mL of the 1.5% HNO_3:4% HCl solution. Weigh and record the weight of the total solution plus the bottle.

3.6.2 1 µg/g Au Standard Solution

1. Label a 60 mL LDPE sample bottle "1 µg/g Au SRM 3121." Weigh and record its weight.
2. Add 1 mL of the 50 µg/g Au standard solution from section 3.6.1 to the bottle. Weigh and record the weight of the standard plus the bottle.
3. Dilute to a total volume of 50 mL by adding 49 mL of the 1.5% HNO_3:4% HCl solution. Weigh and record the weight of the total solution plus the bottle.

3.6.3 Calibration Standards

1. Label and weigh empty 60 mL LDPE sample bottles 0–50 ng/g in 10 ng/g increments (total of 6 bottles) (*see* **Note 6**).
2. From the 1 µg/g solution prepared in section 3.6.2, transfer 0, 0.5, 1, 1.5, 2, and 2.5 mL into the bottles labeled 0, 10, 20, 30, 40, and 50 ng/g Au, respectively. Weigh and record the weight of the samples plus the bottles.
3. If there is sufficient control (blank; untreated) tissue sample digest left after Subheading 3.2, then matrix match the calibration standards. To do this, add the appropriate amount of the blank tissue digest, which when diluted to 50 mL will match the dilution at which the samples will be analyzed (*see* **Note 7**).
4. Dilute the samples to a total volume of 50 mL using the 1.5% HNO_3:4% HCl solution. Weigh and record the weight of the bottle plus the solution.

3.6.4 50 µg/g In Standard

1. The internal standard can be T'ed in with the sample through the use of a separate solution and input line, or can be added individually to each sample. Preferably, the former method is used for internal standards. When choosing an internal standard, it is important to choose an element based on two criteria. First, the element should not interfere with the analyte, i.e., it cannot have isotopes or form polyatomic complexes in the plasma with the same mass as the analyte. Secondly, it should be relatively close in mass to the analyte. In this instance, In was chosen as the internal standard to be used with Au as it fulfills the two prior requirements. Additional elemental standards may also be used.

2. Begin preparation by labeling a 30 mL LDPE sample vial "50 μg/g In." Weigh and record its weight.
3. Add 150 μL of the Stock NIST SRM 3124a In standard to the bottle and weigh and record the weight of the bottle with the standard.
4. Dilute the sample to a total of 30 mL using the 1.5% HNO_3:4% HCl solution. Weigh and record the weight of the bottle with the solution.

3.6.5 Internal Standard Solution

1. Begin preparation by weighing and recording the weight of a 60 mL LDPE sample vial.
2. Add 50 μL of the 50 μg/g NIST SRM 3124a In standard to the bottle and weigh and record the weight of the bottle with the standard.
3. Dilute the sample to a total of 30 mL using the 1.5% HNO_3:4% HCl solution. Weigh and record the weight of the bottle with the solution.

3.7 Quantitative Analysis of the Digested Tissue Samples

1. Turn on and run the normal startup and tuning as recommended by the manufacturer of your ICP-MS instrument. For the Agilent 7500cx used in this experiment, this entails tuning the instrument with a standard solution containing 1 ng/g of Ce, Li, Y, Co, Mg, and Tl. Tuning is done to maximize the signal response for the full range of elements, followed by tuning the Pulse to Analogue factor to ensure linear response as the instrument switches from one detector to the next.
2. Create a sequence file containing the order for the samples to be run. In a typical experiment, generally run two calibration curves, one immediately preceding the samples, and one immediately succeeding them. This is done to average out sensitivity decreases of the instrument over the run time, and is increasingly important as the length of the run increases. Immediately following the first calibration set, five blanks consisting of the 1.5% HNO_3:4% HCl solution should be run. Next the samples should be arranged in the sequence from lowest concentration to highest concentration. This information can be estimated from the semi-quantitative analysis performed in section 3.5. Running the samples from lowest to highest will help insure minimal crossover from sample to sample. Each sample will be run in triplicate, sampling three times from the sample vial. Between each different sample, a minimum of two blanks should be run. After the final sample is run, five more blanks should be run prior to the second calibration curve.
3. Transfer approximately 10 mL of sample into a labeled 18 mL LDPE sample vial. Load the samples into the auto-sampler in the same order that is specified by the sequence. Each sample

Table 2
Acquisition parameters for Au in tissue

Mass	Element		per Point	per Mass
197	Au		0.6	1.8
115	In		0.6	1.8
Before acquisition				
Uptake speed:		0.50 rps		
Uptake time:		40 s		
Stabilization time:		30 s		
After acquisition (rinse port)				
Rinse speed:		0.00 rps		
Rinse time (sample):		0.00 s		
Rinse time (STD):		0.00 s		
After acquisition (rinse vial)				
		Step 1	Step 2	Step 3
Rinse vial:		1	1	1
Rinse speed:		0	0.5	0.1
Rinse time:		0	60	10
Rinse port rinse time:		0	0	0

and calibration standard needs to be loaded only once, since each will contain enough of the sample to complete the necessary runs.

4. "T" in the internal standard solution using a t-mixer. This will create a consistent flow of internal standard for each sample.
5. Set up the acquisition parameters for the sample. A sample of the acquisition parameters used to analyze gold in tissue is presented in Table 2. A total of ten replicates are run per sample analysis. Also, ensure that the analyte stream has stabilized in the instrument prior to starting analysis. To achieve this, the uptake time should be set to 40 s to ensure the analyte stream is in the nebulizer and analysis is delayed by 30 s to ensure that the sample has hit a steady state of introduction. Following each sampling, the sample introduction is rinsed for 60 s to help reduce carry over from sample to sample.
6. Once **steps 1–5** have been completed, execute the programmed sequence.

3.8 Data Analysis

1. The following data analysis procedure will cover exporting the data and using an external spreadsheet program to perform the analysis. This is our preferred method; however, most ICP-MS instruments come with analysis software which may be used with the data analysis. The first step in the data analysis is to normalize the data with respect to the internal standard. This is done by dividing the analyte signal by the internal standard signal. This will reduce any discrepancies in the data caused by variations in flow rate of the sample into the instrument as well as eliminate the effects of instrumental drift, since the ratio of analyte to internal standard should remain consistent throughout analysis.
2. Construct a calibration curve plotting concentration of the Au standards versus the normalized signal for the respective standards. The exact concentrations for the calibration standards can be determined using the concentration and weight data recorded in section 3.7, **steps 1–3**. Once the concentrations of Au in each standard have been determined, average the normalized signals from each standard of the two calibration curves and use the average value for the signal associated with each standard. The calibration curve should look similar to the plot in Fig. 1. Determine the slope of the calibration curve. There is no need to subtract the blank or force the origin though zero, as the y-intercept will correspond with the background or zero signal and will be accounted for in the slope equation for the line.
3. Determine the concentration of Au in the tissue samples using the linear equation for the calibration curve. This concentration will be the concentration of gold at the dilution it was tested. In order to determine the initial concentration of gold

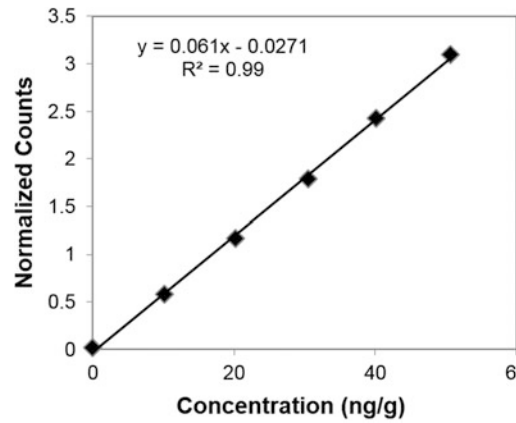

Fig. 1 Typical gold calibration curve. The normalized counts are plotted as a function of standard concentration

in the tissue sample, use the weight data recorded in sections 3.2 and 3.6. Average each set of triplicates to obtain the concentration of gold in each tissue sample (*see* **Note 8**).

4 Notes

1. All solutions should be made up in plastic containers, and contact with glassware should be avoided. This is due in part to glass having metallic impurities which can leach out when exposed to concentrated acids, or dilute acids for prolonged periods of time.
2. Take proper precautions when working with tissue samples and concentrated acids. It is important to wear proper eye wear, clothing, and laboratory gloves, especially when concentrated acid and biological samples are being used. All samples should be processed in a fume hood. Tissue exposed to Aqua Regia will produce a gas that should be properly vented. When mixing acids and water, it is important to add the acid slowly into the water as heat will generate when the two are mixed.
3. It is important to use the appropriate acid matrix for the elemental being analyzed. In this example, the analyte Au needs Aqua Regia in order to fully dissolve, hence the use of HCl and HNO_3. However, if the analyte was silver or any other element that forms an insoluble salt when reacted with a halide, HCl would not be an appropriate acid to use. The resulting salts could fall out of solution creating a non-homogeneous sample and affect the results.
4. Use of weights over volume is preferred for all liquid additions for two reasons. First, volume is dependent on temperature, and unless the temperature is measured for each sample when weighed, the volume can unknowingly fluctuate and introduce error into the measurements. Secondly, when pipetting tens to hundreds of samples, it can be difficult to consciously maintain proper pipeting technique. By weighing each sample after it has been pipetted, the accurate amount of sample added to the vials is known. This will also help to reduce errors in measurement by introducing a secondary check.

   Volumes should compare relatively close to weights provided the density is close to that of water. For samples containing high amounts of acid, the weight will vary, because concentrated acids generally have a higher density than water. Additionally, keeping all sample weights above 50 mg will also help with reducing error. Samples below this amount become increasingly harder to accurately determine.

5. To further validate results, controls can be used. When there is a nanoparticle reference material available (NIST RM 8011-8013 Au NPs or NIST RM 8017 Ag NPs), this should be used as the control in lieu of the dissolved standard. To create the control samples, follow the steps outlined in section 3.1. Digest the nanoparticles in the equivalent amount of acid; however, do not add any tissue to the sample. The sample will be matrix matched similar to the calibration standards, where the digest of the tissue control/blank sample will be added at later dilutions after microwave digestion. When nanoparticle samples are not available, use NIST SRM dissolved standards following the same procedure.
6. In this example, the calibration standards were constructed from a range of 0–50 ng/g. However, it may be necessary to create calibration standards that are well below or above this range. The semi-quantitative analysis will give an idea of whether any changes need to be made to the calibration standards.
7. In the instances where there are no or insufficient control blank tissue samples to complete a matrix-matched calibration curve, a spike recovery examination or standard addition calibration curve can be constructed using the samples with unknown analyte concentration.

   To conduct a spike recovery experiment, in a pre-weighed sample vial weigh a known amount of the 1 μg/g NIST SRM 3121 (in a concentration between 0.5 and 1.5 × the estimated concentration of the unknown). Dilute the sample to a total volume of 10 mL and record the final weight. Run in parallel with the non-spiked sample and determine the concentrations as in section 3.7, **step 3**. Determine the concentration of the NIST SRM 3121 added to the unknown sample. Subtract the concentration of the non-spiked sample from the total concentration of the spiked sample. Divide the remainder by the calculated concentration of the spike added, and convert to a percentage by multiplying by 100. Repeat this for as many samples as deemed necessary.

   Constructing a standard addition calibration curve will be similar to the spike recovery procedure, except multiple spiked samples with different concentrations of NIST SRM added will be required, and no external calibration will be run to calculate the concentration of analyte in the non-spiked sample. Create a standard addition by creating a minimum of four solutions from the sample tissue precursor sample (this will be referred to as Sample A): (1) Sample A without any additional SRM 3121 added, (2) Sample A with SRM 3121 added at a concentration of 10 ng/g Au, (3) Sample A with SRM 3121 added at a concentration of 20 ng/g Au, and (4) Sample A with SRM 3121 added at a concentration of 30 ng/g Au. Run the

standard addition samples along with the other unknown samples. Plot the normalized counts of the four internal standard solutions versus the amount of SRM 3121 added. To determine the concentration of the standard without any added SRM, extrapolate the linear regression line back to the y-intercept. The concentration of Au in the sample will be the absolute value of the y-intercept. To determine the concentration for all other unknown samples, add the concentration of the non-spiked sample to the concentration of all the standard additions calibration standards, re-plot the calibration curve and determine the linear regression. Use this new linear regression equation to determine the amount of Au in the remainder of the unknown samples.

8. At substantially lower concentrations, mid to low pg/g levels, a determination of the limit of quantitation and limit of detection should be carried out to ensure the validity of the results. Both measurements should be made by placing a matrix-matched blank sample (similar in composition to the 0 ng/g standard) prior to both the first and last calibration curve. The sample should be run in triplicate both times. The average background counts and the standard deviation (σ) of the background counts should then be determined. The limit of detection is defined as 3σ and the limit of quantitation is defined as 10σ.

Acknowledgment

This project has been funded in whole or in part with Federal funds from the National Cancer Institute, National Institutes of Health, under Contract No. HHSN261200800001E. The content of this publication does not necessarily reflect the views or policies of the Department of Health and Human Services, nor does mention of trade names, commercial products, or organizations imply endorsement by the U.S. Government.

References

1. Bings NH, Bogaerts A, Broekaert JA (2006) Atomic spectroscopy. Anal Chem 78 (12):3917–3946
2. Rodushkin I, Odman F, Branth S (1999) Multielement analysis of whole blood by high resolution inductively coupled plasma mass spectrometry. Fresen J Anal Chem 364(4):338–346
3. Sonavane G, Tomoda K, Makino K (2008) Biodistribution of colloidal gold nanoparticles after intravenous administration: effect of particle size. Colloid Surf B Biointerfaces 66(2):274–280
4. Yu LL, Wood LJ, Long SE (2010) Determination of gold in rat blood with inductively coupled plasma mass spectrometry. Available via Nanotechnolgy Characterization Laboratory website: https://ncl.cancer.gov/sites/default/files/protocols/NCL_Method_PCC-9.pdf. Accessed October 2015
5. Yu LL, Wood LJ, Long SE (2010) Determination of gold in rat tissue with inductively coupled plasma mass spectrometry. Available via Nanotechnolgy Characterization Laboratory website: https://ncl.cancer.gov/sites/default/files/protocols/NCL_Method_PCC-8.pdf. Accessed October 2015

Chapter 5

PEG Quantitation Using Reversed-Phase High-Performance Liquid Chromatography and Charged Aerosol Detection

Mackensie C. Smith and Jeffrey D. Clogston

Abstract

This chapter describes a method for the quantitation of polyethylene glycol (PEG) in PEGylated colloidal gold nanoparticles using a reversed-phase high-performance liquid chromatography (RP-HPLC) with charged aerosol detection. The method can be used to calculate the total PEG on the nanoparticle, as well as the bound and free unbound PEG fractions after a simple centrifugation step. This is a significant distinction as the bound PEG fraction affects biocompatibility, circulation time, and overall nanoparticle efficacy. PEG quantitation can be achieved through two methods, one involving the dissolution of colloidal gold nanoparticles by potassium cyanide (KCN) and the other by displacement of PEG by dithiothreitol (DTT). The methods outlined herein were applied to 30 nm colloidal gold grafted with 20 kDa PEG, but they can be easily adapted to any size colloidal gold nanoparticle and PEG chain length.

Key words Polyethylene glycol (PEG), Surface characterization, Charged aerosol detector, Gold nanoparticles, Stability, Displacement, Dissolution

1 Introduction

Understanding the nanoparticle surface is one of the challenges in nanoparticle characterization, yet it is an important feature to measure because it defines the nanoparticles' biocompatibility [1–4]. For example, colloidal gold nanoparticles are often surface functionalized with the biocompatible, hydrophilic polymer poly (ethylene) (PEG, i.e., PEGylation) to reduce opsonization, increase circulation half-life, and provide stability by preventing aggregation as a result of its neutral charge [5–9]. Physicochemical characterization techniques such as UV–Vis spectroscopy for gold nanoparticles concentration, dynamic light scattering for hydrodynamic size, and zeta potential analysis indicative of surface charge are commonly employed to characterize PEGylated colloidal gold nanoparticles. These techniques can qualitatively assess the presence of PEG but are not sensitive enough to distinguish differences in PEG quantity, density, or presentation.

Scott E. McNeil (ed.), *Characterization of Nanoparticles Intended for Drug Delivery*, Methods in Molecular Biology, Vol. 1682, DOI 10.1007/978-1-4939-7352-1_5,

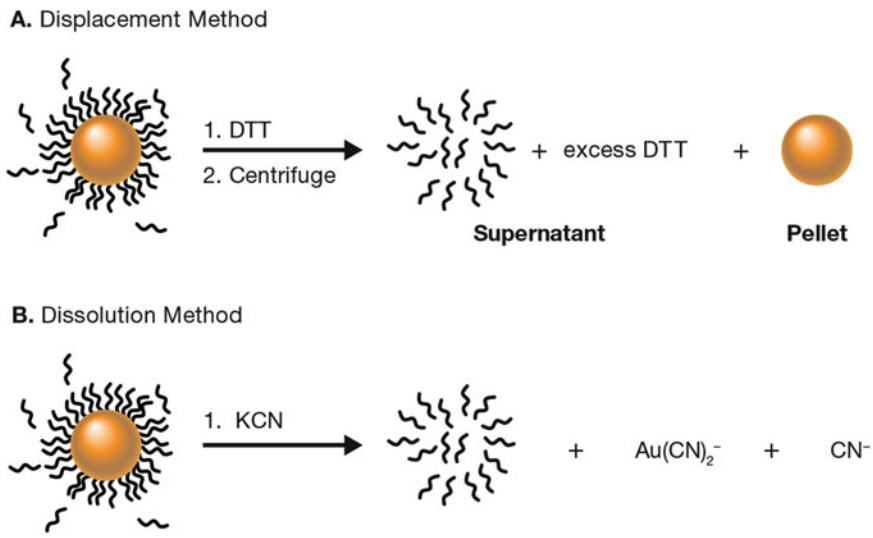

Fig. 1 Displacement and dissolution techniques to quantitate the total (bound and free) PEG on AuNPs. RP-HPLC with CAD is used for both techniques to quantitate the PEG coating. (**A**) The displacement method requires excess DTT to displace PEG from the gold nanoparticle surface. After centrifugation, the displaced PEG and excess DTT make up the supernatant while the gold nanoparticles form a pellet. (**B**) The dissolution method dissolves gold nanoparticles with the addition of potassium cyanide (KCN). RP-HPLC separates the PEG component. Reproduced with permission from ref. 10

To address this characterization gap, two methods have been developed which allow for the quantitative measurement of PEG on PEGylated gold nanoparticles (Fig. 1). In the first method, referred to as the displacement method, dithiothreitol is used to displace PEG from the gold surface. Centrifugation pellets the dithiothreitol-coated gold nanoparticles while the supernatant contains the excess dithiothreitol and dissociated PEG, which are further separated using RP-HPLC. In the second method, referred to as the dissolution method, potassium cyanide is used to dissolve the gold nanoparticles and liberate the PEG. Excess CN^-, $Au(CN)_2^-$, and free PEG are separated using RP-HPLC. In both methods, detection of the PEG is accomplished via charged aerosol detection after RP-HPLC separation. A centrifugation step prior to either of the two methods can be used to separate free PEG from bound PEG (Fig. 2). The displacement and dissolution methods are outlined here using 20 kDa PEGylated 30 nm colloidal gold nanoparticles but can be extended to other size colloidal gold nanoparticles and PEG chain lengths [10].

2 Materials

1. RP-HPLC system consisting of a degasser, capillary pump, well-plate autosampler, PLRP-S column (100 Å, 4.6 mm ID × 150 mm, 5 μm), and charged aerosol detector (CAD).

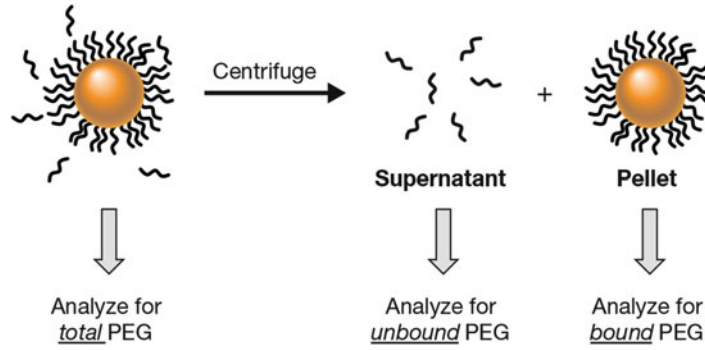

Fig. 2 Separation method to quantitate bound and unbound PEG on AuNPs. A centrifugation step of the PEGylated AuNPs forms a fraction of the unbound PEG in the supernatant and the AuNP-bound PEG in the pellet. Then, PEG can be quantitated for each of these populations by RP-HPLC with CAD. Reproduced with permission from ref. 10

2. Acetonitrile with 0.14% (w/v) trifluoroacetic acid, HPLC grade.
3. Water with 0.14% (w/v) trifluoroacetic acid, HPLC grade.
4. 1 M potassium cyanide (KCN) in water, HPLC grade (*see* **Note 1**).
5. 550 mM dithiothreitol (DTT) in water, HPLC grade, make fresh as required.
6. PEGylated (20 kDa) colloidal gold nanoparticles (AuNP); 50 μg/mL gold concentration.
7. Free 20 kDa PEG, ideally from the same lot of PEG used in the nanoparticles.

3 Methods

3.1 Dissolution Method

3.1.1 Sample Preparation for Total PEG

1. Add 10 μL of 1 M KCN solution to 100 μL PEGylated AuNP (*see* **Note 1**). The red solution (AuNP) will turn clear after several minutes of vortexing, signaling the end of the dissolution process (*see* **Note 2**).

3.1.2 Sample Preparation for Unbound and Bound PEG

1. Centrifuge 200 μL of the PEGylated AuNP sample for 30 min at 17,500 × *g* and 26 °C, yielding a red pellet (*see* **Note 3**).
2. Remove the supernatant and reserve for HPLC analysis to test for free unbound PEG.
3. Record the pellet volume for each sample (typically 6–15 μL) and add the appropriate volume of water to give a total volume ranging from 50 to 100 μL. Resuspension volumes vary to meet the detection limits of the RP-HPLC CAD system. The

pellet fraction is analyzed for bound PEG concentration by HPLC.

4. Add 10 μL of 1 M KCN solution to the resuspended pellet. Vortex sample until it turns clear. Test for bound PEG.

3.2 Displacement Method

3.2.1 Sample Preparation for Total PEG

1. Add 10 μL of 550 mM DTT solution to 100 μL of PEGylated AuNP (*see* **Note 4**). Vortex the sample thoroughly. A minimum of 5 min for incubation is ample time to allow the PEG to be displaced from the surface of the AuNP.
2. Vortex sample and centrifuge for 30 min at 17,500 × *g* and 26 °C, yielding a red pellet (AuNPs). The clear supernatant, containing displaced (bound) PEG and any free unbound PEG, is retained for HPLC analysis.

3.2.2 Sample Preparation for Unbound and Bound PEG

1. Centrifuge 200 μL of the PEGylated AuNP sample for 30 min at 17,500 × *g* and 26 °C, yielding a red pellet (*see* **Note 3**).
2. Remove the supernatant to test for free unbound PEG.
3. The pellet fraction is analyzed for bound PEG concentration. Record the pellet volume for each sample (typically 6–15 μL) and add water for a final volume range of 50–100 μL. Resuspension volumes vary to meet the detection limits of the RP-HPLC CAD system.
4. Add 10 μL of 550 mM DTT solution to the resuspended pellet. Vortex the sample thoroughly. Incubate sample for a minimum of 5 min to allow the PEG to be displaced off the surface of the AuNP.
5. After addition of DTT, vortex the sample and centrifuge for 30 min at 17,500 × *g* and 26 °C, yielding a red pellet (AuNPs). The clear supernatant, containing displaced (bound) PEG, is reserved for HPLC analysis.

3.3 Prepare PEG Calibration Standards

1. Prepare a set of PEG calibration standards in HPLC grade water based on the lower limit of quantification (LLOQ) and limit of detection (LOD) (*see* **Note 5**). Calibration standards are typically prepared at concentrations ranging from 2.5 to 60 μg/mL in HPLC grade water (*see* **Note 6**). A minimum of seven standards are recommended.
2. Mix 100 μL calibration standard with 10 μL 1 M KCN. Standard samples are prepared fresh and used immediately.

3.4 RP-HPLC Conditions

1. The essential component of the chromatographic system needed for PEG quantitation is a charged aerosol detector (CAD). The CAD is operated with a fixed drift-tube temperature of 35 °C. The nebulizer gas consists of compressed nitrogen with a flow rate of 1.68 L/min and pressure of 35.1 psi.

2. The mobile phase consists of water/acetonitrile (A/B, HPLC grade, 0.14% (v/v) trifluoroacetic acid).
3. The elution gradient is 30% B for 3 min, ramp to 50% B in 20 min, hold at 50% B for 3 min, and ramp down to 30% B in 3 min (*see* **Note 7**).
4. The injection volume is 40 μL and the flow rate is 1 mL/min.

3.5 Data Analysis

1. Open the elution profiles of the PEGylated AuNP (Fig. 3) as well as those of the standards.
2. Integrate the PEG peak area for each sample.
3. Create a calibration curve plotting each calibration standard's peak area versus concentration. If the curve is nonlinear, plot log peak area against log of the PEG concentration and use this graph to quantitate the amount of PEG in each sample. While this log–log analysis is more traditional in regards to CAD response, one may be able to plot peak area against PEG concentration on a linear scale with a lower range of standards (in our case 2.5–25 μg/mL) for sample PEG quantitation.

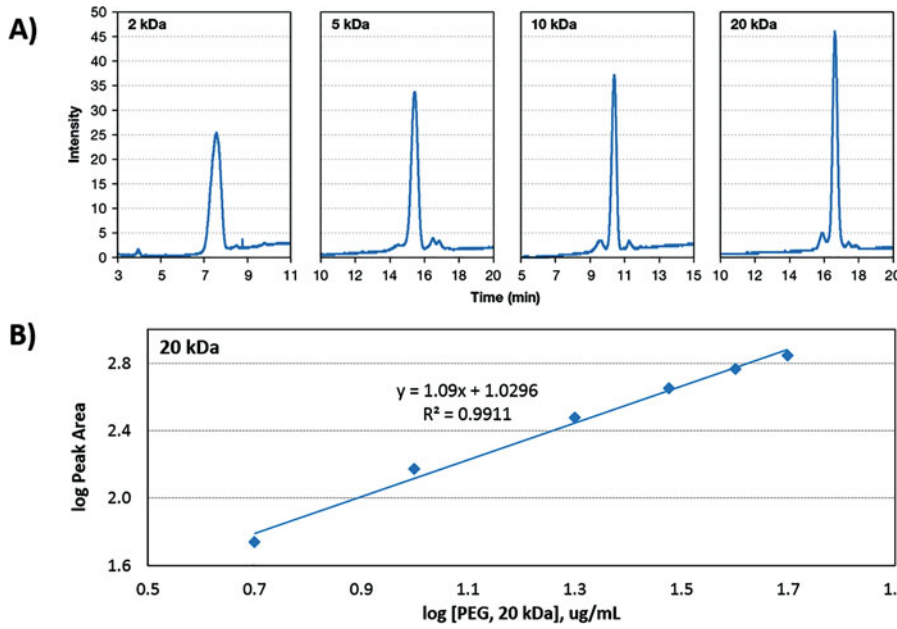

Fig. 3 (**A**) RP-HPLC CAD chromatograms of 2-, 5-, 10-, and 20 kDa mPEG-SH. (**B**) 20 kDa mPEG-SH standard calibration curve. The PEG samples include 50 mM DTT. Separation and quantitation were performed on an RP-HPLC system (Agilent G4225A, Palo Alto, CA) with a capillary pump (Agilent G1312B), well-plate autosampler (Agilent G1329B), Agilent PLRP-S column and CAD (ESA Corona Ultra). The analysis was performed using Agilent Chemstation. Figure (**A**) reproduced with permission from ref. 10

4 Notes

1. Always wear appropriate personal protective equipment and take precautions throughout this procedure. Be especially careful when handling KCN as it is extremely toxic. Follow your lab safety protocols for handling and disposing of such chemicals.
2. When preparing samples for the dissolution method, 1 M KCN diluted 10-fold in the PEGylated AuNP represents a 10-fold molar excess of KCN relative to 50 μg/mL AuNPs, the stock concentration used in our samples. For the AuNP containing samples, vortex thoroughly and observe a color change from red to clear. Be sure the sample has completely turned clear prior to injection. Typically, this color change occurs within 20 min of incubation with KCN.
3. If the amount of bound PEG falls below the LLOQ and there is no detectable free PEG, the sample will need to be concentrated appropriately to increase signal strength. In order to do this, centrifuge the sample down at 17,500 × *g*, 25 °C for 30 min and then remove a known volume of supernatant. For example, spin down 300 μL of sample and remove 150 μL of supernatant. This will concentrate the sample 2-fold and thus increase signal strength. This can be done as many times as necessary to bring the sample to a concentration that falls roughly in the middle of the calibration standards range. As long as the 1:10 ratio of KCN or DTT to PEGylated AuNP is maintained, any appropriate volumes may be used to meet sample injection requirements. Be sure to correct for concentration during data analysis.
4. For the displacement method, 10 μL of 550 mM DTT diluted 10-fold in PEGylated AuNP sample represents a near 1000-fold excess of DTT relative to PEG. After incubating DTT with the PEGylated AuNP, vortex thoroughly and PEG displacement should occur instantly.
5. When determining the LLOQ, construct a calibration curve and probe the lower end until a concentration is reached that does not fall in line with the rest of the curve. The point on the curve above this one is the LLOQ. To determine the LOD, inject consecutively lower concentrations of PEG until there is no apparent peak. The lowest concentration that produces a visible peak is the LOD.
6. In order to fall in the linear range on the calibration curve, standards usually will fall somewhere between 2.5 and 60 μg/mL. This range will also vary instrument to instrument so be sure to test the LLOQ and LOD to construct a proper calibration curve. In addition, signal strength will vary slightly with PEG molecular weight due to peak broadening for the lower

weight PEG chains. For example, 2 kDa and 5 kDa PEG will require a slightly higher calibration range than 10 kDa and 20 kDa PEG. Also note that both methods of PEG quantitation would most likely work for any molecular weight PEG, but was only tested here for 2, 5, 10, and 20 kDa.

7. The elution gradient for 10 kDa PEG was 30% B for 3 min, ramp to 50% B in 20 min, hold at 50% B for 3 min, and ramp down to 30% B in 3 min. The elution gradient for the 5 kDa PEG was 30% B for 3 min, ramp to 50% B in 10 min, hold at 50% B for 3 min, and ramp down to 30% B in 3 min. The elution gradient for the 2 kDa PEG was 30% B for 3 min, ramp to 50% B in 5 min, hold at 50% B for 3 min, and ramp down to 30% B in 3 min.

Acknowledgment

This project has been funded in whole or in part with Federal funds from the National Cancer Institute, National Institutes of Health, under Contract No. HHSN261200800001E. The content of this publication does not necessarily reflect the views or policies of the Department of Health and Human Services, nor does mention of trade names, commercial products, or organizations imply endorsement by the U.S. Government.

References

1. Albanese A, Tang PS, Chan WCW (2012) The effect of nanoparticle size, shape, and surface chemistry on biological systems. Annu Rev Biomed Eng 14:1–16. doi:10.1146/annurev-bioeng-071811-150124
2. Harris JM, Chess RB (2003) Effect of pegylation on pharmaceuticals. Nat Rev Drug Discov 2(3):214–221. doi:10.1038/Nrd1033
3. Jokerst JV, Lobovkina T, Zare RN, Gambhir SS (2011) Nanoparticle PEGylation for imaging and therapy. Nanomedicine 6(4):715–728. doi:10.2217/Nnm.11.19
4. Yowell SL, Blackwell S (2002) Novel effects with polyethylene glycol modified pharmaceuticals. Cancer Treat Rev 28:3–6. doi:10.1016/S0305-7372(02)80002-0
5. Almeida JP, Figueroa ER, Drezek RA (2014) Gold nanoparticle mediated cancer immunotherapy. Nanomedicine 10(3):503–514. doi:10.1016/j.nano.2013.09.011
6. Blanco E, Hsiao A, Mann AP, Landry MG, Meric-Bernstam F, Ferrari M (2011) Nanomedicine in cancer therapy: innovative trends and prospects. Cancer Sci 102(7):1247–1252. doi:10.1111/j.1349-7006.2011.01941.x
7. Cai W, Gao T, Hong H, Sun J (2008) Applications of gold nanoparticles in cancer nanotechnology. Nanotechnol Sci Appl 2008(1):17–32. doi:10.2147/NSA.S3788
8. Jain S, Hirst DG, O'Sullivan JM (2012) Gold nanoparticles as novel agents for cancer therapy. Br J Radiol 85(1010):101–113. doi:10.1259/bjr/59448833
9. van Vlerken LE, Amiji MM (2006) Multifunctional polymeric nanoparticles for tumour-targeted drug delivery. Expert Opin Drug Deliv 3(2):205–216. doi:10.1517/17425247.3.2.205
10. Smith MC, Crist RM, Clogston JD, McNeil SE (2015) Quantitative analysis of PEG-functionalized colloidal gold nanoparticles using charged aerosol detection. Anal Bioanal Chem 407(13):3705–3716. doi:10.1007/s00216-015-8589-2

Chapter 6

Quantitation of Surface Coating on Nanoparticles Using Thermogravimetric Analysis

Alpana A. Dongargaonkar and Jeffrey D. Clogston

Abstract

Nanoparticles are critical components in nanomedicine and nanotherapeutic applications. Some nanoparticles, such as metallic nanoparticles, consist of a surface coating or surface modification to aid in its dispersion and stability. This surface coating may affect the behavior of nanoparticles in a biological environment, thus it is important to measure. Thermogravimetric analysis (TGA) can be used to determine the amount of coating on the surface of the nanoparticle. TGA experiments run under inert atmosphere can also be used to determine residual metal content present in the sample. In this chapter, the TGA technique and experimental method are described.

Key words TGA, Surface coating, Nanoparticles, Colloidal metal nanoparticles, Inorganic nanoparticles

1 Introduction

Thermogravimetric analysis (TGA) is an experimental technique to measure the change in mass of a sample as a function of temperature and/or time in a controlled atmosphere [1]. The thermogravimetric analyzer used for TGA experiments consists of a high-precision thermobalance, which is connected to a pan/crucible holder inside a temperature-controlled furnace. The pan/crucible holder is located on a sensor that is supported with a thermocouple to measure the sample temperature. A purge gas introduced into the furnace, such as nitrogen for an inert atmosphere or air/oxygen for an oxidizing atmosphere, controls the sample environment. TGA experiments are generally run from ambient temperature to 1000 °C [2].

The result of a thermogravimetric measurement is displayed as a mass versus temperature or time curve, known as the thermogravimetric (TGA) curve [1]. A derivative plot of the TGA curve, referred to as the derivative thermogravimetric (DTG) curve, shows the rate at which mass changes and is displayed as a rate of mass loss

Scott E. McNeil (ed.), *Characterization of Nanoparticles Intended for Drug Delivery*, Methods in Molecular Biology, Vol. 1682, DOI 10.1007/978-1-4939-7352-1_6,

versus temperature curve [3]. Mass changes in a sample can occur due to processes such as evaporation, drying, desorption or adsorption, sublimation, and thermal decomposition. These changes in mass are observed as step changes in the TGA curve or peaks in the DTG curve [1].

There are various factors or experimental conditions that affect TGA measurements:

1. Buoyancy. Buoyancy is the upward force exerted on the sample by the surrounding atmosphere which results in an apparent increase in mass [2]. The buoyancy effect is caused by the change in density of the gas due to an increase in temperature and can be corrected by performing a blank measurement without any sample [1]. The blank measurement should be performed with the same temperature program and crucible that would be used for the sample. To get a corrected final curve, the blank curve can be subtracted from the sample measurement curve.
2. Heating rate. An optimum heating rate should be used to obtain a better resolution of the thermal events/transitions occurring during a TGA measurement. Slow heating rates are recommended so that individual thermal events can be resolved. If heating rates are too fast, multiple thermal events may overlap [4].
3. Choice of crucible. The container used for the samples during a TGA measurement is called a crucible. The crucible material should not react with the sample nor undergo any physical changes in the temperature range of interest. Generally, aluminum oxide crucibles are used for TGA measurements. A crucible is closed at the top by a loosely fitted lid containing a very small hole, so it is vented to the atmosphere [1].
4. Furnace atmosphere. A protective gas, such as nitrogen, is introduced into the furnace to protect the balance from any corrosive gases being discharged during the measurement. Additionally, purge gas and/or reactive gas can be introduced in the furnace through separate gas lines at a rate of 30–50 mL/min to help remove gaseous products from the furnace [1].

TGA can be used to determine properties and characteristics of polymers, decomposition temperatures of polymers, absorbed moisture content, or residual metal content in a sample. It can also be interfaced with infrared spectroscopy (IR), mass spectrometry (MS), or gas chromatography (GC) to analyze the residual components or gases involved. Based on these capabilities, TGA is a useful tool to analyze the surface coating of nanoparticles. Herein, we describe the methods and related analysis to measure the amount of surface coating on colloidal metal nanoparticles using TGA. As an example,

we include TGA analysis of polyvinylpyrrolidone (40 kDa PVP)-stabilized silver nanoparticles. The initial measurement will be the blank measurement performed on an empty crucible followed by the sample measurement with the same temperature program. For evaluation, the final TGA curve will be obtained by blank curve correction, and the DTG curve will be generated from the final TGA curve. The final TGA and DTG curves will be used for further analysis and mathematical calculations.

2 Materials

1. Thermogravimetric analyzer.
2. Alumina crucibles with lids (70 μL or 150 μL capacity or ones compatible with the crucible holder and furnace).
3. Tweezers for holding the crucible.
4. Metallic nanoparticle sample for analysis. Polyvinylpyrrolidone (40 kDa PVP)-stabilized silver nanoparticles with a 110 nm nominal size used as example.
5. Spatula for transferring sample into crucible.

3 Methods

3.1 Performing a Blank Measurement Using an Empty Crucible

1. Set up and save an experimental method by defining the temperature program (*see* **Note 1**).
2. Start the experiment and allow the furnace and crucible holder to equilibrate to the starting temperature.
3. After the temperature equilibrates and the instrument's display screen reads a variation of "Insert sample," open the furnace and carefully place an empty crucible along with a lid on the crucible holder using tweezers. Close the furnace.
4. When the crucible weight is displayed on the screen, zero the crucible weight.
5. Allow the weight value indicated on the display to stabilize to zero and proceed with the experiment.

3.2 Performing a Sample Measurement After the Blank Measurement

1. Start the same experimental method as that performed for the blank measurement. Same temperature program and crucible is required for blank curve correction.
2. When the display screen on the instrument reads a variation of "Insert sample," open the furnace and carefully place the empty crucible, which was used for the blank measurement, along with a lid on the crucible holder using tweezers. Close the furnace.

3. When crucible weight is displayed on the screen, tare the crucible weight and allow the weight value indicated on the display to stabilize to zero.
4. Open the furnace again and remove the crucible.
5. Transfer the sample into the crucible using a spatula (*see* **Notes 2–4**). As an example of TGA analysis, the sample used is lyophilized PVP-stabilized silver nanoparticle. Cover the crucible with the lid.
6. Place the crucible filled with sample on the crucible holder and close the furnace.
   Allow the weight value indicated on the display to stabilize (*do not press the tare button again*) and proceed with the experiment.

3.3 Data Analysis

3.3.1 Performing Blank Curve Subtraction

1. Once both the blank measurement and sample measurement are collected, open the evaluation window for data analysis.
2. Open the mass loss versus temperature or time curves for both the measurements simultaneously in one window.
3. For blank curve correction, subtract the blank measurement curve from the sample measurement curve using the curve subtracting function on the analyzer software.
4. The subtracted curve obtained is the blank corrected sample curve and also the final TGA curve that will be used for further analysis. Remove the initial blank and sample measurement curves used for subtraction from the evaluation window.

3.3.2 Generating a Derivative Thermogravimetric (DTG) Curve

1. Select the final TGA curve obtained in Subheading 3.3.1 and generate the DTG curve using the "1st derivative" option in the analyzer software.
2. The final TGA and DTG curves can be displayed in the same evaluation window.

3.3.3 Performing Step Evaluation to Determine Weight Loss

1. The TGA and DTG curves show the decomposition of the surface coating and the metallic content present in the sample from the residual amount left after the measurement. In this example, PVP is the surface coating and silver is the residual metal. To determine the weight loss due to decomposition of the surface coating, draw a frame around the section of the curve that shows a weight loss event; this indicates sample decomposition. Because the weight loss event is best seen in the DTG curve, use the DTG curve to draw a frame around the decomposition event and correlate that frame to the corresponding location in the TGA curve. Then, use the "Step Horizontal" option or a similar selection in the analyzer software to obtain the weight loss value (*see* **Notes 5** and **6**, Figs. 1 and 2, and Table 1).

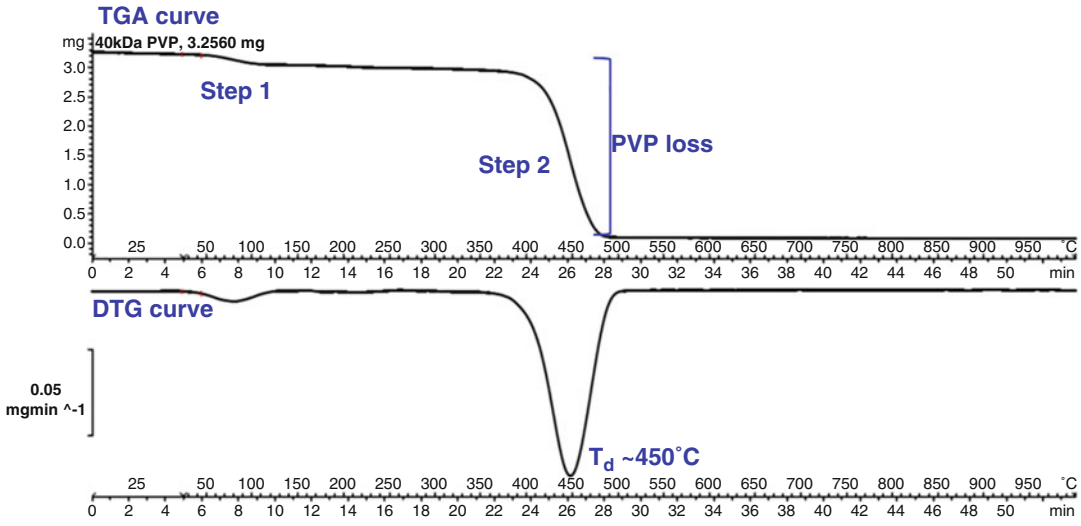

Fig. 1 TGA and DTG curve for the 40 kDa PVP (Control)

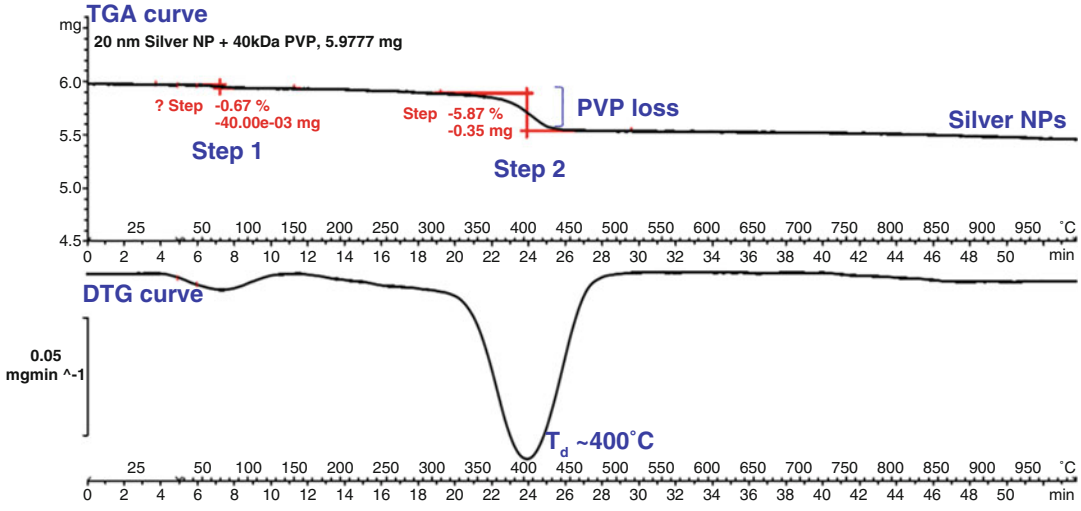

Fig. 2 TGA and DTG curve for the PVP-stabilized silver sample

Table 1
Determination of PVP concentration in the PVP-stabilized silver sample

Weight after water loss (Total construct), mg	PVP loss, mg	Silver NP at 1000 °C, mg	[PVP], μg PVP/mg Ag
5.93	0.35	5.46	64.1

2. To determine the residual metal amount, select the full range of the curve and use the same software option described above to display the total weight loss and residual amount left at the end of the measurement (*see* **Note 7**).

4 Notes

1. For the PVP-stabilized silver nanoparticle analysis, the sample was held at 25 °C for 5 min, after which the temperature was increased to 1000 °C at a heating rate of 20 °C/min. Nitrogen was used as the purge gas at a rate of 40 mL/min.
2. Standard precautions must be taken while handling nanoparticle aqueous solutions and powders. It is important to wear proper clothing, laboratory gloves, and eyewear while performing the experiments. Powdered/lyophilized samples must be prepared and transferred into the crucible in a fume hood. As an extra precaution, a respiratory mask may be used.
3. When loading the sample (aqueous or powdered samples) into the crucible for measurement, care should be taken to add an appropriate amount of sample depending on the capacity of the crucible so as to prevent overflowing of the sample after it is covered with a lid.
4. For the example study, an aqueous suspension of the PVP-stabilized silver nanoparticle sample was measured initially (50 μL of sample was loaded into a 70 μL-capacity crucible for measurement). However, since the samples were in water, water loss was observed below 150 °C of the TGA curve and this peak dominated the curve. Also, the amount of PVP present in the sample was below the level of detection of the instrument. To solve this and achieve better sensitivity, the aqueous sample was lyophilized before TGA measurement. About 20–30 mL of the sample was frozen using dry ice with acetone slurry and lyophilized for 15–18 h to remove water. The resulting lyophilized powder was used for TGA measurement.
5. Figures 1 and 2 show the TGA and corresponding DTG curve for the 40 kDa PVP (control) and PVP-stabilized silver nanoparticle sample. Both the samples decompose in two stages. Initial weight loss (**step 1**) is observed due to water loss (below 150 °C) followed by decomposition of PVP between 300 °C and 500 °C (**step 2**). 40 kDa PVP has a decomposition temperature (T_d) of approximately 450 °C, and it decomposes completely upon heating to 1000 °C. However, the decomposition temperature of PVP in the silver sample is approximately 400 °C, which is lower than that observed in the PVP control

measurement; presumably, silver catalyzes the thermal decomposition of PVP. The residual weight at 1000 °C is attributed to the silver content in the sample.

6. The calculation for PVP concentration in the sample is summarized in Table 1. The resulting weight after water loss is the total construct weight in the sample. This value can be used to calculate the concentration of PVP as mg PVP per mg total construct.
7. If the coating surface material is known, it is good practice to include that material as a control to compare weight loss events between the coated nanoparticle and the coating alone.

Acknowledgment

This project has been funded in whole or in part with federal funds from the National Cancer Institute, National Institutes of Health, under Contract No. HHSN261200800001E. The content of this publication does not necessarily reflect the views or policies of the Department of Health and Human Services, nor does mention of trade names, commercial products, or organizations imply endorsement by the U.S. Government.

References

1. Wagner M (2009) Thermal analysis in practice-Mettler Toledo application handbook. Mettler-Toledo, Switzerland
2. Prime RB, Bair HE, Vyazovkin S, Gallagher PK, Riga A (2008) Thermogravimetric analysis (TGA). In: Menczel JD, Prime RB (eds) Thermal analysis of polymers: fundamentals and applications. John Wiley & Sons Inc., New York, pp 241–317. doi:10.1002/9780470423837.ch3
3. Haines PJ (1995) Thermogravimetry. In: Haines PJ (ed) Thermal methods of analysis: principles, applications and problems. Springer, Netherlands, pp 22–62. doi:10.1007/978-94-011-1324-3
4. Borrachero MV, Payá J, Bonilla M, Monzó J (2008) The use of thermogravimetric analysis technique for the characterization of construction materials. J Therm Anal Calorim 91 (2):503–509. doi:10.1007/s10973-006-7739-3

Chapter 7

Immunoelectron Microscopy for Visualization of Nanoparticles

Sarah R. Anderson, David Parmiter, Ulrich Baxa, and Kunio Nagashima

Abstract

Immunoelectron microscopy (IEM) on a solid phase such as a carbon film is a fast and powerful way to detect and visualize surface antigens on nanoparticles by using a transmission electron microscope (TEM). Nanoparticles, in particular ones for medical applications, are often modified on the surface with soft materials to make them more soluble, less toxic, or targetable to cancerous tumors. Imaging the soft material on the surface of solid nanoparticles by electron microscopy is often a challenge. IEM can overcome this issue in cases where antibodies to any of the surface material are available, which is often the case for proteins, but also for commonly used materials such as polyethylene glycol (PEG). This effective procedure has been used traditionally for viruses and macromolecules, but it can be directly applied to nanoparticles.

Key words Electron microscope, Negative stain, Immune electron microscopy, Indirect solid phase immunolabeling, Nanomaterial

1 Introduction

Many nanoparticles have modified surfaces designed for specific purposes such as increased solubility, reduced immunotoxicity, and site-specific targeting [1]. Imaging such surfaces on nanoparticles in the electron microscope is an important part of development and quality control; but, it can be challenging, especially on solid metal-type nanoparticles and even on soft matter particles such as liposomes. Proteins and lipids can often be imaged with methods like negative staining or dark field scanning transmission electron microscopy (STEM) [2, 3], but other materials, especially soluble polymers such as PEG, are challenging to image in the electron microscope without the use of specialized support films and high-end microscopes [4, 5]. As antibodies become available, IEM is a powerful method for imaging such cases.

IEM on a solid phase has been used traditionally for viruses and macromolecules [6]; but, it can be directly transferred to

Scott E. McNeil (ed.), *Characterization of Nanoparticles Intended for Drug Delivery*, Methods in Molecular Biology, Vol. 1682, DOI 10.1007/978-1-4939-7352-1_7,

nanoparticles. It is a faster and easier method compared to the conventional pre- and post-embedding IEM, because it does not require any plastic embedding. The technique involves three steps: (1) attach the nanomaterial sample on the surface of a carbon coated support film grid, (2) block any non-specific IgG binding sites by commercially available blocking buffer or phosphate buffer containing normal serum and bovine serum albumin, and (3) incubate the grid in a primary antibody followed by gold-conjugated secondary antibody. In the case of soft matter nanoparticles, the procedure can be followed by negative staining with heavy metal salts to give the soft material adequate contrast. The heavy metal salts are typically phosphotungstic acid (PTA), uranyl acetate (UA), or uranyl formate. IEM can also be performed in liquid phase, which involves incubating the sample with primary and secondary antibodies in solution followed by drop-cast mounting on a carbon surface and in some cases negative staining. In such procedures, the concentrations have to be very carefully optimized to avoid aggregation of the sample prior to mounting.

In this chapter, we describe the procedures of solid phase IEM using an indirect immunolabeling method of nanomaterials and show results of two nanoparticle samples—PEG on metal oxide particles (Fig. 1) and 30 nm gold particles coated with tumor necrosis factor alpha (Fig. 2).

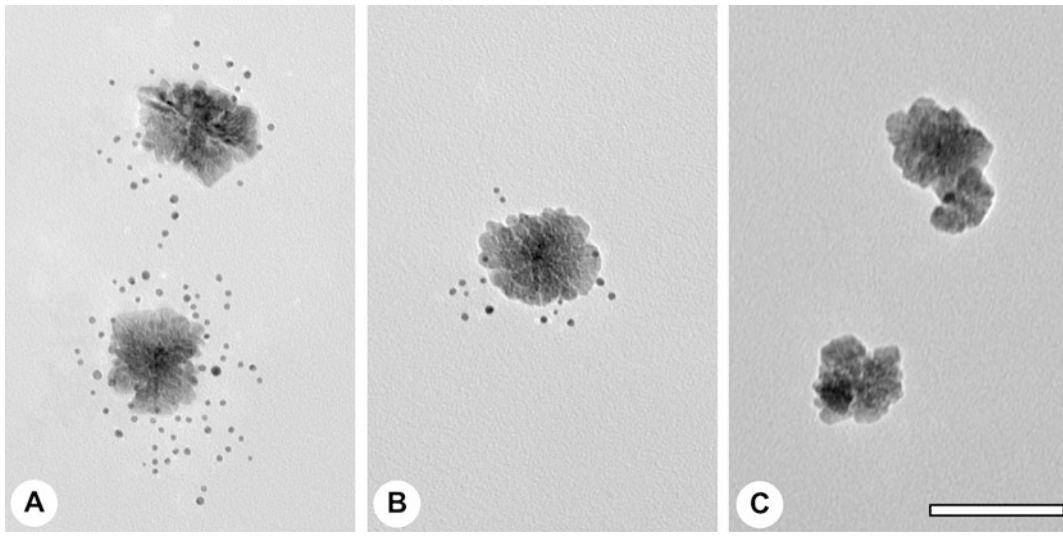

Fig. 1 IEM of PEG-coated metal oxide particles using 10 nm gold secondary antibodies. (**a**) IEM image of particles labeled with the primary antibody specific to PEG main chain (ethylene glycol moiety). Primary antibody: Anti-PEG mouse monoclonal, Clone 9B5-6-25-7 (Life Diagnostics, Inc.); secondary antibody: goat-anti-mouse IgG (Aurion). (**b**) Image of particles labeled with an antibody specific to the methoxy end of PEG chain. Primary antibody: anti-methoxy-PEG mouse monoclonal, Clone 5D6-3 (Life Diagnostics, Inc.); secondary antibody: goat-anti-mouse IgG (Aurion). (**c**) Control image without any primary antibody. Bar = 100 nm for all panels

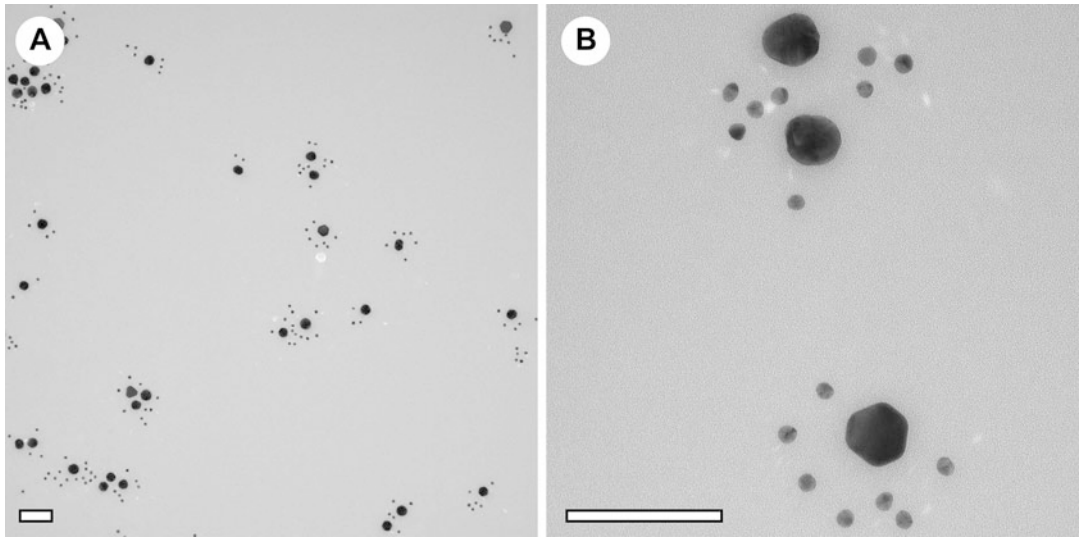

Fig. 2 IEM of 30 nm gold particles coated with tumor necrosis factor alpha (TNF-α). To produce a clear difference in size between the 30 nm core particles and the gold-label, 10 nm gold-labeled secondary antibody was used. (**a**) Low magnification shows the specificity of the reaction. All the gold labels are found close to 30 nm core particles. Almost no gold labels are found on the carbon film, indicating very low background. (**b**) High magnification of the labeling reaction. Bar = 100 nm in both panels

2 Materials

1. Formvar carbon filmed 300 mesh copper grids.
2. Tweezers.
3. Paraffin film.
4. Glow discharger (*see* **Note 1**).
5. Polysorbate 20.
6. 0.1% poly-L-lysine in water.
7. Blocking solution for gold conjugates, proprietary commercial formulae (*see* **Note 2**) or normal serum; bovine serum albumin (BSA); phosphate buffered saline (*see* **Note 3**).
8. Dilution solution, 50 mM Tris buffer containing 125 mM NaCl; 0.1% w/v bovine serum albumin (BSA).
9. Washing solution, 50 mM Tris buffer containing 250 mM NaCl; 0.1% w/v BSA; 0.05% polysorbate 20.
10. Primary antibody (*see* **Note 3**).
11. Gold-conjugated secondary antibody corresponding to primary antibody (*see* **Notes 3** and **4**).
12. 0.5% w/v uranyl acetate aqueous solution (UA).
13. Glass-distilled water (DDH_2O).

3 Methods

3.1 Prepare the Formvar Carbon Film Grids

1. Cut a clean filter paper to 1″ × 2″ and place on a clean glass slide.
2. Place the grids on the filter paper film-side up.
3. Load the slide with the grids on it into the glow discharger's vacuum tube chamber.
4. Introduce a vacuum into the chamber, either by the discharger's automatic setting or through procedure optimization.
5. Under the automatic setting, the glow discharger automatically pumps the chamber and reaches optimal vacuum for glow discharge. After the discharge is done, it automatically vents the chamber. The process takes less than 5 min from beginning to end.
6. Remove the grids for use. The grids can be used within 48 h of preparation without losing much of the hydrophilic property.

3.2 Adsorb the Nanomaterial on the Grid

1. Lay a clean paraffin film sheet (2″ × 4″) on a flat surface.
2. Place a 5 μL drop of sample solution on the paraffin film.
3. Place the grid on the drop with the film-side down using tweezers and float the grid on the sample drop.
4. Let the nanomaterial adsorb to the film for up to 5 min. In many cases, 2 min adsorption time is sufficient.
5. Remove the grid and blot excess solution with a filter paper. Allow the grid to air dry (*see* **Note 5**).
6. Place 5 μL of blocking buffer on the paraffin film and place the grid film-side down to float over the blocking buffer. Block non-specific IgG binding sites for 10 min. Place a petri-dish lid over the drop to prevent evaporation during longer incubations (*see* **Note 6**).
7. Prepare primary antibody dilution. Start with a serial dilution (e.g., 1/50, 1/100, 1/200) using the dilution buffer (*see* **Note 7**).
8. Place the dilution(s) on the paraffin film (5 μL of each dilution is sufficient) and place the grid over the primary antibody drop. Incubate for 1 h. Cover the drop with a petri-dish lid to prevent evaporation.
9. After the primary antibody incubation, the grid is removed using tweezers and blotted with filter paper to remove excess solution.
10. Place 3 drops of 10 μL washing buffer on the paraffin film for each grid. Float the grid on each washing buffer drop for 10 min.
11. After the end of the third washing float, remove the grid and blot excess solution with the filter paper.

12. Place a drop of 10 μL of gold-conjugated secondary antibody (1/25 dilution) for each grid on the paraffin film (*see* **Note 8**).
13. Place the grid over the secondary antibody and incubate for 1 h. Cover the drop with a petri-dish lid to prevent evaporation.
14. After the secondary antibody incubation, remove the grid and blot excess solution from the grid using filter paper.
15. Place 3 drops of 10 μL washing buffer on the paraffin film for each grid and float the grid on each drop for 10 min, as in **step 10** above.
16. At the end of the third washing step, remove the grid and blot excess solution with the filter paper.
17. Wash the grid in a 10 μL drop of water (DDH_2O) for 10 min to remove any remaining salts and BSA from the washing buffer.
18. Proceed directly with negative stain, if necessary. Otherwise air-dry the grid and image in the TEM (*see* **Note 9**).

3.3 If Necessary for Soft Material Nanoparticles, Perform Negative Staining

1. Using a fine tweezer with a rubber *o*-ring, secure the grid.
2. Place 3 μL UA aqueous solution on the grid and quickly blot with a filter paper.
3. Repeat **step 2** above two more times. Then, blot excess solution and allow the grid to air dry.
4. The grid is ready to examine in the TEM (*see* **Notes 9** and **10**).

4 Notes

1. If there is no access to a glow discharger, the formvar carbon film grid can be dipped in 0.1% poly-L-lysine solution and allowed to air dry before adsorbing the nanoparticle sample.
2. Normal serum is added from the same species as the secondary antibody used. Commercial blocking solution used in Fig. 1 contains BSA and cold water fish skin gelatin in phosphate buffered saline with sodium azide as preservative.
3. Make sure the antibody species, subclasses, and blocking solution correspond accordingly to each other. The secondary antibody has to target the correct species and subclass of primary antibody, and the blocking solution should be from the same species as the secondary antibody. For example, if the primary antibody is a monoclonal mouse IgG1, then the corresponding secondary antibody is a goat anti-mouse IgG1 and the matching blocking solution is goat normal serum.
4. Make sure the size of gold on the secondary antibody agrees well with the application. If you are trying to label gold

nanoparticles or other metallic nanoparticles, use a significantly different size of gold for the secondary antibody.

5. The proper amount of nanomaterial adsorbed to the grid can be checked without continuing the complete procedure. Just stop the protocol after this step and proceed to air dry or negative stain, if appropriate. Check the grid in a microscope. There should be plenty of particles visible, but they should be dispersed enough so that labeling specificity can be verified (e.g., label on particle vs. random label binding to the carbon film).
6. During the incubation and washing steps, the grid is often unable to stay afloat because the BSA and Polysorbate 20 reduces the solution's surface tension. To help with this, allow the grid to air dry after each wash cycle before starting the primary and/or secondary antibody incubation. Drying the grid does not reduce immune-reactivity in our hands; however; if there is any concern about loss of structure during air drying (e.g., denaturation of antigen proteins); the complete procedure should be performed without any air drying until the last step. In this case, place the grid film-side up into the solution drops, because it will not stay afloat on the top of the drops.
7. The best primary antibody concentration is highly dependent on the affinity of the antibody–antigen pair under the specific conditions used and has to be optimized for each new primary antibody and for each nanoparticle. It is recommended to start with a dilution series to avoid repeating the experiment many times. Without any prior knowledge, dilutions of 1/50, 1/100, and 1/200 are good starting concentrations. Based on the results, the concentration may have to be adjusted.
8. The gold-conjugated secondary antibody concentration should be optimized based on previous outcomes. Without prior knowledge, a dilution of 1/25 is a good starting concentration.
9. The goal of IEM is to have a low background and high specific labeling (i.e., very few gold particles randomly attached to the carbon film but many gold particles at the targeted area around the nanoparticles). Controls (without primary antibody) can help recognize the specificity. If there is a high background, reduce the concentration of the primary and secondary antibodies. If there is no background but also little specific binding, increase the concentrations of antibodies. High background can also be reduced by increasing the salt concentration in the washing buffer to 0.5 M NaCl, however this reduces the specific binding reaction.

10. UA forms a fir tree-like precipitation with phosphate if PBS was used as a washing buffer. This precipitation can be reduced by extra washing of the grid in DDH_2O.

Acknowledgment

This project has been funded in whole or in part with Federal funds from the National Cancer Institute, National Institutes of Health, under Contract No. HHSN261200800001E. The content of this publication does not necessarily reflect the views or policies of the Department of Health and Human Services, nor does mention of trade names, commercial products, or organizations imply endorsement by the U.S. Government.

References

1. McNeil SE (2005) Nanotechnology for the biologist. J Leukoc Biol 78(3):585–594. doi:10.1189/jlb.0205074
2. Hu M, Qian L, Brinas RP, Lymar ES, Hainfeld JF (2007) Assembly of nanoparticle-protein binding complexes: from monomers to ordered arrays. Angew Chem Int Ed Engl 46 (27):5111–5114. doi:10.1002/anie.200701180
3. Lee YK, Choi EJ, Webster TJ, Kim SH, Khang D (2015) Effect of the protein corona on nanoparticles for modulating cytotoxicity and immunotoxicity. Int J Nanomedicine 10:97–113. doi:10.2147/ijn.s72998
4. Anderson SR, Smith MC, Clogston JD, Patri AK, McNeil SE, Baxa U (2015) Imaging of polyethylene glycol layers on nanoparticles. Microsc Microanal 21(Suppl 3):231–232. doi:10.1017/S1431927615001956
5. Lee Z, Jeon KJ, Dato A, Erni R, Richardson TJ, Frenklach M, Radmilovic V (2009) Direct imaging of soft-hard interfaces enabled by graphene. Nano Lett 9(9):3365–3369. doi:10.1021/nl901664k
6. Doane FW, Anderson N (1987) Electron microscopy in diagnostic virology: a practical guide and atlas. Cambridge University Press, London

Chapter 8

Imaging of Liposomes by Transmission Electron Microscopy

Ulrich Baxa

Abstract

TEM is an important method for the characterization of size and shape of nanoparticles as it can directly visualize single particles and even their inner architecture. Imaging of metal particles in the electron microscope is quite straightforward due to their high density and stable structure, but the structure of soft material nanoparticles, such as liposomes, needs to be preserved for the electron microscope. The best method to visualize liposomes close to their native structure is cryo-electron microscopy, where thin films of suspensions are plunge frozen to create vitrified ice films that can be imaged directly in the electron microscope under liquid nitrogen temperature. Although subject to artifacts, negative staining TEM can also be a useful method to image liposomes, as it is faster and simpler than cryo-EM, and requires less advanced equipment.

Key words Liposomes, Emulsions, Lipids, Transmission electron microscopy, Negative staining, Cryo-electron microscopy

1 Introduction

Size and size distribution of liposomes can have a major effect on its use as a drug or diagnostic. TEM is one of the most frequently used methods to characterize the ultrastructure of nanoparticles in general, and liposomes in particular, along with scanning electron microscopy (SEM), atomic force microscopy (AFM), and other techniques. Liposome samples have to be prepared and stabilized in such a way to survive the high vacuum in the electron microscope. The three main techniques used include negative staining TEM, plunge freezing (also referred to as cryo-EM), and freeze fracture. Each of these has its advantages and disadvantages and results in slightly different information [1, 2].

Negative staining is probably the most commonly used method because it is simple, fast, requires little material or specialized equipment, and results in high contrast images [3, 4]. Essentially, particles will be adsorbed to a carbon film grid, surrounded by a heavy metal salt, and quickly air dried during which the heavy metal salt forms an amorphous film embedding the particles of interest in

Scott E. McNeil (ed.), *Characterization of Nanoparticles Intended for Drug Delivery*, Methods in Molecular Biology, Vol. 1682, DOI 10.1007/978-1-4939-7352-1_8,

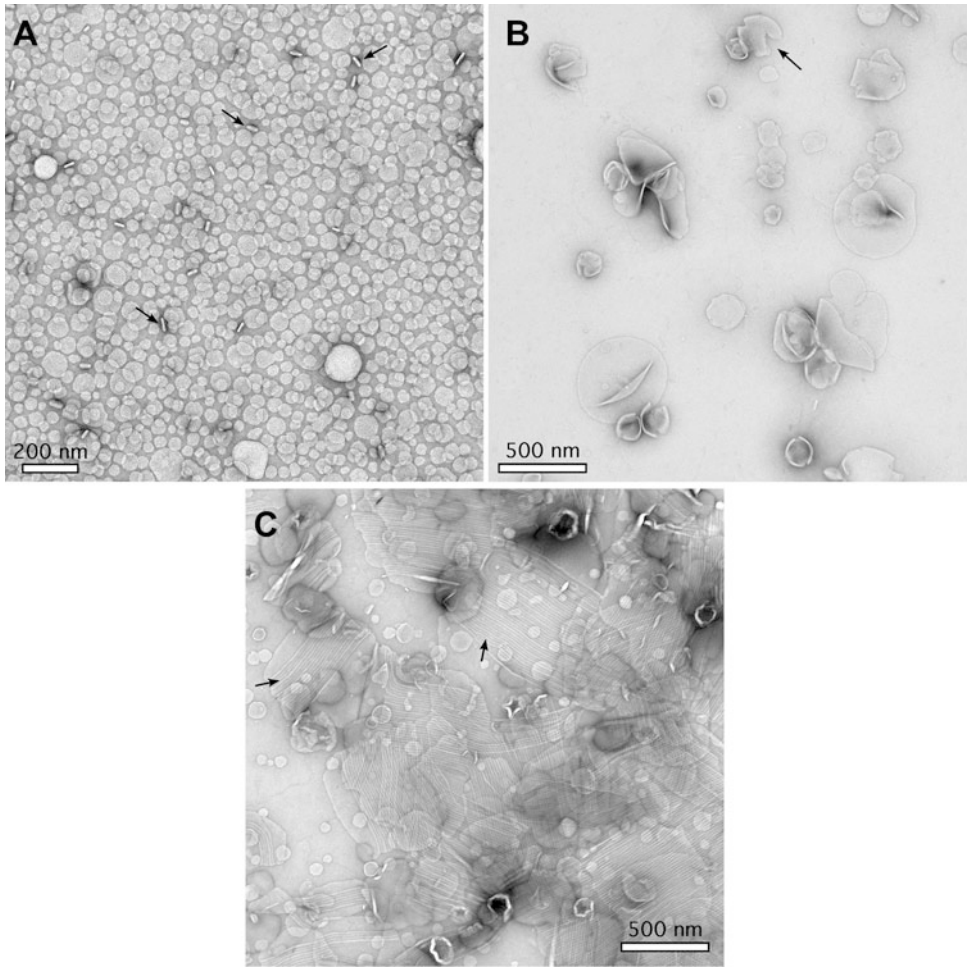

Fig. 1 Examples of negatively stained liposome preparations. (**a**) Liposome preparation with a relatively monodisperse size distribution containing a few bicelles (*arrows*). In negative stain, bicelles can be recognized only when visualized on edge (*side view*). *Top views* of bicelles will appear very similar to liposomes. The bicelles in this preparation have been confirmed by imaging in cryo-EM. (**b**) Liposome preparation with a wide range of sizes. Some of the large liposomes are obviously torn during the drying process (*arrow*). (**c**) Mixture of liposomes and open lipid films. Some parts of the films show a rippled lipid phase (*arrow points* to some areas with rippled phase visible). The lipid films with rippled phases in this preparation have been confirmed by imaging in cryo-EM

the process. The grid is then imaged in the electron microscope where the particles appear bright against the background of the heavy metal stain. The complete protocol is performed at room temperature for a few minutes and the resulting grids can be imaged on any electron microscope and on almost any camera system (Fig. 1). Negative staining works extremely well for protein samples, because proteins are often preserved very close to their native structure [5, 6]. The same is not always true for liposomes and other lipid and emulsion preparations, which are more

susceptible to artifacts in negative stain. Results, therefore, have to be carefully interpreted and examined, and unexpected observations have to be crosschecked with other methods (Fig. 2).

Cryo-EM, on the other hand, can directly visualize particles without any staining in a hydrated (albeit vitrified) state [7–11]. That means that liposomes can be imaged directly, and the liposome structures are preserved very close to their native state in solution (Fig. 3). Cryo-EM can probably be considered the gold standard for liposome imaging, and many review articles and protocols have been published [12–15]. Even for cryo-EM, however, some preparation is still involved. The suspension has to form a thin film (usually <500 nm) before plunge freezing to allow for fast freezing and to result in a thin enough layer for imaging in the electron microscope. Some rearrangement and flattening of larger liposomes are possible in this process, which has to be taken into account when interpreting the results. For cryo-EM imaging of liposomes for size measurements and general morphology, almost any type of TEM can be used; however, if details like membrane thickness are being analyzed, a high-end TEM and imaging system is needed [16].

For preparations that contain larger liposomes (>500 nm), freeze fracture and related methods may be preferred [1, 17]. In freeze fracture a thicker layer of the sample is quickly frozen, then fractured along its length which exposes surfaces with weak molecular interactions (within lipid bilayers) followed by some etching (water sublimation in the vacuum). The exposed surface is then metal shadowed and the replica are eventually imaged in the electron microscope.

This chapter provides detailed protocols and advice for data interpretation on negative staining and cryo-EM of liposomes. Although the freeze fracture technique is not discussed, it is fully described in references 1, 17.

2 Materials

2.1 Negative Staining of Liposomes

1. Choice of negative stain:
   (a) 1% uranyl acetate (UA)
   UA (and uranyl formate, UF) stain has the highest contrast of all stains and is usually a good choice for liposomes—it should be the first choice when new experiments are started. Weigh out the proper amount of UA for the target concentration and dissolve in distilled water—this can be slow at higher concentrations. Can put on shaker overnight. Filter through 0.2 μm membrane and discard the first 0.5 ml to rinse the membrane. This stain can be kept with light protection at 4 °C for up to 1 year.

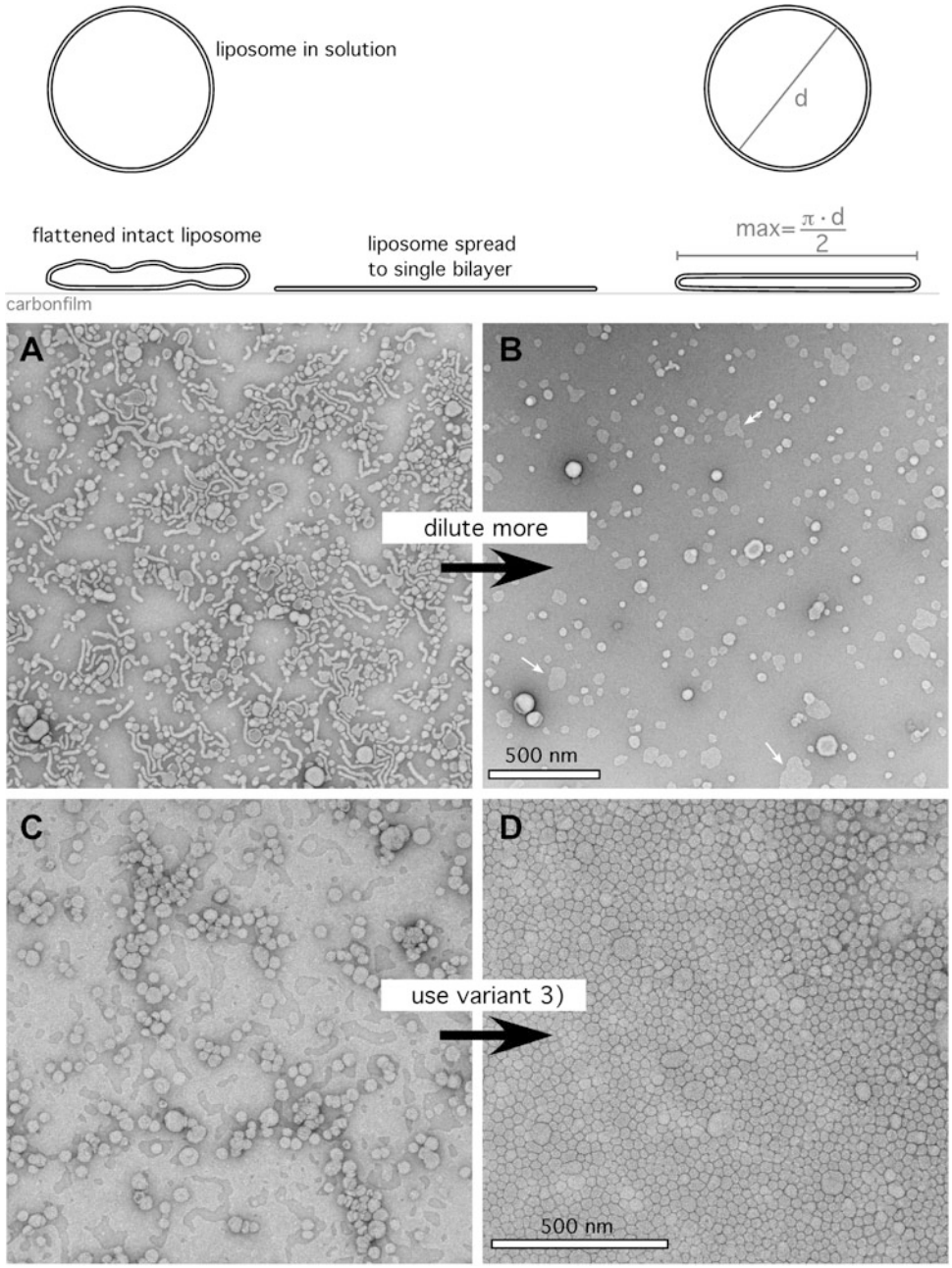

Fig. 2 Interaction of liposomes with the carbon film. Schematic on top shows liposome in solution, intact but flattened liposome in negative stain, and a liposome spread out on the carbon film. The right side explains the size increase of liposomes by flattening. Note that most experimentally observed flattening is by a factor of about ~1.25. (**a**) and (**b**) show a preparation of liposomes that tends to spread on carbon and forms worm-like micelles and tubes at high concentrations. Dilution can resolve the problem of tubes, but the liposomes are still observed to spread on the carbon film (examples shown by *small white arrows*). (**c**) and (**d**) show a liposome preparation that spreads on carbon film and forms a continuous film. Using variation 3 from Subheading 3.2 keeps most of the liposomes intact

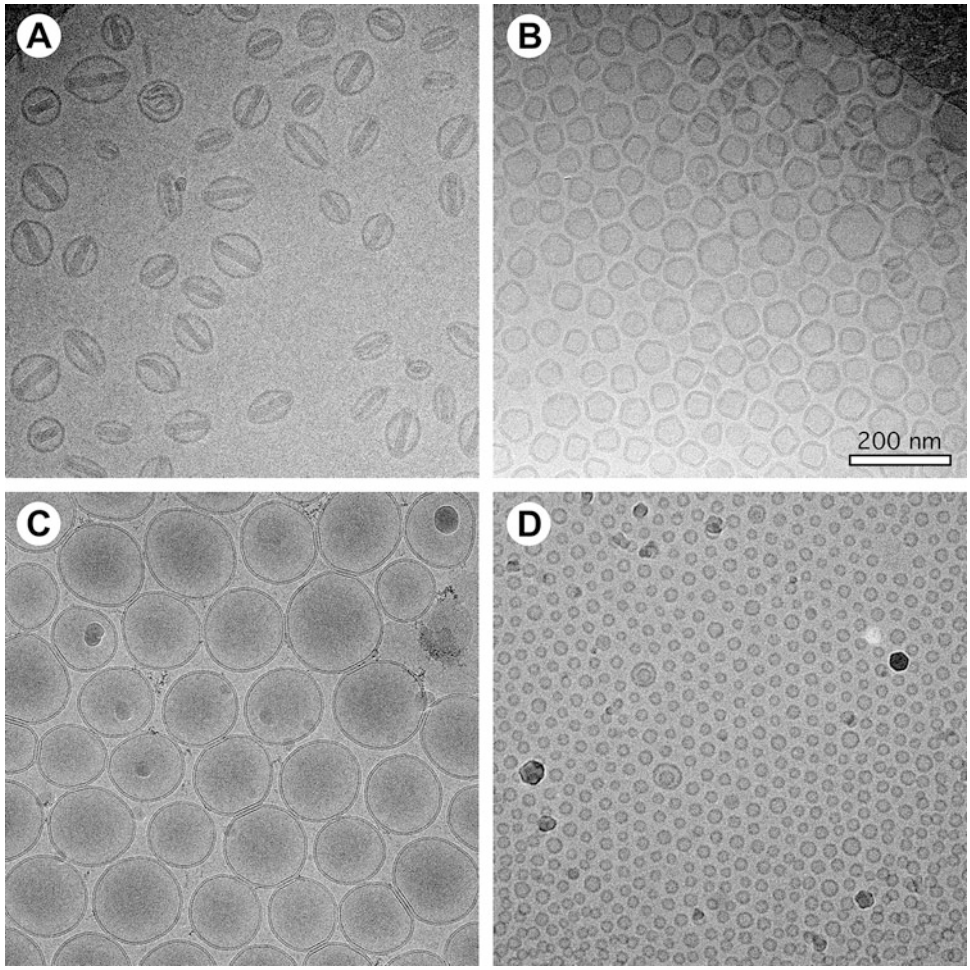

Fig. 3 Examples of cryoEM data of liposome preparations. (**a**) CryoEM images of Doxil®. The typical football-shaped liposomes and striated doxorubicin crystals inside are visible. (**b**) DPPC liposomes showing gel phase at room temperature. (**c**) and (**d**) Highly monodisperse liposome preparations at different sizes

(b) 2% ammonium molybdate
Ammonium molybdate stain has a neutral pH and has some advantage for certain preparations; but, the contrast is significantly reduced compared to UA. Make a 2% solution in distilled water and adjust the pH with ammonium or sodium hydroxide to pH 7.0 or slightly below. Do not exceed pH 7.0 by much as crystallization/precipitation may occur during drying of the stain.

(c) 0.7% uranyl formate (UF)
UF stain has a particularly fine grain and therefore results in very high resolution and detailed imaging of proteins, particularly small proteins. However, for most liposome preparations it does not result in any advantage over UA. The stain can be prepared according to [4].

(d) 2% methylamine tungstate and 2% methylamine vanadate (NanoVan, Nanoprobes, Yaphank, NY)
Methylamine tungstate and methylamine vanadate are both neutral pH stains that result in good high-resolution staining. In particular, methylamine vanadate has a small grain size and shows fine details; however, it has the lowest contrast of all the stains. Methylamine tungstate is a good universal stain with good wetting properties, often creating deeply stained areas.
Inclusion of 1% (w/v) of trehalose or sucrose in any of these stains can reduce flattening and potentially reduce some other artifacts of negative staining, but I have not studied this systematically. When adding trehalose or sucrose it might be advantageous to increase stain concentration (use 4% UA or 5% ammonium molybdate) [3, 18].

2. Biological grade tweezers.
3. Filter paper.
4. Carbon film only grids with around 5–6 mm thickness. Thinner carbon films allow more contrast, but are also less stable.
5. Glow-discharger or plasma cleaner. Home-built glow discharger can be made according to [19].
6. 0.1% polylysine.
7. Transmission electron microscope. Basically, any TEM can be used to image negative stained samples as they have high contrast and need no special treatment. For negative stain imaging of small details at lower doses, high-sensitive cameras might be needed.

2.2 Cryo-EM of Liposomes

1. Plunge freezer (*see* **Note 1**).
2. Transmission electron microscope set up for cryo-EM operation. Requirements for imaging of liposomes are not as stringent as for high-resolution cryo-EM of single particles. Almost any transmission electron microscope can be used. However, a high-quality CMOS or CCD camera is necessary for low-dose imaging. High voltage of the microscope (200–300 kV) is an advantage as the ice for the larger liposomes can be quite thick, but 120 kV will work in many cases.
3. Cryo-holder.
4. Holey carbon film grids.
5. Cryo-grid boxes.
6. Glow-discharger or plasma cleaner.
7. Storage dewar.

3 Methods

3.1 Standard Protocol for Negative Staining of Liposomes

1. Glow-discharge carbon film grids for a short time with the carbon surface toward the plasma, using any type of plasma cleaner. Optimize the time to have good spreading of water/solutions on the grid–longer times are not necessary. Glow-discharged grids should be used the same day (*see* **Note 2**).
2. Hold a glow-discharged grid using high-quality sharp forceps, or anti-capillary forceps with the carbon-coated side facing up (*see* **Note 3**). Lock the forceps with a rubber O-ring or use reverse action forceps and place it in an elevated position (e.g., on top of a closed petri dish) so the grid is easily accessible to pipetting.
3. Apply 4.5 μl of diluted liposome preparation to the glow-discharged grid, and wait for 30 s (*see* **Notes 4** and **5**).
4. Wick off the sample using filter paper and immediately add 4.5 μl of the same buffer—wait 10–15 s (*see* **Notes 6** and **7**).
5. Repeat wicking and adding buffer one more time to remove all sample not adhered to the carbon surface.
6. Wick off the buffer using filter paper and immediately add 4.5 μl of stain solution.
7. Repeat this step three more times in quick succession. Leave the last addition of stain on the grid for 30 s.
8. Wick off stain solution with filter paper. Carefully watch the liquid as it is wicked off and pull away the filter paper just when all visible solution is gone (*see* **Note 8**).
9. Dry the grid by fast movement of the forceps through the air back and forth. An incandescent light bulb can add some heat to increase the speed of drying. If available, a mild stream of compressed air or dry nitrogen can be used for very fast drying (*see* **Notes 9** and **10**).
10. After quick drying, let the grid dry for a few more minutes on the bench. Then image the grid in any TEM. Find properly stained areas (often intermediate stain levels are best) and adjust the protocol based on the observations (*see* **Notes 11–13**).

3.2 Variations of the Negative Staining Protocol for Certain Circumstances

1. To change the charged surface of the carbon film:

   Before adding sample, put a drop of 0.1% polylysine solution on the grid and wait for 30 s. Then wick off the polylysine, wash twice with buffer and continue with adding the sample (*see* **Note 14**). Continue with the same procedure as above.
2. To avoid buffer solution from getting sucking into the forceps and/or wetting the copper backside of the grid (which causes bad staining), use a droplet method for the negative staining procedure:

On a clean piece of parafilm put separate ~40 μl droplets of diluted liposome preparation, wash buffer, and stain. Let the freshly glow-discharged grid swim on the droplet with the carbon surface toward the solution and carefully move the grid from droplet to droplet with the forceps without wetting the backside of the grid. In extreme cases hold the grid with the forceps and keep it slightly away from the droplet so that the solution has no chance to touch the reverse side of the grid. Use the same order of one sample drop, two wash buffer, and four stain droplets as described in the standard protocol. Then dry the grid the same way as described in the standard protocol.

3. To reduce the time of liposome carbon surface interactions (a good choice for cases in which artifacts from liposome spreading are observed):
   Dilute liposome preparation into 1% UA, quickly place 4.5 μl on the carbon film, wick completely, and immediately dry down as fast as possible with a mild nitrogen stream (*see* Fig. 2 and **Note 15**).

3.3 Interpretation and Troubleshooting of Negative Stained Liposome Images

1. Negative staining of liposomes results in artifacts more often than negative staining of protein complexes. Lipids are not "fixed" in their native structure as proteins are by uranyl stains [5, 6], and their interaction with the carbon film surface often leads to spreading of lipids and sometimes recombination of lipids to hydrophilic films or other structures. Large liposomes might break during the drying process or fold into strange shapes (*see* Fig. 2). When liposome preparations interact strongly with the carbon film, further dilution of the preparation and variation of the protocol can alleviate some of the problems. But the results have to be carefully evaluated and interpreted. Unexpected observations/structures (e.g., open lipid films, rippled lipid phases, worm-like micelles and tubular structures, bicelles, micelles, etc.) should not solely rest on negative stain results but have to be confirmed by cryo-EM. Lipid composition likely explains most of the different behavior of liposome preparations toward carbon surfaces; in particular, a large amount of micelle-forming lipids (like DSPE-PEG 2000) probably allows easier transition from closed intact liposomes to open films and could encourage spreading on carbon surfaces. Buffer components (like salt, sucrose, etc.) can also influence interaction of liposomes with the carbon surface and could be varied to result in better negative staining. However, it is very difficult to systematically predict the interaction of liposomes with the carbon film. Some liposome preparations might not produce useful results under any condition (probably because they formed bilayer films very quickly and even at low concentrations).

2. Size measurements: If results of negative staining are free of artifacts, the images can be used to measure size distribution. However, negative stained liposomes are "flattened" and increase therefore in their measured size. At first approximation, the maximum diameter observed for flattened liposomes is half of the circumference of the original spherical liposomes (*see* Fig. 2), and therefore the measured diameter would be $\pi/2$ times the real diameter. Empirically, comparisons between cryo-EM and negative stain measurements have resulted in slightly smaller factors of 1.2–1.3. In cases where liposomes spread out onto the carbon film to form a lipid bilayer or even a lipid monolayer, measured sizes would be even higher and care should be taken to avoid measurements of such structures.

3.4 Cryo-EM of Liposomes

3.4.1 Plunge Freezing of Liposome Preparations (see **Note 1**)

1. Prepare grids in glow discharger with the carbon surface toward the plasma. Grids should be used within 1 h.
2. Prepare Vitrobot by loading 60 ml of water in the humidifier and setting the humidity to 100%.
3. Set up the liquid ethane dish by filling liquid nitrogen on the outside, wait for 5 min and then start slowly flowing ethane gas from a nozzle into the ethane cup. Fill the cup completely with liquid ethane, then remove the "spider tool" and wait for the ethane to solidify. Once a lot of the ethane is solid use a metal rod to melt most of the ethane in the center of the cup, but try to leave some solid ethane on the edges; this indicates that the ethane is at melting temperature and as cold as possible (*see* **Note 16**). Carefully put a grid box into the liquid nitrogen dish without splashing nitrogen into the ethane.
4. Set the Vitrobot to blotting force −5, blotting time 2.5 s (*see* **Note 17**).
5. Pick up a freshly glow discharged grid with the tweezers and secure it with the o-ring. Load the grid into the environmental chamber and start the process. Carefully load 3 μl of the liposome sample (*see* **Notes 18** and **19**) on the grid without touching the grid surface with the pipette tip.
6. Start the process on the Vitrobot. The Vitrobot will blot the grid and plunge it into the liquid ethane. Watch each blotting carefully, as the contact of the grid with the filter paper and the solution on the filter paper after blotting will indicate whether it was a successful process.
7. Remove the tweezers from the plunging rod without taking the grid out of the ethane. Unlock the o-ring and move the grid quickly through the nitrogen atmosphere into liquid nitrogen for a short while and then into the grid box (*see* **Notes 20–22**).
8. Grids can be stored in liquid nitrogen for extended periods of time, but can also be transferred to the cryo-EM holder immediately.

3.4.2 Plunge Freezing for Gels, Emulsions, and Very Viscous Samples

1. Instead of loading the empty grid into the Vitrobot as described in **step 5** of Subheading 3.4.1, apply 3 μl of the gel on the grid and remove almost everything by pulling the edge of a piece of filter paper over it in a shallow angle. This has to be done carefully to not damage the carbon film, but strongly enough to remove all visible gel—the grid should look almost completely fresh after the procedure.
2. Add 3 μl of appropriate buffer on the grid and proceed with the protocol as described above. These grids usually need longer blotting time to create good ice.

3.4.3 Transferring Grid and Loading the Cryo-Holder into the Microscope

1. Place the cryo-holder (*see* **Note 23**) into the transfer station.
2. Cool down the transfer station and the holder by continuously filling with liquid nitrogen. Once the holder dewar and workstation are full and the bubbling has subsided, wait for at least another 5 min to make sure the holder is completely cold.
3. Move the grid box with frozen grids into the transfer station. Transfer one grid with precooled tweezers into the holder tip (*see* **Notes 20** and **24**). Secure the grid with the clip ring or screw ring (depending on exact holder model). Immediately close the holder shutter and fill liquid nitrogen level to cover the holder tip.
4. Prepare the microscope for insertion of cryo-holder (depending on microscope model follow vendor instructions). For a Tecnai F20, fill dewar for anticontaminator with liquid nitrogen and keep cool for at least 1 h before loading the holder. Set stage position to $x = 0$, $y = 0$ and tilt to $-60°$. Prepump the airlock, set the airlock cycle to 90 s, start the turbo pump, and wait until it is at full speed.
5. Transfer the holder quickly but carefully into the airlock. Wait for the airlock cycle to complete (90 s) and insert into the column vacuum smoothly by resetting the stage rotation to 0° and rotating the holder counterclockwise (*see* **Note 25**).
6. Wait for column vacuum to reach levels close to before insertion of the holder. Then proceed with opening the shutter and starting to image the grid in the low-dose mode.

3.4.4 Imaging Liposomes at Low Dose

1. Use the low-dose imaging mode on the TEM to image the samples. On an FEI microscope (like the Tecnai F20) perform the normal alignment, adjust the eucentric height and set up Search, Focus, and Exposure modes (*see* **Note 26**). Use the Search mode to look for promising areas (based on ice thickness and contamination; *see* **Note 27**); use Focus mode to adjust the focus (*see* **Note 28**) and take an image by pressing the Exposure button.

2. If the grid has a good quality, take enough images for a complete analysis of the liposome preparation (*see* **Note 29**).
3. If more grids have to be loaded into the microscope, precool the transfer station after it has been completely warmed up and is at room temperature. Close the shutter and remove the holder from the microscope. Place the holder quickly into the precooled transfer station. The imaged grid can now be removed and a new grid can be loaded.
4. Remove the cryo-holder from the microscope. Place it back into the pumping station and run a warm-up cycle, followed by a zeolite cycle. Run a cryo-cycle on the microscope.

3.5 Interpretation and Troubleshooting of Cryo-EM Liposome Images

1. In most cases, cryo-EM images can be interpreted directly as two-dimensional projections of the three-dimensional structure of the liposomes. Some flattening in the thin ice layer can happen in particular for liposomes larger than about 150 nm. Tilted image pairs (e.g., 45° and 0°) can add additional information and be useful in some cases to confirm particular structures or situations, like checking whether liposomes are slightly compressed or confirming the flatness of bicelles.
2. The contamination of samples with ice from different sources is a common problem in cryo-EM [10, 20]. When contamination is observed, it is useful to know where ice is most likely resulting from so that workflows can be optimized. There are generally four different types of ice contamination each from different sources (*see* Fig. 4):
3. So-called "leopard" ice usually results from bad vacuum in the microscope or problems with the cryo-holder during transfer. When such ice is observed, check the anticontaminator in the microscope and the cryo-holder for problems. Also, blotting liquid ethane before transferring grids into liquid nitrogen can help mitigate such contaminations.
4. Large areas of crystalline (hexagonal) ice usually result from slow freezing or warming up of the grid during transfer. Check the plunge freezing process and the transfer of grid procedure (reduce the number of times that the grid is held in gaseous nitrogen atmosphere).
5. Small amorphous looking blobs of ice crystals (often cubic structure) usually result from transfers of the holder through a humid environment.
6. Large amorphous blobs and large crystals (usually hexagonal ice structure) result from contaminated liquid nitrogen.

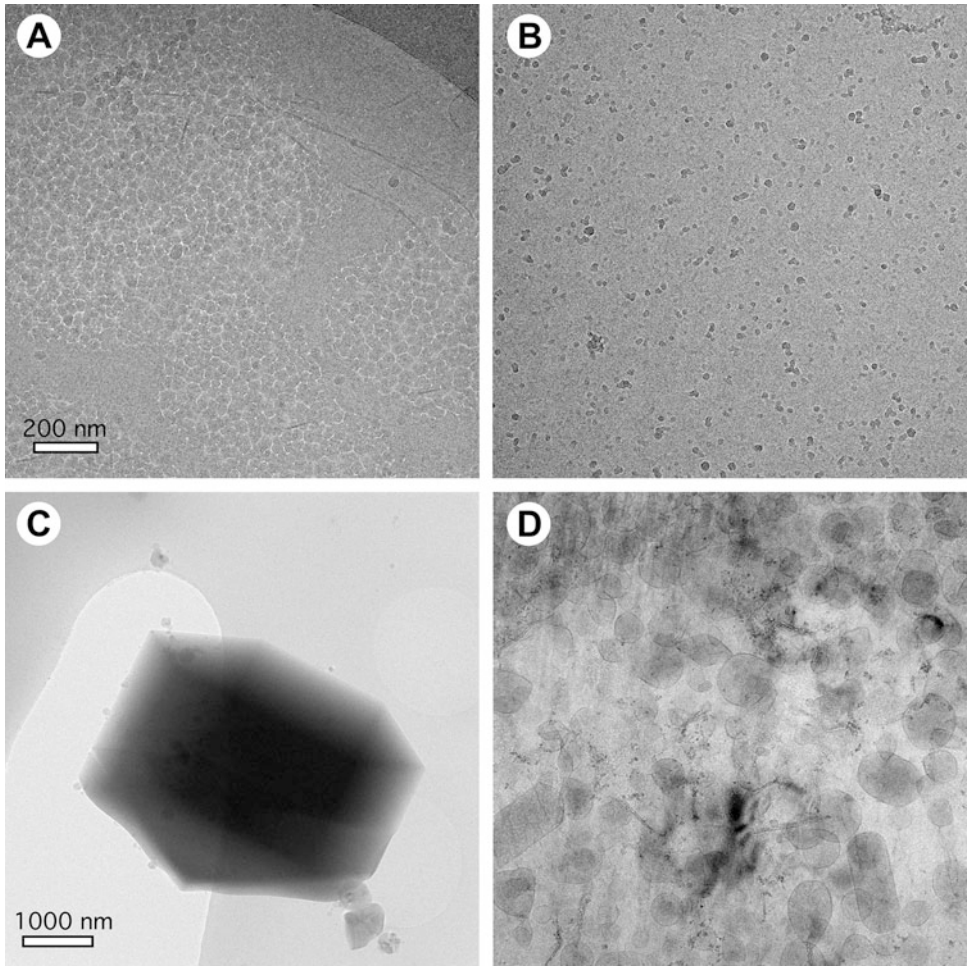

Fig. 4 Examples of ice contamination problems: (**a**) "leopard" ice, (**b**) cubic ice crystals, (**c**) large hexagonal ice crystal, (**d**) hexagonal ice sheets, often present over large areas of the grid

4 Notes

1. Any commercial or homebuilt plunge freezer can be used. However, for liposomes, an environmental chamber (like Vitrobot) can be useful. This allows for a high relative humidity environment for the grid before it is frozen and avoids structural changes due to osmotic pressure and temperature variations [21].
2. Unused grids can be glow-discharged again the next day without damage to the carbon film.
3. It is necessary to use high-quality forceps or anti-capillary forceps. Otherwise, liquid sample will be sucked away from grids by the capillary force between the forceps. If this is a continuous problem, use variation 2 of the negative stain protocol in Subheading 3.2.

4. The dilution of liposomes should be done in the same buffer or something with very similar osmolarity to avoid any osmotic shock to the liposomes as much as possible. The dilution has to be optimized based on observations of the final negative stain result. HEPES, TRIS, MOPS, and many other buffers can be used; phosphate buffer should be avoided. If original liposomes are in phosphate-based buffer try using HEPES with similar salt concentration for dilution and washing (e.g., use 20 mM HEPES, 150 mM NaCl instead of PBS).
5. If liposome solution gets to the reverse side (non-carbon copper side) of the grid, discard this grid and start over—it will result in very bad staining. When this continues to be a problem, reduce the application volume or use variation 2 of the negative stain protocol in Subheading 3.2.
6. Wick the grid from the side; the angle between the plane of the grid and the plane of the filter paper should be between 45° and 90°. Do not touch the carbon film surface of the grid directly.
7. Never let the grid completely dry until the last step of the protocol. Always add the next solution within a few seconds to prevent the grid from drying out.
8. For most stains, this procedure will leave a deep enough layer of stain in all areas of the grid for imaging. However, for higher concentrated stains (2% and higher) keep the filter paper in place a little longer to wick away more solution.
9. The quick drying creates areas with different stain depth on the grid, which enables the choice of optimal depth of staining. One can also leave grids on the bench or in a chemical hood to air dry more slowly. This creates a more even distribution of stain, but in that case it can be a problem to find optimal stain depth for imaging.
10. **Step 8** and in particular **step 9** (final wicking and drying speed) are the most important steps for high-quality staining. The faster the drying speed, the fewer artifacts are usually observed. These parameters should be varied and optimized based on the quality of staining observed.
11. Some samples do not adhere well to the carbon surface (e.g., PEGylated liposomes) and might be washed off by the repeated washing steps. If this is a problem (amount of liposomes is much lower than expected), the wash steps (**steps 5** and 7) can be reduced or completely omitted. For extreme cases, variation 3 of the negative stain protocol can be used (Subheading 3.2). However, this might increase precipitation and crystallization of salts and other buffer components on the grids. The balance between amount of particles and precipitation background has to be optimized in such cases.

12. Negatively stained grids can be stored for many days in a dry place with the exception of ammonium molybdate. Grids stained with ammonium molybdate have to be imaged immediately and cannot be stored even for one night.
13. Any TEM with almost any camera system can be used for imaging. Most stains are very stable under the beam, but use of lower doses can be useful to preserve especially small details in some cases.
14. The polylysine changes the surface of the carbon film from slightly negative to slightly positive, which can change the adhesion of oppositely charged liposomes.
15. This method might create artifacts from salt crystallization/precipitation or other buffer components as washing is minimal. However, it minimizes the time liposomes have to interact with the carbon surface and therefore often reduces artifacts that result from liposomes spreading out onto the carbon film.
16. As the ethane temperature is not controlled in the Vitrobot, make sure to set up the ethane in this way. Homebuilt plungers work in a similar fashion. Other commercial plunge freezers have different ways of controlling ethane temperature—make sure to follow vendors' instructions to get ethane as cold as possible.
17. These are good starting conditions, but for each sample and new buffer this may have to be optimized.
18. The sample volume can be optimized based on observed results. Larger volume will create thicker ice layers, less volume will create thinner ice layers.
19. Liposome suspension should be about 1.0–5.0 mg/ml lipid, which corresponds to about 3×10^{13} liposomes per ml. Buffer additives like glycerol and sucrose should be kept to a minimum, because they can significantly reduce the contrast at high concentrations.
20. Always precool any instruments used to touch the grid directly or indirectly (tweezers to move the grids or screwdrivers to close the grid box).
21. When transferring the grid, reduce the incidents and time that the grid is exposed to the nitrogen atmosphere while held in place by tweezers. During these instances, the grid is not cooled by any medium and the warm tweezers can very quickly warm up the grid to above $-150\ ^{\circ}C$ or higher to cause recrystallization of vitreous ice to hexagonal ice.
22. Sometimes large amounts of solid ethane on the grid can cause the microscope vacuum to crash and yield excessive amounts of leopard skin ice. If this is the case, excess ethane can be removed from the grid before putting it into liquid nitrogen. Precool filter paper in nitrogen atmosphere of the dish for 20 s and then quickly touch the grid to the filter paper.

23. The cryo-holder should be prepared before use by being in the pumping station for at least a 2 h zeolite cycle to create a good vacuum in the holder dewar. Before the zeolite cycle, the holder has to be at room temperature.
24. Grid transfer can be performed with the liquid nitrogen level well above the holder tip or with the liquid nitrogen level slightly below the holder tip (in the gas phase). Avoid levels close to the tip, because the bubbling will cause the grid to move around and jump unexpectedly, resulting in the grid getting lost.
25. A smooth movement without using any unnecessary force on the holder is needed to avoid crashing the microscope column vacuum.
26. Set the Exposure mode magnification to the lowest possible value that still results in an acceptable pixel size for analysis, as that allows for the largest possible field of view. Taking images with different magnifications of the same sample is recommended.
27. Promising areas for liposome imaging often have intermediate ice thickness. If the ice is too thin, no liposomes are observed (depending on their size) as they are excluded. Image areas with different ice thickness on each sample to find optimal conditions. Try to find the thinnest possible ice that still contains liposomes.
28. Choose the amount of defocus based on the necessary analysis. To image high-resolution details (e.g., measuring membrane thickness), it has to be close to focus (defocus of -1.5 to -2 μm); for rougher analysis, like overall size measurements, it can be further from focus (defocus of -4 to -5 μm) to increase contrast. It is often useful to take an image of the same area close to focus and another at higher defocus.
29. It is generally not recommended to save cryo-grids once loaded into the microscope because each transfer will increase ice crystal contamination. But, this can be done for very good grids with important samples.

Acknowledgment

This project has been funded in whole with Federal funds from the National Cancer Institute, National Institutes of Health, under Contract No. HHSN261200800001E. The content of this publication does not necessarily reflect the views or policies of the Department of Health and Human Services, nor does mention of trade names, commercial products, or organizations imply endorsement by the U.S. Government.

References

1. Bibi S, Kaur R, Henriksen-Lacey M, McNeil SE, Wilkhu J, Lattmann E, Christensen D, Mohammed AR, Perrie Y (2011) Microscopy imaging of liposomes: from coverslips to environmental SEM. Int J Pharm 417 (1–2):138–150. doi:10.1016/j.ijpharm.2010.12.021
2. Ruozi B, Belletti D, Tombesi A, Tosi G, Bondioli L, Forni F, Vandelli MA (2011) AFM, ESEM, TEM, and CLSM in liposomal characterization: a comparative study. Int J Nanomedicine 6:557–563. doi:10.2147/IJN.S14615
3. Harris JR (2007) Negative staining of thinly spread biological samples. In: Kuo J (ed) Electron microscopy: methods and protocols. Humana Press, Totowa, NJ, pp 107–142. doi:10.1007/978-1-59745-294-6_7
4. Ohi M, Li Y, Cheng Y, Walz T (2004) Negative staining and image classification—powerful tools in modern electron microscopy. Biol Proced Online 6(1):23–34. doi:10.1251/bpo70
5. Silva MT, Guerra FC, Magalhaes MM (1968) The fixative action of uranyl acetate in electron microscopy. Experientia 24(10):1074
6. Zhao F-Q, Craig R (2003) Capturing time-resolved changes in molecular structure by negative staining. J Struct Biol 141(1):43–52. doi:10.1016/S1047-8477(02)00546-4
7. Cheng Y, Grigorieff N, Penczek PA, Walz T (2015) A primer to single-particle cryo-electron microscopy. Cell 161(3):438–449. doi:10.1016/j.cell.2015.03.050
8. Frank J (2002) Single-particle imaging of macromolecules by cryo-electron microscopy. Annu Rev Biophys Biomol Struct 31:303–319. doi:10.1146/annurev.biophys.31.082901.134202
9. Grassucci RA, Taylor D, Frank J (2008) Visualization of macromolecular complexes using cryo-electron microscopy with FEI Tecnai transmission electron microscopes. Nat Protoc 3(2):330–339. doi:10.1038/nprot.2007.474
10. Grassucci RA, Taylor DJ, Frank J (2007) Preparation of macromolecular complexes for cryo-electron microscopy. Nat Protoc 2(12): 3239–3246. doi:10.1038/nprot.2007.452
11. Milne JL, Borgnia MJ, Bartesaghi A, Tran EE, Earl LA, Schauder DM, Lengyel J, Pierson J, Patwardhan A, Subramaniam S (2013) Cryo-electron microscopy–a primer for the non-microscopist. FEBS J 280(1):28–45. doi:10.1111/febs.12078
12. Almgren M, Edwards K, Karlsson G (2000) Cryo transmission electron microscopy of liposomes and related structures. Colloids Surf A Physicochem Eng Asp 174(1–2):3–21. doi:10.1016/S0927-7757(00)00516-1
13. Friedrich H, Frederik PM, de With G, Sommerdijk NA (2010) Imaging of self-assembled structures: interpretation of TEM and cryo-TEM images. Angew Chem Int Ed Engl 49 (43):7850–7858. doi:10.1002/anie.201001493
14. Helvig S, Azmi IDM, Moghimi SM, Yaghmur A (2015) Recent advances in Cryo-TEM imaging of soft lipid nanoparticles. AIMS Biophys 2 (2):116–130. doi:10.3934/biophy.2015.2.116
15. Kuntsche J, Horst JC, Bunjes H (2011) Cryogenic transmission electron microscopy (cryo-TEM) for studying the morphology of colloidal drug delivery systems. Int J Pharm 417(1-2):120–137. doi:10.1016/j.ijpharm.2011.02.001
16. Tahara Y, Fujiyoshi Y (1994) A new method to measure bilayer thickness: cryo-electron microscopy of frozen hydrated liposomes and image simulation. Micron 25(2):141–149. doi:10.1016/0968-4328(94)90039-6
17. Adler K, Schiemann J (1985) Characterization of liposomes by scanning electron microscopy and the freeze-fracture technique. Micron and Microscopica Acta 16(2):109–113. doi:10.1016/0739-6260(85)90039-5
18. Harris JR, Gerber M, Gebauer W, Wernicke W, Markl J (1996) Negative stains containing Trehalose: application to tubular and filamentous structures. Microsc Microanal 2(1):43–52. doi:10.1017/S1431927696210438
19. Aebi U, Pollard TD (1987) A glow discharge unit to render electron microscope grids and other surfaces hydrophilic. J Electron Microsc Tech 7(1):29–33. doi:10.1002/jemt.1060070104
20. Resch GP, Brandstetter M, Konigsmaier L, Urban E, Pickl-Herk AM (2011) Immersion freezing of suspended particles and cells for cryo-electron microscopy. Cold Spring Harb Protoc 2011(7):803–814. doi:10.1101/pdb.prot5642
21. Frederik PM, Hubert DH (2005) Cryoelectron microscopy of liposomes. Methods Enzymol 391:431–448. doi:10.1016/s0076-6879(05)91024-0

Part IV

Immunology

Chapter 9

Updated Method for In Vitro Analysis of Nanoparticle Hemolytic Properties

Barry W. Neun, Anna N. Ilinskaya, and Marina A. Dobrovolskaia

Abstract

Hemolysis is damage to red blood cells (RBCs), which results in the release of the iron-containing protein hemoglobin into plasma. An in vitro assay was developed and described earlier for the analysis of nanoparticle hemolytic properties. Herein, we present a revised version of the original protocol. In this protocol, analyte nanoparticles and controls are incubated in blood. Undamaged RBCs are removed by centrifugation and hemoglobin, released by the damaged erythrocytes, is converted to cyanmethemoglobin by incubation with Drabkin's reagent. The amount of cyanmethemoglobin in the supernatant is measured by spectrophotometry. This measured absorbance is compared to a standard curve to determine the concentration of hemoglobin in the supernatant. The measured hemoglobin concentration is then compared to the total hemoglobin concentration to obtain the percentage of nanoparticle-induced hemolysis. The revision includes updated details about nanoparticle sample preparation, selection of nanoparticle concentration for the in vitro study, updated details about assay controls and case studies about nanoparticle interference with the in vitro hemolysis assay.

Key words Nanoparticles, Hemolysis, Hemoglobin, Red blood cells (RBC)

1 Introduction

Erythrocytes comprise approximately 45% of whole blood by volume. Hemolysis refers to the damage of red blood cells leading to the release of intracellular erythrocyte content into the blood plasma. When it occurs in vivo, hemolysis can lead to anemia, jaundice, and other pathological conditions, which may become life threatening. Hemoglobin is a dominant protein carried by erythrocytes. When it is contained inside the cell, it plays a key role in carrying oxygen to other cells and tissues. However, extracellular hemoglobin is toxic and may affect vascular, myocardial, renal, and central nervous system tissues. This is why all medical devices and drugs which come in contact with blood are required to be tested for potential hemolytic properties.

Scott E. McNeil (ed.), *Characterization of Nanoparticles Intended for Drug Delivery*, Methods in Molecular Biology, Vol. 1682, DOI 10.1007/978-1-4939-7352-1_9,

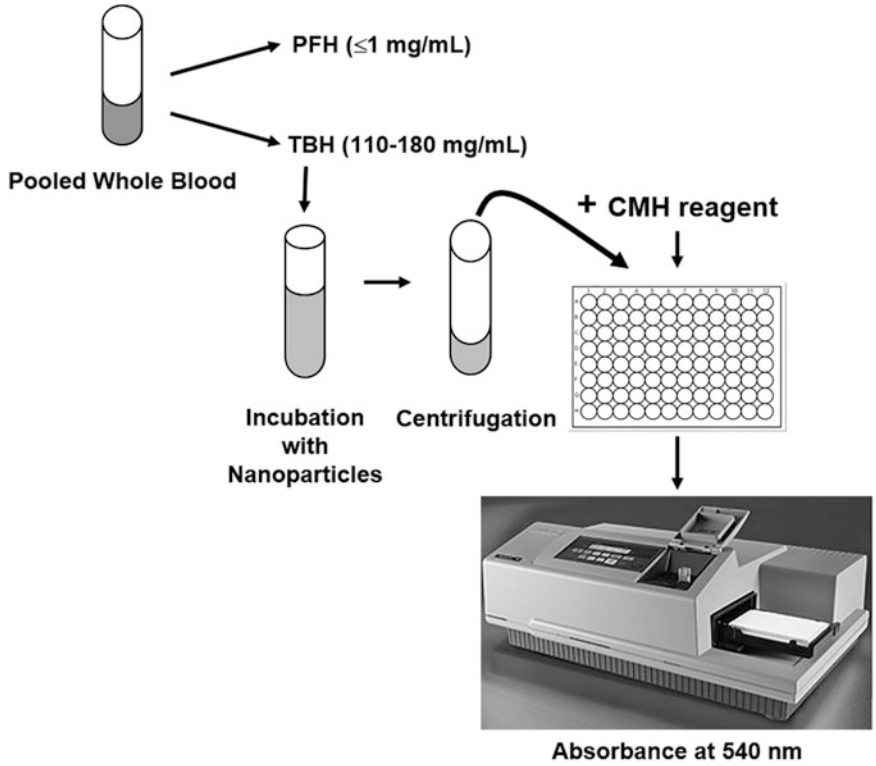

Fig. 1 Schematic illustration of the steps in this in vitro assay to evaluate nanoparticle hemolytic properties. *PFH* plasma-free hemoglobin, *CMH* Cyanmethemoglobin, *TBH* total blood hemoglobin

This chapter describes a revised protocol for quantitative colorimetric determination of total hemoglobin in the whole blood (TBH) and plasma-free hemoglobin (PFH) (Fig. 1). The original protocol was presented in the first edition of this book [1]. The revision includes updated details about nanoparticle sample preparation, selection of nanoparticle concentration for the in vitro study, assay controls, and case studies about nanoparticle interference with the in vitro hemolysis assay.

An increase in the PFH is indicative of erythrocyte damage by the test material (a positive control substance or a nanoparticle). Hemoglobin, released from damaged erythrocytes, is unstable and forms several derivatives with different optical properties. Hemoglobin and its derivatives, except sulfhemoglobin, are oxidized to methemoglobin by ferricyanide in the presence of alkali. Addition of the Drabkin's solution containing cyanide (also called CMH Reagent) converts methemoglobin into CMH form, which is the most stable form of hemoglobin and can then be detected by spectrophotometry at 540 nm. Addition of CMH Reagent to the whole blood sample is needed to lyse erythrocytes and estimate TBH, while its addition to plasma is used to detect PFH. A hemoglobin standard is used to build a standard curve covering the concentration range from 0.025 to

0.80 mg/mL, and to prepare quality control samples at low (0.0625 mg/mL), mid (0.125 mg/mL), and high (0.625 mg/mL) concentrations for monitoring assay performance. The results, expressed as percent of hemolysis, are used to evaluate the acute in vitro hemolytic properties of nanoparticles**.** Other versions of the hemolysis assay are available in the literature; these protocols typically omit reduction of the hemoglobin to its stable CMH form and estimate the amount of hemolysis by measuring oxyhemoglobin at one of its primary absorbance peaks (i.e., 415, 541, or 577 nm). These assays and their limitations have been previously reviewed by Malinauskas [2]. The protocol described in this document is based on ASTM International standards [3, 4]. We recently reviewed the in vitro–in vivo correlation of the hemolysis assays based on both the Nanotechnology Characterization Lab (NCL) experience with this protocol and on the literature using other assay formats [5]. Critical review of nanomaterial hemolytic properties as well as methods for their estimation is also available in a recent review by Wildt et al. [6].

2 Materials

1. Cyanmethemoglobin (CMH) Reagent.
2. Hemoglobin Standard.
3. Ca^{2+}/Mg^{2+}-free Phosphate Buffered Saline (PBS).
4. Normal human whole blood anti-coagulated with Li-heparin from at least 3 donors.
5. 1% Triton X-100 diluted in sterile diluted water.
6. Analyte nanoparticle sample (*see* **Note 1**).
7. 96-well plates suitable for cell culture.
8. Water bath set at 37 °C or incubator set at 37 °C with a tube rotator.
9. Plate reader capable of reading absorbance at 540 nm.

3 Methods

3.1 Preparation of Standards and Controls

1. Prepare fresh hemoglobin *calibration standards* for each experiment, discard leftovers after use. An example of the preparation of standards at concentration range of 0.025 mg/mL–0.8 mg/mL is shown in Table 1. Volumes can be adjusted as needed.
2. Prepare fresh *quality control (QC)* samples for each experiment, discard leftovers after use. An example of the preparation of QC samples at 0.0625, 0.125, and 0.625 mg/mL is shown in Table 2. Volumes can be adjusted as needed.

Table 1
Preparation of calibration samples

Standard	Nominal concentration (mg/mL)	Preparation procedure
Cal 1	0.80	2 mL of stock solution
Cal 2	0.40	1 mL Cal 1 + 1 mL CMH reagent
Cal 3	0.20	1 mL Cal 2 + 1 mL CMH reagent
Cal 4	0.10	1 mL Cal 3 + 1 mL CMH reagent
Cal 5	0.05	1 mL Cal 4 + 1 mL CMH reagent
Cal 6	0.025	1 mL Cal 5 + 1 mL CMH reagent

Table 2
Preparation of quality control samples

Standard	Nominal concentration (mg/mL)	Preparation procedure
QC 1	0.625	1.5 mL of stock solution +0.42 mL CMH reagent
QC 2	0.125	200 μL QC 1 + 800 μL CMH reagent
QC 3	0.0625	100 μL QC 1 + 900 μL CMH reagent

3. Prepare *positive control* sample. Any reagent or a nanomaterial that reproducibly induces ≥8% of hemolysis in this assay can be used as the assay positive control. Triton X-100 at a stock concentration of 1% (10 mg/mL) is an example positive control. Triton X-100 can be prepared in sterile distilled water and kept refrigerated (at a nominal temperature of 4 °C) for up to 2 weeks. Alternatively, a commercial 10% solution can be used and stored according to the manufacturer's instructions.
4. Prepare *negative control* sample. PBS supplied as a sterile solution can be used as the negative control. Store the stock solution at room temperature. Alternatively, a solution of polyethylene glycol or any other material known not to be hemolytic can be used as the negative control. When such reagents are used, please refer to the preparation and storage instructions by the reagent manufacturer.
5. Prepare *vehicle control* sample. Vehicle control is the buffer or media used to formulate test nanomaterials. Common excipients used in nanoformulations are trehalose, sucrose, and albumin. However, other reagents and materials are also used alone or in combination. Vehicle control should match formulation buffer of the test-nanomaterial by both composition and concentration. This control can be skipped if nanoparticles are stored in PBS.
6. Prepare an *inhibition/enhancement control*. This control is needed to estimate potential interaction between nanoparticles

and PFH which masks hemoglobin from detection by the assay. Prepare by spiking cell-free supernatant obtained from the positive control sample with nanoparticles at the concentrations matching those analyzed by the assay. For example, if a nanoparticle is tested at four concentrations (0.008, 0.04, 0.2, and 1 mg/mL), then cell-free supernatant derived from the assay positive control should be spiked with 0.008, 0.04, 0.2, and 1 mg/mL of that nanoparticle. This control is helpful in identifying false-negative results when a material with strong hemolytic potential (i.e., % hemolysis >90) is used as the assay positive control. It also helps identify a potential enhancement type of interference when a low potency positive control (% hemolysis 8–50) is used. Dilution factor of 1.1 is used to adjust the test results derived from these samples to account for the positive control dilution. False-positive interference resulting from nanoparticle optical properties overlapping with the assay wavelength (540 nm) is identified by the nanoparticle-only blood-free control (*see* **step 7**).

7. Prepare *blood-free control*. Nanoparticles diluted in PBS to the same final concentration as those evaluated in the assay using whole blood and subjected to the same manipulation as test samples (i.e., incubation at 37 °C for 3 h, followed by centrifugation and mixing with CMH reagent listed in **steps 16–18**, **21**, and **23** in Subheading 3.3) can serve as an additional control to rule out false-positive assay results.

3.2 Preparation of Blood and Nanoparticle Samples

1. Prepare blood. Collect whole blood in tubes containing Li-heparin as an anticoagulant from at least three donors. Discard first 10 cc. The blood can be used fresh or stored at 2–8 °C for up to 48 h. On the day of the assay, prepare pooled blood by mixing equal proportions of blood from each donor. Donors are preselected so that compatible blood types are mixed. The assay can also be performed in the blood of individual donors.
2. Prepare nanoparticle samples. This assay requires 1.0 mL of nanoparticle solution, at a concentration 9 times the highest final tested concentration, dissolved/resuspended in PBS. The concentration is selected based on the plasma concentration of the nanoparticle at the intended therapeutic dose. For the purpose of this protocol, this concentration is called "theoretical plasma concentration." Considerations for estimating theoretical plasma concentration were reviewed elsewhere [5] and are summarized in Box 1. This assay utilizes human whole blood; therefore, estimation of theoretical plasma concentration should be based on human dose. If a given nanoparticle formulation was tested in animals, conversion of the animal dose into human equivalent dose is needed. For considerations about performing such conversion, please refer to the FDA guidance for industry [7].

Box 1. Example Calculation of Nanoparticle Concentration for In Vitro Test

Assume the mouse dose is known to be 123 mg/kg.

$$\text{human dose} = \frac{\text{mouse dose}}{12.3} = \frac{123\frac{mg}{kg}}{12.3} = 10 \text{ mg/kg}$$

Blood volume makes up approximately 8% of body weight (e.g. a 70 kg human has approximately 5.6 L (8% of 70) of blood). This allows for a very rough estimate of what the maximum blood concentration may be.

$$\text{in vitro concentration}_{human\ matrix} = \frac{human\ dose}{human\ blood\ volume} = \frac{70\ kg\ x\ 10\frac{mg}{kg}}{5.6\ L}$$

$$= \frac{700\ mg}{5.6\ L} = 0.125 \text{ mg/mL}$$

Box 1 Estimation of nanomaterial concentration. The box shows an example of calculating nanoparticle concentration for the in vitro hemolysis assay. Reproduced with permission from ref. 5

3.3 Blood Qualification (Steps 1–8) and Hemolysis Assay (Steps 9–25)

1. Take a 2–3 mL aliquot of the pooled blood and centrifuge 15 min at 800 × *g* (*see* **Note 1**).
2. Collect supernatant. Keep at room temperature while preparing a standard curve, QCs, and total hemoglobin sample. The collected sample is used to determine PFH.
3. Add 200 μL of each calibration standard (CAL), QC, and blank (CMH Reagent, B0) per well on a 96-well plate. Fill 2 wells for each calibrator and 4 wells for each QC and blank. Position test samples so they are bracketed by QC (Fig. 2, Plate Map 1).
4. The assay will evaluate four concentrations: 10× (or when feasible 100×, 30×, or 5×) of theoretical plasma concentration, theoretical plasma concentration, and two 5-fold serial dilutions of the theoretical plasma concentration. When the intended therapeutic concentration is unknown, the highest final concentration is 1 mg/mL or the highest reasonably achievable concentration. For example, if the final theoretical plasma concentration to be tested is 0.2 mg/mL, then a stock of 18 mg/mL will be prepared and diluted 10-fold (1.8 mg/mL), followed by two 1:5 serial dilutions (0.36 and 0.072 mg/mL). When 0.1 mL of each of these samples is added to the test tube and mixed with 0.7 mL of PBS and 0.1 mL of blood, the final nanoparticle concentrations tested in the assay are: 2.0, 0.2, 0.04, and 0.008 mg/mL.
5. Add 200 μL of TBH sample prepared by combining 20 μL of the pooled whole blood and 5.0 mL of CMH Reagent. Fill 6 wells (Fig. 2, Plate Map 1).
6. Add 100 μL of plasma (PFH) per well on a 96-well plate. Fill 6 wells (Fig. 2, Plate Map 1).

Plate 1: Used to determine amount of total blood hemoglobin and plasma free hemoglobin

	1	2	3	4	5	6	7	8	9	10	11	12
A	B0	CAL1	CAL2	CAL3	CAL4	CAL5	CAL6	QC1	QC2	QC3	TBH	TBH
B	B0	CAL1	CAL2	CAL3	CAL4	CAL5	CAL6	QC1	QC2	QC3	TBH	TBH
C	TBH	PFH	PFH	PFH	B0	QC1	QC2	QC3				
D	TBH	PFH	PFH	PFH	B0	QC1	QC2	QC3				
E												
F												
G												
H												

Plate 2 or any subsequent plates: Used to determine hemolysis in nanoparticle samples

	1	2	3	4	5	6	7	8	9	10	11	12
A	B0	CAL1	CAL2	CAL3	CAL4	CAL5	CAL6	QC1	QC2	QC3	TBHd	TBHd
B	B0	CAL1	CAL2	CAL3	CAL4	CAL5	CAL6	QC1	QC2	QC3	TBHd	TBHd
C	TBHd	NP w/Blood	NP w/Blood	NP w/Blood	NP w/Blood	NP w/Blood	NP w/Blood	NP w/Blood	NP w/Blood	NP w/Blood	NP w/Blood	NP w/Blood
D	TBHd	NP w/Blood	NP w/Blood	NP w/Blood	NP w/Blood	NP w/Blood	NP w/Blood	NP w/Blood	NP w/Blood	NP w/Blood	NP w/Blood	NP w/Blood
E	NP w/Blood	NP w/o Blood	NP w/o Blood	NP w/o Blood	NP w/o Blood	NP w/o Blood	NP w/o Blood	NP w/o Blood	NP w/o Blood	NP w/o Blood	NP w/o Blood	NP w/o Blood
F	NP w/Blood	NP w/o Blood	NP w/o Blood	NP w/o Blood	NP w/o Blood	NP w/o Blood	NP w/o Blood	NP w/o Blood	NP w/o Blood	NP w/o Blood	NP w/o Blood	NP w/o Blood
G	NP w/o Blood	PC	PC	NC	NC	B0	QC1	QC2	QC3	IEC	IEC	IEC
H	NP w/o Blood	PC	PC	NC	NC	B0	QC1	QC2	QC3	IEC	IEC	IEC

Fig. 2 Example plate map for a 96-well plate. *B0* blank, *CAL* calibration sample, *QC* quality control sample, *PFH* plasma-free hemoglobin, *TBH* total blood hemoglobin, *TBHd* total blood hemoglobin after dilution to the theoretical value of 10 mg/mL, *NP* nanoparticle sample

7. Add 100 μL of CMH Reagent to each well containing sample (*see* **Note 2**).
8. Cover plate with plate sealer and gently shake on a plate shaker for 1–2 min. Shaker speed settings should be vigorous enough to allow mixing, but should avoid spillage and cross-well contamination (e.g., LabLine shaker speed 2–3).
9. Read the absorbance at 540 nm to determine hemoglobin concentration. Use a dilution factor of 2 for PFH samples and a dilution factor of 251 for TBH. If calculated PFH concentration is below 1 mg/mL, proceed to the next step.
10. Dilute pooled whole blood with Ca^{2+}/Mg^{2+}-free PBS to adjust TBH concentration to 10 ± 2 mg/mL (TBHd).
11. Set up 2 racks. Rack 1 contains tubes for the sample incubation with blood. Rack 2 contains tubes for the nanoparticle-only (no blood) control. Prepare 6 tubes for each test sample and place 3 tubes into Rack 1 and 3 tubes into Rack 2. Place 4 tubes for the positive control, 2 tubes for the negative control and

2 tubes of the vehicle control (if the vehicle is PBS, this samples can be skipped) into Rack 1.

12. Add 100 μL of the test sample or control in corresponding tubes in Rack 1 and Rack 2 as described in **step 10**.
13. Add 700 μL of Ca^{2+}/Mg^{2+}-free PBS to each tube in Rack 1.
14. Add 800 μL of Ca^{2+}/Mg^{2+}-free PBS into each tube in Rack 2.
15. 'Add 100 μL of the TBHd prepared in **step 9** to all tubes in Rack 1.
16. Cover tubes and gently rotate to mix (*see* **Note 3**).
17. Place the tubes in a water bath set at 37 °C and incubate for 3 h ± 15 min, mixing the samples every 30 min. Alternatively, tubes may be incubated on a tube rotator in an incubator set at 37 °C.
18. Remove the tubes from water bath or incubator. If a water bath was used, dry excess water with absorbent paper.
19. Centrifuge the tubes for 15 min at 800 × *g* (*see* **Notes 4** and **5**).
20. Prepare a fresh set of calibrators and QCs.
21. Prepare inhibition enhancement controls by spiking positive control supernatant from **step 18** with nanoparticles at the final particle concentration as in the test samples.
22. To a fresh 96-well plate, add 200 μL of blank reagent, calibrators, QCs, and TBHd prepared by combining 400 μL of blood from **step 9** with 5.0 mL of CMH reagent. Fill 2 wells for each calibrator, 4 wells for blank and each QC, and 6 wells for the TBHd sample. As before, position all test samples between QCs on the plate (Fig. 2, Plate Map 2).
23. Add 100 μL per well of test samples and controls (positive, negative, and vehicle with and without blood) prepared in **step 18** as well as inhibition/enhancement control from **step 20**. Test each sample in duplicate (Fig. 2, Plate Map 2).
24. Add 100 μL of CMH Reagent to each well containing sample and controls (*see* **Note 2**).
25. Cover plate with plate sealer and gently shake on a plate shaker (LabLine shaker speed settings 2–3 or as appropriate for a given shaker).
26. Read the absorbance at 540 nm to determine the concentration of hemoglobin. Use a dilution factor of 18 for samples and controls and a dilution factor of 13.5 for TBHd.

3.4 Calculations and Results Interpretation

Four-parameter regression algorithm is used to build a calibration curve. The following parameters should be calculated for each calibrator and QC sample:

Percent Coefficient of Variation (%CV):

$$\frac{\text{Standard deviation}}{\text{Mean}} \times 100\%$$

%CV should be calculated for each blank, positive control, negative control, and unknown sample.

Percent Difference from Theoretical (PDFT):

$$\frac{(\text{Calculated concentration} - \text{Theoretical concentration})}{\text{Theoretical concentration}} \times 100\%$$

Percent Hemolysis:

$$\frac{\text{Hemoglobin in test sample}}{\text{TBHd}} \text{ x } 100\%$$

Percent hemolysis less than 2 means the test sample is not hemolytic; 2–5% hemolysis means the test sample is slightly hemolytic; and >5% hemolysis means the test sample is hemolytic [2, 3].

3.5 Acceptance Criteria

The acceptance criteria described herein are based on the standard practices for bioanalytical method validation [8, 9]. Please review **Note 6**.

1. %CV and PDFT for each calibration standard and QC should be within 20%. The exception is the lowest calibration standard (Cal 6), for which 30% is acceptable. A plate is accepted if 2/3 of all QC levels and at least one of each level have demonstrated acceptable performance. If not, the entire run should be repeated.
2. %CV for each positive control, negative control, and unknown sample should be within 20%. At least one replicate of positive and negative controls should be acceptable for a run to be accepted.
3. If both replicates of the positive control or negative control fail to meet acceptance criterion described in **step 2**, the run should be repeated.
4. Within the acceptable run, if two of three replicates of unknown sample fail to meet acceptance criterion described in **step 2**, this unknown sample should be re-analyzed.

4 Notes

1. Always wear appropriate personal protective equipment and take appropriate precautions when handling your nanomaterial. Many occupational health and safety practitioners recommend wearing two layers of gloves when handling nanomaterials. Also, be sure to follow your facility's recommended disposal procedure for your specific nanomaterial.
2. *Do not* add CMH Reagent to wells containing calibration standards, QCs, TBH, and TBHd. These samples were already prepared and diluted in CMH reagent.

3. Vortexing may damage erythrocytes and should be avoided.
4. When centrifugation is complete, examine tubes and record any unusual appearance that can help in result interpretation (Fig. 1).
5. If nanoparticles have absorbance at or close to 540 nm, removal of these particles from supernatant will be required before proceeding to the next step. For example, 10–50 nm colloidal gold nanoparticles have absorbance at 535 nm. After **step 18** of Subheading 3.3, supernatants should be transferred to fresh tubes and centrifuged for 30 min at 18,000 × *g*. Removal of nanoparticles from supernatant is specific to the type of nanoparticles; and when applied, appropriate validation experiments should be conducted to ensure that a given separation procedure does not affect assay performance. In certain cases, removal of particles is not feasible. When this is the case, assay results obtained for a particle incubated with blood is adjusted by subtracting results obtained for the same particle in the nanoparticle-only no blood control (*see* **step 10** of Subheading 3.3 and refer to samples in Rack 2). Examples of interference and ways to remove it are shown in Figs. 3 and 4.

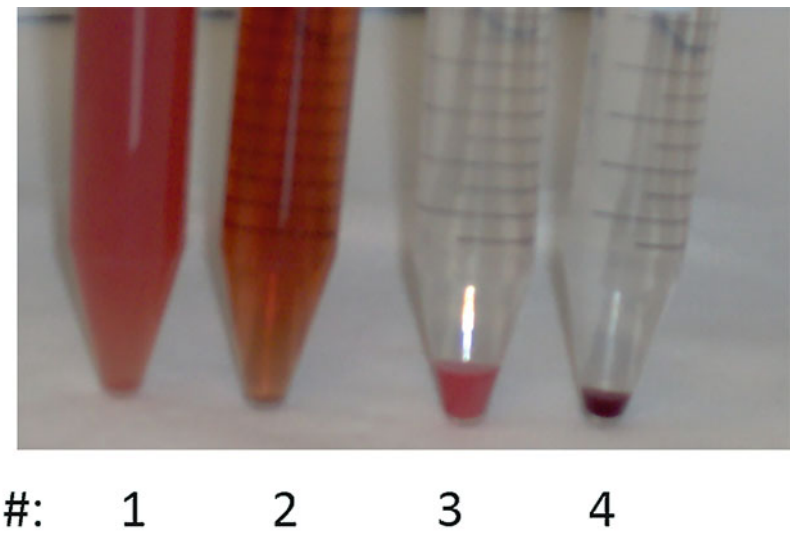

Fig. 3 An example of false-negative interference. This example demonstrates the importance of recording sample appearance after centrifugation to avoid false-negative results. Polystyrene nanoparticles with a size of 20 nm (tube 1) and polystyrene nanoparticles with a size of 50 nm (tube 2) demonstrated hemolytic activity that can be observed by the color of the supernatant. Polystyrene nanoparticles with a size of 80 nm were also hemolytic. However, the 80 nm-sized polystyrene nanoparticles absorbed hemoglobin as seen from the pellet size and color. Sample #4 is the negative control. No hemolytic activity was observed in the supernatant, and intact red blood cells formed a tight dark pellet on the bottom of the tube

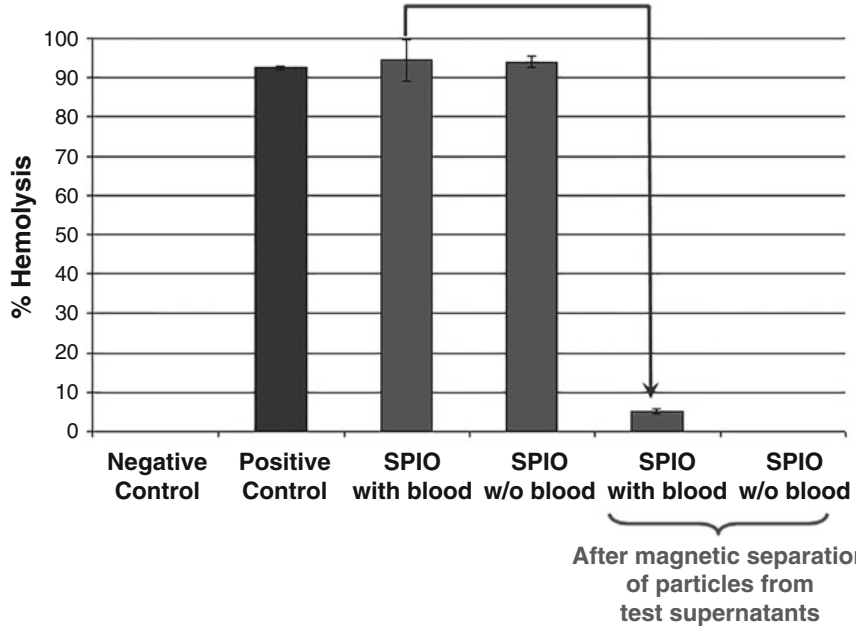

Fig. 4 An example of false-positive interference. In this example, superparamagnetic iron oxide nanoparticles were tested in the hemolysis assay. When the optical density (OD) of the nanoparticles was evaluated against the hemoglobin standard curve, it resulted in 100% hemolysis. When a control sample containing all reaction components, except the blood (without blood control), was evaluated against the same standard curve, the calculated percent hemolysis was also very high, approaching 100%. Before testing on the 96-well plate, the tube containing cell-free supernatant was incubated on a magnet for 16 h. At the end of the incubation, iron oxide nanoparticles accumulated near the magnet which allowed for the collection of the nanoparticle-free supernatant. When this supernatant was evaluated against the standard curve, no percent hemolysis was calculated in the blood-free control and nanoparticle hemolysis was below 2%

6. NCL does not endorse suppliers. However, we found that a new user benefits from knowing catalog information of reagents used in our assays. If you need ideas of what reagents are used at the NCL, please review NCL method ITA-1 available at https://ncl.cancer.gov/resources/assay-cascade-protocols. When other reagents are used, the assay performance may change. When using reagents and instruments from sources other than that used in our protocols, assay performance qualification is needed to verify the assay functionality and validity.

Acknowledgment

This project has been funded in whole or in part with Federal funds from the National Cancer Institute, National Institutes of Health, under Contract No. HHSN261200800001E. The content of this

publication does not necessarily reflect the views or policies of the Department of Health and Human Services, nor does mention of trade names, commercial products, or organizations imply endorsement by the U.S. Government.

References

1. Neun BW, Dobrovolskaia MA (2011) Method for analysis of nanoparticle hemolytic properties in vitro. Methods Mol Biol 697:215–224. doi:10.1007/978-1-60327-198-1_23
2. Malinauskas RA (1997) Plasma hemoglobin measurement techniques for the in vitro evaluation of blood damage called by medical devices. Artif Organs 21(12):1255–1267. doi:10.1111/j.1525-1594.1997.tb00486.x
3. ASTM F756-00 (2000) Standard practice for assessment of hemolytic properties of materials. ASTM Int, West Conshohocken, PA. doi:10.1520/F0756-00
4. ASTM E2524-08 (2013) Standard test method for analysis of hemolytic properties of nanoparticles. ASTM Int, West Conshohocken, PA. doi:10.1520/E2524
5. Dobrovolskaia MA, McNeil SE (2013) Understanding the correlation between in vitro and in vivo immunotoxicity tests for nanomedicines. J Control Release 172(2):456–466. doi:10.1016/j.jconrel.2013.05.025
6. Wildt B, Malinauskas RA, Brown RP (2016) Effects of nanomaterials on erythrocytes. In: Dobrovolskaia MA, McNeil SE (eds) Handbook of immunological properties of engineered nanomaterials. World Scientific Publishing Ltd., Singapore, pp 67–103
7. Food and Drug Administration, Center for Drug Evaluation and Research (2005). Guidance for industry: estimating the maximum safe starting dose in initial clinical trials for therapeutics in adult healthy volunteers http://www.fda.gov/downloads/drugs/guidances/ucm078932.pdf
8. DeSilva B, Smith W, Weiner R, Kelley M, Smolec J, Lee B, Khan M, Tacey R, Hill H, Celniker A (2003) Recommendations for the bioanalytical method validation of ligand-binding assays to support pharmacokinetic assessments of macromolecules. Pharm Res 20(11):1885–1900
9. Food and Drug Administration, Center for Drug Evaluation and Research, Center for Veterinary Medicine (2001). Guidance for Industry: Bioanalytical method validation http://www.fda.gov/downloads/Drugs/Guidance/ucm070107.pdf

Chapter 10

In Vitro Assessment of Nanoparticle Effects on Blood Coagulation

Timothy M. Potter, Jamie C. Rodriguez, Barry W. Neun, Anna N. Ilinskaya, Edward Cedrone, and Marina A. Dobrovolskaia

Abstract

Blood clotting is a complex process which involves both cellular and biochemical components. The key cellular players in the blood clotting process are thrombocytes or platelets. Other cells, including leukocytes and endothelial cells, contribute to clotting by expressing the so-called pro-coagulant activity (PCA) complex on their surface. The biochemical component of blood clotting is represented by the plasma coagulation cascade, which includes plasma proteins also known as coagulation factors. The coordinated interaction between platelets, leukocytes, endothelial cells, and plasma coagulation factors is necessary for maintaining hemostasis and for preventing excessive bleeding. Undesirable activation of all or some of these components may lead to pathological blood coagulation and life-threatening conditions such as consumptive coagulopathy or disseminated intravascular coagulation (DIC). In contrast, unintended inhibition of the coagulation pathways may lead to hemorrhage. Thrombogenicity is the property of a test material to induce blood coagulation by affecting one or more elements of the clotting process. Anticoagulant activity refers to the property of a test material to inhibit coagulation. The tendency to cause platelet aggregation, perturb plasma coagulation, and induce leukocyte PCA can serve as an in vitro measure of a nanomaterial's likelihood to be pro- or anticoagulant in vivo. This chapter describes three procedures for in vitro analyses of platelet aggregation, plasma coagulation time, and activation of leukocyte PCA. Platelet aggregation and plasma coagulation procedures have been described earlier. The revision here includes updated details about nanoparticle sample preparation, selection of nanoparticle concentration for the in vitro study, and updated details about assay controls. The chapter is expanded to describe a method for the leukocyte PCA analysis and case studies demonstrating the performance of these in vitro assays.

Key words Nanoparticles, Thrombogenicity, Platelet aggregation, Platelet, Blood, Plasma coagulation, Coagulation factors, Leukocyte procoagulant activity, Thrombosis, Disseminated intravascular coagulation, DIC

1 Introduction

Formation of a thrombus is a natural mechanism to prevent blood loss upon blood vessel damage. However, when a thrombus is caused by other conditions (e.g., thrombocytosis or a foreign material or drug), it may lead to a life-threatening condition such

Scott E. McNeil (ed.), *Characterization of Nanoparticles Intended for Drug Delivery*, Methods in Molecular Biology, Vol. 1682, DOI 10.1007/978-1-4939-7352-1_10,

as stroke. Undesirable formation of a blood clot may result in partial or complete occlusion of a blood vessel, congestion and at later time points a hemorrhage. Hemorrhage can also result from inhibition of normal blood clotting by certain materials and drugs. Inhibition of blood coagulation is needed to prevent thrombosis, while activation of coagulation is required to prevent a hemorrhage. In health, the pro- and anticoagulant pathways are balanced to maintain hemostasis. Blood clotting is a complex process and involves multiple components. The key players include platelets, leukocytes, endothelial cells, and plasma coagulation factors. Platelets are small cells (~2 μm in size), which originate from megakaryocytes in the bone marrow. Previous studies have demonstrated that some nanomaterials can cause platelet aggregation and that this property largely depends on particle surface characteristics [1]. Procoagulant activity (PCA) of leukocytes, endothelial cells, and some cancer cells is accepted as an important component in the onset of disseminated intravascular coagulation (DIC). DIC is common in acute promyelocytic leukemia (APL) and other forms of cancer [2–6]. DIC in cancer patients is often observed after initiation of therapy with cytotoxic oncology drugs that act by altering DNA replication (e.g., doxorubicin, daunorubicin, and vincristine) [4, 7]. Cytotoxic oncology drugs acting by other mechanisms (e.g., methotrexate and paclitaxel) do not induce DIC [8, 9]. DIC is also a common complication in sepsis [10–13]. Cytotoxic drugs (doxorubicin, daunorubicin, and vincristine) and endotoxin have previously been shown to induce leukocyte PCA in vitro and DIC in vivo [14–22]. When nanoparticles are used for delivery of cytotoxic drugs, induction of the leukocyte PCA can be reduced. However, some carriers are not immunologically inert and can exaggerate this toxicity [23]. Nanoparticles may also contain traces of endotoxin. Besides being a pro-coagulant itself, endotoxin even at low concentrations can induce stronger leukocyte PCA when combined with certain nanocarriers [23]. Some nanocarriers may affect more than one component of the coagulation cascade. For example, cationic PAMAM dendrimers activate platelets and induce platelet aggregation as well as exaggerate endotoxin-mediated PCA [23, 24]. Platelet activation and aggregation and leukocyte PCA are commonly used to assess material/drug-mediated thrombogenicity. In vitro–in vivo correlation for these methods have been described earlier [25].

Plasma coagulation cascade is complex. It involves multiple coagulation factors, whose function is coordinated in several pathways. The three main pathways are intrinsic (also known as the contact activation pathway, because it is activated by a damaged surface); extrinsic (also known as the tissue factor pathway); and the final common pathway. Each pathway can be assessed by a specialized test. For example, the activated partial thromboplastin time (APTT) assay is used to assess the intrinsic pathway, while the

prothrombin time (PT) assay is a measure of the extrinsic pathway. Extrinsic and intrinsic pathways converge into the common pathway. Thrombin time (TT) is an indicator of the functionality of the final common pathway. Each pathway involves many coagulation factors, some of which overlap between pathways. The assays measuring plasma coagulation in APTT, PT, and TT pathways are used in the clinic to assess functionality and reveal deficiency of plasma coagulation factors. The APTT assay assesses the functionality of factors XII, XI, IX, VIII, X, V, and II. The PT assay assesses the activity of factors VII, X, V, and II. All three assays assess the role of fibrinogen. Prolongation of PT and APTT ex vivo is used as a diagnostic marker for DIC [26]. Prolongation of the coagulation pathways in response to a test material in vitro suggests that the test material may interact with and inhibit plasma coagulation pathways. Since nanoparticle interaction with plasma proteins may result in a change in the protein function, the coagulation assays can be used to assess nanoparticle ability to interfere with normal plasma coagulation. It is important not to over-interpret the results of the in vitro plasma coagulation tests for nanoparticles. The positive response obtained for a given nanoformulation in vitro using PT, APTT, and TT assays described in this protocol have to be verified in vivo. Altogether, plasma coagulation, platelet aggregation, and leukocyte PCA assays can be used to assess the compatibility of a test nanomaterial with blood.

In this chapter, we describe three in vitro methods for analysis of a nanoparticle's propensity to affect blood coagulation. These methods include analysis of the nanoparticle's ability to: (1) induce platelet aggregation or interfere with collagen-induced platelet aggregation (Fig. 1), (2) affect the plasma coagulation cascade (Fig. 2), and (3) trigger leukocyte PCA (Fig. 3). All assays are based on human blood derived from healthy donor volunteers.

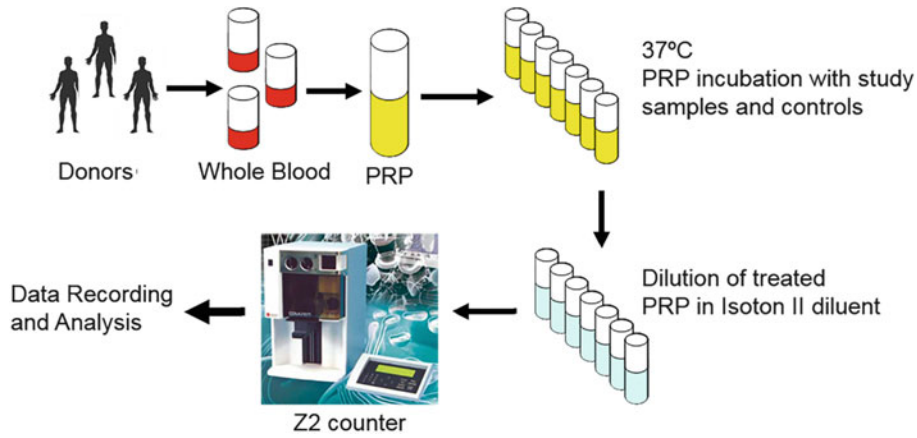

Fig. 1 Schematic diagram of platelet aggregation assay. This figure outlines the main steps of the platelet aggregation assay. *PRP* platelet-rich plasma, *Z2 counter* commercial cell and particle counter

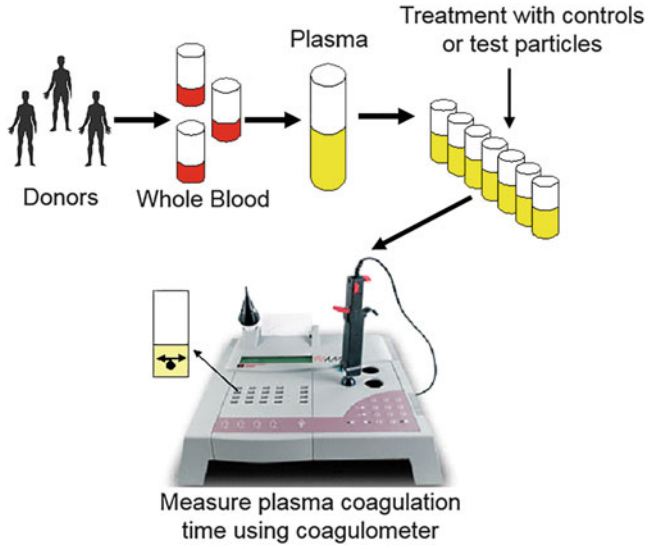

Fig. 2 Schematic diagram of coagulation time measurement. This figure outlines the main steps of the plasma coagulation assay

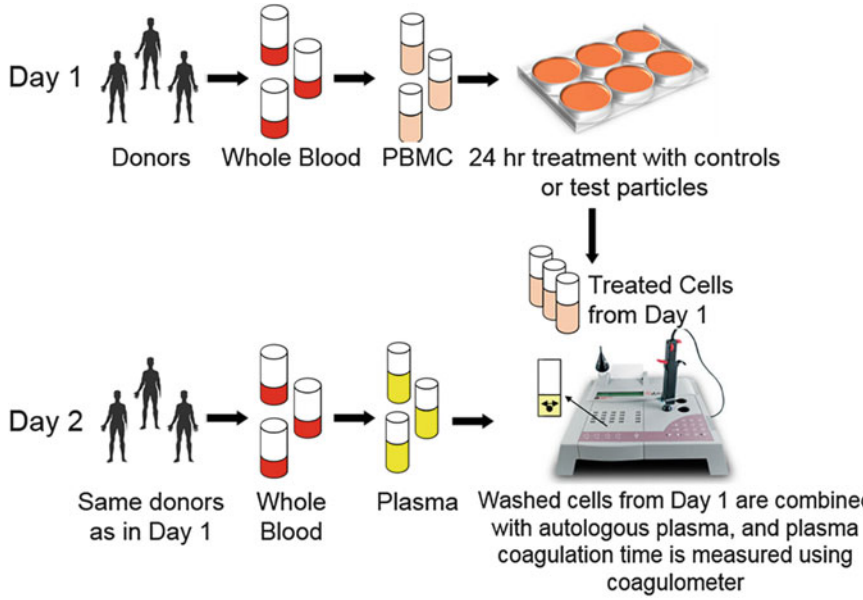

Fig. 3 Schematic diagram of Leukocyte Procoagulant Activity Assay. This figure outlines the main steps of the two-day procedure used to analyze leukocyte procoagulant activity. *PBMC* peripheral blood mononuclear cell

Platelet aggregation and plasma coagulation assays have been described earlier [27]. This chapter presents the revised version of these methods to include updated details about nanoparticle sample preparation, selection of nanoparticle concentration for the in vitro study, and updated details about assay controls as well as to describe a protocol for the assessment of leukocyte PCA.

2 Materials

When planning coagulation experiments, it is important to review Subheading 5. **Notes 1–9** contain technical details helpful in understanding the nuances of individual assay. **Note 10** provides a reference to reagents used in the NCL.

2.1 Platelet Aggregation Assay

1. 5 μm calibration standard. This reagent is needed to set up and qualify the instrument.
2. Isoton II diluent.
3. Coulter Clenz solution. This reagent is needed to clean the instrument after use.
4. Freshly drawn human whole blood anticoagulated with sodium citrate.
5. Collagen.
6. RPMI-1640 Cell Culture Media.
7. Phosphate buffered saline (PBS).
8. Blood cell counter vials with snap caps.
9. 50 μm aperture tube.
10. Particle count and size analyzer.

2.2 Plasma Coagulation Assay

1. Human blood from at least three donors, anticoagulated with sodium citrate.
2. Neoplastine Cl. This reagent is supplied as lyophilized powder along with reconstitution buffer. Reconstitute according to the manufacturer's instructions and use fresh or refrigerate and use within the time specified by the manufacturer.
3. Thrombin.
4. 0.025 M $CaCl_2$.
5. Owren-Koller Buffer.
6. PTTa reagent.
7. Normal and abnormal control plasma (CoagControl N + ABN).
8. RPMI-1640 Cell Culture Media.
9. PBS.
10. 5 mL Finntip pipette tips (ThermoScientific).
11. 4-well cuvettes.
12. Coagulometer (*see* **Note 1**).
13. Metal balls for coagulometer (*see* **Note 1**).

2.3 Leukocyte PCA Assay

1. Human blood from at least three donors, anticoagulated with Li-heparin for peripheral blood mononuclear cell (PBMC) isolation and anticoagulated with sodium citrate for plasma coagulation test.
2. Ficoll-Paque Plus.
3. PBS.
4. Heat-inactivated fetal bovine serum (FBS). Thaw a bottle of FBS at room temperature or thaw overnight at 2–8 °C and allow to equilibrate to room temperature. Incubate for 30 min at 56 °C in a water bath, mixing every 5 min. Fifty mL single-use aliquots may be stored at 2–8 °C for up to 1 month or at a nominal temperature of −20 °C indefinitely.
5. Complete RPMI-1640 medium: 10% FBS (heat inactivated), 2 mM L-glutamine, 100 U/mL penicillin, and 100 μg/mL streptomycin sulfate. Store at 2–8 °C protected from light for no longer than 1 month. Before use, warm in a water bath.
6. 1 mg/mL Lipopolysaccharide (LPS, Stock). Add 1 mL of sterile PBS or cell culture medium per 1 mg of LPS to the vial and vortex to mix. Store daily-use aliquots at a nominal temperature of −20 °C.
7. Buffer A: Prepare Buffer A by dissolving NaCl to a final concentration of 150 mM and $CaCl_2$ to a final concentration of 6.6 mM in 20 mM HEPES, pH 7.4.
8. Hanks balanced salt solution (HBSS).
9. Trypan Blue solution.
10. Neoplastine Cl. This reagent is supplied as lyophilized powder along with reconstitution buffer. Reconstitute according to the manufacturer's instructions and use fresh or refrigerate and use within the time specified by the manufacturer.
11. CoagControl N + ABN (Diagnostica Stago).
12. Calcium ionophore.
13. 5 mL Finntip pipette tips (ThermoScientific).
14. 4-well cuvettes.
15. Coagulometer (*see* **Note 1**).

3 Methods

3.1 Preparation of Study Samples

The concentrations used in these assays are based on an estimated plasma concentration in an average human patient at the intended therapeutic dose. For the purpose of this chapter, we refer to this concentration as the theoretical plasma concentration. Assumptions and considerations for estimating theoretical plasma concentration were reviewed elsewhere [25] and are summarized in Box 1.

Box 1. Example Calculation of Nanoparticle Concentration for In Vitro Test

Assume the mouse dose is known to be 123 mg/kg in this example.

$$\text{human dose} = \frac{mouse\ dose}{12.3} = \frac{123\frac{mg}{kg}}{12.3} = 10\ \text{mg/kg}$$

Blood volume makes up approximately 8% of body weight (e.g. a 70 kg human has approximately 5.6 L (8% of 70) of blood). This allows for a very rough estimate of what the maximum blood concentration may be.

$$\text{in vitro concentration}_{human\ matrix} = \frac{human\ dose}{human\ blood\ volume} = \frac{70\ kg\ x\ 10\frac{mg}{kg}}{5.6\ L}$$

$$= \frac{700\ mg}{5.6\ L} = 0.125\ \text{mg/mL}$$

Box 1 Example calculation of nanoparticle concentration. Reproduced with permission from ref. 25

Each assay evaluates a nanoparticle formulation at four concentrations: 10× (or when feasible 100×, 30×, or 5×) of the theoretical plasma concentration, theoretical plasma concentration, and 25-fold serial dilutions of the theoretical plasma concentration. When the intended therapeutic concentration is unknown, the highest final concentration is 1 mg/mL or the highest reasonably achievable concentration.

1. Platelet Aggregation Assay
   This assay requires 0.4 mL of nanoparticle solution, at 5× the highest test concentration. The nanoparticles should be dissolved/resuspended in RPMI, or other medium, which does not interfere with platelet aggregation. For example, if the final theoretical plasma concentration to be tested is 0.2 mg/mL, then a stock of 10 mg/mL will be prepared and diluted 10-fold (1 mg/mL), followed by two 5-fold serial dilutions (0.2 and 0.04 mg/mL). When 25 μL of each of these samples is added to the test tube and mixed with 0.1 mL of plasma, the final nanoparticle concentrations tested in the assay are: 2.0, 0.2, 0.04, and 0.008 mg/mL. Three 25 μL replicates are tested per each sample concentration.
2. Plasma Coagulation Assay
   This assay requires 500 μL of nanoparticles, at a concentration 10× that of the highest tested concentration, dissolved/resuspended in PBS or other relevant media. For example, if the final theoretical plasma concentration to be tested is 0.2 mg/mL, then a stock of 20 mg/mL will be prepared and diluted 10-fold (2 mg/mL), followed by two 5-fold serial dilutions (0.4 and

0.08 mg/mL). When 0.1 mL of each of these samples is added to the test tube and mixed with 0.9 mL of plasma, the final nanoparticle concentrations tested in the assay are: 2.0, 0.2, 0.04, and 0.008 mg/mL.

3. Leukocyte PCA Assay
   This assay requires 1.5 mL of the test nanoparticles dissolved/resuspended in complete culture medium at a concentration 10× of the highest tested concentration. For example, if the final theoretical plasma concentration to be tested is 0.2 mg/mL, then a stock of 20 mg/mL will be prepared and diluted 10-fold (2 mg/mL), followed by two serial 5-fold dilutions (0.4 and 0.08 mg/mL). When 400 μL of each of these samples is combined in a culture plate well with 3.6 mL of cells, the final concentrations of nanoparticles are 0.008, 0.04, 0.2, and 2 mg/mL. Each nanoparticle concentration is plated in duplicate.

3.2 Preparation of Plasma

During the blood collection procedure, the first 10 mL of blood should be discarded. This is necessary to avoid activation of cells and plasma biochemical cascades (e.g., complement) by venipuncture procedure. Exposure of either blood or plasma to extreme temperatures (<20 °C or >37 °C) may affect the quality of test results and should be avoided. Below we describe preparation procedures specific for each protocol.

1. Platelet Aggregation Assay
   You will need three types of plasma to perform this experiment: platelet-rich plasma (PRP), platelet poor plasma (PPP), and platelet free plasma (PFP). Plasma from individual donors can be analyzed separately or pooled together. Pooled plasma is prepared by mixing plasma from at least two individual donors. For initial screening experiments we use pooled plasma. Analysis of plasma from individual donors may be needed for mechanistic follow-up experiments. Blood is drawn into vacutainer tubes containing sodium citrate as an anticoagulant. Estimate the volume of PRP and PFP needed for this experiment based on the number of test samples. Keep in mind that each 10 mL of whole blood produces ~2 mL of PRP and ~5 mL of PPP. Based on the volume of each type of plasma, divide the vacutainer tubes containing whole blood into two groups. Use one group to make PRP and use the second group to make PPP, which is needed to produce PFP. Follow the guidance below for centrifugation time and speed used to prepare each type of plasma.
   PRP—centrifuge whole blood at 200 × *g* for 8 min, collect plasma and transfer to a fresh tube (*see* **Note 2**).
   PPP—centrifuge whole blood at 2500 × *g* for 10 min, collect plasma and transfer to a fresh tube.

PFP—centrifuge PPP at 18,000 × *g* for 5 min, collect plasma and transfer to a fresh tube.

2. Plasma Coagulation Assay—Normal Test Plasma Preparation
   Use freshly collected whole blood within 1 h after collection. Spin the blood for 10 min at 2500 × *g* at 20–22 °C, collect plasma and pool from at least two donors. Pooled plasma is stable for 8 h at room temperature. Do not refrigerate or freeze. The assay can also be performed in the plasma from individual donors when needed for mechanistic follow-up experiments. Analyze two duplicates (four total samples) of test plasma in each of the coagulation assays. Run one duplicate before the nanoparticle samples analysis and the second duplicate at the end of each run to verify that the plasma functionality is not affected throughout the duration of the experiment.
3. Plasma Coagulation Assay—Normal and Abnormal (Coag N + ABN) Control Plasma Preparation
   Reconstitute each of the lyophilized control plasmas with 1 mL of distilled water. Let the solutions stand at room temperature 30 min prior to use. Mix thoroughly before use. Keep the unused portion refrigerated and use within 48 h after reconstitution. These plasma samples are used as instrument controls.
4. Plasma Coagulation Assay—Nanoparticle-Treated Normal Test Plasma Preparation
   In a microcentrifuge tube, combine 100 μL of nanoparticles and 900 μL of test plasma. Mix well and incubate for 30 min at 37 °C. Prepare three tubes for each test sample (i.e., when each nanoparticle is tested at four concentrations, one needs three tubes for each concentration for a total of 12 tubes per test nanoparticle) (*see* **Note 3**).
5. Leukocyte PCA Assay—Normal Plasma
   Blood should be collected from the same donors used on Day One of the experiment for PBMC preparation. Use freshly collected whole blood within 1 h after collection. Spin the blood for 10 min at 2500 × *g* at 20–22 °C. Collect plasma and label with individual donor number. This plasma is stable for 8 h at room temperature. Do not refrigerate or freeze. Autologous plasma is ideal for this assay. The plasma derived from an individual donor is used to induce coagulation by PBMC prepared from the same donor. If the use of autologous plasma is not feasible, plasma pooled from at least two donors can be used instead of individual donor plasma.
6. Leukocyte PCA Assay—Normal and Abnormal (Coag N + ABN) Control Plasma
   Reconstitute each of the lyophilized control plasmas with 1 mL of distilled water. Let the solutions stand at room temperature 30 min prior to use. Mix thoroughly before use. Keep the

unused portion refrigerated and use within 48 h after reconstitution. These plasma samples are used as instrument controls. The difference between this test and the plasma coagulation described in **step 3** of this section is that this assay will require normal and abnormal controls for the PT assay only.

3.3 Preparation of Controls

1. Platelet Aggregation Assay—Negative Control (PBS)
   Sterile Ca^{2+}/Mg^{2+}-free PBS is used as a negative control. Store at room temperature for up to 6 months.
2. Platelet Aggregation Assay—Vehicle Control (relevant to the given nanoparticle)
   When nanoparticles are formulated in solutions other than saline or PBS, the vehicle of the sample should be tested separately to estimate the effect of excipients on platelet aggregation. This control is specific to each given nanoparticle sample. Vehicle control should match the formulation buffer of the test nanomaterial in both the composition and concentration. Dilute this sample the same way you dilute the test nanomaterials. If PBS is the vehicle, this control can be skipped.
3. Platelet Aggregation Assay—Positive Control (collagen)
   Collagen is provided as a solution with a final concentration of 100 μg/mL contained in sealed glass vials. Keep it at a nominal temperature of 4 °C. After opening, the contents of the vial should be used within 4 weeks.
4. Plasma Coagulation Assay
   Several reagents are used in this assay to initiate plasma coagulation. They are assay-specific and include Neoplastine for PT assay, PTTa-reagent for APTT assay, and thrombin for TT assay. These reagents are supplied as lyophilized powders. Reconstitute the reagents according to the manufacturer's instructions and use fresh or refrigerate and use within the time specified by the manufacturer.
5. Leukocyte PCA Assay—Positive Control
   Dilute stock LPS solution in cell culture medium to a final concentration of 1 μg/mL. Store at room temperature. Discard the unused portion after experiment. Alternatively, calcium ionophore at a final concentration of 500 ng/mL can be used.
6. Leukocyte PCA Assay—Negative Control
   Use PBS as a negative control. Process it the same way as your study samples.
7. Leukocyte PCA Assay—Coagulation Controls (Coag N + ABN)
   Reconstitute lyophilized control plasmas with 1 mL of distilled water. Let the solutions stand at room temperature 30 min prior to use. Mix thoroughly before use. Keep the unused

portion refrigerated and use within 48 h after reconstitution. These plasma samples are used as instrument controls.

8. Leukocyte PCA Assay—Vehicle Control
   Vehicle control is the buffer or media used to formulate test nanomaterials. Common excipients used in nanoformulations are trehalose, sucrose, and albumin. However, other reagents and materials are also used alone or in combination. Vehicle control should match the formulation buffer of the test nanomaterial by both composition and concentration. This control can be skipped if nanoparticles are stored in PBS.

3.4 Preparation of PBMCs for Leukocyte PCA Assay

1. Place freshly drawn blood anticoagulated with Li-heparin into 15 mL or 50 mL conical centrifuge tubes. Add an equal volume of room temperature PBS and mix well.
2. Slowly layer the Ficoll-Paque solution underneath the blood/PBS mixture by placing the tip of the pipet containing the Ficoll-Paque at the bottom of the blood sample tube. Alternatively, the blood/PBS mixture may be slowly layered over the Ficoll-Paque solution. Use 3 mL of Ficoll-Paque solution per 4 mL of blood/PBS mixture (*see* **Note 4**).
3. Centrifuge for 30 min at 900 × *g* at 18–20 °C without brake.
4. Using a sterile pipet, remove the upper layer containing plasma and platelets, and discard.
5. Using a fresh sterile pipet, transfer the mononuclear cell layer into another centrifuge tube.
6. Wash cells by adding an excess of HBSS and centrifuge for 10 min at 400 × *g* at 18–20 °C. The HBSS volume should be about three times the volume of the mononuclear layer (*see* **Note 5**).
7. Discard the supernatant and repeat the wash step (**step 6** above) once more.
8. Resuspend cells in complete RPMI 1640 medium. Count an aliquot of cells and determine viability using trypan blue exclusion.
9. If cell viability is ≥80%, dilute cells in complete culture media to a concentration of 3×10^6 cells/mL and proceed to **step 1** of Subheading 3.7.

3.5 Platelet Aggregation Assay

1. Prepare the Z2 instrument as described in the owner's manual (8). Pre-warm all racks and tubes to 37 °C.
2. Prepare PRP, PPP, and PFP as described in **step 1** of Subheading 3.2, then proceed to the next step.
3. *Part A (Nanoparticle Ability to Induce Platelet Aggregation)*: In a microcentrifuge tube, combine: (1) 100 μL PRP with 25 μL test material; (2) 100 μL PRP with 25 μL of positive

control (collagen); (3) 100 μL PRP with 25 μL of negative control (PBS); and (4) 100 μL PRP with 25 μL of vehicle control (a buffer or media used to formulate nanoparticle; if nanoparticle is formulated in PBS, this sample can be skipped). Prepare in triplicate for each sample.

4. *Part B (Nanoparticle Ability to Interfere with Collagen-Induced Platelet Aggregation)*: In a separate set of tubes combine: (1) 100 μL of PRP with 50 μL of negative control (PBS); (2) 100 μL of PRP with 25 μL of positive control (collagen) and 25 μL of RPMI; (3) 100 μL of PRP with 25 μL of positive control (collagen) and 25 μL of test nanomaterial; (4) 100 μL PRP with 25 μL of vehicle control (a buffer or media used to formulate nanoparticle; if nanoparticle is formulated in PBS, this sample can be skipped) and 25 μL of RPMI. Prepare each test combination in triplicate (*see* **Note 6**).
5. *Part C (Assessment of Nanoparticle Interference with the Assay)*: Prepare 1 control tube, by combining 100 μL of PFP and 25 μL of nanoparticle solution (*see* **Note 7**).
6. Briefly vortex all samples to mix ingredients and incubate for 15 min at a nominal temperature of 37 °C.
7. Add 10 mL of Isoton II diluent into a blood cell counter vial. Prepare two vials for each sample replicate. Each replicate will be diluted into two Isoton II containing vials and a platelet count will be obtained using a Z2 counter. The mean response will then be calculated for each replicate.
8. Add 20 μL of PRP treated with positive control, negative control, vehicle control (if applicable), or test nanomaterial prepared in **steps 3–5** to the Isoton II containing vials from **step 5**. Cover vials and gently invert them to mix diluted samples.
9. Proceed with platelet count determination using the Z2 counter immediately (*see* **Notes 8** and **9**).

3.6 Plasma Coagulation Assay

1. Set-up instrument test parameters for each of the four assays (Table 1). Allow the instrument to warm up 5–10 min prior to use.
2. Prepare all reagents and warm to 37 °C prior to use. Note that lyophilized reagents should be reconstituted at least 30 min prior to use.
3. Place cuvettes into A, B, C, and D test rows on the coagulometer (*see* **Note 1**).
4. Add one metal ball into each cuvette and allow cuvette and ball to warm for at least 3 min prior to use.
5. Add 100 μL of control or test plasma to a cuvette when testing PT or thrombin time, and 50 μL when testing APTT (Table 1).

Table 1
Instrument settings, time, and sample volume requirements for the Plasma Coagulation Assay

Assay	Control	Instrument settings				Volumes		Normal coagulation time (s)
		Max. time (s)	Incubation time (s)	Single/ duplicate	Precision	Plasma and reagent	Coagulation activation reagent	
PT (Neoplastine)	Coag.Control N + ABN	60	120	Duplicate	5%	100 µL plasma	100 µL Neoplastine (PIP position 4)	≤13.4
APTT	Coag.Control N + ABN	120	180	Duplicate	5%	50 µL plasma +50 µL PTT-a	50 µL $CaCl_2$ (PIP position 2)	≤34.1
TT	Coag.Control N + ABN	60	60	Duplicate	5%	100 µL plasma	100 µL Thrombin (PIP position 4)	≤21

PT prothrombin time, *APTT* activated partial thromboplastin time, *TT* thrombin time

Prepare two wells for each test tube prepared in **step 4** of Subheading 3.2.

6. *This step is only for APTT*: Add 50 μL of PTTa reagent to plasma samples in cuvettes.
7. Start the timer for each of the test rows by pressing the A, B, C, or D timer buttons. Ten seconds before the time is up, the timer will beep. When this happens, immediately transfer cuvettes to PIP row and press the PIP button to activate the pipettor (*see* **Note 1**).
8. When time is up, add coagulation activation reagent to each cuvette and record the coagulation time. Refer to Table 1 for the type of coagulation activation reagent and volume for each of the four assays.

3.7 Leukocyte PCA Assay

Performing this experiment requires 2 days. Below we describe the procedure for each of the days.

Day 1

1. Aliquot 3.6 mL of cell suspension into each well of a six-well plate.
2. Add 400 μL of test nanoparticle, positive control, and negative control to respective wells (Fig. 4).
3. Incubate cells with nanoparticles and controls for 24 h.

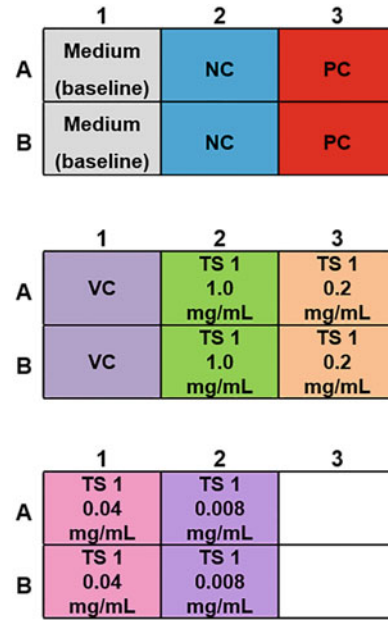

Fig. 4 Example of a plate map for Leukocyte Procoagulant Activity Assay. *TS* test sample, *NC* negative control, *PC* positive control, *VC* vehicle control

Day 2

4. At the end of the incubation time, remove cells from the incubator, transfer cells into 5 mL tubes, and wash cells two times with 1 mL of PBS. For each wash cycle, spin cells at 400 × *g* for 5 min.
5. After last wash, reconstitute cell pellet in 1 mL of Buffer A, which usually results in a cell concentration of 10×10^6 cells/mL and transfer cells into 20 mL scintillation vials or equivalent.
6. Keep cell suspensions at room temperature. Place in an incubator set at 37 °C for 5–10 min prior to testing to warm up. Transfer cells to the 37 °C chamber on the coagulometer when ready to start.
7. Set-up the instrument test parameters as shown below:

   Max Time: 360 s.
   Incubation Time: 120 s.
   Single/Duplicate: Duplicate.
   Precision: 5%.

   Allow instrument to warm up 5–10 min prior to use.
8. Prepare all reagents and cells, and warm them up to 37 °C prior to use. Note that lyophilized reagents should be reconstituted at least 30 min prior to use. It is not advised to keep more than 10 cell samples at 37 °C at on time.
9. Place cuvettes into A, B, C, and D test rows on the coagulometer (*see* **Note 1**).
10. Add one metal ball into each cuvette and allow to warm for at least 3 min before use.
11. Add 100 μL of test plasma from **step 5** of Subheading 3.2 or control plasma from **step 6** of Subheading 3.2 to a cuvette. Prepare one cuvette (1 strip, 4 wells) for each plasma sample.
12. Start timer for each of the test rows by pressing A, B, C, or D buttons. Ten seconds before the time is up, the timer will start beeping. When this happens, immediately transfer cuvettes to PIP row and press PIP button to activate pipettor.
13. When time is up, add 100 μL of Neoplastine reagent to control plasma samples or 100 μL of cell suspension from **step 6** above in lieu of coagulation activation reagent to corresponding cuvettes.
14. Record coagulation time.

4 Calculations and Data Interpretation

Examples of the data generated using individual assays described in this chapter are shown in Figs. 5, 6, and 7. A percent coefficient of variation should be calculated for each control or test sample for all three assays. This parameter is calculated according to the following formula:

$$\%\mathrm{CV} = \frac{\mathrm{SD}}{\mathrm{Mean}} \times 100\%$$

%CV between replicates of test plasma samples should be within 25%. Test samples with %CV greater than 25 should be re-analyzed. This assay performance requirement is based on the requirements for bioanalytical method validation guidance for industry [28].

Other formulas and data interpretation are assay-specific and are discussed below.

4.1 Platelet Aggregation Assay

The following parameters should be calculated for each control and test sample:

1. Platelet Count:

$$\frac{5 \times \text{Instrument count value}}{100} = \#\text{Platelets} \times 10^9/\text{L}$$

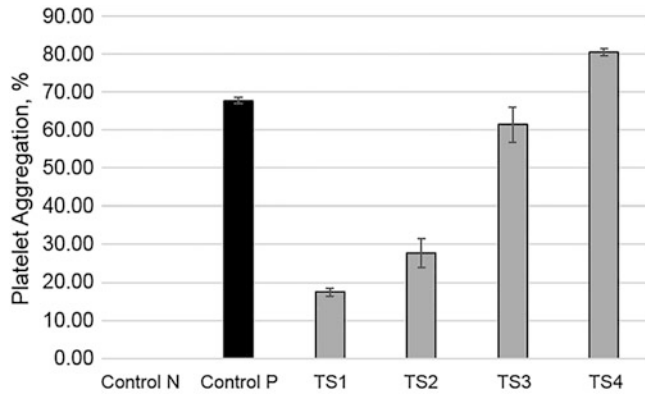

Fig. 5 Example of data generated using the in vitro Platelet Aggregation Assay. This figure shows induction of platelet aggregation by cationic, generation 5 PAMAM dendrimers with various degrees of surface modification. TS1–TS4 refer to the dendrimers with 25, 50, 75, and 100% surface amines, respectively. In this case study, all samples were assessed at the same concentration 50 μg/mL. The purpose of this experiment was to estimate the role of nanoparticle surface properties. Shown is the mean response and standard deviation ($N = 3$). Control N—normal plasma standard: negative control—PBS, Control P: positive control—collagen

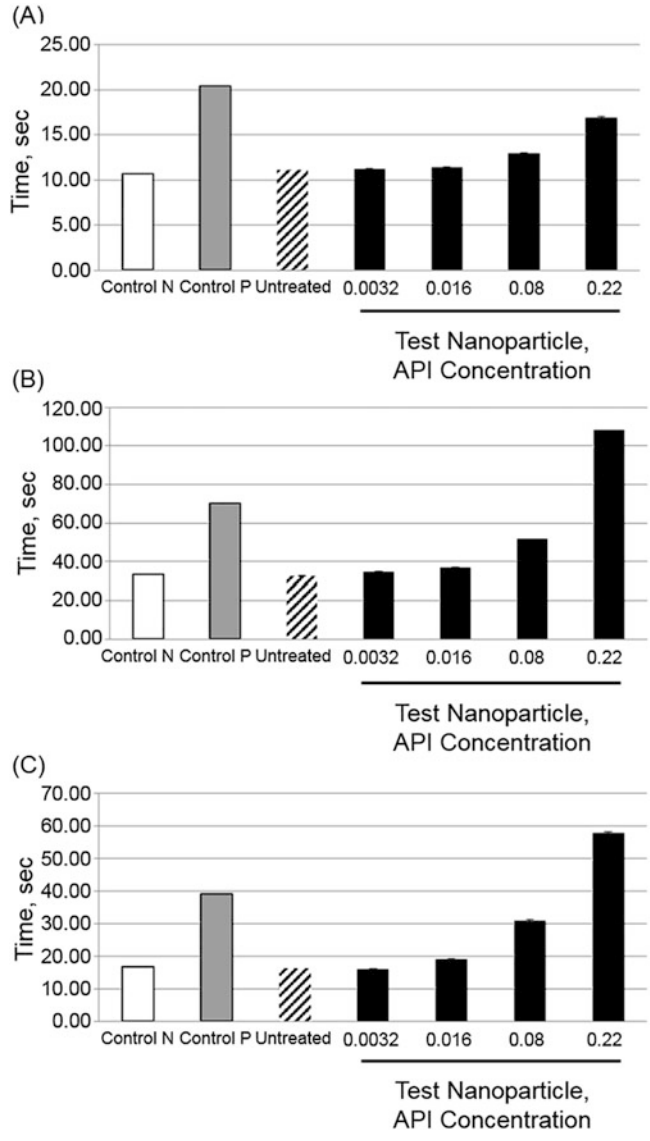

Fig. 6 Example of data generated using the in vitro Plasma Coagulation Assay. A test nanoparticle was evaluated in this assay at four different concentrations on: (**a**) prothrombin time [PT], (**b**) activated partial thromboplastin time [APTT], and (**c**) thrombin time. The concentrations are shown in mg/mL of the active pharmaceutical ingredient (API) formulated using a nanoparticle platform. At high concentrations, it resulted in prolongation of plasma coagulation time in all tests. Based on the results of this assay, the nanoparticle was selected for follow-up studies to investigate its effects on plasma coagulation factors. The prolongation was subsequently attributed to the binding and inhibition of plasma coagulation factors. Shown is the mean response and the standard deviation ($N = 3$). Untreated: sample untreated with nanoparticles, Control N: normal plasma standard, Control P: abnormal plasma standard

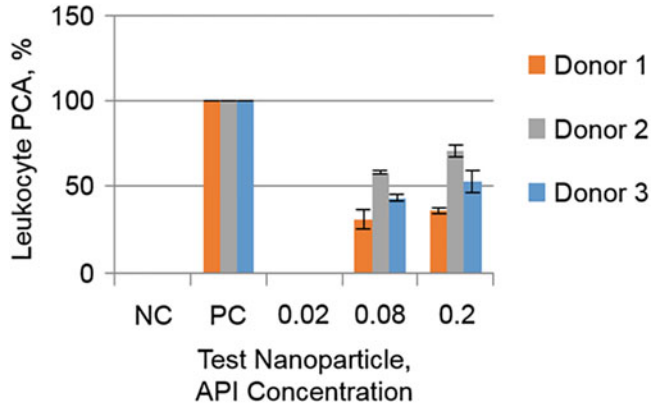

Fig. 7 Example of data generated using the in vitro Leukocyte Procoagulant Activity Assay. This figure shows a case study investigating the induction of leukocyte PCA by a nanoformulation. The nanoformulation was studied at three concentrations. The concentrations are shown in mg/mL of the active pharmaceutical ingredient (API) formulated using a nanoparticle platform. At two high concentrations, this formulation induced leukocyte PCA in PBMC from all tested donors. Shown is the mean response and the standard deviation ($N = 3$). NC: negative control—PBS, PC: positive control—LPS solution

This formula is based on the instrument manufacturer's instructions [29]. If other instrument and/or sample volume is used, the formula may require an adjustment.

2. Percent Platelet Aggregation:

$$\frac{\left(\text{Platelet count}_{\text{negative control}} - \text{Platelet count}_{\text{test sample}}\right)}{\text{Platelet count}_{\text{negative control}}} \times 100\%$$

3. For a positive sample, the assay threshold is 20%. Percent platelet aggregation values above 20% are considered positive, i.e., test material induces platelet aggregation.
4. There is no formal guidance on what degree of inhibition of collagen-induced platelet aggregation is considered significant. Apply scientific judgment to interpret results from part B (**step 4** of Subheading 3.5) of the study. Statistically significant inhibition does not necessarily mean it is physiologically relevant. If an inhibition is observed one should consider a relevant follow-up in vivo study to verify in vitro findings.

4.2 Plasma Coagulation Assay

1. Normal and abnormal control plasma should coagulate within the time established by the certifying laboratory (e.g., for most batches of control plasmas, normal coagulation time in the PT assay is ≤13.4 s, APTT is ≤34.1 s and Thrombin is ≤ 21 s; abnormal control plasma coagulation time should be above these limits). When normal and abnormal control plasma perform as described above and untreated plasma sample

coagulates within normal time limits, both the instrument and the test plasma are qualified for use in this test.

2. Nanoparticles have no effect on the assay coagulation cascade when coagulation time of the test plasma samples after exposure to nanoparticles is within the normal limits.
3. Prolongation of the plasma coagulation time in plasma samples exposed to nanoparticles suggests that the test particle either depletes or inhibits coagulation factors. There is no guidance on the degree of prolongation; but in general, a prolongation of two fold or more than that in the untreated control is considered physiologically significant.

4.3 Leukocyte Procoagulant Activity Assay

1. A percent procoagulant activity of a nanoparticle test sample is calculated according to the following formula:

$$\%\mathrm{PCA} = \frac{\mathrm{Mean\,time}_{\text{positive control sample}}}{\mathrm{Mean\,time}_{\text{test sample}}} \times 100\%$$

2. The positive control is considered positive if the coagulation time in this sample is less than 360 s. Coagulation time of PBMC treated with LPS may vary from donor to donor. Typical coagulation times observed in our lab with PBMC treated with 1 μg/mL LPS is 200–300 s, while that induced by ionophore is about 150 s.

5 Notes

1. The protocol is based on the semi-automatic STArt4 coagulometer from Diagnostica Stago [30]. If using a different instrument, please follow the operational guidelines recommended by the instrument manufacturer.
2. PRP must be prepared as soon as possible and no longer than 1 h after blood collection. PRP must be kept at room temperature and should be used within 4 h.
3. Insoluble nanoparticles, which can be separated from the bulk plasma by centrifugation, may be removed by spinning the test tubes for 5 min at 18,000 × *g*. It is assumed that any proteins involved in the coagulation process and adsorbed onto the particle surface will be removed from the sample in this step and the consequences of such binding on the plasma coagulation pathways will be assessed. Often, nanoparticles are soluble or modified with poly(ethylene glycol), and therefore cannot be easily separated from plasma at the end of the incubation step. In this case, the sample analysis can proceed to the next step in the test procedure without centrifugation.

4. To maintain Ficoll–blood interface, it is helpful to hold the tube at 45° angle.
5. Typically, 4 mL of blood/PBS mixture results in about a 2 mL mononuclear layer and requires 6 mL of HBSS for the wash step.
6. The final concentration of nanoparticles in this case is slightly (1.2 times) lower than that tested in part A. If there is a reason to expect that this difference will affect the test results, adjust the concentration of the stock nanoparticles accordingly.
7. If nanoparticles aggregate to micron size particulates, they either create an artificially high number of single platelet count (if the aggregates resemble the platelet size and pass the aperture) or will not pass through the aperture and prevent accurate counting of single platelets, resulting in false-negative or false-positive result, respectively.
8. Dilutions of tested samples and controls should be performed ex tempore. Counts should be performed within 2 h after removing from the incubator. When planning the experiment, take into account that analysis of one nanoparticle sample with all controls takes approximately 1 h. If the nanoparticle interferes with the assay and results in clogging of the aperture, additional time will be needed to clean the instrument and continue counts. This is not a high-throughput screening assay. Plan your time accordingly.
9. Perform platelet count of the blank PRP used for the experiment in the beginning and the end of the run to confirm that the quality of plasma is not affected by storage and handling. Normal platelet count in human plasma should be between 125 and 690 $\times$ 10^9/L (*8*). Average platelet count in our experiments is between 300 and 450 $\times$ 10^9/L.
10. NCL does not endorse suppliers. However, we found that a new user benefits from knowing catalog information of reagents used in our assays. If you need ideas of what reagents are used at the NCL, please review NCL methods ITA-2, ITA-12, and ITA-17 available at https://ncl.cancer.gov/resources/assay-cascade-protocols. When other reagents are used, the assay performance may change. When using reagents and instruments from sources other than that used in our protocols, assay performance qualification is needed to verify the assay functionality and validity.

Acknowledgment

This project has been funded in whole or in part with Federal funds from the National Cancer Institute, National Institutes of Health, under Contract No. HHSN261200800001E. The content of this

publication does not necessarily reflect the views or policies of the Department of Health and Human Services, nor does mention of trade names, commercial products, or organizations imply endorsement by the U.S. Government.

References

1. Koziara JM, Oh JJ, Akers WS, Ferraris SP, Mumper RJ (2005) Blood compatibility of cetyl alcohol/Polysorbate-based nanoparticles. Pharm Res 22(11):1821–1828. doi:10.1007/s11095-005-7547-7
2. Barbui T, Falanga A (2001) Disseminated intravascular coagulation in acute leukemia. Semin Thromb Hemost 27(6):593–604. doi:10.1055/s-2001-18865
3. Franchini M, Di Minno MN, Coppola A (2010) Disseminated intravascular coagulation in hematologic malignancies. Semin Thromb Hemost 36(4):388–403. doi:10.1055/s-0030-1254048
4. Higuchi T, Toyama D, Hirota Y, Isoyama K, Mori H, Niikura H, Yamada K, Omine M (2005) Disseminated intravascular coagulation complicating acute lymphoblastic leukemia: a study of childhood and adult cases. Leuk Lymphoma 46(8):1169–1176. doi:10.1080/10428190500102662
5. Levi M (2000) Cancer and DIC. Haemostasis 31(Suppl 1):47–48
6. Levi M (2009) Disseminated intravascular coagulation in cancer patients. Best Pract Res Clin Haematol 22(1):129–136. doi:10.1016/j.beha.2008.12.005
7. Uchiumi H, Matsushima T, Yamane A, Doki N, Irisawa H, Saitoh T, Sakura T, Jimbo T, Handa H, Tsukamoto N, Karasawa M, Miyawaki S, Murakami H, Nojima Y (2007) Prevalence and clinical characteristics of acute myeloid leukemia associated with disseminated intravascular coagulation. Int J Hematol 86(2):137–142. doi:10.1532/ijh97.06173
8. Napoleone E, Zurlo F, Latella MC et al (2009) Paclitaxel downregulates tissue factor in cancer and host tumour-associated cells. Eur J Cancer 45(3):470–477. doi:10.1016/j.ejca.2008.10.014
9. Swystun LL, Shin LY, Beaudin S, Liaw PC (2009) Chemotherapeutic agents doxorubicin and epirubicin induce a procoagulant phenotype on endothelial cells and blood monocytes. J Thromb Haemost 7(4):619–626. doi:10.1111/j.1538-7836.2009.03300.x
10. Khemani RG, Bart RD, Alonzo TA, Hatzakis G, Hallam D, Newth CJ (2009) Disseminated intravascular coagulation score is associated with mortality for children with shock. Intensive Care Med 35(2):327–333. doi:10.1007/s00134-008-1280-8
11. Lando PA, Edgington TS (1985) Lymphoid procoagulant response to bacterial endotoxin in the rat. Infect Immun 50(3):660–666
12. Oh D, Jang MJ, Lee SJ, Chong SY, Kang MS, Wada H (2010) Evaluation of modified non-overt DIC criteria on the prediction of poor outcome in patients with sepsis. Thromb Res 126(1):18–23. doi:10.1016/j.thromres.2009.12.008
13. Slofstra SH, ten Cate H, Spek CA (2006) Low dose endotoxin priming is accountable for coagulation abnormalities and organ damage observed in the Shwartzman reaction. A comparison between a single-dose endotoxemia model and a double-hit endotoxin-induced Shwartzman reaction. Thromb J 4(13). doi:10.1186/1477-9560-4-13
14. Fibach E, Treves A, Korenberg A, Rachmilewitz EA (1985) In vitro generation of procoagulant activity by leukemic promyelocytes in response to cytotoxic drugs. Am J Hematol 20(3):257–265
15. Gralnick HR, Abrell E (1973) Studies of the procoagulant and fibrinolytic activity of promyelocytes in acute promyelocytic leukaemia. Br J Haematol 24(1):89–99
16. Hiller E, Saal JG, Ostendorf P, Griffiths GW (1977) The procoagulant activity of human granulocytes, lymphocytes and monocytes stimulated by endotoxin. Coagulation and electron microscopic studies. Klin Wochenschr 55(15):751–757
17. Kwaan HC, Wang J, Boggio LN (2002) Abnormalities in hemostasis in acute promyelocytic leukemia. Hematol Oncol 20(1):33–41
18. Stein E, McMahon B, Kwaan H, Altman JK, Frankfurt O, Tallman MS (2009) The coagulopathy of acute promyelocytic leukaemia revisited. Best Pract Res Clin Haematol 22(1):153–163. doi:10.1016/j.beha.2008.12.007
19. ten Cate H, Falanga A (2008) Overview of the postulated mechanisms linking cancer and thrombosis. Pathophysiol Haemost Thromb 36(3-4):122–130. doi:10.1159/000175150
20. ten Cate H, Falanga A (2008) The pathophysiology of cancer and thrombosis. Summary and

conclusions. Pathophysiol Haemost Thromb 36(3–4):212–214. doi:10.1159/000175159

21. Walsh J, Wheeler HR, Geczy CL (1992) Modulation of tissue factor on human monocytes by cisplatin and adriamycin. Br J Haematol 81 (4):480–488
22. Wheeler HR, Geczy CL (1990) Induction of macrophage procoagulant expression by cisplatin, daunorubicin and doxorubicin. Int J Cancer 46(4):626–632
23. Dobrovolskaia MA, Patri AK, Potter TM, Rodriguez JC, Hall JB, McNeil SE (2012) Dendrimer-induced leukocyte procoagulant activity depends on particle size and surface charge. Nanomedicine (Lond) 7(2):245–256. doi:10.2217/nnm.11.105
24. Dobrovolskaia MA, Patri AK, Simak J, Hall JB, Semberova J, De Paoli Lacerda SH, McNeil SE (2012) Nanoparticle size and surface charge determine effects of PAMAM dendrimers on human platelets in vitro. Mol Pharm 9 (3):382–393. doi:10.1021/mp200463e
25. Dobrovolskaia MA, McNeil SE (2013) Understanding the correlation between in vitro and in vivo immunotoxicity tests for nanomedicines. J Control Release 172(2):456–466. doi:10.1016/j.jconrel.2013.05.025
26. Li WJ, Sha M, Ma W, Zhang ZP, Wu YJ, Shi DM (2016) Efficacy evaluation of D-dimer and modified criteria in overt and nonovert disseminated intravascular coagulation diagnosis. Int J Lab Hematol 38(2):151–159. doi:10.1111/ijlh.12467
27. Neun BW, Dobrovolskaia MA (2011) Method for in vitro analysis of nanoparticle thrombogenic properties. Methods Mol Biol 697:225–235. doi:10.1007/978-1-60327-198-1_24
28. HHS FDA/CDER/CVM. Bioanalytical method validation. Guidance for industry. May 2001. BP. https://www.fda.gov/downloads/Drugs/Guidance/ucm070107.pdf
29. Beckman Coulter Z series User manual # 991 4591-D, section A8.4.2
30. STArt4 Standard Operating procedure and Training manual. Diagnostica Stago, cat#26987, June 2002

Chapter 11

In Vitro Analysis of Nanoparticle Effects on the Zymosan Uptake by Phagocytic Cells

Timothy M. Potter, Sarah L. Skoczen, Jamie C. Rodriguez, Barry W. Neun, Anna N. Ilinskaya, Edward Cedrone, and Marina A. Dobrovolskaia

Abstract

This chapter provides a protocol for analysis of nanoparticle effects on the function of phagocytic cells. The protocol relies on luminol chemiluminescence to detect zymosan uptake. Zymosan is an yeast particle which is typically eliminated by phagocytic cells via the complement receptor pathway. The luminol, co-internalized with zymosan, is processed inside the phagosome to generate a chemiluminescent signal. If a test nanoparticle affects the phagocytic function of the cell, the amount of phagocytosed zymosan and, proportionally, the level of generated chemiluminescent signal change. Comparing the zymosan uptake of untreated cells with that of cells exposed to a nanoparticle provides information about the nanoparticle's effects on the normal phagocytic function. This method has been described previously and is presented herein with several changes. The revised method includes details about nanoparticle concentration selection, updated experimental procedure, and examples of the method performance.

Key words Nanoparticle, Phagocytosis, Immunosuppression, Zymosan A

1 Introduction

Phagocytosis is a receptor-mediated endocytosis unique to the phagocytic cells, e.g., cells of the mononuclear phagocytic system (MPS) [1]. Phagocytosis is an active process and requires actin polymerization. There are four primary receptors which mediate phagocytic uptake. Phagocytosis via three of these receptors (complement receptor (CR), FcγR receptor, and mannose receptor (MR)) is accompanied by inflammatory reactions and cytokine secretion. Phagocytosis via the fourth receptor (scavenger receptor (SR)) is not accompanied by inflammatory responses [1]. Inhibition or suppression of the normal phagocytic function by a test material (e.g. a drug) may lower the host's response to pathogens and transformed cells, and therefore poses a safety concern. Investigation of nanoparticle effects on the normal phagocytic process is

Scott E. McNeil (ed.), *Characterization of Nanoparticles Intended for Drug Delivery*, Methods in Molecular Biology, Vol. 1682, DOI 10.1007/978-1-4939-7352-1_11,

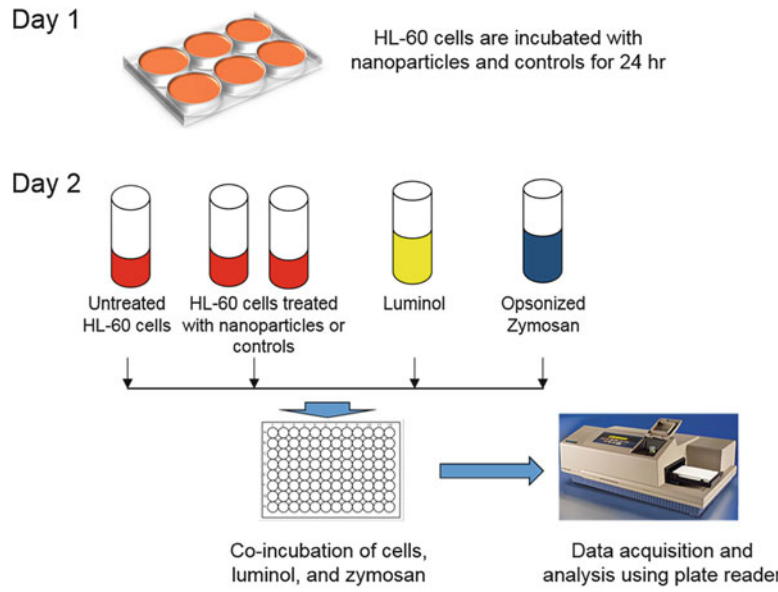

Fig. 1 Schematic illustration of the method described in this chapter

among tests used to establish the safety profile of nanotechnology-formulated drugs and devices. The protocol presented in this chapter was initially described for the analysis of nanoparticle uptake and is based on the luminol reagent [2]. Luminol is a dye which is not luminescent unless exposed to the low pH of the phagolysosome. The chemiluminescent signal generated by the cells is proportional to the amount of test material co-internalized with the luminol. Despite the previous use of this procedure to study nanoparticle uptake [3–5], over recent years, it became evident that internalization of most nanoparticles by the phagocytic cells involves multiple routes and is not limited to phagocytosis [6]. Moreover, due to their small size, the amount of luminol co-ingested by phagocytes during nanoparticle uptake is relatively low. Altogether, these facts limit the sensitivity of the luminol-based assay for monitoring nanoparticle uptake. Herein, we present the revised procedure (Fig. 1). In the updated method, HL-60 promyelocytic cells are used as the model phagocytic cell line, and zymosan A is used as model bioparticle. The phagocytic activity of untreated HL-60 cells and the cells exposed to the test nanomaterial is visualized by monitoring zymosan uptake in the presence of the luminol reagent. Nanoparticles may either enhance or inhibit the function of phagocytic cells. Such effects are identified by comparing the zymosan uptake in control cells with that of the cells exposed to tested nanomaterials 24 h before the addition of zymosan. Nanoparticles, which demonstrate the ability to inhibit phagocytosis of zymosan, may be immunosuppressive. The results of this in vitro method can be used to justify in vivo follow-up studies to verify the consequences of nanoparticle challenge on host immunity.

2 Materials

1. Phosphate buffered saline (PBS).
2. 2 mg/mL Zymosan A stock solution diluted in PBS. Use freshly prepared.
3. Heat-inactivated fetal bovine serum (FBS). Thaw a bottle of FBS at room temperature or overnight at 2–8 °C and allow to equilibrate to room temperature. Incubate for 30 min at 56 °C in a water bath, mixing every 5 min. Single-use aliquots may be stored at 2–8 °C for up to 1 month or at a nominal temperature of −20 °C indefinitely.
4. Complete RPMI-1640: 20% FBS (heat inactivated), 4 mM L-glutamine, 100 U/mL penicillin and 100 μg/mL streptomycin sulfate. Store at 2–8 °C protected from light for no longer than 1 month. Before use, warm in a water bath.
5. Trypan Blue solution
6. Human AB serum or plasma pooled from at least three donors.
7. 10 mM Luminol stock in DMSO. Prepare single-use aliquots and store at −20 °C. Protect from light.
8. 250 μM Luminol working solution diluted in PBS. On the day of the experiment, thaw an aliquot of luminol stock solution and dilute with PBS to a final concentration of 250 μM, e.g., add 250 μL of 10 mM stock into 9.750 mL of PBS. Protect from light. Discard unused portion.
9. Flat bottom 96-well white luminescence plates.
10. HL-60 promyelocytic cells.
11. Hemocytometer.
12. Gel-pack (*see* **Note 1**).
13. Plate reader capable of working in luminescence mode (*see* **Note 2**).

3 Methods

3.1 Preparation of Reagents and Controls

1. Prepare oponized Zymosan A solution. Combine Zymosan A stock and human AB serum or plasma. Use 1 mL of serum/plasma per each 0.5 mL of zymosan A stock. Incubate Zymosan A with serum/plasma for 30 min at 37 °C. Wash Zymosan A particles with PBS (use 1 mL of PBS per each 0.5 mL of original zymosan stock and a centrifuge setting of 2000 × *g* for 2 min) and resuspend in PBS to a final concentration of 2 mg/mL.
2. Prepare *negative control* sample. Use PBS as a negative control. Process this control the same way as test nanoparticle.

3. Prepare *vehicle control* sample. Vehicle control is the buffer or media used to formulate test nanomaterials. Common excipients used in nanoformulations are trehalose, sucrose, and albumin. However, other reagents and materials are also used alone or in combination. Vehicle control should match the formulation buffer of the test nanomaterial by both composition and concentration. This control can be skipped if nanoparticles are stored in PBS.

3.2 Preparation of Nanoparticle Samples

This assay requires 2 mL of nanoparticles at 5× the highest test concentration dissolved/resuspended in PBS. The concentration is selected based on the plasma concentration of the nanoparticle at the intended therapeutic dose. For the purpose of this protocol, this concentration is called "theoretical plasma concentration." Considerations for estimating theoretical plasma concentration were reviewed elsewhere [7] and are summarized in Box 1. The assay will evaluate 4 concentrations: 10× (or when feasible 5×, 30×, 100×) of the theoretical plasma concentration, theoretical plasma concentration, and two 5-fold serial dilutions of the theoretical plasma concentration. When the intended therapeutic concentration is unknown, the highest final concentration is 1 mg/mL or the highest reasonably achievable concentration. For example, if the final theoretical plasma concentration to be tested is 0.2 mg/mL, then a stock of 10 mg/mL will be prepared and diluted 10-fold (1 mg/mL), followed by serial 5-fold dilutions (0.2 and 0.04 mg/mL). When 200 μL of each of these samples are combined in a culture plate well with 800 μL of cells, the final concentrations of nanoparticles are 0.008, 0.04, 0.2, and 2 mg/mL. Each nanoparticle concentration is plated six times.

Box 1. Example Calculation of Nanoparticle Concentration for In Vitro Test

Assume the mouse dose is known to be 123 mg/kg in this example.

$$\text{human dose} = \frac{mouse\ dose}{12.3} = \frac{123\frac{mg}{kg}}{12.3} = 10\ \text{mg/kg}$$

Blood volume makes up approximately 8% of body weight (e.g. a 70 kg human has approximately 5.6 L (8% of 70) of blood). This allows for a very rough estimate of what the maximum blood concentration may be.

$$\text{in vitro concentration}_{human\ matrix} = \frac{human\ dose}{human\ blood\ volume} = \frac{70\ kg\ x\ 10\frac{mg}{kg}}{5.6\ L}$$

$$= \frac{700\ mg}{5.6\ L} = 0.125\ \text{mg/mL}$$

Box 1 Example calculation of nanoparticle concentration for this in vitro test. Reproduced with permission from ref. 7

3.3 Preparation of Cells

HL-60 is a non-adherent promyelocytic cell line derived by S.J. Collins, et al. from a patient with acute promyelocytic leukemia [8]. Cultures can be maintained by the addition of fresh medium or replacement of medium. Alternatively, cultures can be established by centrifugation with subsequent resuspension at 1×10^5 viable cells/mL. Do not allow cell concentration to exceed 1×10^6 cells/mL. Maintain cell density between 1×10^5 and 1×10^6 viable cells/mL. On the day of the experiment, count cells using trypan blue. If the cell viability is ≥90% proceed to the next step.

3.4 Chemiluminescent Assay of Nanoparticle Effects on the Zymosan Uptake by Phagocytic Cells

The experimental procedure involves 2 days.

Day 1

1. Adjust cell concentration to 1.25×10^6 cells per mL using complete medium.
2. Plate 800 μL of the cell suspension per well on a 24-well plate. Prepare 6 wells for each nanoparticle concentration, vehicle control, negative control and 8 wells for untreated cells. Refer to Fig. 2 for example of a plate map.
3. Add 200 μL of test samples to corresponding wells. Cover the plates and incubate at 37 °C overnight (18–24 h).

Day 2

4. Turn on plate reader, allowing it to warm up to 37 °C. Place an empty white 96-well test plate inside the plate reader chamber, allowing it to warm to 37 °C as well. Set up the instrumental parameters.
5. Harvest cells from **step 3** into Eppendorf tubes and wash twice with PBS to remove nanoparticles. Do not pool the content of individual wells within the treatment group; each well serves as a separate replicate.
6. After the last wash, reconstitute the cell pellet in 240 μL of complete media. Use 20 μL of this suspension to determine cell count and viability by acridine orange/propidium iodide (AO/PI) staining or other relevant procedure.
7. Adjust cell concentration to $0.9–1 \times 10^7$ cell/mL using complete medium. Keep at room temperature.
8. Plate 100 μL of cell suspension per well on the 96-well white plate pre-warmed in **step 1**. Prepare 4 wells with 100 μL of PBS for no cell control and another 4 wells with 200 μL of PBS for Luminol only. Refer to Fig. 2 as an example of a plate map (*see* **Note 3**).
9. Add 100 μL of Luminol working solution to each well (*see* **Note 3**).

Example Plate Map - Day 1

1	2	3	4	5	6
Untreated cells	Untreated cells	TS 1 mg/mL	TS 1 mg/mL	TS 0.2 mg/mL	TS 0.2 mg/mL
Untreated cells	Untreated cells	TS 1 mg/mL	TS 1 mg/mL	TS 0.2 mg/mL	TS 0.2 mg/mL
Untreated cells	Untreated cells	TS 1 mg/mL	TS 1 mg/mL	TS 0.2 mg/mL	TS 0.2 mg/mL
Untreated cells	Untreated cells				

1	2	3	4	5	6
TS 0.04 mg/mL	TS 0.04 mg/mL	TS 0.008 mg/mL	TS 0.008 mg/mL	NC	NC
TS 0.04 mg/mL	TS 0.04 mg/mL	TS 0.008 mg/mL	TS 0.008 mg/mL	NC	NC
TS 0.04 mg/mL	TS 0.04 mg/mL	TS 0.008 mg/mL	TS 0.008 mg/mL	NC	NC
VC	VC	VC	VC	VC	VC

Example Plate Map - Day 2

	1	2	3	4	5	6	7	8	9	10	11	12
A	Untreated Cells	Untreated Cells	NC	NC	NC	VC	VC	VC	PBS No cells	PBS No cells		
B	Untreated Cells	Untreated Cells	NC	NC	NC	VC	VC	VC	PBS No cells	PBS No cells		
C	TS 0.008 mg/mL	TS 0.008 mg/mL	TS 0.008 mg/mL	TS 0.04 mg/mL	TS 0.04 mg/mL	TS 0.04 mg/mL	TS 0.2 mg/mL	TS 0.2 mg/mL	TS 0.2 mg/mL	TS 1.0 mg/mL	TS 1.0 mg/mL	TS 1.0 mg/mL
D	TS 0.008 mg/mL	TS 0.008 mg/mL	TS 0.008 mg/mL	TS 0.04 mg/mL	TS 0.04 mg/mL	TS 0.04 mg/mL	TS 0.2 mg/mL	TS 0.2 mg/mL	TS 0.2 mg/mL	TS 1.0 mg/mL	TS 1.0 mg/mL	TS 1.0 mg/mL
E												
F												
G	Untreated Cells	Untreated Cells	PBS	PBS								
H	Untreated Cells	Untreated Cells	PBS	PBS								

These wells receive both Luminol and Zymosan A

These wells receive Luminol only; PBS is used instead of Zymosan A to adjust the volume

Fig. 2 Example plate layout. The wells are labeled as follows: *NC* for negative control (PBS), *VC* for vehicle control, *TS* for test sample

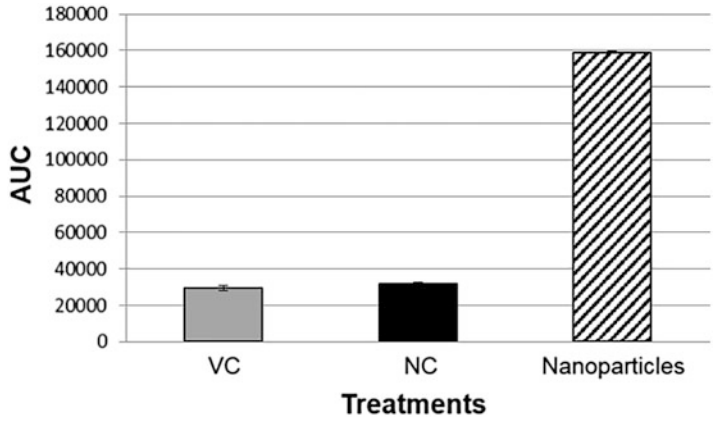

Fig. 3 Example of data generated using this assay. These data demonstrate that a test nanoparticle enhances phagocytosis of zymosan by phagocytic cells. *VC* Vehicle Control, *NC* Negative Control

10. Using a multichannel pipette, quickly add 100 μL of opsonized Zymosan A from **step 1** of Subheading 3.1 to all wells except for the blank wells (*see* **Note 4**).
11. Start kinetic reading on a luminescence plate reader *immediately* (*see* **Notes 5** and **6**).

3.5 Calculations and Data Interpretation

1. Using Excel or other relevant software, compare area under the curve (AUC) for all samples (Fig. 3). Increase in the AUC at least two fold above the negative control (baseline) is considered a positive response. Use relevant statistical analysis to compare AUC values for test samples with that of the baseline.
2. A percent coefficient of variation (%CV) is used to control precision and calculated for each control or test sample according to the following formula:

$$\frac{\text{Standard deviation}}{\text{Mean}} \times 100\%$$

%CV for each control and test sample should be <30%. Samples demonstrating higher variability should be re-analyzed.

3. If the test result in the nanoparticle-treated sample is different from the test result in the un-treated cells more or equal to two fold, then the nanoparticle affects phagocytic function of the cells.

4 Notes

1. This material is optional and may be omitted. It is used to keep the plate warm for optimal phagocytosis; however, if it takes longer than 2 min to transfer the plate to the plate reader after

addition of all reagents, the phagocytosis process will start before one starts analyzing the plate on the plate reader.

2. The plates used for this assay have a solid white bottom, therefore the plate should be read from the top. Depending on the type of plate reader, one may need to use a plate adaptor to provide an optimal condition for the top read.
3. This step can be done at room temperature (20–22 °C). However, when the room temperature is low, keep the plate on a warm gel-pack during these steps.
4. This step can be performed on the bench close to the plate reader to minimize the time between sample addition and initiation of the kinetic reading.
5. If using the plate reader with both top and bottom read capabilities, do not forget to use a plate adaptor before proceeding with the plate analysis on the plate reader. This is important because luminescence reading is performed from the top (the bottom of the plate is not transparent).
6. NCL does not endorse suppliers. However, we found that a new user benefits from knowing catalog information of reagents used in our assays. If you need ideas of what reagents are used at the NCL, please review NCL method ITA-9 available at https://ncl.cancer.gov/resources/assay-cascade-protocols. When other reagents are used, the assay performance may change. When using reagents and instruments from sources other than that used in our protocols, assay performance qualification is needed to verify the assay functionality and validity.

Acknowledgment

This project has been funded in whole or in part with Federal funds from the National Cancer Institute, National Institutes of Health, under Contract No. HHSN261200800001E. The content of this publication does not necessarily reflect the views or policies of the Department of Health and Human Services, nor does mention of trade names, commercial products, or organizations imply endorsement by the U.S. Government.

References

1. Aderem A, Underhill DM (1999) Mechanisms of phagocytosis in macrophages. Annu Rev Immunol 17:593–623. doi:10.1146/annurev.immunol.17.1.593
2. Skoczen SL, Potter TM, Dobrovolskaia MA (2011) In vitro analysis of nanoparticle uptake by macrophages using chemiluminescence. Methods Mol Biol 697:255–261. doi:10.1007/978-1-60327-198-1_27
3. Antonini JM, Van Dyke K, Ye Z, DiMatteo M, Reasor MJ (1994) Introduction of luminol-dependent chemiluminescence as a method to

study silica inflammation in the tissue and phagocytic cells of rat lung. Environ Health Perspect 102(Suppl 10):37–42

4. Gref R, Luck M, Quellec P, Marchand M, Dellacherie E, Harnisch S, Blunk T, Muller RH (2000) 'Stealth' corona-core nanoparticles surface modified by polyethylene glycol (PEG): influences of the corona (PEG chain length and surface density) and of the core composition on phagocytic uptake and plasma protein adsorption. Colloids Surf B Biointerfaces 18(3–4):301–313
5. Leroux JC, Gravel P, Balant L, Volet B, Anner BM, Allemann E, Doelker E, Gurny R (1994) Internalization of poly(D,L-lactic acid) nanoparticles by isolated human leukocytes and analysis of plasma proteins adsorbed onto the particles. J Biomed Mater Res 28(4):471–481. doi:10.1002/jbm.820280410
6. França A, Aggarwal P, Barsov EV, Kozlov SV, Dobrovolskaia MA, Gonzalez-Fernandez A (2011) Macrophage scavenger receptor a mediates the uptake of gold colloids by macrophages in vitro. Nanomedicine (Lond) 6 (7):1175–1188. doi:10.2217/nnm.11.41
7. Dobrovolskaia MA, McNeil SE (2013) Understanding the correlation between in vitro and in vivo immunotoxicity tests for nanomedicines. J Control Release 172(2):456–466. doi:10.1016/j.jconrel.2013.05.025
8. Collins SJ, Ruscetti FW, Gallagher RE, Gallo RC (1978) Terminal differentiation of human promyelocytic leukemia cells induced by dimethyl sulfoxide and other polar compounds. Proc Natl Acad Sci U S A 75(5):2458–2462

Chapter 12

Assessing NLRP3 Inflammasome Activation by Nanoparticles

Bhawna Sharma, Christopher B. McLeland, Timothy M. Potter, Stephan T. Stern, and Pavan P. Adiseshaiah

Abstract

NLRP3 inflammasome activation is one of the initial steps in an inflammatory cascade against pathogen/danger-associated molecular patterns (PAMPs/DAMPs), such as those arising from environmental toxins or nanoparticles, and is essential for innate immune response. NLRP3 inflammasome activation in cells can lead to the release of IL-1β cytokine via caspase-1, which is required for inflammatory-induced programmed cell death (pyroptosis). Nanoparticles are commonly used as vaccine adjuvants and drug delivery vehicles to improve the efficacy and reduce the toxicity of chemotherapeutic agents. Several studies indicate that different nanoparticles (e.g., liposomes, polymer-based nanoparticles) can induce NLRP3 inflammasome activation. Generation of a pro-inflammatory response is beneficial for vaccine delivery to provide adaptive immunity, a necessary step for successful vaccination. However, similar immune responses for intravenously injected, drug-containing nanoparticles can result in immunotoxicity (e.g., silica nanoparticles). Evaluation of NLRP3-mediated inflammasome activation by nanoparticles may predict pro-inflammatory responses in order to determine if these effects may be mitigated for drug delivery or optimized for vaccine development. In this protocol, we outline steps to monitor the release of IL-1β using PMA-primed THP-1 cells, a human monocytic leukemia cell line, as a model system. IL-1β release is used as a marker of NLRP3 inflammasome activation.

Key words Inflammasome, NLRP3, Nanoparticles, IL-1β, THP-1

1 Introduction

Nucleotide-binding oligomerization domain (NOD), leucine-rich-containing family (NLR) pyrin domain-containing-3 (NLRP3) is one of the most versatile pattern-recognition receptors (PRR), making NLRP3 inflammasomes sensitive to a wide variety of stimuli. The NLRP3 inflammasome is a multimeric complex consisting of NLRP3 as a sensor; apoptosis-associated speck-like protein (ASC), an adaptor protein with a caspase recruitment and activation domain; and the catalytic enzyme pro-caspase-1 [1]. NLRP3 inflammasome activation requires two stimuli for in vitro

Scott E. McNeil (ed.), *Characterization of Nanoparticles Intended for Drug Delivery*, Methods in Molecular Biology, Vol. 1682, DOI 10.1007/978-1-4939-7352-1_12,

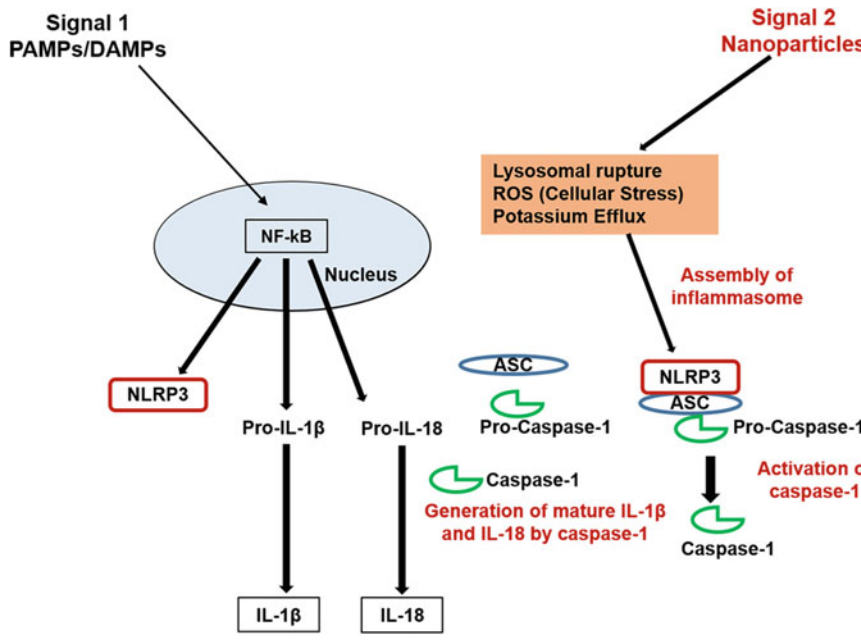

Fig. 1 Schematic overview of inflammasome assembly

experiments. The first stimulus, such as from lipopolysaccharides (LPS) or phorbol-12-myristate-13-acetate (PMA), primes monocytes and macrophages by increasing the transcription and translation of pro-cytokines and NLRP3 inflammasome components (pro-IL-1β, pro-IL-18, NLRP3) [2]. The second stimulus, developed from ATP, nanoparticles [3], environmental toxins, etc., results in NLRP3 inflammasome activation and the conversion of pro-IL-1β to an active IL-1β form [4]. Pathogen-associated molecular patterns (PAMPs) such as microbial nucleic acid, LPS, and glycoprotein, and danger-associated molecular patterns (DAMPs), like those from ATP and uric acid, activate NLRP3 inflammasomes [5, 6] (Fig. 1). Some pathogen-associated molecules can serve as the first and second stimuli to induce inflammasome activation. For example, monocytes and macrophages produce IL-1β in response to bacterial LPS without additional stimuli, although the response can be further potentiated by nanomaterials capable of inflammasome activation [7, 8]. Three models have been proposed through which NLRP3 inflammasome can be activated: (a) lysosomal rupture and release of cathepsin enzymes [9], (b) stimulation of channels (efflux of K^+ or influx of Ca^{2+} through ion channels or influx of ATP via ATP channels) [10, 11], and (c) cellular stress, induced by reactive oxygen species (ROS) [12]. Experimentally, NLRP3 inflammasome activation is monitored by the release of IL-1β and IL-18 cytokines in culture supernatants from immune cells. Recent publications have shown that pro-IL-1β can also be detected after cell necrosis [13], which suggests that nanoparticles causing cell

death can lead to release of detectable pro-IL-1β in the cell supernatants. Western blot analysis of culture supernatants and reporter assays using commercially available cell lines that specifically detect mature IL-1β, such as HEK Blue IL-1β cells, can discern the presence of inactive or active forms of IL-1β.

Physicochemical characteristics of the nanoparticles such as size and surface charge play an important role in the activation of NLRP3 inflammasome. For example, positively charged nanoparticles elicit higher IL-1β secretion when compared to negatively or neutral charged nanoparticles [14]. Similarly, smaller sized silica nanoparticles induce higher levels of IL-1β secretion in murine bone marrow-derived macrophages compared to silica particles with sizes larger than 1 μm [15]. Although moderate immune activation can be beneficial for vaccines, a heightened immune response is generally disadvantageous for most therapeutics. Adjuvants are specifically designed to have immune-potentiating activity to enable the use of lower vaccine doses and dosing frequencies, expanding vaccine supply [16]. However, overt or continuous activation of inflammasomes is known to cause autoimmune and chronic inflammatory diseases, like Crohn's disease and rheumatoid arthritis [17]. The physicochemical attributes of nanoparticles, e.g., silica nanoparticles [18], used for drug or vaccine delivery can influence immune activation; and therefore, it is important to understand this relationship between nanoparticle properties and immunogenicity for successful clinical translation. Nanoparticle's ability to induce cytokines and cytokine-mediated toxicities are monitored in vivo or in vitro using peripheral blood or mononuclear cells (PBMC) cultures. The protocol for such analysis is presented in Chapter 15 of this book. When the results of such tests reveal that the given nanoformulation induces IL-1β, the current protocol can be used for further mechanistic studies. In this chapter, we describe an ELISA-based method to monitor the activation of the NLRP3 inflammasome by silica nanoparticles, using human monocytic leukemia THP-1 cell line as a model system. The protocol is adaptable to any nanomaterial analyte of interest as long as there is an understanding of the nanoparticle's physicochemical characteristics. We utilize three THP-1 cell types to evaluate NLRP3 inflammasome activation: THP-1 Null cells which have all NLRP3 inflammasome components; THP-1 defNLRP3 cells which are deficient in the NLRP3 protein; and THP-1 defCASP1 cells which are deficient in the caspase-1 enzyme. THP-1 defNLRP3 cells are used as a negative control and will not respond to exclusive inducers of the NLRP3 inflammasome, but may respond to inducers of other inflammasomes. THP-1 defCASP1 cells are deficient in the caspase-1 component of the NLRP3 complex and function as an additional negative control for NLRP3 inflammasome activation.

2 Materials

2.1 Cell Culture Reagents and Materials

1. THP-1 Null, THP-1 defNLRP3, and THP-1 defCASP1.
2. Growth medium: RPMI 1640 containing 2 mM L-glutamine, 1.5 g/L sodium bicarbonate, 4.5 g/L glucose, 10 mM HEPES, and 1.0 mM sodium pyruvate with 10% heat-inactivated fetal bovine serum (FBS), 50 U/mL-50 μg/mL Penicillin-Streptomycin, 100 μg/mL Normocin, and 200 μg/mL Hygromycin. Store at 4 °C and warm to 37 °C in water bath before use (*see* **Note 1**).
3. Assay medium: RPMI 1640 containing 2 mM L-glutamine, 1.5 g/L sodium bicarbonate, 4.5 g/L glucose, 10 mM HEPES, and 1.0 mM sodium pyruvate with 10% heat-inactivated fetal bovine serum (*see* **Note 1**).
4. Phorbol-12-myristate-13-acetate (PMA) (*see* **Notes 2** and **3**).
5. T75 flasks.
6. Sterile conical tubes.
7. Automated cell counter or hemocytometer.
8. 96-well flat bottom cell culture plates.

2.2 Control and Nanoparticle Solutions

1. Positive controls: 250 μg/mL alum and 100 μg/mL high purity, high quality, fine ground silica powder with maximum size of 5 μm. Each positive control solution is diluted in RPMI assay medium (*see* **Notes 4** and **5**).
2. Negative control: RPMI assay media.
3. Test material: 20 nm silica nanoparticles diluted in RPMI assay medium to appropriate concentrations (*see* **Notes 4**, **6**–**8**).

2.3 MTT Reagents and Materials

1. MTT reaction mixture: 5 mg/mL 3-(4,5-Dimethyl-2-thiazolyl)-2,5-diphenyl-2H-tetrazolium bromide (MTT) solution in phosphate buffered saline (PBS). Protect stock solution from light and store at 4 °C.
2. Dimethyl sulfoxide (DMSO). Store at room temperature.
3. Glycine buffer: 0.1 M glycine and 0.1 M NaCl, pH 10.5. Store at room temperature.
4. Multichannel or repeat pipettor.
5. Plate shaker.
6. Absorbance plate reader.

2.4 ELISA Reagents and Materials

1. Anti-human IL-1β ELISA components: primary (coating) antibody, secondary (detection) antibody, and recombinant IL-1β (*see* **Note 9**). Store at −80 °C.

2. Blocking buffer: 1× PBS, 1% bovine serum albumin (BSA), and 0.5% Tween 20.
3. Washing buffer: 25 mM Tris, 15 M NaCl at pH 7.2, and 0.05% Tween 20.
4. Streptavidin horseradish peroxidase (SA-HRP). Store at −80 °C.
5. TMB substrate stored at 4 °C.
6. 2 N sulfuric acid.
7. ELISA plates (*see* **Note 10**).
8. Automated plate washer.
9. Absorbance plate reader.

3 Methods

3.1 Cell Culture

1. THP-1 Null, THP-1 defNLRP3, and THP1 defCASP1 cells are cultured in T75 flasks in suspension in 25 mL of growth media.
2. On day 1, centrifuge cells in 50 mL sterile conical tubes at 400 × *g* for 5 min.
3. Aspirate supernatants and resuspend pellets in 5 mL assay media.
4. Count cells using automated cell counter or hemocytometer.
5. Plate THP-1 Null, THP-1 defNLRP3, and defCASP1 cells at 400,000 cells per mL of assay media containing 50 nM PMA in a 96-well format (*see* **Notes 2** and **3**). The cells are incubated for 24 h at 37 °C. All three cell lines display similar morphology (Fig. 2a).
6. On day 2, media is carefully aspirated from the wells in preparation for treatment.

3.2 Treatment of Cells with Nanoparticles

1. Prepare control and test sample solutions by resuspending in assay media (*see* **Notes 4**, **7**, and **8**).
2. Treat cells at 37 °C for 24 h in triplicate with 200 μL of test nanoparticles, silica nanoparticles in this example, in a 96-well plate format. Include no cell wells at each test nanoparticle concentration (Fig. 3, *see* **Note 8**). These wells with no cells are utilized to monitor any interference by nanoparticles in IL-1β ELISA (*see* **Note 11**).
3. Include wells with RPMI assay media alone (wells with no cells) as a "blank," and wells with RPMI assay media and cells as a "negative control" (Fig. 3) (*see* **Note 11**).

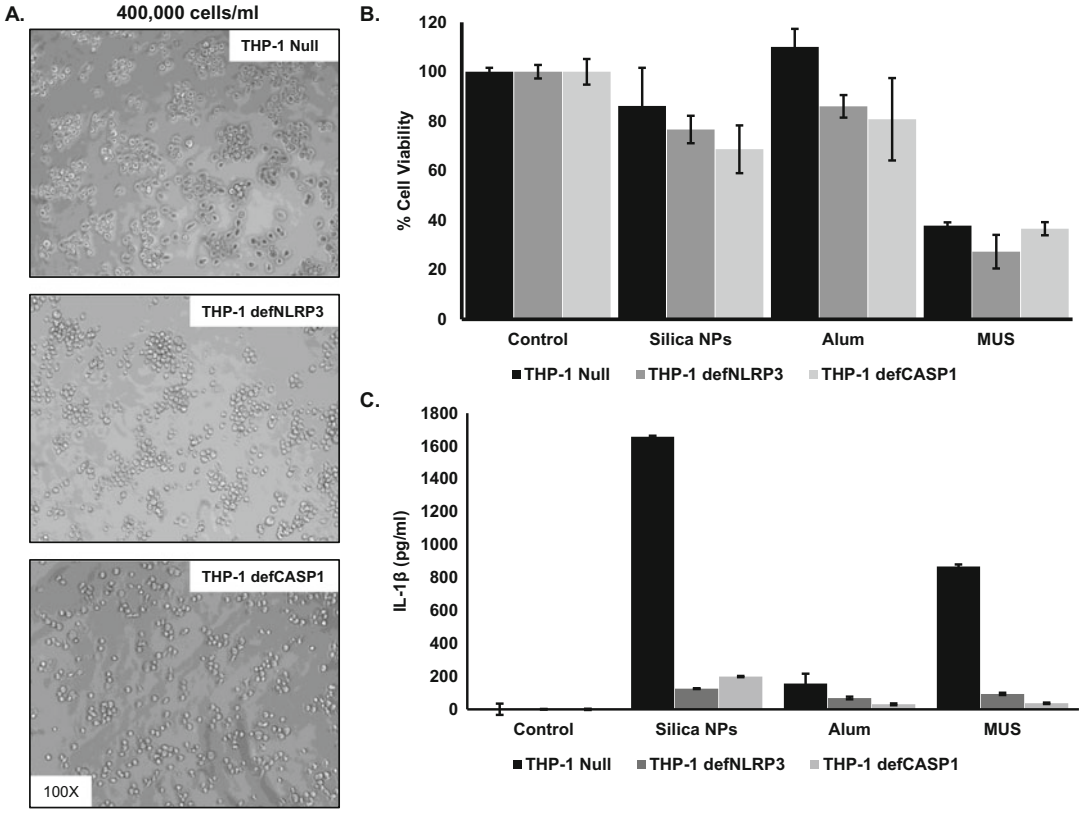

Fig. 2 NLRP3 inflammasome activation in THP-1 cells. (**a**) Morphological images of PMA (50 nM, Sigma) primed THP-1 Null, THP-1 defNLRP3, and THP-1 defCASP1 cells (Invivogen). (**b**) MTT assay showing cell viability after 20 nm silica nanoparticles (NanoComposix, Silica NPs, 250 μg/mL), alum (Imject Alum, 250 μg/mL, Thermo Fisher Scientific) and ground silica (Min-U-sil 5; MUS, 100 μg/mL, US Silica, Berkley Spring, WV) treatment in THP-1 Null, THP-1 defNLRP3, and THP-1 defCASP1 cells. (**c**) IL-1β expression as determined by ELISA (R&D Systems) after 20 nm silica nanoparticles (Silica NPs), alum and Min-U-sil (MUS) treatment in THP-1 Null, defNLRP3 and defCasp1 cells. ELISA values were normalized with basal IL-1β levels in each cell type to account for differences in cell number

4. Add 100 μg/mL of fine ground silica and 250 μg/mL of alum diluted in assay media to wells with cells as "positive controls" for NLRP3 inflammasome activation. Prepare wells in triplicate for each positive control Fig. 3, *see* **Note 5**).
5. Incubate plate at 37 °C for 24 h.
6. Centrifuge plate at 120 × *g* for 5 min and transfer supernatants into a 96-well collection plate for ELISA (*see* **Notes 12–14**). Maintain collection plates at −20 °C (same/next day storage) or −80 °C (longer storage) until ready to start ELISA.

	Assay Media			Null			NLRP3-/-			CASP1-/-		
	1	2	3	4	5	6	7	8	9	10	11	12
A	Media	Media	Media	Media	Media	Media	Media	Media	Media	Media	Media	Media
B	P1	P1	P1	P1	P1	P1	P1	P1	P1	P1	P1	P1
C	P2	P2	P2	P2	P2	P2	P2	P2	P2	P2	P2	P2
D	P3	P3	P3	P3	P3	P3	P3	P3	P3	P3	P3	P3
E	Alum 250 ug/ml	Alum 250 ug/ml	Alum 250 ug/ml	Alum 250 ug/ml	Alum 250 ug/ml	Alum 250 ug/ml	Alum 250 ug/ml	Alum 250 ug/ml	Alum 250 ug/ml	Alum 250 ug/ml	Alum 250 ug/ml	Alum 250 ug/ml
F	MSU 100 ug/ml	MSU 100 ug/ml	MSU 100 ug/ml	MSU 100 ug/ml	MSU 100 ug/ml	MSU 100 ug/ml	MSU 100 ug/ml	MSU 100 ug/ml	MSU 100 ug/ml	MSU 100 ug/ml	MSU 100 ug/ml	MSU 100 ug/ml
G												
H												

Fig. 3 Plate map for MTT assay. Null: THP-1 Null cells; NLRP3−/−: THP-1 defNLRP3 cells; CASP1−/−: THP-1 defCASP1 cells; MSU: MIN-U-SIL, fine ground silica; P1: analyte concentration 1; P2: analyte concentration 2; P3: analyte concentration 3

3.3 MTT Assay to Monitor Cell Viability

1. Aspirate any remaining media from the plate with cells and replace with fresh 200 μL assay media. No wash step is involved.
2. Add 50 μL of 5 mg/mL MTT solution to each well and incubate at 37 °C for 2–4 h. Cover plates with aluminum foil to protect from light. MTT should be added using multichannel or repeat pipettor to avoid delay in chromogen development among wells.
3. After incubation, aspirate media and add 200 μL of DMSO and 25 μL of glycine buffer to each well. DMSO is used to solubilize the formazan crystals, while glycine buffer stops the reaction.
4. Mix contents of each well by placing the plate on a shaker for 5 min with continuous gentle shaking.
5. Read optical density (OD) of entire plate at 570 nm on a plate reader with a reference wavelength of 680 nm.
6. Normalize MTT results with averaged OD values from cell-free "blank" wells for each treatment. Percent cell viability is measured as:

$$\%\text{Cell Viability} = \frac{\text{Cell Treatment OD-Mean}^{\text{“Blank”}}\text{ OD}}{\text{Mean Normalized Media Control OD}} \times 100$$

where Normalized Media Control OD = media control OD – cell-free "Blank" OD

7. Cell viability (%) is calculated for each OD value (triplicate treatments) and then the mean and standard deviation of the three values is plotted on a graph (Fig. 2b).

3.4 IL-1β ELISA Assay

This part of the protocol has been adapted from another chapter in this book (refer to Chapter 15).

1. ELISA plates (96-well format) are coated with primary antibody at a concentration of 1 μg/mL in 0.2 M sodium carbonate-bicarbonate buffer, pH 9.4. To coat one ELISA plate, a 10 mL volume of primary antibody solution is required (*see* **Note 9**).
2. Incubate plates at 4 °C overnight.
3. Next day, aspirate remaining primary antibody from the wells and tap plate gently on blotting paper to remove excess antibody. Add 100 μL of blocking buffer to each well for 1 h at room temperature to reduce background signal.
4. Prepare standards in duplicate. Recombinant IL-1β protein standards are made starting at a 250 pg/mL concentration diluted in assay media. Perform serial dilutions at 1:2 ratios. The concentration range for the standards used in the experiment shown is 250 pg/mL–3.9 pg/mL (*see* **Notes 15** and **16**).
5. Prepare samples in triplicate. If using frozen samples prepared during **step 7** of Subheading 3.2, spin plates before using them. Make 1:5 dilutions of samples in assay media in an intermediate plate before adding the solutions to the ELISA plate. For example, combine 30 μL of the supernatant sample with 120 μL of assay media (*see* **Note 16**).
6. Prepare quality control standards in duplicate using recombinant IL-1β protein at 100, 50, and 12.5 pg/mL concentrations from the stock solution. Do not use the same dilution tubes as used for the standard.
7. Prepare inhibition enhancement controls in duplicate. To check for interference by nanoparticles, use nanoparticle blank solutions from **step 2** in Subheading 3.2 in the intermediate plate. Spike nanoparticle blank wells with IL-1β protein to make a 50 pg/mL final concentration of the protein in the wells. If wells are limited in the intermediate or ELISA plates, use the highest concentration of nanoparticles tested.
8. Aspirate blocking buffer and blot ELISA plate to remove excess buffer.
9. Once all standards and samples are prepared, transfer 100 μL from each well of the intermediate plate to the ELISA plate, which was blocked in **step 3** above (Fig. 4). ELISA plate should include test samples, quality controls, and assay standards.
10. Incubate at room temperature for 1 h.

	Assay Media			Null			NLRP3-/-			CASP1-/-		
	1	2	3	4	5	6	7	8	9	10	11	12
A	P1	P1	P1	P1	P1	P1	P1	P1	P1	P1	P1	P1
B	P2	P2	P2	P2	P2	P2	P2	P2	P2	P2	P2	P2
C	P3	P3	P3	P3	P3	P3	P3	P3	P3	P3	P3	P3
D	ALUM	ALUM	ALUM	ALUM	ALUM	ALUM	ALUM	ALUM	ALUM	ALUM	ALUM	ALUM
E	MSU	MSU	MSU	MSU	MSU	MSU	MSU	MSU	MSU	MSU	MSU	MSU

Assay Media (unless otherwise noted)

F	Q1 100 pg/ml	Q1 100 pg/ml	Q2 50 pg/ml	Q2 50 pg/ml	Q3 12.5 pg/ml	Q3 12.5 pg/ml	CTL1 **Null**	CTL1 **Null**	CTL2 **NLRP3-/-**	CTL2 **NLRP3-/-**	CTL3 **Casp1-/-**	CTL3 **Casp1-/-**
G	Blank	IEC1	IEC2	IEC3	IEC4	STD1 250 pg/ml	STD2 125 pg/ml	STD3 62.5 pg/ml	STD4 31.2 pg/ml	STD5 15.6 pg/ml	STD6 7.8 pg/ml	STD7 3.9 pg/ml
H	Blank	IEC1	IEC2	IEC3	IEC4	STD1 250 pg/ml	STD2 125 pg/ml	STD3 62.5 pg/ml	STD4 31.2 pg/ml	STD5 15.6 pg/ml	STD6 7.8 pg/ml	STD7 3.9 pg/ml

Fig. 4 Plate map for IL-1β ELISA. Null: THP-1 Null cell supernatants; NLRP3−/−: THP-1 defNLRP3 cell supernatants; CASP1−/−: THP-1 defCASP1 cell supernatants; P1: analyte, concentration 1; P2: analyte concentration 2; P3: analyte concentration 3; MSU: MIN-U-SIL, fine ground silica; Q: Quality control; CTL: Media control for each cell type; Blank: Assay media only, no cells; IEC: Inhibition enhancement control; STD: Standard

11. After incubation, aspirate samples and wash ELISA plate with washing buffer in two rounds. Each round of washing is made up of three washes using an automated plate washer.
12. Blot plates dry on blotting paper to remove excess wash buffer.
13. Add 100 µL of 0.5 µg/mL detection (biotinylated secondary) antibody to the wells and incubate at room temperature for 1 h (*see* **Note 9**).
14. After incubation with the detection antibody, aspirate the antibody and repeat washing **steps 11** and **12**.
15. Add 100 µL of SA-HRP (0.1µg/mL) to each well and incubate for 1 h at room temperature.
16. Repeat **steps 11** and **12**.
17. Add 100 µL of TMB substrate to each well. Incubate at room temperature for 15–30 min and protect the plate from light. Monitor the development of blue color.
18. To stop the reaction, add 50 µL of 2 N sulfuric acid to each well. The color in the well will change from blue to yellow. Read the plate within 30 min of stopping the reaction at 450 nm using a plate reader.
19. Average OD values of blank wells and subtract averaged value from OD values of all wells (Fig. 2c).

20. Plot a standard curve with averaged OD values of standards (Y-axis) vs. IL-1β protein concentration (X-axis, pg/mL) used in the assay.
21. Interpolate the IL-1β concentrations of the samples using the standard curve equation with the normalized OD values:

$$\text{IL-1}\beta \text{ Concentration } (\rho\text{g/mL}) = (\text{Sample OD-Blank OD}) \times \text{Concentration at 1 OD} \times \text{Dilution Factor}$$

where Blank OD is the average of duplicate values, Concentration at 1 OD is from the standard curve fit, and the Dilution Factor is 5 based on **step 5** above.

22. Normalize concentration to account for any differences in cell number per well (*see* **Note 17**).
23. OD values of the inhibition enhancement controls are compared to the quality controls with the same recombinant protein concentrations. If the values are within 25% of each other, no interference by the nanoparticle can be inferred. If the values differ, then the nanoparticle may interfere with the ELISA. To account for the interference, one can subtract the nanoparticle blank ELISA OD values from the treatment well OD values.

4 Notes

1. Different cell types may require different media with other antimicrobial reagents. Follow the cell supplier's recommendations. THP-1 Null, THP-1 defNLRP3, and THP-1 defCASP1 cells shown in Fig. 2 are purchased from Invivogen.
2. PMA is used as a first signal for inflammasome activation and for the differentiation of THP-1 cells to macrophage-like cells, which makes THP-1 cells adherent [2].
3. PMA stocks are maintained at 1 mM concentration in DMSO in 50 μL aliquots. The working concentration of PMA (50 nM) is obtained by diluting the stock in cell culture media.
4. Test particles should be monitored for the presence of endotoxin. Particles contaminated with bacterial endotoxin can lead to false-positive results as endotoxin triggers IL-1 gene expression through Toll-like receptor 4 and can also activate inflammasome. LAL assay is one of the most commonly used assays for endotoxin detection. Detection and quantitative evaluation of endotoxin contamination in nanoparticle formulations using LAL-based assays has been described before [19].

5. Fine ground silica used in studies shown in Fig. 2 is MIN-U-SIL®. MIN-U-SIL (100 μg/mL) is made fresh from powdered stock in media for the assay. Fine ground silica should be weighed and diluted in an aseptic biological safety cabinet (HEPA filtered BSL-2 class, type B2 biological safety cabinet). While dealing with powdered silica, wear all personal protective equipment, because this material is toxic and can cause silicosis when inhaled.
6. This protocol utilizes silica nanoparticles as the test analyte. The methods described here can be adapted to other test analytes, which should be characterized for their physicochemical properties.
7. Use the recommended diluent for the nanoparticle analyte and make the final dilution in assay media. Make sure the majority of the final solution is in assay media.
8. The concentration range for the analyte and treatment time to cells is best chosen with an understanding of the nanoparticle's toxicity and its IC_{50} value using assays like an MTT cell viability assay or lactate dehydrogenase (LDH) leakage assay. Ideally, the concentration series should encompass clinically relevant concentrations if known.
9. Concentrations of ELISA components (antibodies, SA-HRP, protein) may vary depending upon the manufacturer. Please follow the manufacturer's recommendations.
10. ELISA plates designed for high protein binding are recommended for detection of IL-1β. Assay shown as an example in Fig. 2 was performed using Nunc Maxisorp flat bottom 96-well plates (eBioscience, San Diego, CA).
11. Platemap should contain cell-free "blank" wells to monitor nanoparticle interference (e.g., inhibition or enhancement) with the MTT assay or ELISA results.
12. If nanoparticle treatment causes cell death in the tested cell model, Western blot analysis of supernatants or commercially available cell-based reporter assays can be incorporated in this protocol to detect the mature form of IL-1β.
13. The lactate dehydrogenase (LDH) leakage assay can also be performed on the culture supernatant (50–100 μL) to monitor the effect of nanoparticles on cell viability in addition to the MTT assay.
14. To monitor lysosomal damage or dysfunction as one of the mechanisms of NLRP3 inflammasome activation, 50 μL of the culture supernatants can be used to measure cathepsin B release (using Z-LR-AMC Fluorogenic substrate assay, R&D Systems). Use of phenol-free media is recommended to avoid interference with the assay.

15. Intermediate controls (25,000 pg/mL and 2500 pg/mL) were made first from the recombinant IL-1β stock (25 μg/mL) maintained at −80 °C. The standard concentrations for the assays are diluted from the intermediate controls.
16. Ensure that the analyte concentrations span the detection range. IL-1β levels in the sample may vary depending on the cell type and cell density. The dilution of samples may need to be optimized depending upon the experimental settings.
17. If cells used in the experiment grow differently or one cell type exhibits more treatment-related cytotoxicity than the other cells, ELISA data can be normalized to media control wells for each cell type (basal IL-1β levels in the cells) or % loss of viability relative to control.

Acknowledgment

This project has been funded in whole or in part with Federal funds from the National Cancer Institute, National Institutes of Health, under Contract No. HHSN261200800001E. The content of this publication does not necessarily reflect the views or policies of the Department of Health and Human Services, nor does mention of trade names, commercial products, or organizations imply endorsement by the U.S. Government.

References

1. Guo H, Callaway JB, Ting JPY (2015) Inflammasomes: mechanism of action, role in disease, and therapeutics. Nat Med 21(7):677–687. doi:10.1038/nm.3893
2. Lund ME, To J, O'Brien BA, Donnelly S (2016) The choice of phorbol 12-myristate 13-acetate differentiation protocol influences the response of THP-1 macrophages to a pro-inflammatory stimulus. J Immunol Methods 430:64–70. doi:10.1016/j.jim.2016.01.012
3. Kim M-G, Park JY, Shon Y, Kim G, Shim G, Oh Y-K (2014) Nanotechnology and vaccine development. Asian J Pharm Sci 9 (5):227–235. http://dx.doi.org/10.1016/j.ajps.2014.06.002
4. Sharma D, Kanneganti TD (2016) The cell biology of inflammasomes: Mechanisms of inflammasome activation and regulation. J Cell Biol 213(6):617–629. doi:10.1083/jcb.201602089
5. Agostini L, Martinon F, Burns K, McDermott MF, Hawkins PN, Tschopp J (2004) NALP3 forms an IL-1beta-processing inflammasome with increased activity in Muckle-Wells autoinflammatory disorder. Immunity 20 (3):319–325
6. Mariathasan S, Weiss DS, Newton K, McBride J, O'Rourke K, Roose-Girma M, Lee WP, Weinrauch Y, Monack DM, Dixit VM (2006) Cryopyrin activates the inflammasome in response to toxins and ATP. Nature 440 (7081):228–232. doi:10.1038/nature04515
7. Meunier E, Coste A, Olagnier D, Authier H, Lefèvre L, Dardenne C, Bernad J, Béraud M, Flahaut E, Pipy B (2012) Double-walled carbon nanotubes trigger IL-1β release in human monocytes through Nlrp3 inflammasome activation. Nanomed Nanotechnol Biol Med 8 (6):987–995
8. Luo Y.-H, Chang L.W, Lin P (2015) Metal-Based Nanoparticles and the Immune System: Activation, Inflammation, and Potential Applications. BioMed Res Int 2015:1–12
9. Okada M, Matsuzawa A, Yoshimura A, Ichijo H (2014) The lysosome rupture-activated TAK1-JNK pathway regulates NLRP3

inflammasome activation. J Biol Chem 289 (47):32926–32936. doi:10.1074/jbc.M114.579961

10. Yaron JR, Gangaraju S, Rao MY, Kong X, Zhang L, Su F, Tian Y, Glenn HL, Meldrum DR (2015) K(+) regulates Ca(2+) to drive inflammasome signaling: dynamic visualization of ion flux in live cells. Cell Death Dis 6:e1954. doi:10.1038/cddis.2015.277
11. Ferrari D, Pizzirani C, Adinolfi E, Lemoli RM, Curti A, Idzko M, Panther E, Di Virgilio F (2006) The P2X7 receptor: a key player in IL-1 processing and release. J Immunol 176 (7):3877–3883
12. Tschopp J, Schroder K (2010) NLRP3 inflammasome activation: The convergence of multiple signalling pathways on ROS production? Nat Rev Immunol 10(3):210–215. doi:10.1038/nri2725
13. Cullen SP, Kearney CJ, Clancy DM, Martin SJ (2015) Diverse activators of the NLRP3 inflammasome promote IL-1beta secretion by triggering necrosis. Cell Rep 11 (10):1535–1548. doi:10.1016/j.celrep.2015.05.003
14. Neumann S, Burkert K, Kemp R, Rades T, Rod Dunbar P, Hook S (2014) Activation of the NLRP3 inflammasome is not a feature of all particulate vaccine adjuvants. Immunol Cell Biol 92:535–542. 2014/04/02 edn. doi:10.1038/icb.2014.21
15. Kusaka T, Nakayama M, Nakamura K, Ishimiya M, Furusawa E, Ogasawara K (2014) Effect of silica particle size on macrophage inflammatory responses. PLoS One 9(3):e92634. doi:10.1371/journal.pone.0092634
16. Reed SG, Orr MT, Fox CB (2013) Key roles of adjuvants in modern vaccines. Nat Med 19 (12):1597–1608. doi:10.1038/nm.3409
17. Lamkanfi M, Dixit VM (2014) Mechanisms and functions of inflammasomes. Cell 157 (5):1013–1022. doi:10.1016/j.cell.2014.04.007
18. van der Zande M, Vandebriel RJ, Groot MJ, Kramer E, Herrera Rivera ZE, Rasmussen K, Ossenkoppele JS, Tromp P, Gremmer ER, Peters RJ, Hendriksen PJ, Marvin HJ, Hoogenboom RL, Peijnenburg AA, Bouwmeester H (2014) Sub-chronic toxicity study in rats orally exposed to nanostructured silica. Part Fibre Toxicol 11(1):8. doi:10.1186/1743-8977-11-8
19. Neun BW, Dobrovolskaia MA (2011) Detection and quantitative evaluation of endotoxin contamination in nanoparticle formulations by LAL-based assays. Methods Mol Biol 697:121–130. doi:10.1007/978-1-60327-198-1_12

Chapter 13

Analysis of Complement Activation by Nanoparticles

Barry W. Neun, Anna N. Ilinskaya, and Marina A. Dobrovolskaia

Abstract

The complement system is a group of proteins, which function in plasma to assist the innate immunity in rapid clearance of pathogens. The complement system also contributes to coordination of the adaptive immune response. Complement Activation Related Pseudo Allergy or CARPA is a life-threatening condition commonly reported with certain types of drugs and nanotechnology-based combination products. While CARPA symptoms are similar to that of anaphylaxis, the mechanism behind this pathology does not involve IgE and is mediated by the complement system. In vitro assays using serum or plasma derived from healthy donor volunteers correlate with the in vivo complement-mediated reactions, and therefore are helpful in understanding the propensity of a given drug formulation to cause CARPA in patients. In the first edition of this book, we have described an in vitro method for qualitative assessment of the complement activation by nanomaterials using western blotting. Herein, we present a similar method utilizing enzyme-linked immunoassay for quantitative analysis of the complement activation, and we compare the performance of this approach to that of the qualitative western blotting technique. The revised chapter also includes new details about nanoparticle sample preparation.

Key words Nanoparticles, Complement, Anaphylaxis, C3, Western blot, Immunoassay, EIA

1 Introduction

The complement system is comprised of several components organized into a biochemical cascade serving to assist the immune system in the clearance of pathogens [1]. The biochemical cascade includes three main pathways—classical, alternative, and lectin (Fig. 1). Activation of each of these pathways is triggered by different factors. For example, an immune complex composed of an antibody and an antigen is required to activate the classical pathway. Activation of the alternative pathway does not oblige an antibody and depends on spontaneous hydrolysis of a C3 component of the complement and properdin. Mannose-binding lectin triggers activation of the mannose pathway. These pathways converge on C3 component [1]. Cleavage of the C3 protein results in activation of the common pathway that culminates with formation of the terminal or membrane attack complex. Complement cleavage products

Scott E. McNeil (ed.), *Characterization of Nanoparticles Intended for Drug Delivery*, Methods in Molecular Biology, Vol. 1682, DOI 10.1007/978-1-4939-7352-1_13,

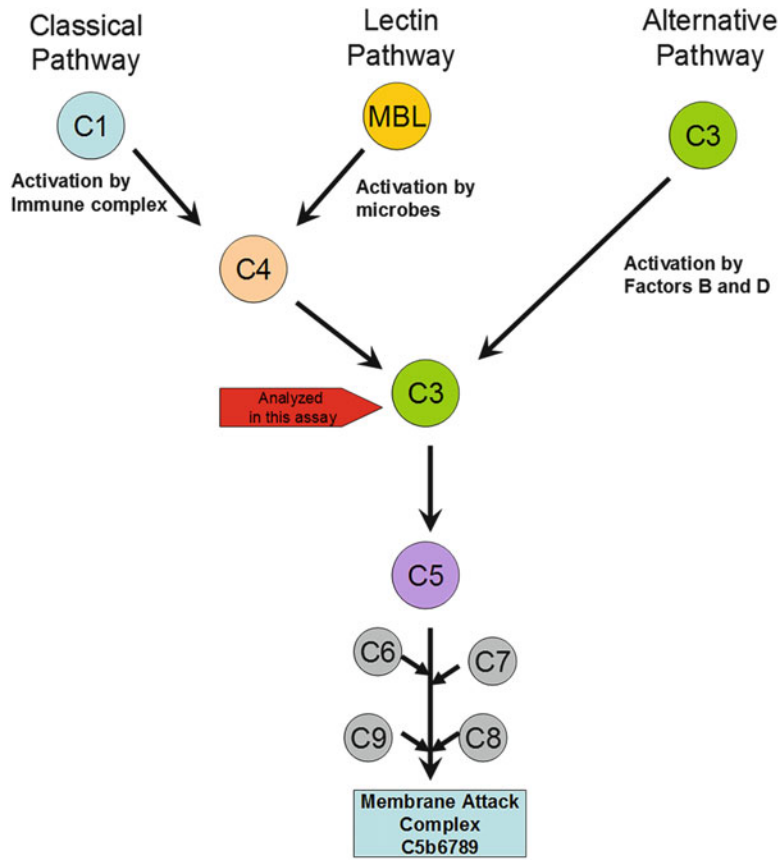

Fig. 1 Complement activation pathways. The antibodies used in this assay detect split product of C3 component of complement

C4a, C3a, and C5a are potent immunostimulants also known as anaphylatoxins. The presence of these proteins in the bloodstream is associated with induction of inflammation, generation of oxygen radicals, increase in vascular permeability, the IgE-independent release of histamine from mast cells, and smooth muscle contraction [1]. The complement terminal complex functions to destroy the pathogen, and in the absence of such (e.g., during drug-mediated complement activation) it damages healthy host cells [2–5]. Altogether these responses produce anaphylaxis and tissue damage. Since complement activation enhances antigen presentation, a certain degree of complement activation is desirable for vaccines [6]. However, for systemically administered drugs and combination products, the complement activation is undesirable due to the CARPA reaction [2–5, 7–12].

Complement-mediated infusion reactions and CARPA are common dose-limiting toxicities for particular types of drug products including therapeutic oligonucleotides [9–11] and PEGylated liposomal formulations of small molecules [4, 5, 12].

For example, liposomal formulations of doxorubicin (Doxil) and amphotericin (Ambisome), when administered into systemic circulation, activate the complement and result in complement-mediated hypersensitivity reactions in sensitive individuals [3, 5, 7, 8, 12]. In contrast, subcutaneously administered polymer-based nanoparticles, which lead to local complement activation, improve vaccine efficacy by enhancing antigen uptake by dendritic cells, activating T cells and supplementing the antigen-specific immune response [6].

Nanoparticle physicochemical properties, including size, charge, shape, and surface functionalities, determine the particle interaction with the complement system. For example, charged nanoparticles were shown to be more potent activators of the complement system than their neutral counterparts in studies investigating polypropylene sulfide nanoparticles, lipid nanocapsules, cyclodextrin-containing polycation-based nanoparticles, and polystyrene nanospheres [13–18]. Polymer coatings (such as polyethylene glycol (PEG) and poloxamine 908), which partially neutralize surface charge, have been shown to reduce nanoparticle-mediated complement activation [13, 16]. Similar studies using dextran and chitosan coatings reported that charge in combination with size and conformation of the polymer played the key role in complement activation by these particles [17]. In the case of Doxil, the combination of three factors, including particle shape, PEG coating, and the presence of doxorubicin crystals, determines complement activation [8, 19, 20]. Dr. Janos Szebeni proposed using analysis of complement activation by PEGylated liposomal drugs to assess the bioequivalence of generic formulations [3]. In vitro–in vivo correlation of complement activation is reviewed elsewhere [21].

In the first edition of this book, we described an in vitro method utilizing western blotting technique to perform qualitative analysis of the complement activation by nanoparticles [22]. Herein, we describe a similar method using quantitative analysis of the C3 component of complement split product iC3b. In this protocol, a test sample is incubated with human plasma, and the amounts of iC3b protein are measured by an enzyme-linked immunoassay (EIA). The amount of iC3b is proportional to the level of complement activation. Other split products, such as C3a, can also be used to perform this analysis. We selected iC3b because this analysis generates a higher signal-to-noise ratio (Fig. 2). The revised method includes considerations for selecting nanoparticle concentrations for in vitro analysis. We also compare the performance of qualitative western blotting and quantitative EIA methods for analysis of the complement activation by nanomaterials. This comparison demonstrates that western blotting is a more sensitive technique than EIA (Fig. 3). The greater sensitivity is explained by the use of polyclonal antibodies which capture all

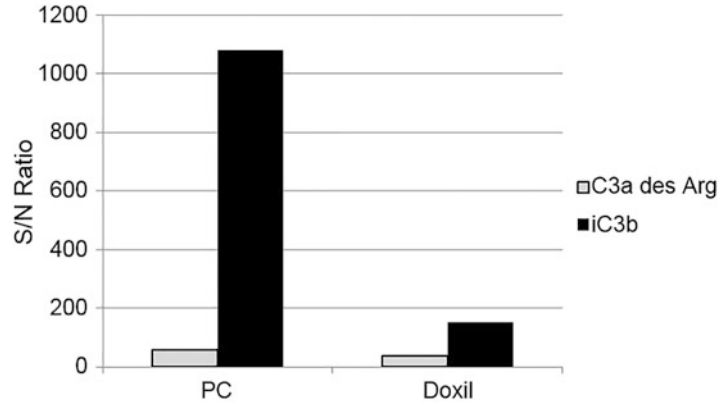

Fig. 2 Comparison between C3a and iC3b EIAs. Plasma samples treated with negative control, positive (cobra venom factor), and Doxil were analyzed by C3a des Arg and iC3b EIA. Each sample was analyzed in duplicate (%CV < 10). The mean responses from positive control (PC) and Doxil samples were divided by the mean response of the negative control sample to estimate the signal-to-noise (S/N) ratio for each EIA. The background in the C3a EIA was higher. Due to the differences in the background, the S/N ratio of iC3b assay was higher

split products. Despite the difference in sensitivities, EIA allows detection of the complement at the levels relevant to CARPA induction in vivo. The western blot detects lower levels of complement split products which may be asymptomatic in vivo. While both methods can be used for analysis of the complement activation, EIA overcomes limitations of the western blotting technique such as low throughput. Although the protocol described herein focuses on measuring iC3b component of the complement, supernatants generated in this test can be used to measure other complement components (e.g., C4a, C4d, and Bb) when identification of the pathway responsible for the complement activation by a test nanomaterial is needed.

2 Materials

1. Sterile Ca^{2+}/Mg^{2+}-free phosphate buffered saline (PBS).
2. Cobra venom factor as the positive control.
3. Veronal buffer.
4. Pooled human plasma, anti-coagulated with sodium citrate.
5. iC3b EIA kit (e.g., MicroVue by Quidel Corp.).
6. 1.0 N HCl, as stop solution. Stop solution is provided with each kit, but can also be prepared separately. Dilute stock hydrochloric acid to a final concentration of 1.0 N. Filter and store and room temperature for up to 2 weeks.

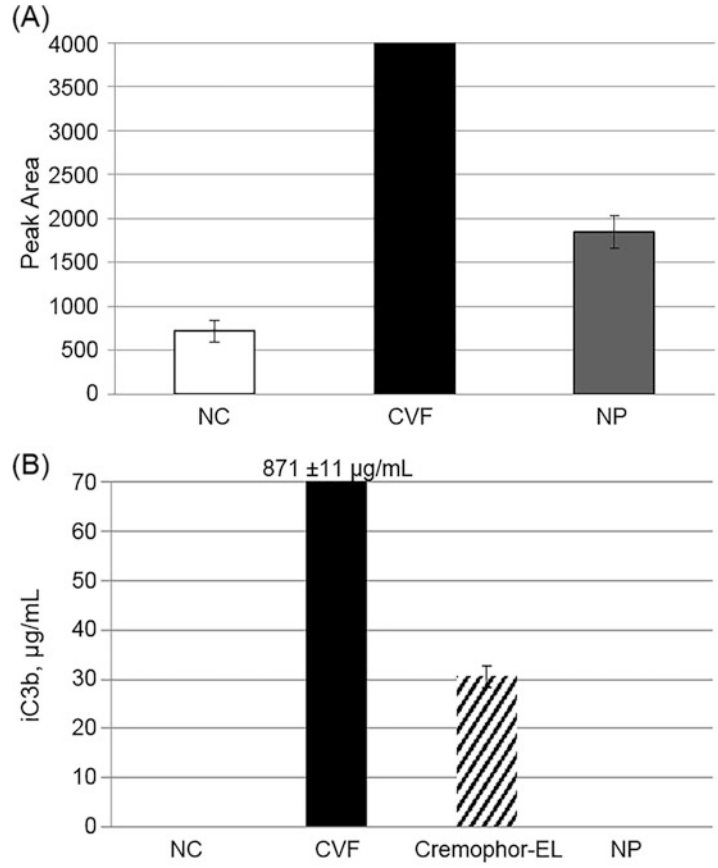

Fig. 3 Comparison between western blotting and EIA of iC3b. The samples of plasma treated with negative control, positive control, and nanoparticle were analyzed by western blot (**a**) and EIA (**b**). Each bar shows mean and SD of duplicate response. (**a**) Cremophor-EL was not analyzed in western blot assay because the presence of oil affects protein mobility and results in smeared bands. Western blot results were analyzed by the NIH ImageJ software and shown is the peak intensity of the band corresponding to C3 split products. (**b**) The scale was changed to show levels of iC3b in Cremophor-EL and nanoparticle-treated samples (NP). The level of iC3b in the positive control sample (CVF) is 871 ± 11 µg/mL. NC: negative control, NP: nanoparticle, CVF: cobra venom factor

7. Doxil (Doxorubicin HCl, liposome, injection). This is a prescription medication available from a licensed pharmacy. It may not be available to some research laboratories.
8. Cremophor.
9. Taxol (Paclitaxel in Cremophor EL). This is a prescription medication available from a licensed pharmacy. This drug may not be available to some research laboratories.
10. Multichannel (8–12 channel) pipettor for 50–300 µL volumes.

11. Reagent reservoirs.
12. ELISA plate reader capable of operating at 405 nm.
13. *See* **Note 1**.

3 Methods

3.1 Preparation of Controls and Plasma

1. Prepare Cobra Venom Factor (CVF) as Positive Control 1, a traditional substance known to activate complement. CVF is supplied as a frozen solution. Thaw this stock, prepare single-use aliquots and store them at a nominal temperature of −80 °C as long as performance is acceptable. Avoid repeated freeze/thaw cycles. After thawing single-use aliquot and using it in the assay, discard any leftover material. For this experiment, use 30 μL (1.1–50 U) of CVF solution. This control activates the complement system through the alternative pathway (*see* **Note 2**).
2. Prepare Positive Control 2, a nanoparticle-relevant control.

   Cremophor-EL is an excipient commonly used in the pharmaceutical industry to dissolve hydrophobic drugs. Cremophor-EL is a nanosized micelle, which is known to induce CARPA syndrome [5], and therefore is used as a nanoparticle-relevant control. The following procedure can be used to prepare Cremophor-EL with the composition similar to that in clinical formulation of paclitaxel (Taxol): 527 mg of purified Cremophor® EL* (polyoxyethylated castor oil) and 49.7% (v/v) dehydrated alcohol, USP and 2 mg of citric acid per 1 mL. Store at room temperature. To prepare Cremophor-EL mix commercial Cremophor 1:1 with ethanol containing 2 mg/mL of citric acid to mimic the concentration of Cremophor-EL, citric acid, and ethanol used in Taxol® and the generic formulation of paclitaxel.

   Cremophor-EL-formulated Paclitaxel (Taxol) can be used as an alternative for this nanoparticle-relevant positive control. It is supplied at a stock concentration of 6 mg/mL of paclitaxel. When used in this assay, the final concentration of Paclitaxel is 2 mg/mL. Store at 2–8 °C.

   PEGylated liposomal doxorubicin (Doxil) can also be used as a nanoparticle-relevant positive control [3]. Doxil is doxorubicin formulated in nanoliposomes. It is available through the pharmacy as 20 mg of Doxorubicin HCl in 10 mL of vehicle. Store at 2–8 °C.
3. Prepare the Inhibition/Enhancement Control. Use the positive control sample after incubation. Prior to loading this sample onto the ELISA plate, add nanoparticles at the same final concentrations as in the study samples. For example, one can

mix 20 μL of the positive control sample and 10 μL of the test nanoparticle. The test result for this sample needs to be adjusted by the dilution factor 1.5 prior to comparison to the test value of the positive control sample. If the test results do not differ more than 25% of each other, the test nanoparticle at the given concentration does not interfere with the detection of the complement split product by ELISA.

4. Prepare the Negative Control. Sterile Ca^{2+}/Mg^{2+}-free PBS is used as a negative control. Store at room temperature for up to 6 months.
5. Prepare the Vehicle Control, which is relevant to the given nanoparticle. When nanoparticles are formulated in a vehicle other than saline or PBS, the vehicle sample should be tested to estimate the effect of excipients on the complement system. This control is specific to each given nanoparticle sample. It should be prepared to match the formulation buffer of the nanoparticle by both the composition and the concentration.
6. To prepare plasma, the blood is spun down in a centrifuge for 10 min at 2500 × *g* (*see* **Note 3**).

3.2 Preparation of Nanoparticle Samples

This assay requires 400 μL of nanoparticles in PBS at a concentration three times higher than the highest final tested concentration. The concentration is selected based on the plasma concentration of the nanoparticle at the intended therapeutic dose. For the purpose of this protocol, this concentration is called the "theoretical plasma concentration." Considerations for estimating theoretical plasma concentration were reviewed elsewhere [21] and are also summarized in Box 1. The assay will evaluate four concentrations: 10× (or when feasible 100×, 30×. or 5×) of the theoretical plasma concentration, theoretical plasma concentration, and two serial 5-fold dilutions of the theoretical plasma concentration. When the intended therapeutic concentration is unknown, the highest final concentration is 1 mg/mL or the highest reasonably achievable concentration. For example, if the final theoretical plasma concentration to be tested is 0.2 mg/mL, then a stock of 6 mg/mL will be prepared and diluted 10-fold (0.6 mg/mL), followed by two serial 5-fold dilutions (0.12 and 0.024 mg/mL). When 0.1 mL of each of these samples is added to the test tube and mixed with 0.1 mL of plasma and 0.1 mL of veronal buffer, the final nanoparticle concentrations tested in the assay are: 2.0, 0.2, 0.04, and 0.008 mg/mL.

3.3 Assay

1. In a microcentrifuge tube, combine equal volumes (100 μL of each) of veronal buffer, human plasma, and a test sample (i.e., positive control, negative control, nanoparticles, or vehicle control if different than PBS). Prepare two replicates of each sample.

Box 1. Example Calculation of Nanoparticle Concentration for In Vitro Test

Assume the mouse dose is known to be 123 mg/kg.

$$\text{human dose} = \frac{mouse\ dose}{12.3} = \frac{123\frac{mg}{kg}}{12.3} = 10\ \text{mg/kg}$$

Blood volume constitutes approximately 8% of body weight (e.g. a 70 kg human has approximately 5.6 L (8% of 70) of blood). This allows for a very rough estimation of what the maximum blood concentration may be.

$$\text{in vitro concentration}_{human\ matrix} = \frac{human\ dose}{human\ blood\ volume} = \frac{70\ kg\ x\ 10\frac{mg}{kg}}{5.6\ L}$$

$$= \frac{700\ mg}{5.6\ L} = 0.125\ \text{mg/mL}$$

Box 1 Example calculation of nanoparticle concentrations for in vitro tests. Reproduced with permission from ref. 21

2. Vortex tubes to mix all reaction components, spin briefly in a microcentrifuge to bring any drops down, and incubate in an incubator at a nominal temperature of 37 °C for 30 min.
3. Prepare 100 μL aliquots and either use in EIA immediately or freeze at −20 °C for later analysis.
4. Follow the manufacturer's instruction to reconstitute complement standard, buffers, and controls.
5. Dilute plasma samples prepared in **step 3** in complement specimen diluent reagent (provided with each kit). Use the following dilution guide for each individual assay (*see* **Note 4**):

   iC3b—1:1500 for positive control sample; 1:75 for negative control, and other test samples.
   C4d—1:30 for all samples.
   Bb—1:75 for all samples.
6. Follow the manufacturer's instruction for plate loading volumes, incubation time, and plate washing.

3.4 Calculations and Results Interpretation

Do not forget to use the appropriate dilution factor for control and study samples. Compare determined amount of complement components between positive control or study samples with that in the negative control. An increase in the complement component species two fold or higher above the background (negative control) constitutes a positive response. If a nanoparticle under study generated a positive response in any of the EIA assays, compare the degree of activation between this particle and Doxil or other nanoparticle-relevant controls. Doxil is used in the clinic and is

known to induce complement activation-related hypersensitivity reactions in sensitive patients [5]. Using Doxil helps to interpret results of this in vitro study for a test nanoparticle. If the degree of activation observed for the test nanoparticle is equal to or greater than that observed for Doxil, this nanoparticle formulation will most likely cause similar or stronger hypersensitivity reactions in patients and may require modifications before entering in vivo preclinical and clinical phases. If the degree of activation is lower than that of Doxil, complement activation should be considered when designing the in vivo evaluation phase for the given particle; but, it is less likely to cause concerns similar to Doxil.

4 Notes

1. NCL does not endorse suppliers. However, we found that a new user benefits from knowing catalog information of reagents used in our assays. If you need ideas of what reagents are used at the NCL, please review NCL method ITA-5 available at https://ncl.cancer.gov/resources/assay-cascade-protocols. When other reagents are used, the assay performance may change. When using reagents and instruments from sources other than that used in our protocols, assay performance qualification is needed to verify the assay functionality and validity.
2. *Heat Aggregated Gamma Globulin (HAGG)* acts similarly to naturally occurring immune complexes and is a very potent activator of complement through the classical pathway. HAGG can be used as Positive Control 1 when activation of the complement through the classical pathway is desired. This control is available from Quidel under the name "Complement Activator." Handling and storage are according to the manufacturer's instructions. Avoid repeated freeze/thaw cycles when stored at −20 °C.
3. Blood is drawn into vacutainer tubes containing anticoagulant. Sodium citrate is an ideal anticoagulant for this assay. However, depending on phlebotomy paraphernalia, plasma anticoagulated with sodium citrate may result in a high background in the ELISA assay. In this case, using K2 EDTA as an anticoagulant is acceptable. The first 5–10 mL of blood should be discarded and not used to prepare plasma. For optimal results, it is important to keep blood at 20–24 °C to avoid exposure to high temperatures (summer time) and low temperatures (winter time), and to avoid prolonged (> 1 h) storage. Blood is transported to the lab in a contained Styrofoam box with warm packs (20–24 °C). After centrifugation to separate plasma, the plasma is evaluated for the presence of hemolysis. Discolored

plasma (an indication of hemolysis) is not used to prepare the pool. Individual plasma specimens that did not show any indication of hemolysis are pooled and mixed in a conical tube. Plasma must be used for complement testing within 1 h after collection. Pooled plasma can be used and prepared by mixing plasma from at least 2 individual donors. The assay can also be performed in plasma from individual donors. In this case, analyze plasma from at least 3 donors. Inter-individual variability and comparison to pooled plasma is shown in Fig. 4.

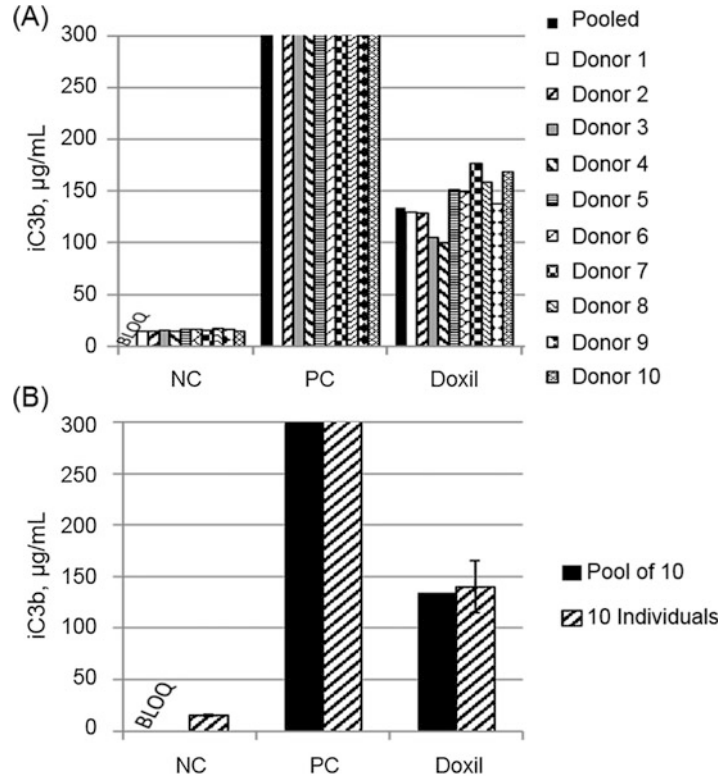

Fig. 4 Analysis of complement activation by Doxil in individual and pooled plasma. Plasma from ten donors was used to analyze Doxil. The plasma was tested either individually or after pooling. To prepare pooled plasma equal volumes of individual plasmas were mixed. The analysis was performed according to the experimental procedure described in this chapter. (**a**) Shows results for controls and Doxil in individual plasma from 10 donors. Each bar represents a mean and SD from 2 replicates, %CV between replicates is less than 10. (**b**) Compares result generated in plasma pooled from 10 donors (*black bar*, pooled plasma) and the mean result of ten individual responses analyzed side-by-side (*hatched bars*, ten individuals). *Black bar* shows a mean and SD from two replicates, %CV between replicates is less than 10. Hatched bars show the mean result and SD ($N = 10$)

It is possible to use pooled sodium citrate plasma from commercial suppliers; however, when placing the order, one needs to notify the supplier that the plasma is intended for complement testing so no delays between blood draw and plasma collection occur. The supplier then freezes the plasma immediately after collection and ships it to the lab on dry ice. When using frozen plasma for the complement activation assay, it is important to avoid repeated freeze/thaw cycles. The frozen plasma should be thawed in a water bath containing ambient tap water, mixed gently, and used immediately after thawing. It is also advised to avoid indefinite storage of frozen plasma at −20 °C. The sooner the frozen plasma is used, the better the results are. In general, the degree of complement activation estimated by comparing intensity of the C3 split product in the positive control with that of the negative control is greater in fresh plasma than in thawed plasma.

4. The dilution factors should be determined by each laboratory and adjusted as needed.

Acknowledgment

This project has been funded in whole or in part by federal funds from the National Cancer Institute, National Institutes of Health, under contract HHSN261200800001E. The content of this publication does not necessarily reflect the views or policies of the Department of Health and Human Services, nor does mention of trade names, commercial products, or organizations imply endorsement by the U.S. Government.

References

1. Calame DG, Mueller-Ortiz SL, Wetsel RA (2016) Innate and adaptive immunologic functions of complement in the host response to Listeria monocytogenes infection. Immunobiology 221(12):1407–1417. doi:10.1016/j.imbio.2016.07.004
2. Szebeni J, Fishbane S, Hedenus M, Howaldt S, Locatelli F, Patni S, Rampton D, Weiss G, Folkersen J (2015) Hypersensitivity to intravenous iron: classification, terminology, mechanisms and management. Br J Pharmacol 172 (21):5025–5036. doi:10.1111/bph.13268
3. Szebeni J, Storm G (2015) Complement activation as a bioequivalence issue relevant to the development of generic liposomes and other nanoparticulate drugs. Biochem Biophys Res Commun 468(3):490–497. doi:10.1016/j.bbrc.2015.06.177
4. Rampton D, Folkersen J, Fishbane S, Hedenus M, Howaldt S, Locatelli F, Patni S, Szebeni J, Weiss G (2014) Hypersensitivity reactions to intravenous iron: guidance for risk minimization and management. Haematologica 99 (11):1671–1676. doi:10.3324/haematol.2014.111492
5. Szebeni J (2014) Complement activation-related pseudoallergy: a stress reaction in blood triggered by nanomedicines and biologicals. Mol Immunol 61(2):163–173. doi:10.1016/j.molimm.2014.06.038
6. Reddy ST, van der Vlies AJ, Simeoni E, Angeli V, Randolph GJ, O'Neil CP, Lee LK, Swartz

MA, Hubbell JA (2007) Exploiting lymphatic transport and complement activation in nanoparticle vaccines. Nat Biotechnol 25 (10):1159–1164. doi:10.1038/nbt1332

7. Moghimi SM, Wibroe PP, Szebeni J, Hunter AC (2013) Surfactant-mediated complement activation in beagle dogs. Int Immunopharmacol 17(1):33–34. doi:10.1016/j.intimp.2013.05.012
8. Szebeni J, Muggia F, Gabizon A, Barenholz Y (2011) Activation of complement by therapeutic liposomes and other lipid excipient-based therapeutic products: prediction and prevention. Adv Drug Deliv Rev 63 (12):1020–1030. doi:10.1016/j.addr.2011.06.017
9. Shen L, Engelhardt JA, Hung G, Yee J, Kikkawa R, Matson J, Tayefeh B, Machemer T, Giclas PC, Henry SP (2016) Effects of repeated complement activation associated with chronic treatment of Cynomolgus monkeys with 2′-O-Methoxyethyl modified antisense oligonucleotide. Nucleic Acid Ther 26(4):236–249. doi:10.1089/nat.2015.0584
10. Shen L, Frazer-Abel A, Reynolds PR, Giclas PC, Chappell A, Pangburn MK, Younis H, Henry SP (2014) Mechanistic understanding for the greater sensitivity of monkeys to antisense oligonucleotide-mediated complement activation compared with humans. J Pharmacol Exp Ther 351(3):709–717. doi:10.1124/jpet.114.219378
11. Henry SP, Beattie G, Yeh G, Chappel A, Giclas P, Mortari A, Jagels MA, Kornbrust DJ, Levin AA (2002) Complement activation is responsible for acute toxicities in rhesus monkeys treated with a phosphorothioate oligodeoxynucleotide. Int Immunopharmacol 2(12):1657–1666
12. Chanan-Khan A, Szebeni J, Savay S, Liebes L, Rafique NM, Alving CR, Muggia FM (2003) Complement activation following first exposure to pegylated liposomal doxorubicin (Doxil®): possible role in hypersensitivity reactions. Ann Oncol 14(9):1430–1437
13. Vonarbourg A, Passirani C, Saulnier P, Simard P, Leroux JC, Benoit JP (2006) Evaluation of pegylated lipid nanocapsules versus complement system activation and macrophage uptake. J Biomed Mater Res A 78 (3):620–628. doi:10.1002/jbm.a.30711
14. Bartlett DW, Davis ME (2007) Physicochemical and biological characterization of targeted, nucleic acid-containing nanoparticles. Bioconjug Chem 18(2):456–468. doi:10.1021/bc0603539
15. Nagayama S, Ogawara K, Fukuoka Y, Higaki K, Kimura T (2007) Time-dependent changes in opsonin amount associated on nanoparticles alter their hepatic uptake characteristics. Int J Pharm 342(1–2):215–221. doi:10.1016/j.ijpharm.2007.04.036
16. Al-Hanbali O, Rutt KJ, Sarker DK, Hunter AC, Moghimi SM (2006) Concentration dependent structural ordering of poloxamine 908 on polystyrene nanoparticles and their modulatory role on complement consumption. J Nanosci Nanotechnol 6(9–10):3126–3133
17. Bertholon I, Vauthier C, Labarre D (2006) Complement activation by core-shell poly(isobutylcyanoacrylate)-polysaccharide nanoparticles: influences of surface morphology, length, and type of polysaccharide. Pharm Res 23 (6):1313–1323. doi:10.1007/s11095-006-0069-0
18. Xu Y, Ma M, Ippolito GC, Schroeder HW Jr, Carroll MC, Volanakis JE (2001) Complement activation in factor D-deficient mice. Proc Natl Acad Sci U S A 98(25):14577–14582. doi:10.1073/pnas.261428398
19. Szebeni J, Bedocs P, Rozsnyay Z, Weiszhar Z, Urbanics R, Rosivall L, Cohen R, Garbuzenko O, Bathori G, Toth M, Bunger R, Barenholz Y (2012) Liposome-induced complement activation and related cardiopulmonary distress in pigs: factors promoting reactogenicity of Doxil and AmBisome. Nanomedicine 8 (2):176–184. doi:10.1016/j.nano.2011.06.003
20. Szebeni J, Baranyi L, Savay S, Milosevits J, Bunger R, Laverman P, Metselaar JM, Storm G, Chanan-Khan A, Liebes L, Muggia FM, Cohen R, Barenholz Y, Alving CR (2002) Role of complement activation in hypersensitivity reactions to doxil and hynic PEG liposomes: experimental and clinical studies. J Liposome Res 12(1–2):165–172. doi:10.1081/lpr-120004790
21. Dobrovolskaia MA, McNeil SE (2013) Understanding the correlation between in vitro and in vivo immunotoxicity tests for nanomedicines. J Control Release 172(2):456–466. doi:10.1016/j.jconrel.2013.05.025
22. Neun BW, Dobrovolskaia MA (2011) Qualitative analysis of total complement activation by nanoparticles. Methods Mol Biol 697:237–245. doi:10.1007/978-1-60327-198-1_25

Chapter 14

Methods for Analysis of Nanoparticle Immunosuppressive Properties In Vitro and In Vivo

Timothy M. Potter, Barry W. Neun, and Marina A. Dobrovolskaia

Abstract

Adverse drug effects on the immune system function represent a significant concern in the pharmaceutical industry, because 10–20% of the drug withdrawal from the market is accounted to immunotoxicity. Immunosuppression is one such adverse effect. The traditional immune function test used to estimate materials' immunosuppression is a T-cell-dependent antibody response (TDAR). This method involves a 28 day in vivo study evaluating the animal's antibody titer to a known antigen (KLH) with and without challenge. Due to the limited quantities of novel drug candidates, an in vitro method called human leukocyte activation (HuLa) assay has been developed to substitute the traditional TDAR assay during early preclinical development. In this test, leukocytes isolated from healthy donors vaccinated with the current year's flu vaccine are incubated with Fluzone in the presence or absence of a test material. The antigen-specific leukocyte proliferation is then measured by ELISA analyzing incorporation of BrdU into DNA of the proliferating cells. Here, we describe the experimental procedures for investigating immunosuppressive properties of nanoparticles by both TDAR and HuLa assays, discuss the in vitro–in vivo correlation of these methods, and show a case study using the iron oxide nanoparticle formulation, Feraheme.

Key words Nanoparticles, Immunosuppression, Leukocyte proliferation, Antigen, TDAR

1 Introduction

Approximately 10–20% of drugs were withdrawn from clinical use between 1969 and 2005 due to their adverse effects on the immune system function [1–4]. These concerns were described in several reports from academia [1], the pharmaceutical industry [2] and the US Food and Drug Administration [3, 4]. The range of adverse immune reactions responsible for the drug withdrawal included anaphylaxis, allergy, hypersensitivity, idiosyncratic reactions, and immunosuppression [1–4]. Nanotechnology-formulated complex drug formulations are a relatively new class of therapeutics. Investigation of nanoparticle immunotoxicity is performed according to the framework established for other therapeutics and includes analysis of immunosuppressive properties [5–7]. The traditional

Scott E. McNeil (ed.), *Characterization of Nanoparticles Intended for Drug Delivery*, Methods in Molecular Biology, Vol. 1682, DOI 10.1007/978-1-4939-7352-1_14,

immune function test used to estimate materials' immunosuppression is a T-cell-dependent antibody response (TDAR) [8]. Although the likelihood of identifying immunotoxicity increases with progression from preclinical in vitro to in vivo studies, in vitro methods are often the first choice in the early phases of the drug's safety investigation. In addition to the higher throughput and lower cost, in vitro methods are also helpful when quantities of novel drug candidates are limited. To study immunosuppressive properties of novel drugs, an in vitro method called human leukocyte activation (HuLa) assay has been developed to substitute the traditional in vivo TDAR assay [9]. The schematics of both methods are shown in Fig. 1. The HuLA assay was validated across a wide range of immunosuppressive agents with different mechanisms of action (cyclosporine, dexamethasone, rapamycin, mycophenolic acid, and methotrexate) and demonstrated sensitivity to these drugs at their respective therapeutic concentrations. The primary endpoints of TDAR and HuLa assays are antigen-specific antibody response and leukocyte proliferation, respectively. Collinge et al. demonstrated that cell proliferation in the HuLA assay is specific to the flu antigen and involves CD4+ and CD8+ T cells and B lymphocytes [9]. They further confirmed that cell proliferation is accompanied by an increase in flu-specific, antibody-secreting cells.

In this chapter, we describe experimental procedures for analyzing nanoparticle immunosuppressive properties by both TDAR and HuLa assays. Furthermore, using iron oxide nanoparticle

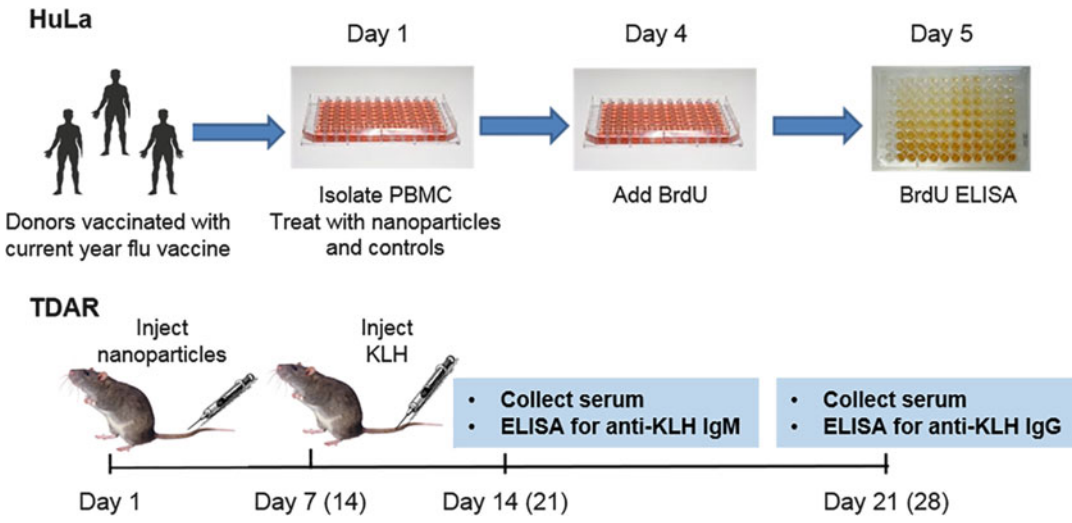

Fig. 1 Schematic of TDAR and HuLa assays. This figure shows major experimental steps of HuLa and TDAR methods. For the TDAR assay, the day number for KLH injection and IgM/IgG blood collection may change, because it depends on the test nanomaterial's clinically intended dosing regimen. However, there is always 7 days interval between the KLH injection and IgM blood collection. The IgG blood collection can be done at day 14 or 21 after the KLH injection

formulation Feraheme, we show a correlation between HuLa and TDAR assays (Fig. 2a, b). We chose Feraheme as a model particle for the in vitro–in vivo comparison because several literature reports demonstrated immunosuppressive properties of another commercial iron oxide formulation Resovist [10–12], and because immunosuppression was a commonly observed toxicity of investigational iron oxide formulations that we analyzed in the NCL immunological assay cascade. The main limitation of this immunosuppressive assay pair is that in vitro assays cannot account for the nanoparticle biodistribution, potential inter-gender differences in particle metabolism, and sensitivity to the particle-mediated toxicity (Fig. 2c). Therefore, an in vitro assay is useful for identifying potential immunosuppressive nanoparticle candidates, while an in vivo method is still needed to confirm the results of the in vitro test.

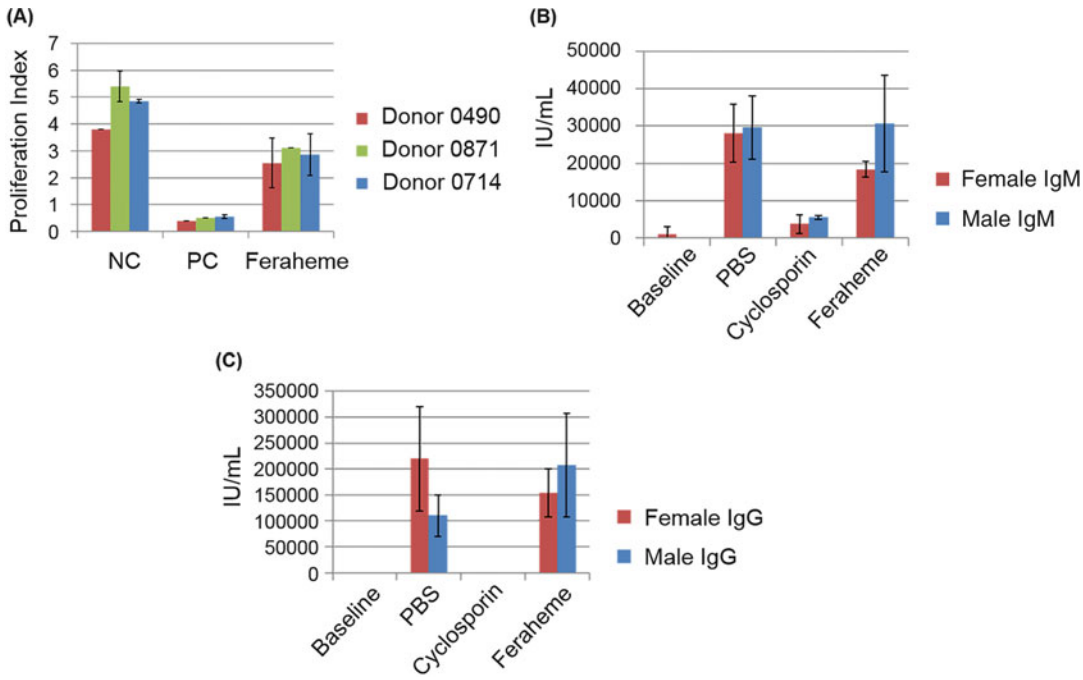

Fig. 2 Correlation between HuLa and TDAR assays. Iron oxide nanoparticle Feraheme was analyzed in vitro and in vivo. (**a**) The results of HuLa assay show statistically significant ($p < 0.05$) decrease in leukocyte proliferation in response to 0.3 mg/mL of Feraheme. *NC* Negative Control (PBS), *PC* Positive Control (Dexamethasome). (**b**) TDAR investigation was conducted in 6-week-old CD1 mice. Each treatment group included five males and five females. The animals received i.v. injection of PBS as a negative control (PBS), or were fed daily with a clinical formulation of cyclosporine in oil for the positive control (Cyclosporin). Feraheme treatment groups received a single injection of 30 mg/kg of Feraheme (the dose is provided in terms of iron) 1 h prior to KLH injection. The results show a decrease ($p < 0.05$) in anti-KLH IgM titer in females but not in males. (**c**) The same animals as in (**b**) were sacrificed and terminal blood was collected at day 21 of the study for the analysis of serum IgG. The results show no significant change in the IgG levels or difference between males and females

2 Materials

2.1 HuLa

1. Review **Note 1**.
2. Human blood from at least three prescreened donors, anticoagulated with Li-heparin. The blood from at least three donor volunteers vaccinated with the current season flu vaccine should be drawn in vacutainers containing Li-heparin as an anticoagulant. First 10 cc collected during phlebotomy should be discarded. Cells from each donors should be tested separately.
3. Ficoll-Paque Plus.
4. Phosphate buffered saline (PBS).
5. 4 mg/mL clinical-grade dexamethasone (DXM) stock.
6. Fluzone (Sanofi Pasteur). This is a prescription medication that is seasonal and may not be available to all research laboratories. Fluzone is supplied as a stock with a final concentration of 90 μg/mL of influenza hemagglutinin. Dilute the commercial stock 1:50 with complete culture media. The vaccine is available in both single and multidose vials. Mutidose vials usually contain preservatives (e.g., mercury) which may interfere with this assay. Use only preservative-free versions.
7. Heat-inactivated fetal bovine serum (FBS). Thaw a bottle of FBS at room temperature or overnight at 2–8 °C and allow to equilibrate to room temperature. Incubate for 30 min at 56 °C in a water bath mixing every 5 min to heat-inactivate it. Single-use aliquots may be stored at 2–8 °C for up to 1 month or at a nominal temperature of −20 °C.
8. Complete RPMI medium: RPMI-1640, 10% FBS (heat-inactivated), 2 mM L-glutamine, 100 U/mL penicillin, 100 μg/mL streptomycin sulfate. Store at 2–8 °C protected from light for no longer than 1 month. Before use, warm the medium in a water bath to 37 °C.
9. Hank's balanced salt solution (HBSS).
10. Trypan Blue solution.
11. MTT (3-(4, 5-dimethyl-2-thiazolyl)-2,5-diphenyl-2H-tetrazolium bromide).
12. Glycine.
13. Sodium chloride.
14. Commercial BrdU cell proliferation assay (e.g., Calbiochem, QIA58). After initial thaw of the commercially supplied material, divide it into small aliquots and store at −20 °C. On the day of the experiment, thaw the required number of aliquots and dilute BrdU label 1:2000 in fresh complete media. Prepare

immediately before use. Dilute BrdU-specific antibody by 1:100 in Antibody Diluent. Prepare immediately before use. After initial thaw, divide into small aliquots and store at −20 °C. Reconstitute Peridoxase Goat Anti-Mouse IgG HRP Conjugate in 250 μL of PBS and let incubate at room temperature for 10 min. Once reconstituted, divide into small aliquots and store at −20 °C. For use, dilute Peridoxase Goat Anti-Mouse IgG HRP Conjugate in Conjugate Diluent *according to the dilution instructions on the vial as the dilution factor is lot specific*. Prepare immediately before use. Allow the Fixative/Denaturing Solution to sit at room temperature for 4 h prior to use. Thaw the Conjugate Diluent, Substrate, Plate Wash Concentrate, and Stop Solution overnight at 4 °C. Once thawed, these components can be stored at 4 °C. Dilute Plate Wash Concentrate (20×) to 1× by adding 25 mL of Concentrate to 475 mL of deionized water. Store at 4 °C.

15. 96-well flat bottom plates for BrdU plate.
16. 96-well round bottom plates for MTT plate.
17. Hemocytometer.
18. Test nanomaterial and the buffer or media it was formulated in.

2.2 TDAR

1. 6-week-old male and female mice of CD-1 strain.
2. Keyhole Limpet Hemocyanin (KLH). KLH is supplied as lyophilized powder. Reconstitute the KLH in PBS to a final concentration of 8 mg/mL. Filter through sterile 0.2 mm filter and keep at room temperature for no longer than 2 h. Discard any leftovers. Each animal should receive 0.25 mL of this stock solution. The dose per animal is 2 mg (*see* **Note 2**).
3. 100 mg/mL Cyclosporin A (Neoral). Cyclosporin is supplied as an oral solution with a concentration of 100 mg/mL. The dose, 100 mg/kg/day, is administered to mice via oral gavage. The maximum volume of the gavage is 10 mL/kg or 0.2 mL per 20 g animal. To deliver a 100 mg/kg dose by gavage, dilute the commercial 100 mg/mL stock of cyclosporine to 10 mg/mL for a 20 g animal for example. To adjust the stock solution concentration, perform dilutions of the commercial stock in corn oil (*see* **Note 3**).
4. PBS.
5. Corn oil, any brand available in a grocery store.
6. Mouse anti-KLH IgM ELISA commercial kit (e.g., Life Diagnostics Inc., 4000–1).
7. Mouse anti-KLH IgG ELISA commercial kit (e.g., Life Diagnostics Inc., 4010–1).
8. Test nanomaterial.

3 Methods

3.1 Preparation of Controls and Study Sample for HuLa

1. Prepare *negative control*. Use PBS and process this control in the same way as the test samples.
2. Prepare *positive control* of stock DXM. Clinical grade DXM is provided at a stock concentration of 4 mg/mL. Dilute the commercial stock in culture medium for a final concentration of 250 μg/mL.
3. Prepare *vehicle control* sample. Vehicle control is the buffer or media used to formulate the test nanomaterials. Common excipients used in nanoformulations are trehalose, sucrose, and albumin. However, other reagents and materials are also used alone or in combination. Vehicle control should match the formulation buffer of the test nanomaterial by both composition and concentration. This control can be skipped if nanoparticles are stored in PBS.
4. This assay requires 0.5 mL of nanoparticles dissolved/resuspended in complete culture medium to a concentration of 16× the highest tested concentration. The concentration is selected based on the plasma concentration of the nanoparticle at the intended therapeutic dose. For the purpose of this protocol, this concentration is called the "theoretical plasma concentration." Considerations for estimating theoretical plasma concentration were reviewed elsewhere [13] and are summarized in Box 1. The assay will evaluate four concentrations: 10X (or when feasible 100×, 30×, or 5×) of theoretical plasma

Box 1. Example Calculation of Nanoparticle Concentration for In Vitro Test

In this example, assume the mouse dose is known to be 123 mg/kg.

$$\text{human dose} = \frac{mouse\ dose}{12.3} = \frac{123\frac{mg}{kg}}{12.3} = 10\ \text{mg/kg}$$

Blood volume constitutes approximately 8% of body weight (e.g. a 70 kg human has approximately 5.6 L (8% of 70) of blood), allowing for a very rough estimation of the maximum blood concentration.

$$\text{in vitro concentration}_{human\ matrix} = \frac{human\ dose}{human\ blood\ volume} = \frac{70\ kg\ x\ 10\frac{mg}{kg}}{5.6\ L}$$

$$= \frac{700\ mg}{5.6\ L} = 0.125\ \text{mg/mL}$$

Box 1 Estimation of nanomaterial concentration for in vitro assay. The box shows an example of calculating the nanoparticle concentration for the in vitro HuLa assay. Reproduced with permission from ref. 13

concentration, theoretical plasma concentration, and two 5-fold serial dilutions of the theoretical plasma concentration. When the intended therapeutic concentration is unknown, the highest final concentration is 1 mg/mL or the highest reasonably achievable concentration. For example, if the final theoretical plasma concentration to be tested is 0.2 mg/mL, then a stock of 32 mg/mL will be prepared and diluted 10-fold (3.2 mg/mL), followed by two serial 5-fold dilutions (0.64 and 0.13 mg/mL, respectively). When 0.01 mL of each sample is added to the plate and mixed with 0.05 mL of Fluzone and 0.1 mL of the cell suspension, the final nanoparticle concentrations tested in the assay are: 2.0, 0.2, 0.04, and 0.008 mg/mL.

3.2 Preparation of Study Sample for TDAR

Prepare test nanoparticles in appropriate vehicle, which is specific to each formulation. Nanomaterials are tested at three doses, selected based on the existing information about the test nanomaterial from previous toxicological studies, at the: (1) no observable adverse effect level (NOAEL), (2) maximum tolerated dose (MTD) (e.g., a dose which demonstrated a moderate decrease in leukocyte count and was not accompanied by life-threatening abnormalities), and (3) dose between dose levels 1 and 2. The frequency and the route of administration for each test nanomaterial is selected based on its intended clinical use (e.g., once a week, every day, every other day, etc., and i.v., s.c., oral, etc.).

3.3 Human Leukocyte Activation (HuLa) Assay

1. Place freshly drawn blood into 15 mL or 50 mL conical centrifuge tubes, add an equal volume of room temperature PBS, and mix well.
2. Slowly layer the Ficoll-Paque solution underneath the blood/PBS mixture by placing the tip of the pipet containing Ficoll-Paque at the bottom of the blood sample tube. Alternatively, the blood/PBS mixture may be slowly layered over the Ficoll-Paque solution. Use 3 mL of Ficoll-Paque solution per 4 mL of blood/PBS mixture. For example, use 15 mL of Ficoll-Paque solution per 20 mL of diluted blood.
3. Centrifuge for 30 min at 900 × *g* at 18–20 °C, without brake.
4. Using a sterile pipet, remove the upper layer containing plasma and platelets and discard it.
5. Using a fresh sterile pipet, transfer the mononuclear cell layer into another centrifuge tube.
6. Wash cells by adding an excess of HBSS and centrifuging for 10 min at 400 × *g* at 18–20 °C. The HBSS volume should be about three times the volume of the mononuclear layer.
7. Discard the supernatant and repeat wash **step 6** one more time.
8. Resuspend cells in complete RPMI-1640 medium. Dilute cells 1:5 or 1:10 with trypan blue, count cells, and determine

	1	2	3	4	5	6	7	8	9	10	11	12
A	Medium (baseline)	NC	VC	PC		TS1 (0.008 mg/mL)	TS1 (0.008 mg/mL)	TS1 (0.008 mg/mL)	TS1 (0.04 mg/mL)	TS1 (0.04 mg/mL)	TS1 (0.04 mg/mL)	TS1 (0.2 mg/mL)
B	Medium (baseline)	NC	VC	PC		TS1 (0.008 mg/mL)	TS1 (0.008 mg/mL)	TS1 (0.008 mg/mL)	TS1 (0.04 mg/mL)	TS1 (0.04 mg/mL)	TS1 (0.04 mg/mL)	TS1 (0.2 mg/mL)
C	TS1 (0.2 mg/mL)	TS1 (0.2 mg/mL)	TS1 (2.0 mg/mL)	TS1 (2.0 mg/mL)	TS1 (2.0 mg/mL)	NC	VC	PC	Medium (baseline)	Cells, No Fluzone	Cells, No Fluzone	Cells, No BrdU
D	TS1 (0.2 mg/mL)	TS1 (0.2 mg/mL)	TS1 (2.0 mg/mL)	TS1 (2.0 mg/mL)	TS1 (2.0 mg/mL)	NC	VC	PC	Medium (baseline)	Cells, No Fluzone	Cells, No Fluzone	Cells, No BrdU
E	Cells, No BrdU											
F	Cells, No BrdU											
G	TS1 (0.008 mg/mL)	TS1 (0.04 mg/mL)	TS1 (0.2 mg/mL)	TS1 (2.0 mg/mL)								
H	TS1 (0.008 mg/mL)	TS1 (0.04 mg/mL)	TS1 (0.2 mg/mL)	TS1 (2.0 mg/mL)								

Fig. 3 Example of the plate map for HuLa assay. Wells 1–4 in Rows G and H are the cell-free, test samples; they do not receive cells. *NC* Negative Control, *PC* Positive Control, *TS* Test Sample, *VC* Vehicle Control

viability using trypan blue exclusion. If viability is at least 90%, proceed to the next step.

9. Adjust cell concentration to 1×10^6/mL with complete medium.
10. Aliquot 100 µL of cell suspension to the appropriate wells of two 96-well plates (Fig. 3). Repeat this step for each individual donor.
11. Add 10 µL of test nanoparticle, positive control and negative control to the respective wells. Prepare no cell, control wells containing nanoparticles only (Fig. 3).
12. Incubate at 37 °C for 1 h.
13. Add 50 µL of media or Fluzone vaccine to appropriate wells. Do not add Fluzone to "No Fluzone" wells.
14. Incubate at 37 °C for 72 h.
15. Add 20 µL of BrdU label to appropriate wells on BrdU plate, taking care not to add BrdU to "No BrdU" wells.
16. Incubate at 37 °C for 24 h.
17. Spin BrdU plate for 4 min at 400 × *g*.

18. Aspirate media from BrdU plate, add 200 µL of fixative per well, and incubate at room temperature for 30 min. Remove fixative and tap the plate on paper towel.
19. Aspirate plate and add 100 µL of diluted BrdU-specific antibody to all wells.
20. Incubate at room temperature for 1 h.
21. Aspirate plate.
22. Wash plate three times using 250 µL/well of 1× Wash Buffer. Blot the plate on paper towels to remove excess buffer.
23. Add 100 µL of Peroxidase-conjugated Goat Anti Mouse IgG to all wells.
24. Incubate at room temperature for 30 min.
25. Aspirate plate.
26. Wash plate three times using 250 µL/well of 1× Wash Buffer. Blot the plate on paper towels to remove excess buffer.
27. Fill wells completely with distilled water.
28. Aspirate plate. Blot the plate on paper towels to remove excess buffer.
29. Add 100 µL of Substrate Solution to all wells.
30. Incubate at room temperature for 30 min in the dark.
31. Add 100 µL of Stop Solution.
32. Read plate at dual wavelengths of 450 nm (Lm1) and 540 nm (Lm2) within 30 min of addition of Stop Solution. The final result is recorded as OD = Lm1-Lm2.

3.4 TDAR Assay

1. On Day 1 of the study, weigh each animal and administer nanoparticles using dose level and route of administration, as discussed in Subheading 3.2. The typical treatment groups, each containing five males and five females, include: untreated control, vehicle alone, KLH alone, Cyclosporin/KLH (positive control), Nanoparticles/KLH (test sample).
2. On Day 11, administer KLH (*see* **Note 4**).
3. On Day 17 weigh each animal, then collect 100 µL of blood from each mouse via tail vein. Allow blood to clot. Collect and freeze serum in a fresh tube for the subsequent IgM analysis (*see* **Note 4**).
4. On Day 25 weigh each animal, then collect 100 µL of blood from each mouse via tail vein. Allow blood to clot. Collect and freeze serum in a fresh tube for the subsequent IgG analysis. Humanely euthanize the animals, according to your institute's animal care and use policies, for example via carbon dioxide asphyxiation (*see* **Note 4**).
5. Analyze serum using a commercial ELISA kit for the presence of KLH-specific IgM and IgG.

3.5 Calculations and Data Interpretation for HuLa

1. A percent coefficient of variation should be calculated for each control or test according to the following formula:

$$\frac{\text{Standard deviation}}{\text{Mean}} \times 100\%$$

%CV for each control and test sample should be less than 30%.

2. Calculate the Stimulation Index (SI) using the following formula:

$$\frac{\text{Mean OD}_{test\ sample} - \text{Mean OD}_{\text{cells, no BrdU}}}{\text{Mean OD}_{\text{No Fluzone sample}} - \text{Mean OD}_{\text{cells, no BrdU}}}$$

A good SI in the absence of an immunosuppressive agent is $\geq$3. Preferable SI is $\geq$6–7.

3. If positive control or negative control fails to meet acceptance criterion in **step 1** above, the assay should be repeated.
4. Within the acceptable assay, if two of three replicates of unknown sample fail to meet acceptance criterion described in **step 1**, this unknown sample should be re-analyzed.
5. If significant variability is observed in results obtained using leukocytes from three initial donors, the experiment needs to be repeated with additional donor cells.
6. The positive control is considered positive if it results in at least a two fold reduction in SI, when compared to the baseline sample.
7. Statistical analysis is used to identify the nanoparticle candidate with potential immunosuppressive properties.

3.6 Calculations and Data Interpretation for TDAR

1. %CV for each sample analyzed on ELISA plate should be calculated as described in **step 1** of Subheading 3.5 for HuLa assay. %CV should be no more than 25%.
2. Compare IgM and IgG levels in the treatment groups with that in the control group immunized with KLH alone. Perform statistical analysis using traditional methods.

4 Notes

1. NCL does not endorse suppliers. However, we found that a new user benefits from knowing catalog information of reagents used in our assays. If you need ideas of what reagents are used at the NCL, please review NCL method ITA-18 available at https://ncl.cancer.gov/resources/assay-cascade-protocols. When other reagents are used, the assay

performance may change. When using reagents and instruments from sources other than that used in our protocols, assay performance qualification is needed to verify the assay functionality and validity.

2. Check your institutional Animal Care and Use Committee (ACUC) requirements for the needle size. We do not recommend using needles larger than 25 gauge for i.v. injections.
3. Commercial formulation of cyclosporine A contains castor oil. Castor oil will cause diarrhea in animals which may lead to dehydration. To avoid diarrhea in the positive control group, corn oil should be used for the preparation of the working stock of cyclosporine, which is administered to animals via oral gavage.
4. The timing between nanoparticle administration and that of KLH may be modified to select the most relevant schedule mimicking the clinically intended use. For example, nanoparticles and KLH can be administered on Day 1 with an hour interval. This dosing regimen is appropriate for nanoparticles intended for a single dose administration. Such a change will result in a different number of days of the study. Blood collection for IgM and IgG assessment is done 7 and 14–21 days after KLH administration, respectively.

Acknowledgment

This project has been funded in whole or in part by federal funds from the National Cancer Institute, National Institutes of Health, under contract HHSN261200800001E. The content of this publication does not necessarily reflect the views or policies of the Department of Health and Human Services, nor does mention of trade names, commercial products, or organizations imply endorsement by the U.S. Government.

References

1. Wilke RA, Lin DW, Roden DM, Watkins PB, Flockhart D, Zineh I, Giacomini KM, Krauss RM (2007) Identifying genetic risk factors for serious adverse drug reactions: current progress and challenges. Nat Rev Drug Discov 6 (11):904–916. doi:10.1038/nrd2423
2. Smith DA, Schmid EF (2006) Drug withdrawals and the lessons within. Curr Opin Drug Discov Devel 9(1):38–46
3. Wysowski DK, Nourjah P (2004) Analyzing prescription drugs as causes of death on death certificates. Public Health Rep 119(6):520. doi:10.1016/j.phr.2004.09.001
4. Wysowski DK, Swartz L (2005) Adverse drug event surveillance and drug withdrawals in the United States, 1969-2002: the importance of reporting suspected reactions. Arch Intern Med 165(12):1363–1369. doi:10.1001/archinte.165.12.1363
5. Tyner K, Sadrieh N (2011) Considerations when submitting nanotherapeutics to FDA/CDER for regulatory review. Methods Mol Biol 697:17–31. doi:10.1007/978-1-60327-198-1_3
6. Tyner KM, Zou P, Yang X, Zhang H, Cruz CN, Lee SL (2015) Product quality for

nanomaterials: current U.S. experience and perspective. Wiley Interdiscip Rev Nanomed Nanobiotechnol 7(5):640–654. doi:10.1002/wnan.1338

7. Bancos S, Tyner K, Weaver JL (2013) Immunotoxicity testing for drug–nanoparticle conjugates: regulatory considerations. In: Dobrovolskaia MA, SE MN (eds) Handbook of immunological properties of engineered nanomaterials. World Scientific Publishing, Singapore
8. Dobrovolskaia MA, Germolec DR, Weaver JL (2009) Evaluation of nanoparticle immunotoxicity. Nat Nanotechnol 4(7):411–414. doi:10.1038/nnano.2009.175
9. Collinge M, Cole SH, Schneider PA, Donovan CB, Kamperschroer C, Kawabata TT (2010) Human lymphocyte activation assay: an in vitro method for predictive immunotoxicity testing. J Immunotoxicol 7(4):357–366. doi:10.3109/1547691x.2010.523881
10. Shen CC, Liang HJ, Wang CC, Liao MH, Jan TR (2011) A role of cellular glutathione in the differential effects of iron oxide nanoparticles on antigen-specific T cell cytokine expression. Int J Nanomedicine 6:2791–2798. doi:10.2147/ijn.s25588
11. Shen CC, Liang HJ, Wang CC, Liao MH, Jan TR (2012) Iron oxide nanoparticles suppressed T helper 1 cell-mediated immunity in a murine model of delayed-type hypersensitivity. Int J Nanomedicine 7:2729–2737. doi:10.2147/ijn.s31054
12. Shen CC, Wang CC, Liao MH, Jan TR (2011) A single exposure to iron oxide nanoparticles attenuates antigen-specific antibody production and T-cell reactivity in ovalbumin-sensitized BALB/c mice. Int J Nanomedicine 6:1229–1235. doi:10.2147/ijn.s21019
13. Dobrovolskaia MA, McNeil SE (2013) Understanding the correlation between in vitro and in vivo immunotoxicity tests for nanomedicines. J Control Release 172(2):456–466. doi:10.1016/j.jconrel.2013.05.025

Chapter 15

Analysis of Pro-inflammatory Cytokine and Type II Interferon Induction by Nanoparticles

Timothy M. Potter, Barry W. Neun, Jamie C. Rodriguez, Anna N. Ilinskaya, and Marina A. Dobrovolskaia

Abstract

Cytokines, chemokines, and interferons are released by the immune cells in response to cellular stress, damage and/or pathogens, and are widely used as biomarkers of inflammation. Certain levels of cytokines are needed to stimulate an immune response in applications such as vaccines or immunotherapy where immune stimulation is desired. However, undesirable elevation of cytokine levels, as may occur in response to a drug or a device, may lead to severe side effects such as systemic inflammatory response syndrome or cytokine storm. Therefore, preclinical evaluation of a test material's propensity to cause cytokine secretion by healthy immune cells is an important parameter for establishing its safety profile. Herein, we describe in vitro methods for analysis of cytokines, chemokines, and type II interferon in whole blood cultures derived from healthy donor volunteers. First, whole blood is incubated with controls and tested nanomaterials for 24 h. Then, culture supernatants are analyzed by ELISA to detect IL-1β, TNFα, IL-8, and IFNγ. The culture supernatants can also be analyzed for the presence of other biomarkers secreted by the immune cells. Such testing would require additional assays not covered in this chapter and/or optimization of the test procedure to include relevant positive controls and/or cell types.

Key words Cytokines, Chemokines, Interferons, Inflammation, Whole blood, Immunostimulation

1 Introduction

Cytokine storm is a condition characterized by high plasma levels of inflammatory cytokines, chemokines, and interferons which can be commonly induced by pathogens or their components (endotoxin, lipoproteins, DNA, RNA, etc.). Cytokine storm can also be caused by certain drugs, for example recombinant proteins, therapeutic antibodies, macromolecular nucleic acid-based therapeutics. It is often accompanied by fever, hypo- or hypertension and may progress to a more severe life-threatening condition called systemic inflammatory response syndrome (SIRS). For example, cytokine storm was a serious side effect in the phase I clinical trial of an experimental monoclonal antibody therapeutic, TGN1412, which

Scott E. McNeil (ed.), *Characterization of Nanoparticles Intended for Drug Delivery*, Methods in Molecular Biology, Vol. 1682, DOI 10.1007/978-1-4939-7352-1_15,

caused six healthy volunteer enrollees to become critically ill, requiring intensive care [1]. All patients had high serum levels of TNFα, IFNγ, and other pro-inflammatory messengers [1]. Cytokine storm was not observed in preclinical studies of this drug using rats and cynomolgus monkeys [1], but was readily detectable in vitro using a cytokine release assay in human primary blood cells [2].

Nanoparticles can be employed for delivery of therapeutic proteins and antibodies, use biologicals (e.g., antibodies, proteins, peptides) as targeting agents, or can be made of biological molecules (e.g., self-assembling peptides). This warrants investigation of the nanotechnology platforms, as well as their macromolecular payload and targeting agents, for their propensity to induce pro-inflammatory cytokines. Human whole blood is considered a reliable and predictive model for this purpose. The data obtained from such in vitro studies are intended to supplement other preclinical data to create a safety profile for the technology, and ensure the safe transition of nanomedicines toward clinical development.

The protocol described herein uses whole blood derived from healthy donor volunteers and cultures these specimens in the presence of controls and nanoparticles to identify the potential to induce a cytokine storm. The culture supernatants are subsequently analyzed by ELISA assays specific to IL-8, IL-1β, TNFα, and IFNγ. Commercial ELISA assays and multiplex kits can also be used, following the instructions from relevant manufacturers. This chapter does not describe a protocol for the detection of type I interferons. If analysis of type I interferons is desired, another model (e.g., PBMC or pDC cultures) and other positive controls (e.g., oligonucleotides) should be used. There is no harmonized approach for the type of assay to use or for the choice between singleplex and multiplex analysis. One should rely on scientific judgment, focusing on the particular type of nanoparticles, the kind of the cytokines, and the method for analysis of supernatants. It takes 24 h to culture whole blood and collect supernatants. An additional 5–6 h are needed to complete the ELISA or multiplex analysis. If ELISA or multiplex analysis cannot be conducted immediately after incubation of whole blood with nanoparticles, the culture supernatants can be frozen at −20 °C. Different cytokines have different stability at room temperature (RT) and upon repeated freeze/thaw (FT) cycles. Please refer to **Note 1** or manufacturer's instruction of commercial kits for the information about RT and FT stabilities. When such information is not available, as in the case of some commercial kits, analyze supernatants immediately and prepare multiple aliquots for repeat analysis to avoid multiple FT cycles.

2 Materials

1. *See* **Note 2**.
2. Human blood, anticoagulated with Li-heparin from at least three healthy donors.
3. Phosphate Buffered Saline (PBS).
4. Complete RPMI-1640 Medium. Prepare with 10% FBS (heat-inactivated), 2 mM L-glutamine, 100 U/mL penicillin, and 100 μg/mL streptomycin. Store at 2–8 °C, protected from light for no longer than 1 month. Warm the media in a water bath before use. To prepare heat-inactivated FBS, thaw a 50 mL aliquot of FBS stock and equilibrate to room temperature. Place the tube in a 56 °C water bath and incubate with mixing for 35 min. Chill the serum and use to prepare complete culture media.
5. 1 mg/mL ultrapure lipopolysaccharide (LPS) from K12 *E. coli*. Add 1 mL of sterile water to 1 mg LPS and vortex to mix. Aliquot 20 μL and store at a nominal temperature of −20 °C. Avoid repeated freeze–thaw cycles. On the day of the experiment thaw one aliquot and use at a final concentration of 20 ng/mL.
6. 1 mg/mL Phytohemagglutinin (PHA-M) stock. Add 1 mL sterile PBS or cell culture medium to 1 mg PHA-M. Gently rotate to mix. Store daily use aliquots at a nominal temperature of −20 °C. Avoid repeated freezing/thawing. On the day of the experiment thaw one aliquot and use at a final concentration of 10 μg/mL.
7. Coating Buffer (BupH Carbonate-Bicarbonate): Dissolve one pack of BupH Carbonate-Bicarbonate in 500 mL distilled water and mix well. This produces 0.2 M carbonate-bicarbonate buffer with pH 9.4. Filter through 0.2 μm filter and store at room temperature for up to 1 month.
8. Wash Buffer: 1× TBS in 0.05% Tween-20. Dissolve one pack of BupH Tris Buffered Saline Pack in 500 mL distilled water mix well and add 250 μL of Tween-20. Store at room temperature for up to 1 month.
9. Blocking Buffer: 1× PBS with 1% BSA and 0.5% Tween-20. Weigh 5 g BSA and dissolve in 500 mL of 1× PBS. Then, add 2.5 mL Tween-20 and mix well. Filter through 0.2 μm low protein binding filter and store at 4 °C for up to 1 month.
10. 1 mg/mL NeutrAvidin Horseradish Peroxidase Conjugate stock solution. This conjugate is supplied as 2 mg lyophilized powder. Reconstitute with 0.4 mL distilled water and further dilute to 2 mL by adding 1.6 mL sterile PBS to achieve a stock

concentration of 1 mg/mL. For long-term storage freeze reconstituted product in single use 5 μL aliquots. Avoid repeated freezing and thawing.

11. Stop Solution: 2 N sulfuric acid (H_2SO_4). Slowly add 27.7 mL H_2SO_4 into 200 mL of dH_2O water, mix the solution thoroughly, let it cool and bring the solution to 500 mL with dH_2O using a 1000 mL graduated cylinder. Mix well and store in a bottle at room temperature.
12. Ultra TMB-ELISA Substrate.
13. Human IL-8 monoclonal antibody.
14. Human IL-8 Biotinylated Affinity Purified polyclonal antibody.
15. Recombinant Human IL-8.
16. Human IL-1β monoclonal antibody.
17. Human IL-1β Biotinylated Affinity Purified polyclonal antibody.
18. Recombinant Human IL-1β.
19. Human TNF-α monoclonal antibody.
20. Human TNF-α Biotinylated Affinity Purified polyclonal antibody.
21. Recombinant Human TNF-α.
22. Human IFNγ monoclonal antibody.
23. Human IFNγ Biotinylated Affinity Purified polyclonal antibody.
24. Recombinant Human IFNγ.
25. 24-well round bottom plates.
26. 96-well flat bottom plates.
27. Sealing tape for 96-well plates.
28. Plate reader, 450 nm.

3 Methods

3.1 Preparation of Reagents and Controls

1. *Negative Control.* Use PBS as the negative control. Process this control the same way as the test samples.
2. *Vehicle Control.* The vehicle control is the buffer or media used to formulate test nanomaterials. Vehicle control should match formulation buffer of the test-nanomaterial by both composition and concentration. This control can be skipped if nanoparticles are stored in PBS.
3. *Assay Diluent.* Collect whole blood into heparinized tubes. Centrifuge for 10 min at 2500 × *g* and 2–8 °C; collect and pool plasma from at least three donors. Plasma must be

prepared within 2 h after blood collection and either used immediately or aliquoted and stored at −20 °C. Avoid repeated freeze–thaw cycles. Follow one of the approaches described below to prepare working diluent.

Approach A: Thaw pooled Li-Heparin plasma, pulse-spin in a microcentrifuge or 10 min at 2500 × *g* to remove fibrinogen fibers or any other aggregated material. Dilute plasma in complete RPMI to a final concentration of 20%. The plasma does not have to match the donors used in a given experiment; a large pool of plasma from various donors can be prepared in advance, aliquoted and stored at −20 °C.

Approach B: Autologous plasma collected from the same donors as used in the culture experiment can be utilized. The limitation of this approach is that a separate standard curve and quality control set should be prepared for each donor. Use fresh; discard any leftover amount after experiment is complete (*see* **Note 3**).

Approach C: Utilize the unused portion of the blood diluted for the experiment to prepare untreated blood supernatants from each individual donor and pool these supernatants to make pooled assay diluent representing all donors used in the given experiment. Add 1 mL of complete RPMI per each 4 mL of the pooled supernatant to match the matrix of study samples by both composition and concentration. Use fresh; discard any leftover amount after experiment is complete (*see* **Note 4**).

4. *Inhibition/Enhancement Controls (IEC)*. Two approaches can be used to prepare IECs.

   Approach A: Use culture supernatant from the positive control sample and spike with test nanoparticle at four concentrations (refer to Subheading 3.2). For example, add 100 μL of nanoparticle working dilution into 400 μL of positive control supernatant. The final concentration of nanoparticle in this sample will mimic that in supernatants from nanoparticle-treated cells. The concentration of the analyte (cytokine, chemokine, or IFN) in the positive control supernatant will be 1.3 times lower. Compare the analyte level in the positive control supernatant with that in IEC × 1.3 to account for the dilution factor. If the difference in test results is within 25%, test-nanoparticle does not interfere with ELISA.

   Approach B: Use cell-free controls and spike with analyte (cytokine, chemokine, or IFN) standard at a concentration equal to that in Quality Control 2 (QC 2, Tables 1B, 2B, 3B). Compare this IEC to QC 2. If the difference in test results is within 25%, test-nanoparticle does not interfere with ELISA.

5. *Quality Controls (QCs)*. QC samples are prepared by dilution of recombinant cytokine, chemokine, or IFN stock in the Assay Diluent. Follow Table 1B for IL-8 QC preparation, Table 2B

Table 1
Preparation of calibration standard and quality controls for IL-8 ELISA. Table A shows concentrations and volumes used to prepare calibration standards for the IL-8 ELISA. Table B shows concentrations and volumes used to prepare quality controls for the IL-8 ELISA

Sample	Nominal concentration (pg/mL)	Preparation procedure
A. Calibration standards		
Int A	100,000	2.5 µL of stock +2497.5 µL of assay diluent
Std 1	2000	40 µL of Int A + 1960 µL of assay diluent
Std 2	1000	250 µL of Std 1 + 250 µL of assay diluent
Std 3	500	250 µL of Std 2 + 250 µL of assay diluent
Std 4	250	250 µL of Std 3 + 250 µL of assay diluent
Std 5	125	250 µL of Std 4 + 250 µL of assay diluent
Std 6	62.5	250 µL of Std 5 + 250 µL of assay diluent
Std 7	31.3	250 µL of Std 6 + 250 µL of assay diluent
B. Quality controls		
Int A	100,000	2.5 µL of stock +2497.5 µL of assay diluent
Int B	2000	40 µL of Int A + 1960 µL of assay diluent
QC 1	800	400 µL of Int B + 600 µL of assay diluent
QC 2	200	100 µL of Int B + 900 µL of assay diluent
QC 3	100	500 µL of QC 2 + 500 µL of assay diluent

Int intermediate solution, *Std* standard

for IL-1β, Table 3B for TNFα, and Table 4B for IFNγ. Int A and Int B are intermediate solutions used to prepare QCs only. Although Int A has the same nominal concentration as Int A used to prepare calibration standards, the latter should not be used to prepare QC in order to avoid duplicating errors if such an error occurs. Prepare Int A for QC separately from that used to make calibration standards.

6. *Coating Antibody.* Prepare appropriate monoclonal antibody by reconstituting lyophilized powder in sterile PBS to afford a final concentration of 0.5 mg/mL. Prepare single use aliquots of 10, 20, 40, and 20 µL for IL-8, IL-1β, TNFα, and IFNγ, respectively. Store aliquots at −70 °C for up to 6 months. On the day of the assay, thaw a single-use aliquot at room temperature and add the entire amount to 10 mL of Coating Buffer (*see* **Note 5**).
7. *Recombinant Human Cytokine Stock.* Prepare appropriate recombinant human stocks by reconstituting lyophilized

Table 2
Preparation of calibration standard and quality controls for IL-1β ELISA. Table A shows concentrations and volumes used to prepare calibration standards for the IL-1β ELISA. Table B shows concentrations and volumes used to prepare quality controls for the IL-1β ELISA

Sample	Nominal concentration (pg/mL)	Preparation procedure
A. Calibration standards		
Int A	25,000	5 μL of stock +4995 μL of assay diluent
Int B	2500	100 μL of Int A + 900 μL of assay diluent
Std 1	250	100 μL of Int B + 900 μL of assay diluent
Std 2	125	250 μL of Std 1 + 250 μL of assay diluent
Std 3	62.5	250 μL of Std 2 + 250 μL of assay diluent
Std 4	31.3	250 μL of Std 3 + 250 μL of assay diluent
Std 5	15.6	250 μL of Std 4 + 250 μL of assay diluent
Std 6	7.8	250 μL of Std 5 + 250 μL of assay diluent
Std 7	3.9	250 μL of Std 6 + 250 μL of assay diluent
B. Quality controls		
Int A	25,000	5 μL of stock +4995 μL of assay diluent
Int B	2500	100 μL of Int A + 900 μL of assay diluent
QC 1	100	150 μL of Int B + 3600 μL of assay diluent
QC 2	50	500 μL of QC 1 + 500 μL of assay diluent
QC 3	12.5	200 μL of QC 2 + 600 μL of assay diluent

Int intermediate solution, *Std* standard

powder in sterile PBS containing 0.1% BSA to a final concentration of 100, 25, 100, and 200 μg/mL for IL-8, IL-1β, TNFα, and IFNγ, respectively. Prepare single-use aliquots of 5 μL and store at −70 °C for up to 6 months. This stock solution is used to prepare the calibration standards and QCs (*see* **Note 5**).

8. *Secondary Antibody.* Prepare appropriate secondary antibody by reconstituting lyophilized powder in sterile PBS to a final concentration of 0.2 mg/mL. Prepare single-use 25 μL aliquots and store at −70 °C for up to 6 months. On the day of the assay, thaw a single-use aliquot at room temperature and add the entire amount to 10 mL of Blocking Buffer (*see* **Note 5**).

3.2 Preparation of Nanoparticle Samples

When the experiment is conducted in 24-well plates, the assay requires 5 mL of nanoparticles dissolved/resuspended in complete culture medium at a concentration five times greater than the

Table 3
Preparation of calibration standard and quality controls for TNFα ELISA. Table A shows concentrations and volumes used to prepare calibration standards for the TNFα ELISA. Table B shows concentrations and volumes used to prepare quality controls for the TNFα ELISA

Sample	Nominal concentration (pg/mL)	Preparation procedure
A. Calibration standards		
Int A	100,000	5 μL of stock +4995 μL of assay diluent
Int B	10,000	100 μL of Int A + 900 μL of assay diluent
Std 1	4000	200 μL of Int B + 300 μL of assay diluent
Std 2	2000	250 μL of Std 1 + 250 μL of assay diluent
Std 3	1000	250 μL of Std 2 + 250 μL of assay diluent
Std 4	500	250 μL of Std 3 + 250 μL of assay diluent
Std 5	250	250 μL of Std 4 + 250 μL of assay diluent
Std 6	125	250 μL of Std 5 + 250 μL of assay diluent
Std 7	62.5	250 μL of Std 6 + 250 μL of assay diluent
B. Quality controls		
Int A	100,000	5 μL of stock +4995 μL of assay diluent
Int B	10,000	100 μL of Int A + 900 μL of assay diluent
QC 1	1500	600 μL of Int B + 3399 μL of assay diluent
QC 2	750	500 μL of QC 1 + 500 μL of assay diluent
QC 3	375	500 μL of QC 2 + 500 μL of assay diluent

Int intermediate solution, *Std* standard

highest final test concentration. The concentration is selected based on the theoretical plasma concentration of the nanoparticle at the intended therapeutic dose. Considerations for estimating the theoretical plasma concentration have been reviewed elsewhere [3] and are summarized in Box 1. The assay examines four nanoparticle test concentrations: 10× (or when feasible 100×, 30×, or 5×) of the theoretical plasma concentration, the theoretical plasma concentration, and two 5-fold serial dilutions of the theoretical plasma concentration.

When the intended therapeutic concentration is unknown, the highest final concentration is either 1 mg/mL, or the highest reasonably achievable concentration. For example, if the final theoretical plasma concentration to be tested is 0.2 mg/mL, then a stock of 10 mg/mL will be prepared and diluted 10-fold (1 mg/mL), followed by two 5-fold serial dilutions (0.2 and 0.04 mg/mL). When 200 μL of each of these samples are combined in a

Table 4
Preparation of calibration standard and quality controls for IFNγ ELISA. Table A shows concentrations and volumes used to prepare calibration standards for the IFNγ ELISA. Table B shows concentrations and volumes used to prepare quality controls for the IFNγ ELISA

Sample	Nominal concentration (pg/mL)	Preparation procedure
A. Calibration standards		
Int A	200,000	5 μL of stock +4995 μL of assay diluent
Int B	20,000	100 μL of Int A + 900 μL of assay diluent
Std 1	2000	100 μL of Int B + 900 μL of assay diluent
Std 2	1000	250 μL of Std 1 + 250 μL of assay diluent
Std 3	500	250 μL of Std 2 + 250 μL of assay diluent
Std 4	250	250 μL of Std 3 + 250 μL of assay diluent
Std 5	125	250 μL of Std 4 + 250 μL of assay diluent
Std 6	62.5	250 μL of Std 5 + 250 μL of assay diluent
Std 7	31.3	250 μL of Std 6 + 250 μL of assay diluent
B. Quality controls		
Int A	200,000	5 μL of stock +4995 μL of assay diluent
Int B	20,000	100 μL of Int A + 900 μL of assay diluent
QC 1	800	150 μL of Int B + 3600 μL of assay diluent
QC 2	400	500 μL of QC 1 + 500 μL of assay diluent
QC 3	200	300 μL of QC 2 + 300 μL of assay diluent

Int intermediate solution, *Std* standard

culture plate with 800 μL of cells, the final concentrations of nanoparticles are 0.008, 0.04, 0.2, and 2 mg/mL. Each nanoparticle concentration is plated three times. An additional 600 μL is required for a cell-free control. When the cell-free control is prepared for the whole blood plate, an aliquot of blood diluted in PBS from Subheading 3.3 is spun down for 10 min at 2500 × *g* and 800 μL of this cell-free supernatant is combined with 200 μL of test nanoparticles.

3.3 Preparation of Whole Blood

1. Collect whole blood from healthy donor volunteers who have been clear from infection and unmedicated for at least 2 weeks prior to blood donation. Use Li-heparin tubes and discard the first 10 cc. For best results, whole blood should be used within 1 h after collection. Prolonged storage (>2 h) of whole blood will lead to a decrease in cell function.

Box 1. Example Calculation of Nanoparticle Concentration for In Vitro Test

In this example, we assume the mouse dose is known to be 123 mg/kg.

$$\text{human dose} = \frac{mouse\ dose}{12.3} = \frac{123\frac{mg}{kg}}{12.3} = 10\ \text{mg/kg}$$

Blood volume constitutes approximately 8% of body weight (e.g. a 70 kg human has approximately 5.6 L (8% of 70) of blood). This allows for a very rough estimation of what the maximum blood concentration may be.

$$\text{in vitro concentration}_{human\ matrix} = \frac{human\ dose}{human\ blood\ volume} = \frac{70\ kg\ x\ 10\frac{mg}{kg}}{5.6\ L}$$

$$= \frac{700\ mg}{5.6\ L} = 0.125\ \text{mg/mL}$$

Box 1 Example of calculation of nanoparticle concentrations for in vitro test. Reproduced with permission from ref. 3

	1	2	3	4	5	6
A	NC	PC	TS 1	TS 2	VC 1	VC 2
B	NC	PC	TS 1	TS 2	VC 1	VC 2
C	NC	PC	TS 1	TS 2	VC 1	VC 2
D	TS 1 Cell free	TS 2 Cell free	TS 1 Cell free	TS2 Cell free	VC 1 Cell free	VC 2 Cell free

Fig. 1 Example 24-well Plate Template for Culturing Whole Blood. Row D does not contain cells; *NC* negative control, *PC* positive control; *TS 1* and *2* test nanoparticle at concentrations 1 and 2, respectively; *VC1* and *2* vehicle control at concentrations 1 and 2, respectively

2. Dilute whole blood four times with complete culture media (e.g., 3 mL of whole blood and 9 mL of complete culture media).
3. Dispense 800 µL of diluted blood from **step 1** per well in a 24-well plate. *See* Fig. 1 for plate layout (*see* **Note 6**).
4. Dispense 200 µL of blank media (baseline), negative control, positive control, vehicle control, and test samples into corresponding wells on a 24-well plate containing 800 µL of diluted blood from **step 1**. Prepare triplicate wells for each

sample. Prepare cell-free control by dispending 200 μL of nanoparticles into 800 μL of cell-free supernatant prepared by spinning an aliquot of whole blood from **step 1** for 10 min at 2500 × *g*. Gently shake plates to mix (*see* **Note 7**).

5. Repeat **steps 1–3** for cells obtained from each individual donor. There is no limit to the number of donors that can be used. It is advised to test each nanoparticle formulation using blood derived from at least three donors.
6. Incubate 24 h in a humidified 37 °C, 5% CO_2 incubator.
7. Collect cultured blood in 1.5 mL centrifuge tubes and spin in a microcentrifuge at 18,000 × *g* for 5 min.
8. Transfer supernatants into fresh tubes and either proceed with ELISA analysis or aliquot and store at −20 °C (*see* **Note 8**).

3.4 ELISA

1. Before starting, please *see* **Notes 1** and **9**.
2. Refer to Fig. 2 for an ELISA plate template to determine the number of plates needed. Coat the plate with capture antibody

	1	2	3	4	5	6	7	8	9	10	11	12
A	B0	Std1	Std2	Std3	Std4	Std5	Std6	Std7	QC1	QC2	QC3	TS1
B	B0	Std1	Std2	Std3	Std4	Std5	Std6	Std7	QC1	QC2	QC3	TS1
C	TS1	TS1	TS2	TS2	TS2	TS3	TS3	TS3	TS4	TS4	TS4	TS1 CF
D	TS1	TS1	TS2	TS2	TS2	TS3	TS3	TS3	TS4	TS4	TS4	TS1 CF
E	TS1 CF	TS1 CF	TS2 CF	TS2 CF	TS2 CF	TS3 CF	TS3 CF	TS3 CF	TS4 CF	TS4 CF	TS4 CF	IEC1
F	TS1 CF	TS1 CF	TS2 CF	TS2 CF	TS2 CF	TS3 CF	TS3 CF	TS3 CF	TS4 CF	TS4 CF	TS4 CF	IEC1
G	IEC2	IEC3	IEC4	NC	NC	PC	PC	VC	VC	QC1	QC2	QC3
H	IEC2	IEC3	IEC4	NC	NC	PC	PC	VC	VC	QC1	QC2	QC3

Fig. 2 Example ELISA Plate Template. This figure shows an example of the ELISA plate layout. *Std* standard; *TS* test sample; *QC* quality control; *B0* blank (assay diluent); *NC* negative control supernatant; *PC* positive control supernatant; *VC* vehicle control supernatant; *TS1*, *TS2*, *TS3* and *TS 4* supernatant from nanoparticle test sample at concentrations 1, 2, 3, and 4, respectively; *IEC1*, *IEC2*, *IEC3*, and *IEC4* inhibition enhancement controls for nanoparticles at test concentrations 1, 2, 3, and 4, respectively; *CF* cell free

by adding 100 μL of working solution to each well; Cover plate with a plate sealer and incubate overnight at 4 °C.

3. Aspirate coating solution and dry the plate by tapping on a paper towel. Add 100 μL of blocking buffer per well and incubate for 1 h at room temperature.
4. During incubation time in **step 3**, prepare calibration standards, QCs, and IECs.
5. Aspirate blocking buffer, tap-dry the plate and add 100 μL of standards, test samples, QCs, and IECs to appropriate wells. Carefully cover the plate with an adhesive plate cover. Ensure that all edges and strips are sealed tightly. Incubate for 1 h at room temperature. All standards, controls, and samples are analyzed in duplicate (*see* **Note 10**).
6. Carefully remove the adhesive plate cover. Wash the plate six times with wash buffer. When using an automatic plate washer, turn plates after first cycle (i.e., first three washes). After final wash, tap the plate on absorbent paper to remove traces of wash buffer from wells.
7. Add 100 μL of Secondary Antibody working solution per well, cover the plate with a plate sealer and incubate for 1 h at room temperature.
8. Wash the plate six times with wash buffer. When using an automatic plate washer, turn plates after first cycle (i.e., first three washes). After final wash, tap plate thoroughly on absorbent paper to remove traces of wash buffer from the wells.
9. Add 100 μL of NeutrAvidin Horseradish Peroxidase Conjugate working solution to each well, cover the plate with a plate sealer and incubate for 1 h at room temperature.
10. Wash the plate six times with wash buffer. When using an automatic plate washer turn plates after first cycle (i.e., first three washes). After final wash, tap plate thoroughly on absorbent paper to remove traces of wash buffer from the wells.
11. Add 100 μL of TMB-ELISA substrate per well, cover the plate with a plate sealer and incubate plate for 20–30 min at room temperature. Protect from light (*see* **Note 11**).
12. Add 50 μL of Stop Solution to each well. The color in the wells should change from blue to yellow. If the color change does not appear uniform, gently tap the plate to ensure thorough mixing.
13. Determine the optical density of each well within 30 min, using a microplate reader set to 450 nm.

3.5 Calculations and Results Interpretation

1. The % CV for each test sample, including supernatants from cell/blood cultures treated with positive control, negative control, and nanoparticle sample, should be within 20%. At least

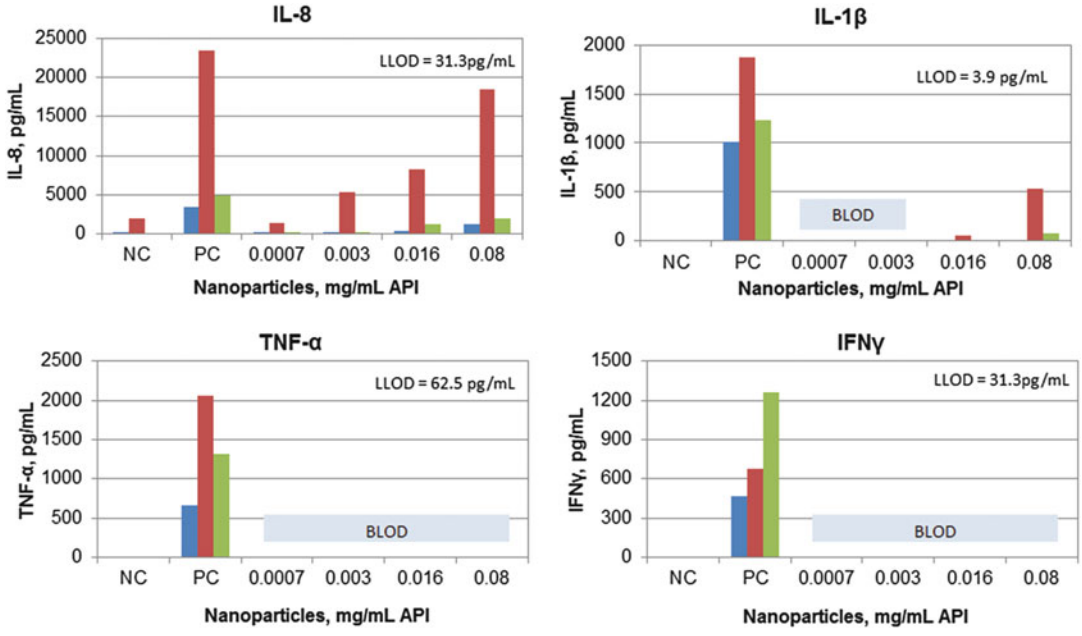

Fig. 3 Example of data generated using this assay. A nanoparticle formulation was analyzed according to the protocol described in this chapter. The data show that the formulations induced IL-8 in all tested donors and IL-1β in two of three tested donors. Induction of TNFα and IFNγ was not observed

one replicate of positive and negative controls should be acceptable for run to be accepted.

2. If both replicates of positive control or negative control fail to meet acceptance criterion described in **step 1**, the run should be repeated.
3. Within the acceptable run, if two of three replicates of unknown sample fail to meet acceptance criterion described in **step 1**, this unknown sample should be re-analyzed.
4. Elevation of cytokine level in the test sample ≥two fold above that observed in the baseline sample is considered a positive response. Please *see* Fig. 3 for an example of the data generated using this assay.
5. Nanoparticles do not interfere with ELISA if the difference in test results between IEC and QC or positive control is within 25%.

4 Notes

1. When analysis of cytokines and interferon are performed using ELISA as described in this chapter, the acceptable number of freeze/thaw cycles is as follows: one for IL-8, three for IL-1β and TNFα, and two for IFNγ.

2. NCL does not endorse suppliers. However, we found that a new user benefits from knowing catalog information of reagents used in our assays. If you need ideas of what reagents are used at the NCL, please review NCL methods ITA-10, ITA-22, ITA-23, ITA-24, and ITA-25 available at https://ncl.cancer.gov/resources/assay-cascade-protocols. When other reagents are used, the assay performance may change. For ELISA assays, the limits of detection and quantification, the calibration curve and QCs, and the number of acceptable freeze/thaw cycles may also change. When using reagents and instruments from sources other than that used in our protocols, assay performance qualification is needed to verify the assay functionality and validity.
3. If autologous plasma was frozen, pulse-spin in a microcentrifuge for 10 min at 2500 × *g* to remove fibrinogen fibers or any other aggregated material.
4. If the experiment cannot be completed within the same day, it is OK to freeze this diluent at −20 °C. If this diluent is stored frozen and thawed prior to use in the assay, pulse-spin the diluent in a microcentrifuge for 10 min at 2500 × *g* to remove fibrinogen fibers or any other aggregated material.
5. If the protein or antibody from another source is used, the final dilution of this protein should be adjusted to provide optimal assay performance (i.e., minimum background, high signal-to-noise ratio).
6. If positive control supernatants are used to prepare IECs, do not forget to add extra replicates of the positive control sample.
7. The cell-free sample will be processed the same way as the whole blood samples and will serve as a control for false-positive results. To test for potential false-negative results, supernatant from the positive control can be spiked with nanoparticle at a final nanoparticle concentration identical to that in the test sample. Alternatively, a cell-free supernatant containing nanoparticles can be spiked with cytokine standard in each individual ELISA assay and analyzed against relevant quality controls. If the nanoparticle inhibits detection of the cytokine, a decrease in the cytokine level will be seen when compared to the level of cytokine in the positive control or QC samples. Additionally, to understand whether a nanoparticle may potentiate or inhibit cellular responses to the assay positive control (LPS or PHA-M), the positive control can be co-cultured with nanoparticles in the presence of cells.
8. To avoid multiple freeze/thaw cycles, it is better to prepare multiple (200 or 300 μL) aliquots for each supernatant.
9. The described procedure is uniform for all ELISAs. Please refer to Subheading 3.1 for instructions on preparation of coating antibody, detection antibody, calibration standards and QCs

specific to individual analytes (IL-8, IL-1β, TNFα, and IFNγ). Also review **Note 1**.

10. If samples were stored frozen, pulse-spin in a microcentrifuge to remove fibrinogen fibers or any other aggregated material. If it takes longer than 5–10 min to load all samples onto the plate, prepare an intermediate plate and use a multichannel pipettor to transfer the diluted samples from the intermediate plate onto ELISA plate.
11. You can pre-read plate at 650 nm at about 15–20 min of incubation to decide whether to stop or continue incubation up to 30 min. Criteria for decision to stop and/or continue the incubation are acceptance of calibration standards and QC and steepness of the standard curve. (It is better to avoid high concentration standards reaching maximum OD.) OD units seen at 650 nm will be lower after addition of stop solution and analysis at 450 nm.

Acknowledgment

This project has been funded in whole or in part by federal funds from the National Cancer Institute, National Institutes of Health, under contract HHSN261200800001E. The content of this publication does not necessarily reflect the views or policies of the Department of Health and Human Services, nor does mention of trade names, commercial products, or organizations imply endorsement by the U.S. Government.

References

1. Suntharalingam G, Perry MR, Ward S, Brett SJ, Castello-Cortes A, Brunner MD, Panoskaltsis N (2006) Cytokine storm in a phase 1 trial of the anti-CD28 monoclonal antibody TGN1412. N Engl J Med 355(10):1018–1028. doi:10.1056/NEJMoa063842
2. Stebbings R, Findlay L, Edwards C, Eastwood D, Bird C, North D, Mistry Y, Dilger P, Liefooghe E, Cludts I, Fox B, Tarrant G, Robinson J, Meager T, Dolman C, Thorpe SJ, Bristow A, Wadhwa M, Thorpe R, Poole S (2007) "Cytokine storm" in the phase I trial of monoclonal antibody TGN1412: better understanding the causes to improve preclinical testing of immunotherapeutics. J Immunol 179 (5):3325–3331. doi:10.4049/jimmunol.179.5.3325
3. Dobrovolskaia MA, McNeil SE (2013) Understanding the correlation between in vitro and in vivo immunotoxicity tests for nanomedicines. J Control Release 172(2):456–466. doi:10.1016/j.jconrel.2013.05.025

Chapter 16

Analysis of Nanoparticle-Adjuvant Properties In Vivo

Barry W. Neun and Marina A. Dobrovolskaia

Abstract

Nanoparticles can be engineered for targeted antigen delivery to the immune cells and for stimulating the immune response to improve the antigen immunogenicity. This approach is commonly used to develop nanotechnology-based vaccines. In addition, some nanotechnology platforms may be initially designed for drug delivery, but in the course of subsequent characterization, their additional immunomodulatory functions may be discovered that can potentially benefit vaccine efficacy. In both of these scenarios, an in vivo proof of concept study to verify the utility of the nanocarrier for improving vaccine efficacy is needed. Here, we describe an experimental approach and considerations for designing an animal study to test adjuvant properties of engineered nanomaterials in vivo.

Key words Nanoparticles, Vaccines, Adjuvant, Antigen, Antibody

1 Introduction

Nanoparticles can provide a wide variety of advantages over conventional adjuvants. Some benefits include improved solubility of hydrophobic antigens, option to control antigen release, lower frequency and severity of side effects, protection of the antigen from degradation, and concurrent delivery of multiple antigens, as reviewed elsewhere [1, 2]. Different nanomaterials, including but not limited to polymeric, chitosan, magnetic, latex, gold, silica, and polystyrene nanoparticles, have been described as successful antigen carriers and vaccine adjuvants [3–10]. The most common target cells for nanoparticle-based vaccines are the antigen-presenting cells (APC) such as dendritic cells (DC). DC can internalize nanoparticles loaded with antigens via multiple routes [6, 11]. Macrophages have also shown to utilize multiple pathways for nanoparticle internalization [12]. Nanoparticle physicochemical properties, such as size, zeta potential, and surface functionalities, play a fundamental role in the particle interaction with the immune cells. Several studies demonstrate that smaller particles generate stronger immune responses than their larger counterparts [3,

Scott E. McNeil (ed.), *Characterization of Nanoparticles Intended for Drug Delivery*, Methods in Molecular Biology, Vol. 1682, DOI 10.1007/978-1-4939-7352-1_16,

6–8, 11, 13]. This property can be explained by the ability of smaller particles to travel to the draining lymph nodes (LN) where they target LN-resident DC, B-cells, and macrophages [13, 14]. Particles with sizes of 100 nm or larger tend to stay at the site of injection where they stimulate resident APC. A nanoparticle size of about 50 nm is suggested to be the most optimal for particle uptake by DC [15–17]. It has been further demonstrated that smaller particles are more potent in inducing IFN-α responses, while larger particles preferentially stimulate the production of TNF-α [18]. Moreover, smaller particles promote Th1 and CD8+ T-cell responses, while their larger counterparts preferentially stimulate Th2 responses [3, 6, 8]. Engineering the particle surface is another approach commonly used in vaccine design. For example, positively charged particles demonstrate greater uptake by DC [19–21], stronger induction of DC maturation [14, 22–25], and higher cytotoxic T lymphocyte responses [26]. A comprehensive review of nanotechnology-based vaccines is available elsewhere [27, 28].

Nanotechnology platforms are also used to formulate drugs and imaging agents. Sometimes, in the course of characterization of such particles, one may discover immunomodulatory functions, which may potentially benefit vaccine efficacy. In this case, the carrier may be re-purposed for the delivery of an antigen. In both situations, when the adjuvant property was intentionally created and when it was unexpectedly discovered, a proof of concept experiment is needed to verify the nanoparticle-adjuvant property. Here, we describe an experimental approach which can be used for such a proof of concept study along with considerations about the route of administration and dosing regimen (Fig. 1).

2 Materials

1. Six-week-old male and female mice of C57BL6 strain.
2. Phosphate buffered saline (PBS).
3. Model antigen, Ovalbumin-Endofit. Ovalbumin is supplied as a lyophilized powder. Reconstitute in sterile PBS or saline before injection to a final concentration of 1 mg/mL. Use freshly prepared material, discard any leftovers.
4. ELISA to detect antibody to the model antigen: Mouse anti-OVA ELISA kit. OVA specific IgM are assessed at Day 7. At Day 21, IgG levels are evaluated.
5. ELISA to detect antibody to target antigen.
6. Test nanomaterial and its formulation buffer (vehicle control).

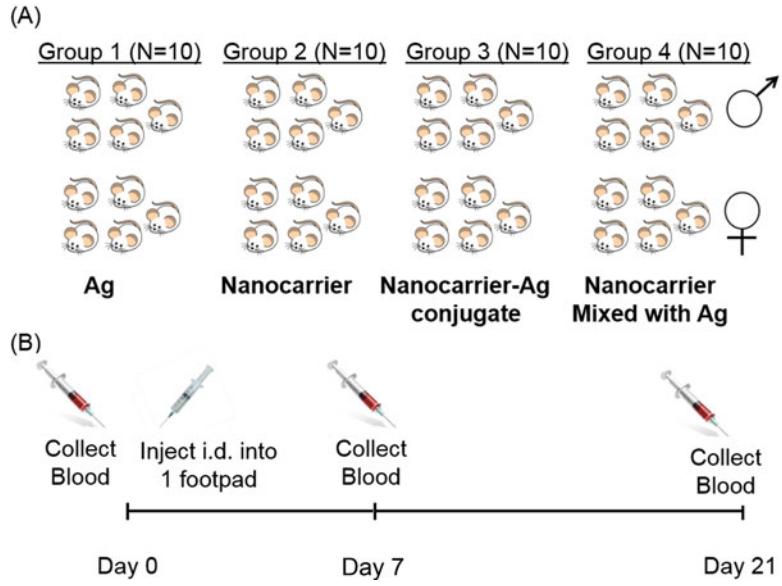

Fig. 1 Schematic of the study protocol. This figure shows the main experimental steps of the method used to assess adjuvanticity of nanoparticles. (**a**) Treatment groups and number of animals. (**b**) Study outline. *Ag* antigen, *i.d.* intradermal

3 Methods

3.1 Preparation of Control, Test Antigen, and Test Nanoparticle

1. Prepare *vehicle control*. Vehicle control is the buffer or media used to formulate test nanomaterials. Typical excipients employed in nanoformulations are trehalose, sucrose, and albumin. However, other reagents and materials are also used alone or in combination. Vehicle control should match the formulation buffer of the test nanomaterial by both composition and concentration. This control can be skipped if nanoparticles are stored in PBS.
2. Prepare *test antigen* of interest, according to the manufacturer's instructions or based on the information unique to this antigen.
3. Prepare *test nanoparticles* in an appropriate vehicle, which is specific to each formulation. Nanomaterials are tested at three doses, selected based on the existing information about the test nanomaterial from previous immunological studies.

3.2 In Vivo Assay

1. On Day 0, determine the weight of each animal and collect 100 μL of blood via the tail vein to establish antibody background for each animal (*see* **Notes 1**–**4**).
2. Inject test samples and controls intradermally into the dorsal foot skin as a 30 μL total volume bolus (*see* **Notes 2** and **5**).
3. On Day 7, determine the weight of each animal and collect 100 μl of blood via tail vein.

4. On Day 21, determine the weight of each animal, then euthanize the animals via CO_2 asphyxiation. Perform terminal blood collection via cardiac puncture (*see* **Note 6**).
5. Allow the blood to clot, centrifuge the tubes for 5 min at 2500 × *g*, and transfer serum to fresh tubes. The serum can be analyzed immediately or stored frozen at −20 °C.
6. On the day of analysis, thaw sera at room temperature and analyze by ELISA for the presence of antibodies. Day 7 samples are used for IgM analysis; Day 21 samples are used for IgG analysis.

3.3 Calculations and Results Interpretation

1. Percent Coefficient of Variation (%CV) should be calculated for each sample analyzed on ELISA plate according to the following formula:

$$\frac{\text{Standard Deviation}}{\text{Mean}} \times 100\%$$

2. %CV for each sample should be less than 25%.
3. Compare IgM and IgG levels in the treatment groups with that in the control group immunized with antigen alone. Perform statistical analysis using traditional methods.

4 Notes

1. Conduct thorough physicochemical, immunological, and toxicological characterization of a nanomaterial-based formulation before its testing in the animal study. Ensure that the test nanoparticle is endotoxin-free. Endotoxin is a potent immunostimulant and can also act as a vaccine adjuvant.
2. Check your Institutional ACUC requirements for animal husbandry and the needle size. We do not recommend using needles larger than 29 gauges for injections. Perform injections into only one hind foot per animal. Provide soft bedding and ensure the ability of animals to reach food and water. Monitor animals daily for pain/distress or complications at the injection site for the duration of the experiment or until there is no evidence of pain or discomfort. Consider humane euthanasia for mice exhibiting signs of severe pain or distress.
3. The following test groups are included in a typical study: (1) nanoparticle-formulated antigen [10 animals: 5 males and 5 females]; (2) antigen alone [10 animals: 5 males and 5 females]; (3) nanoparticle carrier only [10 animals: 5 males and 5 females]; (4) nanoparticle carrier mixed with model antigen (i.e., antigen is not bound or conjugated to the particle surface

or entrapped into the particle) [10 animals: 5 males and 5 females]. Group 1 can be skipped if the test antigen is not conjugated to the nanoparticle carrier. The inclusion of the standard adjuvant (e.g., alum or complete Freund adjuvant (CFA)) should be considered to estimate the potency of the nanoparticle carrier.

4. When designing a study, one may also consider a traditional immunization protocol, which includes prime and boost dosing regimen on Days 0 and 7, respectively. The traditional protocol will require s.c. vaccination on two flanks of each animal, and therefore will require larger material quantity. When traditional protocol is used, the blood is also collected on Day 14 (7 days after the last immunization). However, if the test nanoparticle hydrodynamic size is less than 100 nm, nanoparticles can deliver the antigen directly into the draining lymph nodes. Intradermal injection into the footpad described in this protocol is optimal and provides better efficacy for such carriers (Fig. 2). If, however, the test nanoparticle size is over 100 nm, nanoparticles will stimulate the immune cells at the site of injection, and a traditional immunization regimen including s.c. vaccination should be considered.

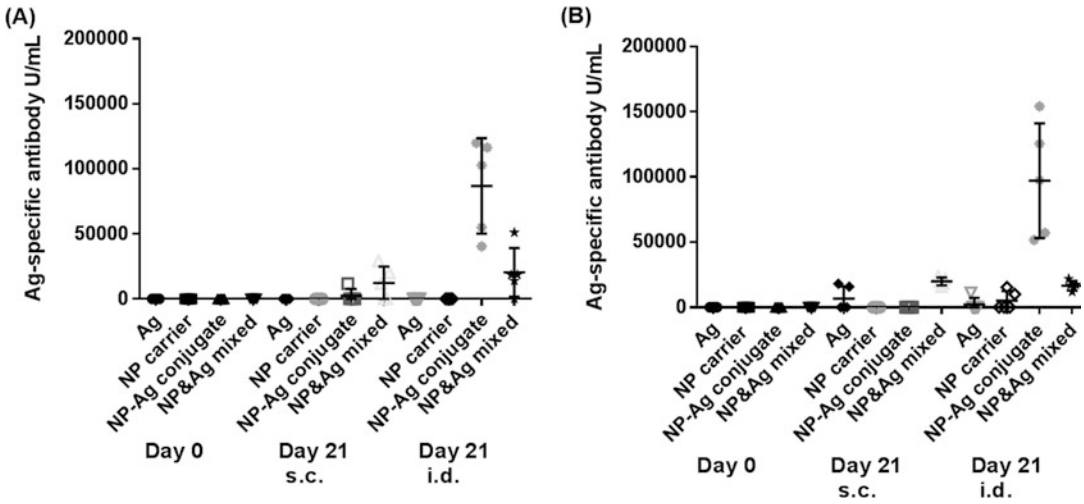

Fig. 2 An example of data generated using this protocol. The hydrodynamic size of the test nanoparticle was <100 nm. Therefore, it was expected that lymphatic drainage would be essential for the efficacy of the formulation. The intradermal (i.d.) injection was performed according to the protocol described in this chapter. In parallel, the same particle was also administered to animals via the traditional subcutaneous (s.c.) route and dosed using a traditional prime and boost regimen on Days 0 and 7, respectively. Individual animal responses are shown for (**a**) males and (**b**) females. The data demonstrate that immunization using a single footpad injection described in this protocol resulted in greater antibody levels than repeated administration of the same nanoparticles via s.c. route. The total dose of antigen delivered via the s.c. route was four times greater than that delivered via i.d. route. Antibody levels for all animals at Day 0 were the same. *Ag* antigen, *NP* nanoparticle

5. Nanoparticle dose per injection typically does not exceed 500 μg (i.e., per 30 μL volume). The dose of the model antigen (OVA) is 30 μg per injection (i.e., per 30 μL volume). The concentration of the target antigen may be different and should be determined experimentally. Using 30 μg per injection can be considered as a starting point.

Acknowledgment

This project has been funded in whole or in part by federal funds from the National Cancer Institute, National Institutes of Health, under contract HHSN261200800001E. The content of this publication does not necessarily reflect the views or policies of the Department of Health and Human Services, nor does mention of trade names, commercial products, or organizations imply endorsement by the U.S. Government.

References

1. Xiang SD, Scalzo-Inguanti K, Minigo G, Park A, Hardy CL, Plebanski M (2008) Promising particle-based vaccines in cancer therapy. Expert Rev Vaccines 7(7):1103–1119. doi:10.1586/14760584.7.7.1103
2. Xiang SD, Selomulya C, Ho J, Apostolopoulos V, Plebanski M (2010) Delivery of DNA vaccines: an overview on the use of biodegradable polymeric and magnetic nanoparticles. Wiley Interdiscip Rev Nanomed Nanobiotechnol 2 (3):205–218. doi:10.1002/wnan.88
3. Fifis T, Mottram P, Bogdanoska V, Hanley J, Plebanski M (2004) Short peptide sequences containing MHC class I and/or class II epitopes linked to nano-beads induce strong immunity and inhibition of growth of antigen-specific tumour challenge in mice. Vaccine 23(2):258–266
4. Pavelic K, Hadzija M, Bedrica L, Pavelic J, Dikic I, Katic M, Kralj M, Bosnar MH, Kapitanovic S, Poljak-Blazi M, Krizanac S, Stojkovic R, Jurin M, Subotic B, Colic M (2001) Natural zeolite clinoptilolite: new adjuvant in anticancer therapy. J Mol Med 78(12):708–720
5. Walsh MC, Banas JA, Mudzinski SP, Preissler MT, Graziano RF, Gosselin EJ (2003) A two-component modular approach for enhancing T-cell activation utilizing a unique anti-FcgamaRI-streptavidin construct and microspheres coated with biotinylated-antigen. Biomol Eng 20(1):21–33
6. Fifis T, Gamvrellis A, Crimeen-Irwin B, Pietersz GA, Li J, Mottram PL, McKenzie IF, Plebanski M (2004) Size-dependent immunogenicity: therapeutic and protective properties of nano-vaccines against tumors. J Immunol 173(5):3148–3154
7. Minigo G, Scholzen A, Tang CK, Hanley JC, Kalkanidis M, Pietersz GA, Apostolopoulos V, Plebanski M (2007) Poly-L-lysine-coated nanoparticles: a potent delivery system to enhance DNA vaccine efficacy. Vaccine 25(7): 1316–1327. doi:10.1016/j.vaccine.2006.09.086
8. Mottram P, Leong D, Crimeen-Irwin B, Gloster S, Xiang SD, Meanger J, Ghildyal R, Vardaxis N, Plebanski M (2007) Type 1 and type 2 immunity following vaccination is influenced by nanoparticle size: formulation of a model vaccine for respiratory syncytial virus. Mol Pharm 4(1):73–84. doi:10.1021/mp060096p
9. Tighe H, Corr M, Roman M, Raz E (1998) Gene vaccination: plasmid DNA is more than just a blueprint. Immunol Today 19(2):89–97. doi:10.1016/s0167-5699(97)01201-2
10. Weiss R, Scheiblhofer S, Freund J, Ferreira F, Livey I, Thalhamer J (2002) Gene gun bombardment with gold particles displays a particular Th2-promoting signal that over-rules the Th1-inducing effect of immunostimulatory CpG motifs in DNA vaccines. Vaccine 20 (25–26):3148–3154. doi:10.1016/s0264-410x(02)00250-5

11. O'Hagan DT, MacKichan ML, Singh M (2001) Recent developments in adjuvants for vaccines against infectious diseases. Biomol Eng 18(3):69–85
12. Franca A, Aggarwal P, Barsov EV, Kozlov SV, Dobrovolskaia MA, Gonzalez-Fernandez A (2011) Macrophage scavenger receptor A mediates the uptake of gold colloids by macrophages in vitro. Nanomedicine (Lond) 6 (7):1175–1188. doi:10.2217/nnm.11.41
13. Manolova V, Flace A, Bauer M, Schwarz K, Saudan P, Bachmann MF (2008) Nanoparticles target distinct dendritic cell populations according to their size. Eur J Immunol 38 (5):1404–1413
14. Reddy ST, van der Vlies AJ, Simeoni E, Angeli V, Randolph GJ, O'Neil CP, Lee LK, Swartz MA, Hubbell JA (2007) Exploiting lymphatic transport and complement activation in nanoparticle vaccines. Nat Biotechnol 25 (10):1159–1164
15. Aoyama Y, Kanamori T, Nakai T, Sasaki T, Horiuchi S, Sando S, Niidome T (2003) Artificial viruses and their application to gene delivery. Size-controlled gene coating with glycocluster nanoparticles. J Am Chem Soc 125(12):3455–3457
16. Nakai T, Kanamori T, Sando S, Aoyama Y (2003) Remarkably size-regulated cell invasion by artificial viruses. Saccharide-dependent self-aggregation of glycoviruses and its consequences in glycoviral gene delivery. J Am Chem Soc 125(28):8465–8475
17. Wang J, Fu L, Gu F, Ma Y (2011) Notch1 is involved in migration and invasion of human breast cancer cells. Oncol Rep 26 (5):1295–1303. doi:10.3892/or.2011.1399
18. Rettig L, Haen SP, Bittermann AG, von Boehmer L, Curioni A, Krämer SD, Knuth A, Pascolo S (2010) Particle size and activation threshold: a new dimension of danger signaling. Blood 115(22):4533–4541. doi:10.1182/blood-2009-11-247817
19. Foged C, Brodin B, Frokjaer S, Sundblad A (2005) Particle size and surface charge affect particle uptake by human dendritic cells in an in vitro model. Int J Pharm 298:315–322. doi:10.1016/j.ijpharm.2005.03.035
20. Villanueva A, Cañete M, Roca AG, Calero M, Veintemillas-Verdaguer S, Serna CJ, Morales Mdel P, Miranda R (2009) The influence of surface functionalization on the enhanced internalization of magnetic nanoparticles in cancer cells. Nanotechnology 20(11):115103. doi:10.1088/0957-4484/20/11/115103
21. Thiele L, Merkle HP, Walter E (2003) Phagocytosis and phagosomal fate of surface-modified microparticles in dendritic cells and macrophages. Pharm Res 20(2):221–228
22. Little SR, Lynn DM, Ge Q, Anderson DG, Puram SV, Chen J, Eisen HN, Langer R (2004) Poly-beta amino ester-containing microparticles enhance the activity of nonviral genetic vaccines. Proc Natl Acad Sci U S A 101 (26):9534–9539
23. Thiele L, Rothen-Rutishauser B, Jilek S, Wunderli-Allenspach H, Merkle HP, Walter E (2001) Evaluation of particle uptake in human blood monocyte-derived cells in vitro. Does phagocytosis activity of dendritic cells measure up with macrophages? J Control Release 76(1-2):59–71
24. Jilek S, Merkle HP, Walter E (2005) DNA-loaded biodegradable microparticles as vaccine delivery systems and their interaction with dendritic cells. Adv Drug Deliv Rev 57 (3):377–390. doi:10.1016/j.addr.2004.09.010
25. Jilek S, Ulrich M, Merkle HP, Walter E (2004) Composition and surface charge of DNA-loaded microparticles determine maturation and cytokine secretion in human dendritic cells. Pharm Res 21(7):1240–1247
26. Singh M, Briones M, Ott G, O'Hagan D (2000) Cationic microparticles: a potent delivery system for DNA vaccines. Proc Natl Acad Sci U S A 97(2):811–816
27. Fesenkova V (2013) Nanoparticles and dendritic cells. In: Dobrovolskaia MA, McNeil SE (eds) Handbook of immunological properties of engineered nanomaterials. World Scientific Publishing Ltd., Singapore
28. Xiang SD, Fuchsberger M, JKarlson TDL, Hardy CL, Selomulya C, Plebanski M (2013) Nanoparticles, immunomodulation and vaccine delivery. In: Dobrovolskaia MA, McNeil SE (eds) Handbook of immunological properties of engineered nanomaterials. World Scientific Publishing Ltd., Singapore

Chapter 17

In Vitro and In Vivo Methods for Analysis of Nanoparticle Potential to Induce Delayed-Type Hypersensitivity Reactions

Timothy M. Potter, Barry W. Neun, and Marina A. Dobrovolskaia

Abstract

Delayed-type hypersensitivity (DTH) reactions are among the common reasons for drug withdrawal from clinical use during the post-marketing stage. Several in vivo methods have been developed to test DTH responses in animal models. They include the local lymph node assay (LLNA) and local lymph node proliferation assay (LLNP). While LLNA is instrumental in testing topically administered formulations (e.g., creams), the LLNP was proven to be predictive of drug-mediated DTH in response to small molecule pharmaceuticals. Global efforts in reducing the use of research animals lead to the development of in vitro models to predict test-material-mediated DTH. Two such models include analysis of surface marker expression in human cell lines THP-1 and U-937. These tests are known as the human cell line activation test (hCLAT) and myeloid U937 skin sensitization test (MUSST or U-SENS), respectively. Here we describe experimental procedures for all these methods, discuss their in vitro–in vivo correlation, and suggest a strategy for applying these tests to analyze engineered nanomaterials and nanotechnology-formulated drug products.

Key words Nanoparticles, Hypersensitivity, Leukocyte proliferation, Sensitizer, Allergen, Irritant, LLNA, LLNP, hCLAT, MUSST

1 Introduction

According to several reports from industry, academia, and regulatory agencies, many drugs are withdrawn from clinical use due to their adverse effects on immune system function [1–4]. Although nanotechnology-formulated drugs represent a relatively new category of pharmaceutical products, their safety assessment is conducted using the regulatory framework established for other products, such as small molecules, therapeutic nucleic acids, and biologics; and, among other tests, it includes analysis of immunotoxicity. Acute immunotoxicity commonly observed in response to nanomaterials is related to hemolysis, complement activation, opsonization, phagocytosis, and cytokine secretion, and can be accurately tested using in vitro assays [1]. Identifying changes in

Scott E. McNeil (ed.), *Characterization of Nanoparticles Intended for Drug Delivery*, Methods in Molecular Biology, Vol. 1682, DOI 10.1007/978-1-4939-7352-1_17,

the immune system function is more complex and requires more sophisticated approaches. Since many low molecular weight compounds can induce allergic contact dermatitis, evaluation of skin sensitization is one of the key safety endpoints for materials used in cosmetics [2]. Delayed-type hypersensitivity (DTH) reactions to systemically administered drugs are also a safety concern which cannot be revealed by standard toxicity studies [3]. Estimation of a material's potential to allergic contact dermatitis in human was historically done using Guinea Pig Maximization Test, Buehler's Test, and more recently by Local Lymph Node Assay (LLNA). Local Lymph Node Proliferation Assay (LLNP) is a modification of LLNA which was shown to accurately predict DTH reaction to systemically administered pharmaceuticals [3]. The change in LLNP involves subcutaneous (s.c.) injection of a test material instead of topical application onto a skin surface like in LLNA. Both LLNA and LLNP require administration of a test material to mice once a day for three consecutive days, followed by 2 days of rest and then intravenouos (i.v.) administration of 3H-thymidine. Animals are sacrificed 5 h after thymidine injections and draining lymph nodes are analyzed by scintillation counting. 3H-thymidine incorporation into DNA of lymph node resident leukocytes is used as an indication of T-cell activation involved in allergic sensitization. Several years ago, the European Cosmetics Association (COLIPA), through a number of inter-laboratory studies, validated two in vitro assays that are proposed to decrease and possibly eliminate animal use in analysis of DTH reactions. These tests are the human cell line activation test (hCLAT) and myeloid U937 skin sensitization test (MUSST or U-SENS) [2, 4–8]. For the purpose of this chapter, we will refer to the MUSST/U-SENS assay as MUSST. They were originally developed by several researchers in Japan [2, 9–13], and subsequently adopted by several European labs [14–17]. The principle of these methods is based on the fact that allergic sensitization requires formation of T-cell memory and the essential step in the process is the activation of antigen-presenting cells such as dendritic cells. Due to the complexity of isolation and high inter-donor variability between primary human dendritic cell cultures, the researchers have selected monocyte-macrophage cell lines THP-I and U-937. They found that these cells possess one of the properties of activated primary dendritic cells, i.e., they express CD86 and/or CD54 in response to allergens. Despite original publications describing the expression of both CD54 and CD86 by THP-I cells, both our laboratory and BD Biosciences found that THP-1 lack CD86 (NCL unpublished data and reference 18). The hCLAT and MUSST tests described in this chapter are adaptations of previously published methods and evaluate the expression of surface markers CD54 and CD86 in THP-1 and U937 cell lines, respectively. Both in vitro and in vivo DTH tests are schematically depicted in Fig. 1. These assays apply to engineered nanomaterials

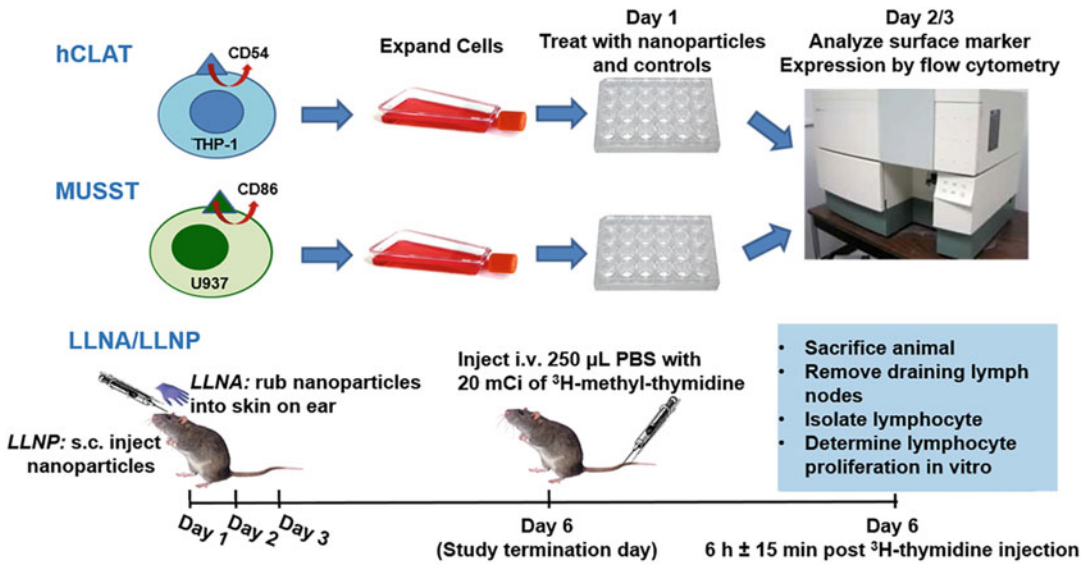

Fig. 1 Schematic of LLNA, LLNP, MUSST, and hCLAT methods. This figure depicts the major experimental steps of in vitro MUSST and hCLAT, and in vivo LLNA and LLNP methods

and nanotechnology-formulated drug products. However, due to the complexity of these novel materials, the in vitro–in vivo correlation between LLNA, LLNP, and hCLAT, MUSST assays may be observed for some but not all nanoparticles (Fig. 2). In vitro methods have a greater rate of positive response than in vivo tests; moreover, among in vitro assays MUSST is more sensitive in identifying positive responses than hCLAT (Fig. 3). Therefore, the in vitro assays can be used for rapid screening of multiple nanoformulations. However, positive responders established in these in vitro tests require verification using a relevant in vivo method.

2 Materials

2.1 hCLAT and MUSST

1. Phosphate buffered saline (PBS).
2. Heat-inactivated fetal bovine serum (FBS). Thaw a bottle of FBS at room temperature or overnight at 2–8 °C and allow to equilibrate to room temperature. Incubate for 30 min at 56 °C in a water bath mixing every 5 min to heat-inactivate it. Single-use aliquots may be stored at 2–8 °C for up to 1 month or at a nominal temperature of −20 °C for a longer duration.
3. 10 mg/mL stock glycerol. Prepare 10 mg/mL stock by adding 80 µL of glycerol into 9.92 mL sterile water and filter through 0.2-µm filter. Make sure to use pyrogen-free water.
4. Reagent to distinguish between life and dead cells, such as trypan blue solution or arcindine orange/propidium iodide (AO/PI) staining solution.

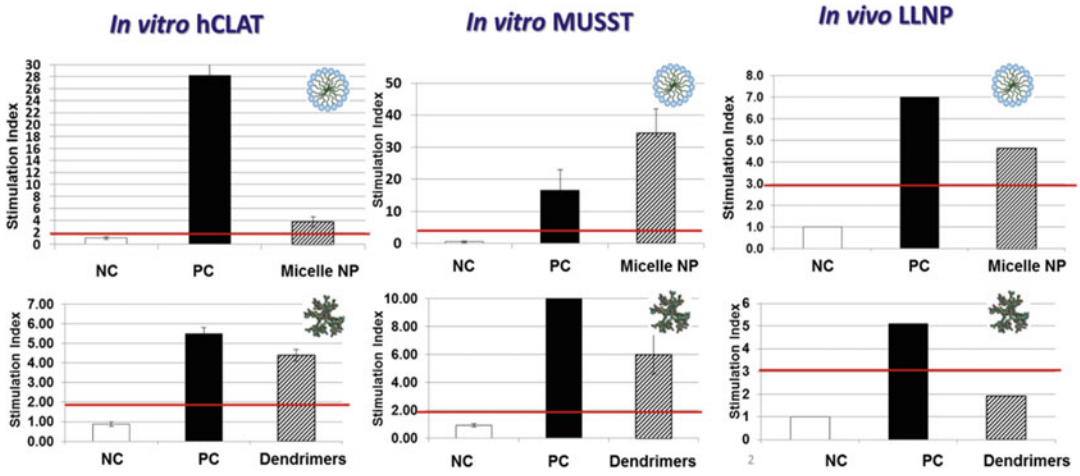

Fig. 2 Correlation between hCLAT, MUSST, and LLNP assays is observed for some but not all nanomaterials. Micelle nanoparticle (Cremophor EL) and dendrimers (generation 6 carboxy-terminated PAMAM dendrimers) were tested in vitro in hCLAT and MUSST, and in vivo in LLNP assay. The concentration of dendrimers tested in vitro is 100 μg/mL. That of Cremophor is 8.5 mg/mL and is equivalent to the cremophor concentration present in Taxol when the API (paclitaxel) concentration is 25 μM. Taxol is the cremophor-based formulation of paclitaxel used in the clinic. It is associated with both acute and delayed-type hypersensitivity. Animals were s.c. injected with 100 μL of nanoparticle stock solution. The concentration of the stock was 8.5 mg/mL and 0.1 mg/mL for cremophor and dendrimers, respectively. NC: negative control (1 mg/mL glycerol in hCLAT and MUSST and PBS in LLNP), PC: positive control (250 μg/mL Nickel sulfate, 250 μM TNBS, and 50 mg/kg Streptozotocin in hCLAT, MUSST, and LLNP, respectively). Shown are mean ± SD ($N = 3$). The red line depicts the minimum positive stimulation index of 3

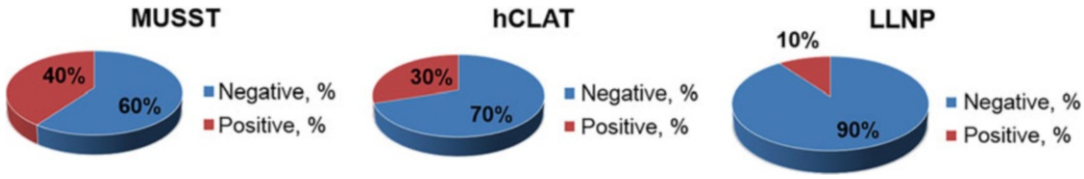

Fig. 3 Comparison of positive response rates between in vitro and in vivo tests. Twenty formulations including colloidal gold and colloidal silver nanoparticles with various sizes and surface coatings, generations 3, 4, 5, and 6 PAMAM dendrimers with different surface functionalities, iron oxide nanoparticles, liposomes, and emulsions were analyzed in vitro using hCLAT and MUSST and in vivo using LLNP assay. Particles producing a stimulation index ≥3 were considered positive, while those with a stimulation index of less than 3 were considered negative. Percentage of positive and negative responders in each test is presented in the charts. Not all particles that were positive in vitro were positive in vivo, indicating that results correlated between in vitro and in vivo conditions for some but not all nanoparticles (Fig. 2, for example). The data show that in vitro assays have a greater rate of positive responses

5. Albumin from bovine serum (BSA).
6. Bovine Serum Albumin (BSA) blocking buffer. BSA reagent is provided as lyophilized powder. Dissolve 50 mg of the reagent and in 50 mL ice-cold PBS. Mix well and place on ice. Prepare fresh before each use. Discard any leftover after the experiment is complete.

7. Globulins Cohn fraction II bocking buffer. Globulins Cohn fraction II, III human is provided as lyophilized powder. Dissolve 5 mg of the reagent in 50 mL of ice cold PBS. Mix well and place on ice. Prepare fresh before each use. Discard any leftover after the experiment is complete.
8. 7-Amino-Actinomycin D (7-AAD).
9. Cellometer (NexCelome) or Hemacytometer to perform cell count.
10. Flow Cytometer (e.g., FACSCalibur) (*see* **Notes 1** and **2**).

2.2 hCLAT Only

1. Monocytic leukemia cell line THP-1 (ATCC).
2. R-phycoerythrin (PE) mouse IgG1 isotype control (BD Pharmingen, cat# 34076) (*see* **Note 2**).
3. PE mouse anti-human CD54 (BD Pharmingen, cat# 555511).
4. 10 mg/mL nickel(II) sulfate hexahydrate stock solution. Weight 100 mg of nickel(II) sulfate and dissolve in 10 mL of sterile water to obtain a 10 mg/mL stock solution. Filter this stock through 0.2-μm filter.
5. Complete RPMI solution: 20% heat-inactivated FBS, 4 mM L-glutamine, 2-mercaptoethanol to a final concentration of 0.05 mM, and 100 U/mL penicillin. Store at 2–8 °C protected from light for no longer than 1 month. Before use warm the medium in a water bath to 37 °C.

2.3 MUSST Only

1. Monocytic leukemia cell line U937 (ATCC).
2. Fluorescein isothiocyanate (FITC) mouse IgG1 isotype control (BD Pharmingen, cat# 555748).
3. FITC mouse anti-human CD86 (BD Pharmingen, cat# 555657).
4. 170 mM 2,4,6-Trinitrobenzenesulfonic acid solution (TNBS) stock.
5. Complete RPMI medium: 20% FBS (heat-inactivated), 4 mM L-glutamine, 100 U/mL penicillin. Store at 2–8 °C protected from light for no longer than 1 month. Before use warm the medium in a water bath to 37 °C.

2.4 LLNP and LLNA

1. 7–12 weeks old male and female mice of the following strains: CBA/Ca, CBA/j, or Balb/c.
2. Streptozotocin.
3. PBS.
4. 1 mCi ^{3}H-thymidine.
5. 5% trichloroacetic acid (TCA) solution. Prepare 5% solution by dissolving 5 g of TCA in 100 mL of distilled water.

6. Tuberculin 1 mL syringe.
7. 12 × 75 mm tube with cell strainer cap.
8. Scintillation liquid.
9. Scintillation counter.
10. 20 mL scintillation vials.

3 Methods

3.1 Preparation of Controls and Cell Lines

1. For *hCLAT* and *MUSST*, prepare glycerol as negative control. Use 100 μL of 10 mg/mL glycerol stock per 900 μL of cell suspension to achieve a final concentration of 1 mg/mL.
2. For *hCLAT*, prepare THP-I cell line. Cultures can be maintained by the addition of fresh medium or replacement of culture medium. Alternatively, cultures can be established by centrifugation with subsequent resuspension at 2–4 × 10^5 viable cells/mL. Subculture is needed when cell concentration reaches 8 × 10^5 cells/mL. It is important not to allow cell concentration to exceed 1 × 10^6 cells/mL. Maintain cell density between 1 × 10^5 and 1 × 10^6 viable cells/mL. Do not use cells exceeding 22 passages.
3. For *hCLAT*, prepare nickel(II) sulfate hexahydrate as a positive control. Dilute the 10 mg/mL stock solution by adding 1 mL of the stock to 3 mL of media to obtain a 2.5 mg/mL intermediate solution. Add 100 μL of the 2.5 mg/mL intermediate solution to 900 μL of cell suspension to obtain a final concentration of 250 μg/mL.
4. For *MUSST*, prepare U937 cell line. Cultures can be maintained by the addition of fresh medium or replacement of culture medium. Alternatively, cultures can be established by centrifugation with subsequent resuspension at 1–2 × 10^5 viable cells/mL. Subculture is needed when cell concentration reaches 8 × 10^5 cells /mL. It is important not to allow cell concentration to exceed 1 × 10^6 cells/mL. Maintain cell density between 1 × 10^5 and 2 × 10^6 viable cells/mL. Do not use cells exceeding 22 passages.
5. For *MUSST*, prepare TNBS solution as a positive control. Dilute the 170 mM TNBS stock solution by adding 18 μL of the stock to 982 μL of the media to obtain a 3 mM working stock. Add 100 μL of the 3 mM working stock solution to 900 μL of the cell suspension to obtain a final concentration of 300 μM.
6. For *LLNP*, prepare ^{3}H-thymidine dosing solution. Add 11.5 mL of PBS to a dosing vial. Remove stock of the radiolabeled material from storage and add 1 mL of this stock to

the dosing vial containing PBS. Mix well to prepare a dosing solution. To confirm the concentration of this dosing solution, remove two 8 μL aliquots of the solution and mix with 20 mL of water, then use 1 mL aliquots of these diluted dosing solutions and mix each with 10 mL of the scintillation liquid. These aliquots are used to confirm that each milliliter of the dosing solution contains ~80 μCi of ^{3}H-thymidine. Dispose of all radioactive material and perform post work contamination survey according to the protocol approved by your institutional committee.

7. Prepare streptozotocin by dissolving lyophilized powder in sterile PBS or saline at concentration 1.5–2 mg/mL. The final dose of streptozotocin is 50 mg/kg and the injection volume is 50–100 μL per animal.

3.2 Preparation of Study Samples

1. The *hCLAT* and *MUSST* require 0.4 mL of nanoparticles dissolved/resuspended in complete culture medium to a concentration of 10× the highest tested concentration. The concentration is selected based on the plasma concentration of the nanoparticle at the intended therapeutic dose. For the purpose of this protocol, this concentration is called "theoretical plasma concentration." Considerations for estimating theoretical plasma concentration were reviewed elsewhere [1] and are summarized in Box 1. The assay will evaluate four concentrations: 10× (or when feasible 100×, 30×, or 5×) of theoretical plasma concentration, theoretical plasma concentration,

Box 1. Example Calculation of Nanoparticle Concentration for In Vitro Test

In this example, assume the mouse dose is known to be 123 mg/kg.

$$\text{human dose} = \frac{mouse\ dose}{12.3} = \frac{123\frac{mg}{kg}}{12.3} = 10\ \text{mg/kg}$$

Blood volume constitutes approximately 8% of body weight (e.g. a 70 kg human has approximately 5.6 L (8% of 70) of blood), allowing for a very rough estimation of the maximum blood concentration.

$$\text{in vitro concentration}_{human\ matrix} = \frac{human\ dose}{human\ blood\ volume} = \frac{70\ kg\ x\ 10\frac{mg}{kg}}{5.6\ L}$$
$$= \frac{700\ mg}{5.6\ L} = 0.125\ \text{mg/mL}$$

Box 1 Estimation of nanomaterial concentration for in vitro assay. The box shows an example of calculating nanoparticle concentrations for the in vitro assays. Reproduced with permission from ref. 1

and two 5-fold serial dilutions of the theoretical plasma concentration. When the intended therapeutic concentration is unknown, the highest final concentration is 1 mg/mL or the highest reasonably achievable concentration. For example, if the final theoretical plasma concentration to be tested is 0.1 mg/mL, then a stock of 10 mg/mL will be prepared and diluted 10-fold (1 mg/mL), followed by two 5-fold serial dilutions (0.2 and 0.04 mg/mL, respectively). When 0.1 mL of each sample is added to the plate and mixed with 0.9 mL of cell suspension, the final nanoparticle concentrations tested in the assay are 1.0, 0.1, 0.02, and 0.004 mg/mL.

2. For *LLNP* and *LLNA*, prepare test nanoparticles in an appropriate vehicle which may be peculiar to each formulation. Nanomaterials are tested at three doses, selected based on the existing information about the test nanomaterial from previous toxicological studies: (1) at the maximum tolerated dose (MTD) (e.g., a dose which demonstrated a moderate decrease in leukocyte count and was not accompanied by life-threatening abnormalities), (2) half of MTD, and (3) quarter of MTD.

3.3 hCLAT Experimental Procedure

1. Adjust THP-1 cell number to 1×10^6 viable cells/mL and aliquot 900 μL of the cell suspension to each well on the 24-well plate.
2. Add 100 μL of test nanoparticles or controls to appropriate wells. Prepare duplicate wells for each sample. Incubate for 24 h at 37 °C and 5% CO_2.
3. After 24 h of incubation with test materials and controls, harvest the cells and determine cell viability by trypan blue or another relevant method.
4. Harvest cells into round bottom 12×75 mm^2 tubes and centrifuge at $400 \times g$ for 5 min.
5. Aspirate supernatant and wash cells with 2 mL of ice-cold PBS.
6. Resuspend cells in 400 μL of ice-cold Cohn fraction blocking buffer and incubate on ice for 10 min.
7. Wash cells two times with 1 mL of BSA blocking buffer using centrifugation at $400 \times g$ at 4 °C for 5 min to pellet the cells. Discard wash supernatant.
8. After final wash, resuspend cells in 100 μL of ice-cold BSA blocking buffer.
9. Add 20 μL of monoclonal antibody against CD54 and isotype control antibody to appropriate tubes (final concentration of antibody is 5 μg/mL).
10. Incubate at 4 °C for 30 min.

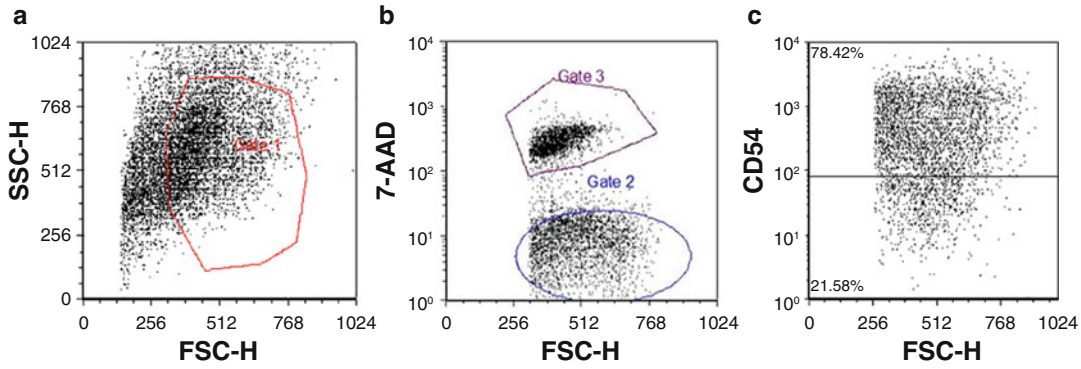

Fig. 4 An example of flow cytometry analysis of CD54 expression in THP-1 cells. (**a**) Forward scatter (FSC) vs. side scatter (SSC) dot plot gated on cells of interest. (**b**) FSC vs. FL3 cells stained with 7AAD dot plot showing 7AAD negative cells (gate 2). Gate 3 shows dead cells. (**c**) FSC vs. FL2 profile of cells stained with mouse anti-human CD54-PE dot plot gated to show only cells from gate 2

11. Wash cells twice with 1 mL of BSA blocking buffer and centrifugation at 400 × *g* for 5 min to pellet the cells and discard the wash supernatant.
12. After final wash resuspend the cells in 400 μL of BSA blocking buffer.
13. Add 5 μL of 7AAD to each sample.
14. Analyze the samples using flow cytometer (*see* **Notes 1** and **2**; Fig. 4).

3.4 MUSST Experimental Procedure

1. Adjust U937 cell count to 1.25×10^5 cells/mL and aliquot 900 μL of the cell suspension to each well on the 24-well plate.
2. Add 100 μL of test nanoparticles or controls to appropriate wells. Prepare duplicate wells for each sample.
3. After 48 h of incubation with test materials and controls, harvest the cells and determine cell viability using trypan blue or another similar approach.
4. Harvest cells into polystyrene round bottom 12 × 75 mm^2 tubes and centrifuge at 400 × *g* for 5 min.
5. Aspirate supernatant and wash cells with 2 mL of ice-cold PBS.
6. Resuspend cells in 400 μL of ice-cold Cohn fraction blocking buffer and incubate on ice for 10 min.
7. Wash cells two times with 1 mL of BSA blocking buffer using centrifugation at 400 × *g* at 4 °C for 5 min to pellet the cells and discard wash supernatant.
8. After final wash, resuspend cells in 100 μL of ice-cold BSA blocking buffer.
9. Add 20 μL of monoclonal antibody against CD86 and isotype control antibody to appropriate tubes (final concentration of the antibody is 5 μg/mL).

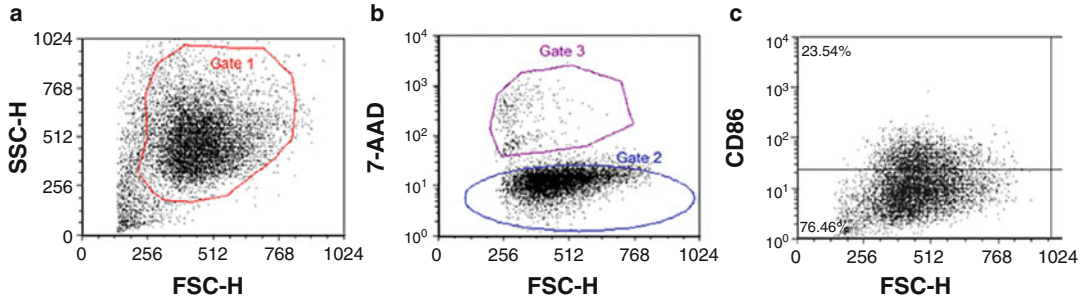

Fig. 5 An example of flow cytometry analysis of CD86 expression in U937 cells. (**a**) Forward scatter (FSC) vs. side scatter (SSC) dot plot gated on cells of interest. (**b**) FSC vs. FL3 cells stained with 7AAD dot plot showing 7AAD negative cells (gate 2). Gate 3 shows dead cells. (**c**) FSC vs. FL1 profile of cells stained with mouse anti-human CD86 FITC dot plot gated to show only cells from gate 2

10. Incubate at 4 °C for 30 min.
11. Wash cells twice with 1 mL of BSA blocking buffer and centrifuge at 400 × *g* for 5 min to pellet the cells. Discard the wash supernatant.
12. After final wash, resuspend the cells in 400 μL of BSA blocking buffer.
13. Add 5 μL of 7AAD to each sample.
14. Analyze the samples using flow cytometer (*see* **Notes 1** and **2**; Fig. 5).

3.5 LLNA and LLNP Experimental Procedure

1. On Day 1, weight each mouse before applying treatment (*see* **Note 3**). If using LLNA, apply 25 μL of the test solution (either negative control [PBS], positive control [10% neutral buffered formalin], or nanoparticles) topically to the dorsal surface of both ears (*see* **Note 4**). Just before application of the treatment, wipe the dorsal surface of each ear with acetone to aid in absorption. If using LLNP, inject 100 μL of the test solution (either negative control [PBS], positive control [streptozotocin], or nanoparticles) s.c. in the midline of the head (*see* **Notes 5** and **6**).
2. Repeat Day 1 treatment on two subsequent days (Days 2 and 3). Observe each animal for signs of local irritation.
3. On Days 4, 5, and 6 of the study, observe each animal for signs of local irritation and record animal weights.
4. On Day 6 (72 ± 3 h) after the first treatment, inject each animal intravenously (i.v.) with 250 μL of sterile PBS containing 20 μCi of ^{3}H-thymidine via the lateral tail vein. Use a 1 mL syringe with a needle size no larger than 25 guage (*see* **Note 7**).
5. Sacrifice the animals 5 h ±45 min after injection of the thymidine using carbon dioxide asphyxiation or another technique approved by your institute's animal care committee. Isolate the

draining lymph nodes of each ear and collect them into vials containing sterile PBS (*see* **Note 8**).

6. Place lymph nodes into the top compartment of the cell strainer cap. Using the plunger from the 1 mL syringe, press the lymph node into the 5 mL round bottom tube. Prepare one tube per individual animal.
7. Rinse the cap with 5 mL of PBS to move all single cells into the tube. Discard the strainer cap and remaining tissue debris.
8. Centrifuge for 10 min at 190 × *g* and 4 °C. Remove supernatant and leave 1 mL of solution above the pellet.
9. Repeat **step 8** two more times.
10. After the final wash, remove all PBS and gently agitate to break up the pellet.
11. Add 3 mL of 5% TCA and incubate at 4 °C overnight.
12. Centrifuge for 10 min at 190 × *g* and 4 °C. Remove supernatant and resuspend the pellet in 1 mL of 5% TCA.
13. Transfer each sample to a scintillation vial and add 10–15 mL of scintillation fluid.
14. Shake well. Dark adapt the samples for 30 min.
15. Analyze the samples using a scintillation counter.

3.6 Calculations and Data Interpretation—hCLAT and MUSST

1. A percent coefficient of variation should be calculated for each control or test according to the following formula:

$$\%\mathrm{CV} = \frac{\text{Standard deviation}}{\text{Mean}} \times 100\%$$

2. Measure the stimulation index (SI) using the following formula:

$$\mathrm{SI} = \frac{\text{Mean \% positive cells}_{\text{test sample}}}{\text{Mean \% positive cells}_{\text{negative control}}}$$

   An SI $\geq$3 is considered a positive response.
3. %CV for each control and test sample should be less than 30%.
4. If a positive control or negative control fails to meet acceptance criterion described above, the assay should be repeated.
5. Within the acceptable assay, if two of three replicates of unknown sample fail to meet acceptance criterion described in **step 3** above, this unknown sample should be re-analyzed.

3.7 Calculations and Data Interpretation—LLNA and LLNP

1. The proliferative response (PR) in each sample is determined by the number of radioactive disintegrations per minute per lymph node, using the following formula:

$$\mathrm{PR} = \frac{\left(\mathrm{DPM}_{\text{test sample}} - \mathrm{DPM}_{\text{background}}\right)}{\mathrm{LN}}$$

where DPM is the result reported by the scintillation counter and LN is the number of the lymph nodes in the sample. The background DPM ($\mathrm{DPM}_{\text{background}}$) is determined by analyzing 10 mL of the scintillation liquid without any sample.

2. Measure SI according to the formula:

$$\mathrm{SI} = \frac{\mathrm{PR}_{\text{test sample}}}{\mathrm{PR}_{\text{negative control}}}$$

An SI of ≥ 3 is considered a positive response.

4 Notes

1. To set up the instrument for data acquisition and analysis, please refer to the operation manual of your flow cytometer. The protocol described in this chapter was developed using a FACSCalibur. With this instrument, we first optimize the instrument settings to bring the cells in focus using forward and side scatter. Next, we create a gate around the cell population and analyze cells from this gate on the fluorescent channel 3 (FL-3) to distinguish between dead and live cells. We create a gate around the live cell population in FL-3. Cells negative for 7-AAD staining detected in this channel are the live cells, while cells positive in 7-AAD staining are dead cells and they are excluded from the analysis. We acquire CD54+ cells and CD86+ cells from the 7-AAD negative population using fluorescent channels 2 and 1 (FL-2 and FL-1), respectively. The FL-1 and FL-2 on the FACSCalibur instrument detect the FITC and PE labels of the antibodies, respectively. Each test sample is also stained using the isotype control antibody. The percent positive cells in each sample stained with CD54 or CD86 antibody is determined against respective isotype controls of the same sample. If antibodies with different fluorophores are used, one would need to select the appropriate isotype control and adjust both the antibody concentration and the acquisition channel.
2. NCL does not endorse suppliers. However, we found that a new user benefits from knowing the instruments and catalog information of reagents used in our assays. Therefore, ideas of

reagents used at the NCL are included in this chapter in parentheses. When using reagents and instruments from other sources, the assay performance may change. We recommend performing assay qualification to verify the assay functionality and validity before proceeding with test samples.

3. This procedure requires an animal study protocol and radiation program approved by relevant institutional committees at your organization.
4. Consider using a collar to prevent animals from ingesting the treatments during the grooming process.
5. The point of injection is very important. It should be in the midline, between the eyes on the top of the head. Point the needle toward the back of the animal so that the end of the needle is just forward of the point between the ears. Injection should be performed slowly so that the bulk of the liquid is placed either between or just forward of the ears. Injecting too far to the rear will result in reduced response in the draining lymph nodes.
6. Typical injection volume is 100 μL, but it may be lower and vary between 50 and 100 μL. The volume should not exceed 5 mL/kg, and the needle size should be 25 G or smaller.
7. Placing animals on a warm plate may be needed to dilate veins for easier i.v. injections.
8. The lymph nodes should be processed as soon as possible within 2 h after isolation from the animals.

Acknowledgment

This project has been funded in whole or in part by federal funds from the National Cancer Institute, National Institutes of Health, under contract HHSN261200800001E. The content of this publication does not necessarily reflect the views or policies of the Department of Health and Human Services, nor does mention of trade names, commercial products, or organizations imply endorsement by the U.S. Government.

References

1. Dobrovolskaia MA, McNeil SE (2013) Understanding the correlation between in vitro and in vivo immunotoxicity tests for nanomedicines. J Control Release 172(2):456–466. doi:10.1016/j.jconrel.2013.05.025
2. Sakaguchi H, Ryan C, Ovigne JM, Schroeder KR, Ashikaga T (2010) Predicting skin sensitization potential and inter-laboratory reproducibility of a human cell line activation test (h-CLAT) in the European Cosmetics Association (COLIPA) ring trials. Toxicol In Vitro 24(6):1810–1820. doi:10.1016/j.tiv.2010.05.012
3. Weaver JL, Chapdelaine JM, Descotes J, Germolec D, Holsapple M, House R, Lebrec H, Meade J, Pieters R, Hastings KL, Dean JH

(2005) Evaluation of a lymph node proliferation assay for its ability to detect pharmaceuticals with potential to cause immune-mediated drug reactions. J Immunotoxicol 2(1):11–20. doi:10.1080/15476910590930100

4. Bauch C, Kolle SN, Fabian E, Pachel C, Ramirez T, Wiench B, Wruck CJ, van Ravenzwaay B, Landsiedel R (2011) Intralaboratory validation of four in vitro assays for the prediction of the skin sensitizing potential of chemicals. Toxicol In Vitro 25(6):1162–1168. doi:10.1016/j.tiv.2011.05.030
5. Nukada Y, Ashikaga T, Miyazawa M, Hirota M, Sakaguchi H, Sasa H, Nishiyama N (2012) Prediction of skin sensitization potency of chemicals by human cell line activation test (h-CLAT) and an attempt at classifying skin sensitization potency. Toxicol In Vitro 26 (7):1150–1160. doi:10.1016/j.tiv.2012.07.001
6. Natsch A, Ryan CA, Foertsch L, Emter R, Jaworska J, Gerberick F, Kern P (2013) A dataset on 145 chemicals tested in alternative assays for skin sensitization undergoing prevalidation. J Appl Toxicol 33(11):1337–1352. doi:10.1002/jat.2868
7. Piroird C, Ovigne JM, Rousset F, Martinozzi-Teissier S, Gomes C, Cotovio J, Alepee N (2015) The myeloid U937 skin sensitization test (U-SENS) addresses the activation of dendritic cell event in the adverse outcome pathway for skin sensitization. Toxicol In Vitro 29 (5):901–916. doi:10.1016/j.tiv.2015.03.009
8. Urbisch D, Mehling A, Guth K, Ramirez T, Honarvar N, Kolle S, Landsiedel R, Jaworska J, Kern PS, Gerberick F, Natsch A, Emter R, Ashikaga T, Miyazawa M, Sakaguchi H (2015) Assessing skin sensitization hazard in mice and men using non-animal test methods. Regul Toxicol Pharmacol 71(2):337–351. doi:10.1016/j.yrtph.2014.12.008
9. Sakaguchi H, Ashikaga T, Miyazawa M, Yoshida Y, Ito Y, Yoneyama K, Hirota M, Itagaki H, Toyoda H, Suzuki H (2006) Development of an in vitro skin sensitization test using human cell lines; human cell line activation test (h-CLAT). II An inter-laboratory study of the h-CLAT. Toxicol In Vitro 20(5):774–784. doi:10.1016/j.tiv.2005.10.014
10. Ashikaga T, Yoshida Y, Hirota M, Yoneyama K, Itagaki H, Sakaguchi H, Miyazawa M, Ito Y, Suzuki H, Toyoda H (2006) Development of an in vitro skin sensitization test using human cell lines: the human cell line activation test (h-CLAT). I Optimization of the h-CLAT protocol. Toxicol In Vitro 20(5):767–773. doi:10.1016/j.tiv.2005.10.012
11. Sakaguchi H, Ashikaga T, Miyazawa M, Kosaka N, Ito Y, Yoneyama K, Sono S, Itagaki H, Toyoda H, Suzuki H (2009) The relationship between CD86/CD54 expression and THP-1 cell viability in an in vitro skin sensitization test–human cell line activation test (h-CLAT). Cell Biol Toxicol 25(2):109–126. doi:10.1007/s10565-008-9059-9
12. Miyazawa M, Ito Y, Yoshida Y, Sakaguchi H, Suzuki H (2007) Phenotypic alterations and cytokine production in THP-1 cells in response to allergens. Toxicol In Vitro 21(3):428–437. doi:10.1016/j.tiv.2006.10.005
13. Yoshida Y, Sakaguchi H, Ito Y, Okuda M, Suzuki H (2003) Evaluation of the skin sensitization potential of chemicals using expression of co-stimulatory molecules, CD54 and CD86, on the naive THP-1 cell line. Toxicol In Vitro 17(2):221–228. doi:S0887233303000067 [pii]
14. Ball N, Gordon N, Casal E, Parish J (2011) Evaluation of auto bi-level algorithm to treat pressure intolerance in obstructive sleep apnea. Sleep Breath 15(3):301–309. doi:10.1007/s11325-010-0381-0
15. Aeby P, Ashikaga T, Bessou-Touya S, Schepky A, Gerberick F, Kern P, Marrec-Fairley M, Maxwell G, Ovigne JM, Sakaguchi H, Reisinger K, Tailhardat M, Martinozzi-Teissier S, Winkler P (2010) Identifying and characterizing chemical skin sensitizers without animal testing: Colipa's research and method development program. Toxicol In Vitro 24 (6):1465–1473. doi:10.1016/j.tiv.2010.07.005
16. Maxwell G, Aeby P, Ashikaga T, Bessou-Touya S, Diembeck W, Gerberick F, Kern P, Marrec-Fairley M, Ovigne JM, Sakaguchi H, Schroeder K, Tailhardat M, Teissier S, Winkler P (2011) Skin sensitisation: the Colipa strategy for developing and evaluating non-animal test methods for risk assessment. ALTEX 28(1):50–55
17. Luebke R (2012) Immunotoxicant screening and prioritization in the twenty-first century. Toxicol Pathol 40(2):294–299. doi:10.1177/0192623311427572
18. Mittar T, Parambar R, McIntyre C (2011) Flow cytometry and high-content imaging to identify markers of monocyte-macrophage differentiation. Application Note URL: https://www.bdbiosciences.com/documents/BD_Multicolor_MonocyteMacrophageDiff_AppNote.pdf. Last accessed 8/10/2017

Chapter 18

Autophagy Monitoring Assay II: Imaging Autophagy Induction in LLC-PK1 Cells Using GFP-LC3 Protein Fusion Construct

Pavan P. Adiseshaiah, Sarah L. Skoczen, Jamie C. Rodriguez, Timothy M. Potter, Krishna Kota, and Stephan T. Stern

Abstract

Autophagy is a catabolic process involved in the degradation and recycling of long-lived proteins and damaged organelles for maintenance of cellular homeostasis, and it has also been proposed as a type II cell death pathway. The cytoplasmic components targeted for catabolism are enclosed in a double-membrane autophagosome that merges with lysosomes, to form autophagosomes, and are finally degraded by lysosomal enzymes. There is substantial evidence that several nanomaterials can cause autophagy and lysosomal dysfunction, either by prevention of autophagolysosome formation, biopersistence or inhibition of lysosomal enzymes. Such effects have emerged as a potential mechanism of cellular toxicity, which is also associated with various pathological conditions. In this chapter, we describe a method to monitor autophagy by fusion of the modifier protein MAP LC3 with green fluorescent protein (GFP; GFP-LC3). This method enables imaging of autophagosome formation in real time by fluorescence microscopy without perturbing the MAP LC3 protein function and the process of autophagy. With the GFP-LC3 protein fusion construct, a longitudinal study of autophagy can be performed in cells after treatment with nanomaterials.

Key words Autophagy, MAP LC3, Fluorescence imaging, Autophagosomes, Lysosomal dysfunction

1 Introduction

Autophagy is a survival pathway that is evolutionarily conserved from yeast to mammals [1]. The discoveries of mechanisms for autophagy by Dr. Yoshinori Ohsumi led to the 2016 Nobel Prize in Physiology or Medicine [2]. Autophagy is induced when cells are exposed to various stressors (e.g., nutrient deprivation; exposure to chemotherapy, ionizing radiation, infection, and select nanomaterials) resulting in recycling of misfolded or aggregated proteins and damaged subcellular organelles by the lysosomal enzymes in order to maintain cell homeostasis. Induction of autophagy results in the formation of double-layered vacuoles called autophagosomes that sequester the cytoplasmic contents for degradation by fusing with

Scott E. McNeil (ed.), *Characterization of Nanoparticles Intended for Drug Delivery*, Methods in Molecular Biology, Vol. 1682, DOI 10.1007/978-1-4939-7352-1_18,

the lysosomes [3]. Exposure to nanomaterials has resulted in increased accumulation of autophagosomes in various cell types [4]. The enhanced accumulation of autophagosome can be due to either increased autophagy induction or blocking of maturation/degradation of autophagosomes by lysosomal enzymes [5]. Several methods can monitor autophagy, which include electron microscopy, lysotracker assay, and immunoblotting techniques, to evaluate the autophagosomal marker microtubule-associated protein light chain 3-I (MAP LC3-I) lipidation product—LC3-II (MAP LC3-II) [6]. MAP LC3-II, a phosphatidylethanolamine-conjugated form of MAP LC3-I, is incorporated in the autophagosome membrane making it a commonly assessed marker for autophagy [7].

In this chapter, we present a method to monitor induction of autophagy by first stably transfecting a green fluorescent protein-MAP LC3 (GFP-LC3) construct in LLC-PK1 cells (porcine kidney proximal tubule cell line) and then imaging GFP-LC3 in the cells using fluorescence microscopy after treatment with nanomaterials, and positive and negative autophagy controls. The cytosolic GFP-LC3-I is converted to the autophagosome membrane-bound GFP-LC3-II upon autophagy induction (Fig. 1), causing GFP-LC3 to appear as fluorescent puncta under microscopy. The number of GFP-LC3 puncta is a measure of autophagy induction and/or blockade in the transfected LLC-PK1 cells. Unlike the methods used to assess autophagy discussed earlier, the GFP-LC3-transfected cell line method enables both temporal and spatial analysis of autophagosomes directly for a longitudinal study. The protocol

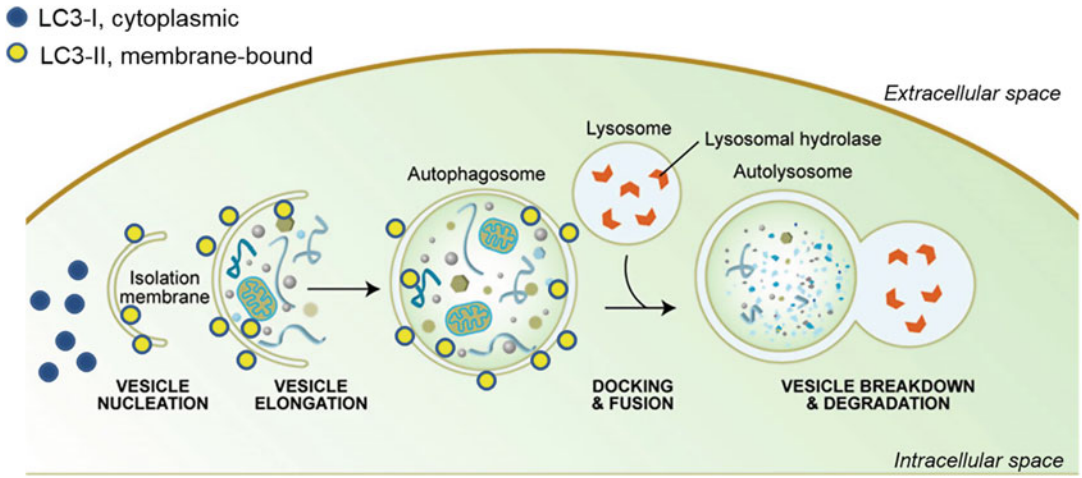

Fig. 1 Schematic depiction of the role of LC3 protein in autophagy. During autophagy, the cytoplasmic LC3-I is conjugated to phosphatidylethanolamine to form LC-3-phosphatidylethanolamine conjugate, LC3-II. LC3-II is recruited to the membranes of autophagosomes. When autophagosomes fuse with lysosomes to make autolysosomes, LC3-II is degraded by lysosomal hydrolases. Image adapted from ref. 8

presented here describes methods to stably transfect LLC-PK1 cells with the GFP-LC3 protein fusion construct and to perform image analysis of GFP-LC3 puncta.

2 Materials

2.1 Equipment

1. T-75 cell culture flasks.
2. Cloning cylinders.
3. Ninety six well cellular imaging plates.
4. Six-well cell culture plates.
5. Inverted wide-field fluorescent microscope with illuminations/filters appropriate for GFP (488 nm) visualization.
6. Automated imager with 20× water objective and 405 nm, 488 nm, and 640 nm lasers.
7. Image analysis software with nuclei, cytoplasmic, and spot detection libraries.

2.2 Reagents

1. LLC-PK1 cells.
2. M199 cell culture media with 3% v/v fetal bovine serum.
3. Serum-free M199 cell culture media.
4. pSELECT-GFP-LC3 plasmid (Invivogen Cat # psetz-gfplc3).
5. Transfecting agent (*see* **Note 1**).
6. Zeocin (Life Technologies Cat # R25001) (*see* **Note 2**).
7. Nanomaterial treatment solution (*see* **Note 3**).
8. Chloroquine solution (25 μM) as positive control.
9. Cellular nuclear stain with an excitation around 350 nm (e.g., Hoechst 33342).
10. Cytoplasm stain with excitation around 650 nm (e.g., HCS CellMask Deep Red).
11. 4% Paraformaldehyde in Phosphate Buffered Saline Solution (PBS), prepared fresh.

3 Methods

3.1 Stable Transfection of LLC-PK1 Cells

1. Seed LLC-PK1 cells in T-75 flask to achieve 50–80% confluence the following day. Use M199 cell culture media with 3% fetal bovine serum.
2. After cells reach appropriate confluence, replace media from the flask with serum-free media for about 30 min at 37 °C.

3. Dilute pSELECT-GFP-LC3 plasmid DNA to get 24 μg of DNA in 1.5 mL of serum-free media and incubate solution for 5 min at room temperature.
4. Dilute 60 μL of transfecting agent with 1.5 mL of serum-free media and incubate solution for 5 min at room temperature.
5. Mix transfecting agent solution from **step 4** with DNA solution from **step 3** in a 1:2.5 ratio and incubate solution for 20 min at room temperature (*see* **Note 4**).
6. Add 2.1 mL of solution complex from **step 5** to flask of cells and incubate at 37 °C for about 3 h.
7. Change media to complete media after incubation period.
8. After transfection for 24 h, visualize the cells under a fluorescence microscope to evaluate the transfection efficiency (*see* **Note 5**).
9. After 72 h of transient transfection, split cells at a 1:10 dilution into M199 medium containing 250 μg/mL Zeocin.
10. Replace M199 cell culture media containing Zeocin every couple of days to maintain the antibiotic selection.
11. After several rounds of selection of cells in M199 media containing the antibiotics, seed the cells at a low density in a 6-well culture plate to get single colonies (*see* **Note 6**).
12. Isolate single colonies using a sterile cloning cylinder.
13. Seed each colony in a T-25 flask for cell expansion (*see* **Note 5**).
14. Freeze 1 mL of early passage stable cells at 2×10^6 cells/mL in a cryovial tube and store in cell repository for future use.

3.2 Cell Imaging

1. Plate GFP-LC3-transfected LLC-PK1 cells onto 96 well imaging plates at a volume of 100 μL/well and 5×10^5 cells/mL and incubate the cells for 24 h.
2. Treat cells with nanomaterial solution, 25 μM chloroquine as a positive control and complete media as a negative control (Fig. 2; *see* **Notes 3** and **7**).
3. To determine the best time point for cell fixation, image cells under a fluorescence microscope with live cell imaging capabilities including CO_2 flow, humidity, and above ambient temperature control (37 °C). Then, monitor changes in the GFP-LC3 puncta with appropriate illumination and filters for GFP visualization. Select the time point with the most visible puncta (*see* **Note 8**).
4. At the predetermined time point depending on the treatment from **step 3**, fix cells using formaldehyde. First, rinse the tissue-culture dish twice with ice-cold PBS, incubate cells in 4% paraformaldehyde for 20 min at 4 °C, and wash cells twice with ice-cold PBS.

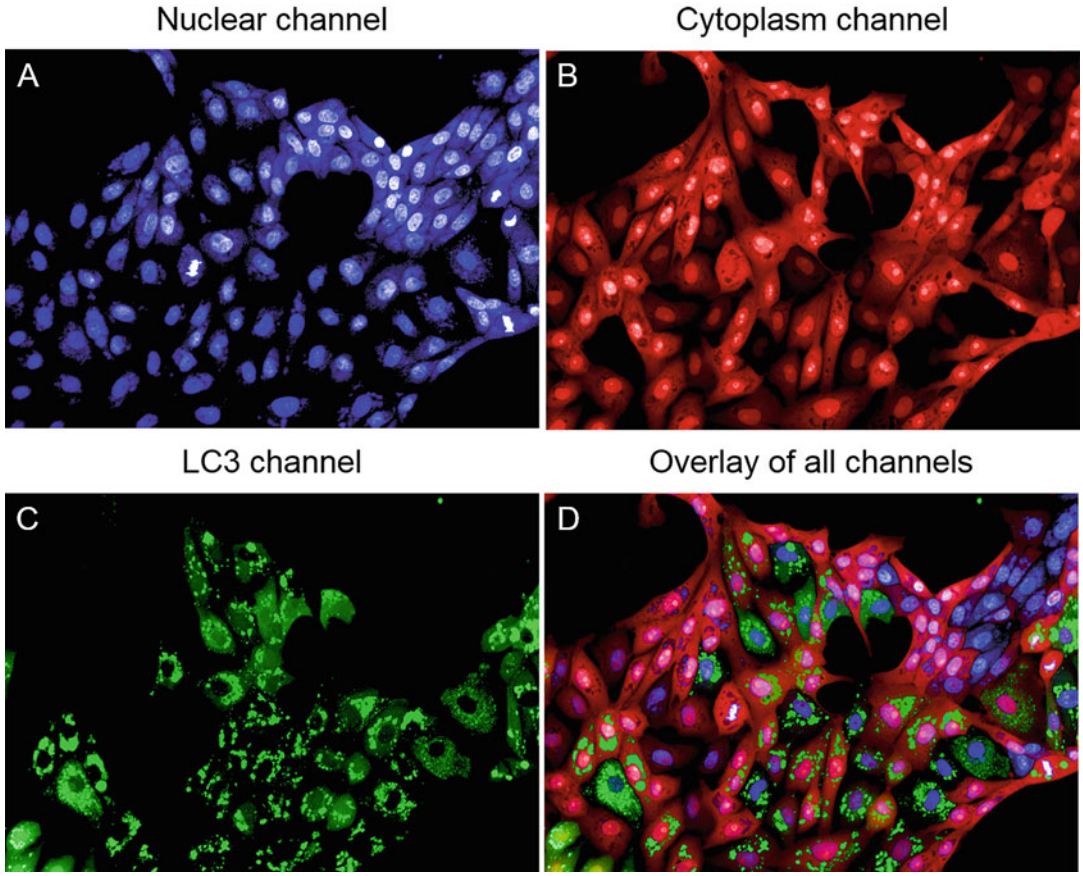

Fig. 2 Fluorescent images of GFP-LC3 in LLC-PK1 cells to monitor autophagy induction. Porcine proximal tubular cells (LLC-PK1) with stable expression of GFP-LC3 construct were treated with chloroquine (25 μg/mL) for 24 h. Cellular staining was used to monitor the location of the LC3 protein. (**a**) *Blue* indicates nuclei stained with Hoechst 33342 (excitation/emission (nm): 405/450; Thermo Fisher Scientific, Waltham, MA 02451), (**b**) *red* indicates cytoplasm stained with HCS CellMask *Deep Red* (excitation/emission (nm): 640/690; Thermo Fisher Scientific), and (**c**) *green* indicates GFP-LC3 fusion protein captured using a 488 nm excitation laser. (**d**) Overlay of all three channels is shown. High content data was acquired on an Opera confocal reader (model 3842-Quadruple Excitation High Sensitivity (QEHS), Perkin Elmer, Waltham, MA 02451). Imaging was performed with a 20× high NA water objective

5. Add nuclear and cytoplasmic dyes to cells as per the manufacturer's instructions (*see* **Notes 9** and **10**).
6. Image cells using appropriate illumination/filters for visualization of GFP and nuclear/cellular stains as described in Subheading 3.3. Take cell images at predetermined post-treatment time (Fig. 2; *see* **Note 8**).

3.3 Image Acquisition and Analysis

1. On a fluorescence microscope, use two exposures to acquire images and minimize bleed over to other channels (*see* **Note 11**).

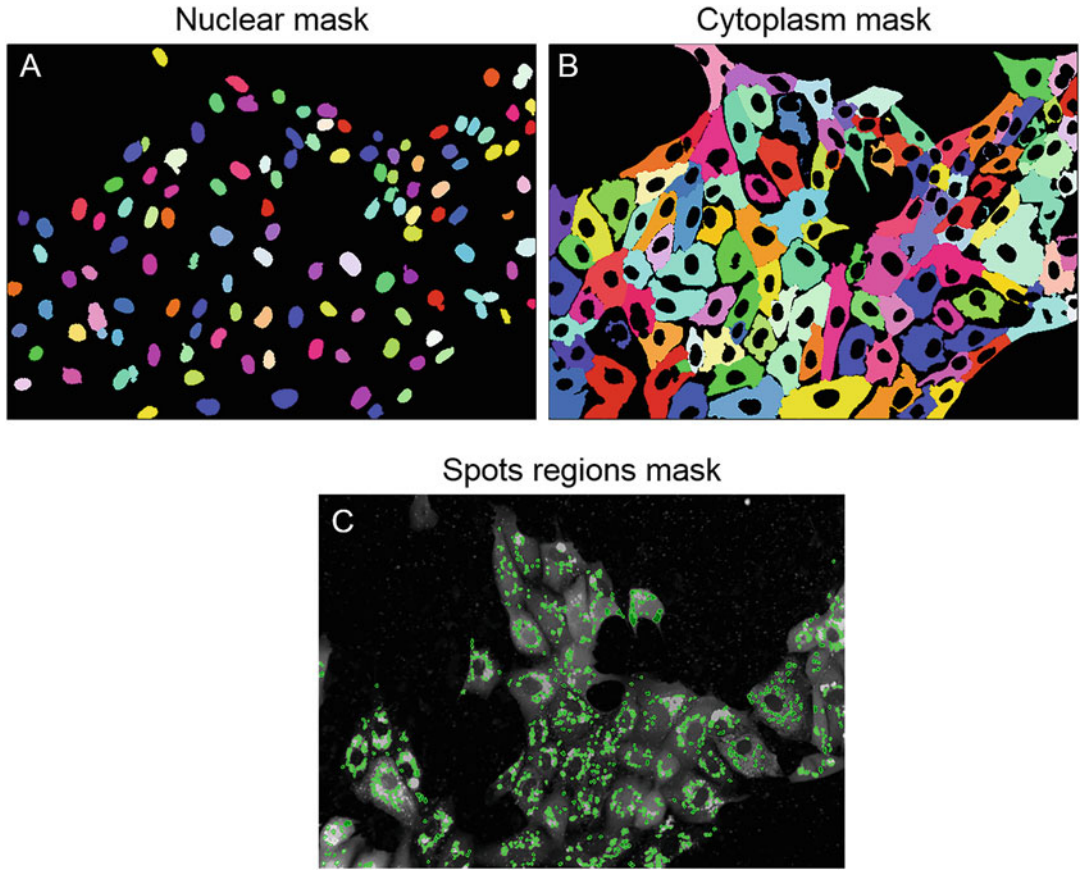

Fig. 3 Determination of nuclear, cytoplasmic, and LC3 puncta spots in cells. Image analysis was accomplished within the Opera environment using standard Acapella scripts (Perkin Elmer). During image analysis, the use of separate nuclear Hoechst dye and whole cell CellMask *Deep Red* stain enabled accurate identification and segmentation of the nuclei and the cells, respectively. Using the above-segmented nuclei and cytoplasmic regions, a nuclear mask, whole cell mask (HCS CellMask *Deep Red* stain; Thermo Fisher Scientific), and spot regions mask were created on the single image

2. Determine nuclei and cytoplasmic regions of the cells (Fig. 3). For nuclear detection, fluorescence emitted by a nuclear stain (e.g., Hoechst 33342) using a UV excitation channel (excitation/emission (nm): 405/450) can be used. For cytoplasm detection, fluorescence from a visible excitation channel cytoplasmic stain (excitation/emission (nm): 640/690) can be exploited (e.g., HCS CellMask Deep Red).
3. To detect the autophagy puncta, visualize and capture emitted GFP fluorescence with a 488 nm laser (excitation/emission (nm): 488/520).
4. Image analysis software provides a nuclei detection library with different nuclear algorithms. Each algorithm comes with advanced parameters to further fine tune nuclei detection.

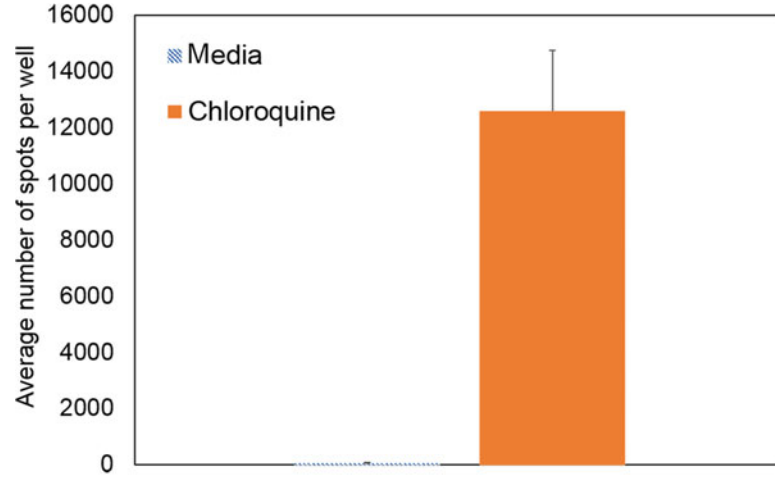

Fig. 4 The quantitation of autophagy induction as monitored by LC3 puncta. The plot shows an average number of spots per well for media alone and cells treated with chloroquine (25 μg/mL). The data shown are mean ± S.D. ($n = 6$)

For example, separation between background and nuclei can be controlled by two parameters—Threshold Adjustment and Individual Threshold Adjustment (*see* **Note 12**).

5. Image analysis software provides a cytoplasmic library consisting of cytoplasmic detection algorithms to aid in the differentiation among the background, nucleus, and cytoplasm of a cell (*see* **Note 12**).
6. A cell is considered to have autophagy induction (positive response) if the average number of green fluorescent puncta per well are above the background in the negative control cells and within the boundaries of the cell, as determined by nuclear, cytoplasmic, and spot detection algorithms (Figs. 3 and 4, *see* **Note 12**).

4 Notes

1. A commonly used transfecting agent is Lipofectamine 2000 reagent (Invitrogen). However, a number of different reagents can be used to achieve effective transfection.
2. The antibiotic serves as a selection marker for cells transfected with pSELECT-GFP-LC3 plasmid. If a different plasmid is selected, the corresponding selection marker should be used.
3. Take appropriate precautions when handling nanomaterials. Work in the hood and wear appropriate personal protective equipment. Follow the facility and institutional guidelines for proper disposal/storage of nanomaterials.

4. The ratio of transfection reagent and plasmid has to be optimized based on the cell type and transfection reagent used.
5. Transfection efficiency is the ratio of fluorescent cells to the total number of seeded cells. If efficiency is below 50%, you may need to adjust DNA concentration and/or increase transfection time to reach appropriate transfection efficiency.
6. Seeding density will depend on the plate format, e.g., 96- or 6-well plate.
7. Appropriate concentrations of nanomaterial should be evaluated by conducting an in vitro cytotoxicity assay [9]. Nanomaterials should be tested at the physiological pH and osmolarity, either in buffer or complete media. Appropriate control wells should be maintained with buffer or complete media for the same time period.
8. Choose the best time points for imaging based on the nanomaterial's activity. Time point selection may depend on the nanomaterial treatment concentration, cell line, and autophagy induction time-course. If the nanomaterial treatment group induces autophagy at early time points and cells quickly undergo cell death, earlier and more frequent time points may need to be monitored to track and capture GFP-LC3 puncta.
9. Depending on the cell type, the staining time will vary significantly. Optimize cell staining time to avoid saturation in nuclear/cytoplasmic stains.
10. Protect the stained cells from light to avoid photobleaching. Protect dye-containing solutions from light.
11. Wavelengths will depend on the nuclear and cytoplasmic stains used. When using CellMask Deep Red and Hoechst, the following method is suggested. For the first exposure, consider using 488 nm and 640 nm lasers to excite the GFP-tagged autophagy marker (GFP-LC3) and cytoplasmic fluorophores, respectively. For the second exposure, use a 405 nm laser to excite the nuclear stain (e.g., Hoechst).
12. Spot Detection algorithm was used to detect autophagosomes and quantify cell-associated autophagosomes within the confocal reader environment using standard scripts (*see* Fig. 3). Autophagosomes were detected as spots (LC3-GFP puncta) in a specified search region (Whole cell) having a higher intensity than its surroundings. To separate the spatial noise peaks and other artifacts, all spots detected initially were regarded as spot candidates. Spot candidates were then separated as "Classified Spots" based on two parameters: (1) contrast (i.e., contrast between the maximum intensity and the local background intensity near the spot candidate) and (2) spot-to-cell intensity (i.e., the ratio between the maximum intensity of the spot

candidate and the average intensity of the cell to which the spot object belongs). The final number of autophagosomes is exported as the mean spots per well (*see* Fig. 4).

Acknowledgment

This project has been funded in whole or in part with Federal funds from the National Cancer Institute, National Institutes of Health, under Contract No. HHSN261200800001E. The content of this publication does not necessarily reflect the views or policies of the Department of Health and Human Services, nor does mention of trade names, commercial products, or organizations imply endorsement by the U.S. Government.

References

1. Guimaraes RS, Delorme-Axford E, Klionsky DJ, Reggiori F (2015) Assays for the biochemical and ultrastructural measurement of selective and nonselective types of autophagy in the yeast Saccharomyces cerevisiae. Methods 75: 141–150. doi:10.1016/j.ymeth.2014.11.023
2. The Nobel Prize in Physiology or Medicine 2016. Nobel Media AB 2014. http://www.nobelprize.org/nobel_prizes/medicine/laureates/2016/. Accessed 14 Oct 2016
3. Klionsky DJ, Emr SD (2000) Autophagy as a regulated pathway of cellular degradation. Science 290(5497):1717–1721
4. Johnson-Lyles DN, Peifley K, Lockett S, Neun BW, Hansen M, Clogston J, Stern ST, McNeil SE (2010) Fullerenol cytotoxicity in kidney cells is associated with cytoskeleton disruption, autophagic vacuole accumulation, and mitochondrial dysfunction. Toxicol Appl Pharmacol 248(3):249–258. doi:10.1016/j.taap.2010.08.008
5. Adiseshaiah PP, Clogston JD, McLeland CB, Rodriguez J, Potter TM, Neun BW, Skoczen SL, Shanmugavelandy SS, Kester M, Stern ST, McNeil SE (2013) Synergistic combination therapy with nanoliposomal C6-ceramide and vinblastine is associated with autophagy dysfunction in hepatocarcinoma and colorectal cancer models. Cancer Lett 337(2):254–265. doi:10.1016/j.canlet.2013.04.034
6. Stern ST, Adiseshaiah PP, Crist RM (2012) Autophagy and lysosomal dysfunction as emerging mechanisms of nanomaterial toxicity. Part Fibre Toxicol 9:20. doi:10.1186/1743-8977-9-20
7. McLeland CB, Rodriguez J, Stern ST (2011) Autophagy monitoring assay: qualitative analysis of MAP LC3-I to II conversion by immunoblot. Methods Mol Biol 697:199–206. doi:10.1007/978-1-60327-198-1_21
8. Melendez A, Levine B (2009) Autophagy in C. elegans. WormBook:1–26. doi:10.1895/wormbook.1.147.1
9. Potter TM, Stern ST (2011) Evaluation of cytotoxicity of nanoparticulate materials in porcine kidney cells and human hepatocarcinoma cells. Methods Mol Biol 697:157–165. doi:10.1007/978-1-60327-198-1_16

Part V

Drug Release and In Vivo Efficacy

Chapter 19

Improved Ultrafiltration Method to Measure Drug Release from Nanomedicines Utilizing a Stable Isotope Tracer

Sarah L. Skoczen and Stephan T. Stern

Abstract

An important step in the early development of a nanomedicine formulation is the evaluation of stability and drug release in biological matrices. Additionally, the measurement of encapsulated and unencapsulated nanomedicine drug fractions is important for the determination of bioequivalence (pharmacokinetic equivalence) of generic nanomedicines. Unfortunately, current methods to measure drug release in plasma are limited, and all have fundamental disadvantages including non-equilibrium conditions and process-induced artifacts. The primary limitation of current ultrafiltration (and equilibrium dialysis) methods for separation of encapsulated and unencapsulated drug and determination of drug release is the difficulty in accurately differentiating protein bound and encapsulated drug. Since the protein binding of most drugs is high (>70%) and can change in a concentration- and time-dependent manner, it is very difficult to accurately account for the fraction of non-filterable drug that is encapsulated within the nanomedicine and how much is bound to protein. The method in this chapter is an improvement of existing ultrafiltration protocols for nanomedicine fractionation in plasma, in which a stable isotope tracer is spiked into a nanomedicine containing plasma sample in order to precisely measure the degree of plasma protein binding. Determination of protein binding then allows for accurate calculation of encapsulated and unencapsulated nanomedicine drug fractions, as well as free and protein-bound fractions.

Key words Nanomedicine, Drug release, Stability, Stable isotope, Bioanalytical

1 Introduction

An important step in the early development of a nanomedicine formulation is the evaluation of stability and drug release in biological matrices. Additionally, the measurement of encapsulated and unencapsulated nanomedicine drug fractions is important for the determination of bioequivalence (pharmacokinetic equivalence) of generic nanomedicines [1]. Unfortunately, current methods to measure drug release in plasma are limited, and all have fundamental disadvantages including non-equilibrium conditions and process-induced drug release. The ultrafiltration method detailed in this protocol represents a substantial improvement over existing ultrafiltration methods to measure nanomedicine

Scott E. McNeil (ed.), *Characterization of Nanoparticles Intended for Drug Delivery*, Methods in Molecular Biology, Vol. 1682, DOI 10.1007/978-1-4939-7352-1_19,

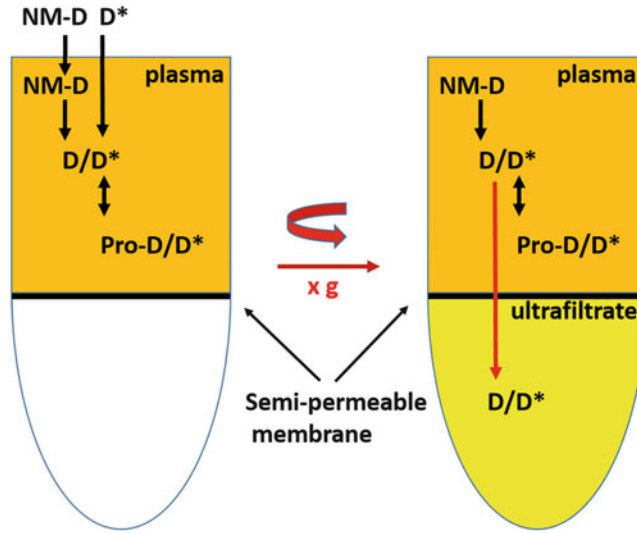

Fig. 1 Stable isotope tracer ultrafiltration method. Stable isotopically labeled drug (D*) is spiked into nanomedicine (NM-D) containing plasma, and behaves identically to normoisotopic drug (D) with regard to protein binding (Pro-D/D*). Following the attainment of protein binding equilibrium, the plasma sample is transferred to an ultrafiltration device and the filtrate is separated by centrifugation. The stable isotope tracer free fraction, represented as the ultrafilterable fraction, can be used to calculate protein bound, unencapsulated, and encapsulated drug fractions, according to Eqs. (1), (2), and (3) in the text, respectively

encapsulated and unencapsulated drug fractions in plasma and assess nanomedicine drug release. The primary issue with existing equilibrium methods for nanomedicine fractionation in plasma, including ultrafiltration and equilibrium dialysis, is accounting for the protein bound component of the non-filterable or dialyzable drug fractions, respectively, in order to accurately determine the encapsulated and unencapsulated drug fractions [1]. Since plasma protein binding for most marketed drugs is in excess of 70% [2] and can change in a concentration-, time-, and even formulation-dependent manner [3], accurate determination of the protein bound fraction is a considerable challenge. This method utilizes a stable isotope tracer (*see* **Note 1**) of the nanomedicine-encapsulated drug to measure protein binding [4] (Fig. 1).

The method explained below details how to conduct an in vitro drug release study in human plasma, comparing a bilayer-loaded docetaxel (DTX) nanoliposome to the commercial DTX formulation, Taxotere®, and solvent solubilized DTX. However, this method can also be used to fractionate nanomedicine-containing plasma from an in vivo pharmacokinetic study, such as a bioequivalence trial. Following collection of the nanomedicine-containing plasma sample, the stable isotope is spiked into the plasma.

The sample is then incubated to allow equilibration of the stable isotope with plasma protein, an aliquot of the sample is taken for analysis of total drug, and the remaining sample is transferred to an ultrafiltration apparatus for collection of the filterable fraction by centrifugation. The initial aliquot (reservoir drug), used to measure total drug, and the filtrate, used to measure free/unbound drug, are analyzed by mass spectrometry to determine both the formulation (normoisotopic) and stable isotope tracer drug concentrations.

Since the stable, isotopically labeled drug (**D***) and unlabeled, normoisotopic drug (**D**) released from the nanomedicine formulation equilibrate with protein and formulation components to the same degree, the ultrafilterable fraction of the isotopically labeled drug is an accurate measure of free unbound fraction. The bound fraction can be calculated from Eq. (1):

$$\%\text{Bound D}^* = \frac{([\text{Reservoir D}^*] - [\text{Ultrafilterable D}^*]) \times 100}{[\text{Reservoir D}^*]} \tag{1}$$

The encapsulated and unencapsulated nanomedicine fractions can then be calculated using simple Eqs. (2) and (3):

$$[\text{Unencapsulated D}] = \frac{[\text{Ultrafilterable D}]}{\left(1 - \frac{(\%\text{Bound D}^*)}{100}\right)} \tag{2}$$

$$[\text{Encapsulated D}] = [\text{Reservoir D}] - [\text{Unencapsulated D}] \tag{3}$$

2 Materials

1. Human plasma (pooled) collected fresh from six human donors in K_2EDTA tubes.
2. 1 M HEPES buffer solution.
3. 4 mL plastic blood collection tubes with K_2EDTA.
4. 10 kDa molecular weight cutoff (MWCO) cellulose membrane ultrafiltration device, 0.5 mL capacity.
5. 30 kDa MWCO centrifugal filter units, 4 mL capacity.
6. Acetonitrile (ACN).
7. Docetaxel (DTX).
8. Docetaxel-d5 (DTX-d5).
9. Docetaxel-d9 (DTX-d9).
10. 20 mg/mL docetaxel (Taxotere®), prepared as directed by the manufacturer (Sanofi-Aventis Corporation, Bridgewater, NJ).
11. Docetaxel nanoliposome (bilayer-loaded) test nanoparticle.

12. Liquid chromatography-mass spectrometry (LC-MS) instrumentation.
13. Formic acid.
14. C18 high-performance liquid chromatography column, 2.1 mm × 100 mm and matching C18 guard column, 2.1 mm × 10 mm.
15. Amber glass screw top HPLC vial with fixed Teflon insert and cap.
16. Evaporator and concentrator workstation.

3 Methods

3.1 Protein Binding Comparison

The first step in this method is the determination of the time for the normoisotopic drug to reach equilibrium with plasma proteins. If the normoisotopic drug is in equilibrium with both protein and formulation components, then the free fraction should not vary over progressive time points. The amount of time for the free drug to come to equilibrium with the protein bound form is generally from 10 to 30 min. Free DTX equilibration time in this example was determined by incubation for 5, 10, 15, and 30 min and identifying the earliest time at which protein binding stabilized. This equilibration time was found to be 10 min, which was then used in the stable isotope tracer protein binding comparison study below.

Following the determination of equilibrium binding time, the next step is to evaluate the protein binding characteristics of the stable isotope tracer, to ensure that the stable isotope behaves identically to the normoisotopic drug. Deuteration, for instance, can lead to changes in the physicochemical properties of drugs that can potentially influence the protein binding characteristics.

1. Prepare human plasma. Collect and pool human blood in K_2EDTA tubes from six donors. Prepare plasma from the pooled blood by centrifugation at 2500 × *g* for 10 min. Add 50 μL of HEPES buffer for every 2 mL of plasma and adjust the pH to 7.4. To prepare protein-free plasma, transfer plasma into a 4 mL centrifugal filter unit with a 30 kDa MWCO, centrifuge for 5000 × *g* for 1 h, and collect filtrate.
2. Solubilize DTX in ACN and spike into 1 mL of prewarmed plasma samples (37 °C) in triplicate to yield final DTX concentrations of 0.5, 1, 2, 5, and 10 μg/mL. Then, spike plasma samples with ACN solubilized stable isotope tracer DTX-d5 to yield a final DTX-d5 concentration of 0.5 μg/mL (*see* **Note 2**).
3. Add 400 μL of plasma samples to prewarmed 10 kDa MWCO centrifuge devices and incubate for 10 min at 37 °C (*see* **Note 3**). Spin samples at 6000 × *g* for 10 min at 37 °C.

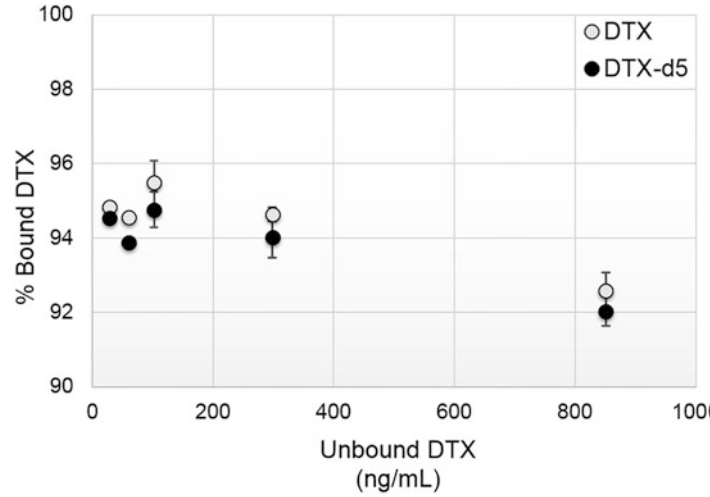

Fig. 2 Protein binding of DTX and DTX-d5 in human plasma. Displayed are the free/unbound docetaxel concentration (Unbound DTX), measured as the ultrafilterable drug concentration (ng/mL), and the percent bound docetaxel (% Bound DTX), calculated from Eq. (1) ($N = 3$, Mean ± SD)

4. Analyze 50 μL of the ultrafiltrate by LC-MS. Plasma samples (400 μL) incubated in centrifuge devices at 37 °C and not spun are also analyzed by LC-MS to determine total drug concentration in the reservoir (*see* **Note 4**). LC-MS method is described in Subheading 3.4.
5. Calculate percent bound drug using Eq. (1).
6. Compare percent bound drug values between the stable isotope tracer and the normoisotopic drug. Ideally, values would be within 15% of each other.

Protein binding of DTX, over a clinically relevant concentration range of 500–10,000 ng/mL, was compared to protein binding of a constant 500 ng/mL deuterated DTX-d5 spike. The isotopically labeled DTX-d5 behaved identically to the normoisotopic drug, DTX with percent protein binding between 92% and 96% (Fig. 2). These data suggest that DTX protein binding characteristics of the stable isotope tracer were not impacted by deuteration.

3.2 Drug Release in Human Plasma

This method gives an example of an in vitro drug release experiment in human plasma using DTX liposome as a model nanomedicine formulation. Drug release is compared to commercial Taxotere™ and ACN solubilized DTX. The time points chosen in advance were 0, 10, 30, and 60 min. These may be adjusted depending upon the drug release kinetics. The concentrations of DTX equivalents chosen for this study were 2, 5, and 10 μg/mL, as they were clinically relevant concentrations based upon its clinical dose and pharmacokinetic profile.

1. Collect and pool human blood in K_2EDTA tubes from six donors. Prepare plasma from the pooled blood by centrifugation at 2500 × *g* for 10 min. Add 50 μL HEPES buffer for every 2 mL of plasma and adjust the pH to 7.4.
2. Spike 4 mL of prewarmed plasma samples (37 °C) with DTX liposome and commercial Taxotere or ACN solubilized DTX in triplicate to yield final DTX concentrations of 2, 5 and 10 μg/mL in glass vials. Incubate samples for 0, 10, 30, and 60 min at 37 °C with agitation (*see* **Note 5**).
3. At each time point, spike 400 μL aliquots of the plasma samples with DTX-d5 to make a final DTX-d5 concentration of 0.5 μg/mL and vortex. Transfer sample to 10 kDa MWCO centrifuge devices and incubate for 10 min at 37 °C with agitation.
4. Centrifuge samples at 6000 × *g* for 10 min and analyze 50 μL of the ultrafiltrate by LC-MS. Plasma samples (400 μL) incubated in centrifuge devices at 37 °C and not spun were also analyzed by LC-MS to determine total drug concentration in the reservoir (*see* **Note 4**). The LC-MS method is described in Subheading 3.4.
5. Calculate unencapsulated and encapsulated drug fractions according to Eqs. (2) and (3), respectively.

A liposomal DTX release study was conducted in human plasma. The stable isotope tracer method determined rapid release of DTX from the liposome, with >90% of the drug released within 10 min, and the remainder released over a 30 min period (Fig. 3,

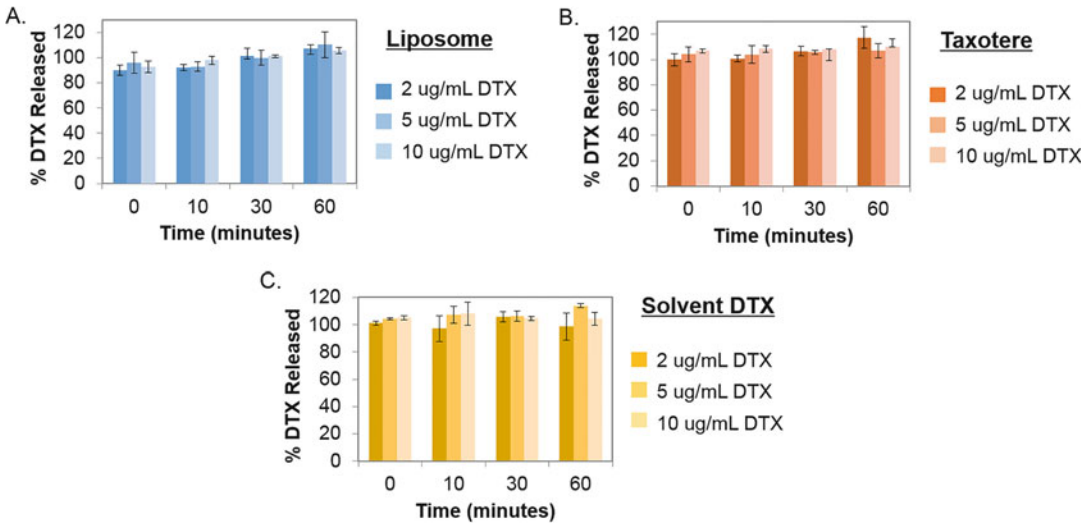

Fig. 3 DTX release. Displayed are the percent unencapsulated values (% DTX Released) for (**a**) Liposome, (**b**) Taxotere, and (**c**) solvent DTX formulations, calculated from Eq. (2) after 0, 10, 30, and 60 min incubation ($N = 3$, mean ± SD)

Table 1
DTX release from liposomal formulation. Displayed are the % bound, % encapsulated, and % unencapsulated DTX for Liposome, Taxotere, and solvent formulations, calculated from Eqs. (1), (2), and (3), respectively, over time (*N* = 3, Mean ± SD). *TZ* time zero, *SD* standard deviation

		% Bound DTX-d5	Encapsulated DTX ng/mL	Unencapsulated DTX ng/mL	% Encapsulated DTX	% Unencapsulated DTX
Liposome						
TZ	2 μg/mL	96 ± 0.7	172 ± 70	1535 ± 70	10 ± 4	90 ± 4
	5 μg/mL	95 ± 0.3	183 ± 375	4217 ± 375	4 ± 9	96 ± 9
	10 μg/mL	95 ± 0.4	617 ± 376	7819 ± 376	7 ± 4	93 ± 4
10 min	2 μg/mL	95 ± 0.3	134 ± 43	1598 ± 43	8 ± 2	92 ± 2
	5 μg/mL	96 ± 1	318 ± 162	4177 ± 162	7 ± 4	93 ± 4
	10 μg/mL	96 ± 1	177 ± 256	8098 ± 256	2 ± 3	98 ± 3
30 min	2 μg/mL	97 ± 0.2	−26 ± 50	1910 ± 50	−1 ± 3	101 ± 3
	5 μg/mL	96 ± 0.7	7 ± 284	4722 ± 284	0.2 ± 6	100 ± 6
	10 μg/mL	96 ± 0.6	−99 ± 118	9376 ± 118	−1 ± 1	101 ± 1
Taxotere						
TZ	2 μg/mL	94 ± 0.4	5 ± 97	2014 ± 97	0.2 ± 5	100 ± 5
	5 μg/mL	94 ± 0.2	−203 ± 289	5044 ± 289	−4 ± 6	104 ± 6
	10 μg/mL	90 ± 4	−675 ± 148	10,607 ± 148	−7 ± 1	107 ± 1
10 min	2 μg/mL	95 ± 1	−18 ± 71	2521 ± 71	−0.7 ± 3	101 ± 3
	5 μg/mL	94 ± 1	−219 ± 392	5861 ± 392	−4 ± 7	104 ± 7
	10 μg/mL	94 ± 0.2	−983 ± 305	12,588 ± 305	−8 ± 3	108 ± 3
30 min	2 μg/mL	95 ± 0.3	−165 ± 97	2647 ± 97	−7 ± 4	107 ± 4
	5 μg/mL	95 ± 0.3	−320 ± 79	5963 ± 79	−6 ± 1	106 ± 1
	10 μg/mL	94 ± 0.2	−861 ± 73	11,899 ± 73	−8 ± 0.7	108 ± 0.7
DTX solvent						
TZ	2 μg/mL	96 ± 0.3	−26 ± 34	2229 ± 34	−1 ± 2	101 ± 2
	5 μg/mL	94 ± 0.4	−249 ± 35	5902 ± 35	−4 ± 0.6	104 ± 0.6
	10 μg/mL	93 ± 0.4	−543 ± 135	11,247 ± 135	−5 ± 1	105 ± 1
10 min	2 μg/mL	96 ± 0.4	54 ± 186	1896 ± 186	3 ± 10	97 ± 10
	5 μg/mL	94 ± 0.5	−345 ± 292	5032 ± 292	−7 ± 6	107 ± 6
	10 μg/mL	93 ± 1	−717 ± 732	9633 ± 732	−8 ± 8	108 ± 8
30 min	2 μg/mL	96 ± 0.3	−133 ± 82	2353 ± 82	−6 ± 4	106 ± 4
	5 μg/mL	94 ± 0.1	−355 ± 209	6029 ± 209	−6 ± 4	106 ± 4
	10 μg/mL	93 ± 0.9	−493 ± 145	11,138 ± 145	−5 ± 1	105 ± 1

Table 1). By comparison, Taxotere™ and solvent formulations released all drug immediately. If the stable isotope was not an accurate control of free fraction, the percent release estimates for the various formulations would have lacked precision and accuracy, and varied dramatically from the theoretical 100% release, based upon the amount of DTX equivalents added to the plasma sample.

3.3 Control Studies

To insure the validity of results, studies should incorporate spike recovery controls. To determine the accuracy of the unencapsulated drug estimation, a free normoisotopic drug can be spiked into plasma with the formulation. An additional control study to examine the possibility of processing artifacts with regard to encapsulated drug release can be performed by double processing the formulation containing plasma, in which a single formulation containing plasma sample undergoes two successive filtration processes. Lastly, a control for the organic spike can be performed whereby identical formulation containing plasma samples are compared. One sample receives the stable isotope tracer spike, and the other does not. If the organic spike does not disrupt the formulation, then the concentration of normoisotopic drug in the filtrate of both samples should be identical, ideally within 15% of each other.

1. Collect and pool human blood in K_2EDTA tubes from six donors. Centrifuge the pooled blood at 2500 × *g* for 10 min to prepare plasma. Add 50 μL of HEPES buffer for every 2 mL of plasma and adjust the pH to 7.4.
2. Spike three sets of 4 mL of prewarmed plasma samples (37 °C) in glass vials with DTX liposome in triplicate to yield final concentrations of 600 ng/mL. Incubate samples for 10 min at 37 °C with agitation (*see* **Note 5**). The three sets are used for: (1) double spin study, (2) 300 ng/mL spike recovery study, and (3) organic stable isotope spike study.
3. For the **double spin study**, spike DTX-d5 into 400 μL aliquots of plasma from set one to make a final DTX-d5 concentration of 0.5 μg/mL and vortex. Transfer the spiked samples to a 10 kDa MWCO centrifuge device and incubate for 10 min at 37 °C with agitation. Centrifuge the samples at 6000 × *g* for 10 min at 37 °C. Analyze 50 μL of the ultrafiltrate by LC-MS (*see* LC-MS method in Subheading 3.4). Following this initial spin, transfer the samples to new centrifuge devices, spin samples again at 6000 × *g* for 10 min at 37 °C, and collect and analyze a second 50 μL sample of the ultrafiltrate. Plasma samples (400 μL) incubated in centrifuge devices at 37 °C and not spun are also analyzed by LC-MS to determine total drug concentration in the reservoir (*see* **Note 4**). Calculate the unencapsulated DTX concentrations according to Eq. (2).

4. For the **spike recovery study**, spike 300 ng/mL of free DTX and 0.5 μg/mL of DTX-d5 into 400 μL plasma aliquots from set two and vortex. Transfer samples to 10 kDa MWCO centrifuge devices and incubate for 10 min at 37 °C with agitation. Centrifuge samples at 6000 × *g* for 10 min and analyze 50 μL of the ultrafiltrate by LC-MS (*see* LC-MS method in Subheading 3.4). Plasma samples (400 μL) incubated in centrifuge devices at 37 °C and not spun are also analyzed by LC-MS to determine total drug concentration in the reservoir (*see* **Note 4**). Determine unencapsulated DTX concentrations according to Eq. (2). To determine spike recovery, the mean of the calculated DTX concentrations for the first spin of the double spin study (*see* **step 3** in Subheading 3.3) is subtracted from the mean of the spiked sample concentrations. Ideally, the protein binding value of the spike recovery samples would be within 15% of the theoretical value.
5. For the **organic stable isotope spike study**, take 400 μL of plasma aliquots from set three and do **not** spike with ACN solubilized DTX-d5. Vortex the sample and transfer to 10 kDa MWCO centrifuge devices. Incubate samples for 10 min at 37 °C with agitation and then centrifuge samples at 6000 × *g* for 10 min at 37 °C. Analyze 50 μL of the ultrafiltrate by LC-MS (*see* LC-MS method in Subheading 3.4). Plasma samples (400 μL) incubated in centrifuge devices at 37 °C and not spun were also analyzed by LC-MS to determine total drug concentration in the reservoir (*see* **Note 4**). Determine percent protein binding of the normoisotopic drug, calculated as:

$$\%\text{Protein binding} = \frac{([\text{Total DTX in reservoir}] - [\text{DTX in ultrafiltrate}])}{[\text{Total DTX in reservoir}]} \times 100,$$

for set one and set three in order to determine the effect of the organic spike on formulation stability. Ideally, the percent protein binding values between the two sets would be within 15% of each other.

Double processing of the DTX liposome containing plasma did not alter the unencapsulated DTX estimate, supporting the fact that the centrifugation/filtration step does not alter formulation stability (Fig. 4). The 300 ng/mL spike recovery was within 10% of theoretical (Fig. 4). The organic stable isotope spike did not change the protein binding estimate (within 15%), confirming that the organic stable isotope spike does not alter formulation stability in this example (Fig. 5).

3.4 LC-MS Set Up and Analysis

3.4.1 LC-MS Set Up

1. Set HPLC conditions at: 5 μL injection volume, water-ACN gradient (30% ACN/0.1% formic acid from 0 to 1.5 min, linear increase to 80% ACN/0.1% formic acid from 1.5 to 4.5 min, hold at 80% ACN/0.1% formic acid from 4.5 to 8.5 min, and

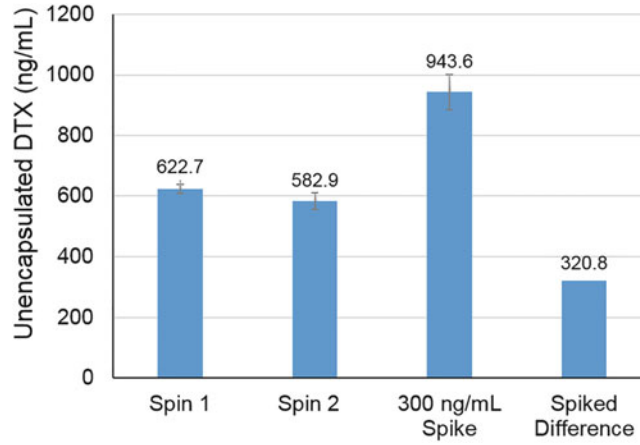

Fig. 4 Double processing and spike recovery controls. Displayed are the unencapsulated DTX concentrations, calculated from Eq. (2), for the first (Spin 1) and second spin (Spin 2) of the double processing controls and the 300 ng/mL spike control. The "Spiked Difference" is the difference between the 300 ng/mL spike and Spin 1 controls. The concentration of liposome was 600 ng DTX/mL in plasma, and the incubation time was 0 min ($N = 3$, mean $\pm$ SD)

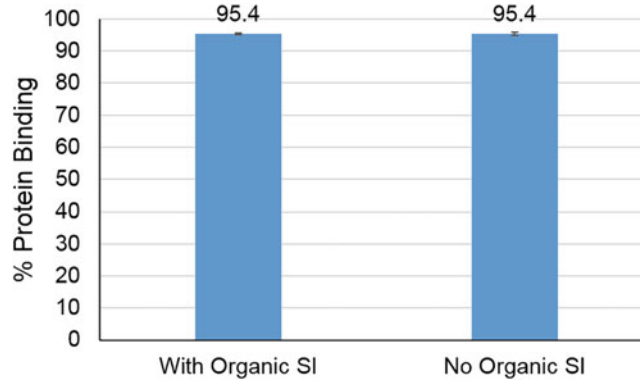

Fig. 5 Organic stable isotope spike controls. Displayed are the percent protein binding values for the normoisotopic drug, calculated as % protein binding $=$ (total DTX in reservoir-DTX in ultrafiltrate)/total DTX in reservoir $\times$ 100, for liposome containing samples with or without organic stable isotope (SI) spike. The concentration of liposome was 600 ng DTX/mL in plasma ($N = 3$, mean $\pm$ SD)

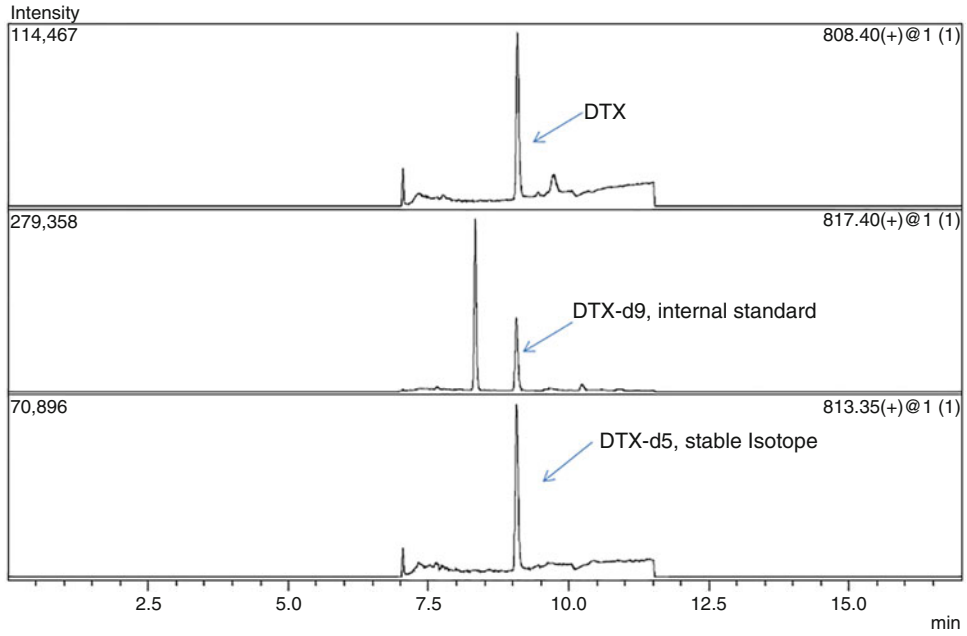

Fig. 6 Example Selected Ion Monitoring Spectrometry Spectrograms in plasma matrix of DTX (*top*), DTX-d9 (*middle*), and DTX-d5 (*bottom*). Spectrograms collected on LC/MS 2020 single quad, LC-20AT pump, SPD-20AC autoinjector, and C-R3A integrator (Shimadzu Scientific Instruments, Inc.)

linear decrease to 30% ACN/0.1% formic acid from 8.5 to 10.5 min), flow rate of 0.35 mL/min, and column temperature of 32 °C. The column regeneration time between injections is 6.5 min.

2. Use an MS instrument with an electrospray ionization source in positive ion mode. Set detector voltage at 0.2 kV and the desolvation line (DL) and heat block temperature at 200 °C. Use high-pressure liquid nitrogen as the drying gas at a rate of 1.5 L/min. DTX, DTX-d5, and DTX-d9 elution times were all 8.9 min, and m/z ions monitored by selected ion monitoring (SIM) were 808, 813, and 817 respectively (Fig. 6).
3. Measure the peak area ratio of the analyte to the internal standard, DTX-d9, and use it to interpolate DTX concentrations of unknowns from a linear fit of calibration curves. The calibration curve range can vary depending on the assay analyte concentrations using calibration standards prepared in appropriate assay matrix. For each calibration run, include quality control samples from the low, mid, and high points of the calibration curve prepared in appropriate assay matrix. For specifics as to how the calibration and quality control samples are to be prepared, please refer to Subheading 3.4.2 below.

Table 2
Example of the DTX calibration curve data in human plasma. Percent accuracy between the theoretical and actual values is shown along with Quality Control (QC) samples

Theoretical ng/mL	Actual ng/mL	% Accuracy
25*	63	251
25	22	87
50	45	90
50	47	93
125	132	106
125	128	103
500	542	108
500	525	105
1,000	1,084	108
1,000	1,081	108
5,000	5,174	104
5,000	5,268	105
10,000	10,087	101
10,000	9,878	99
25,000	26,101	104
25,000	23,265	93
QC		
125	128	102
125	129	103
1,000	1,054	105
1,000	1,091	109
10,000	9,718	97
10,000	10,233	102

*Value omitted from standard curve

3.4.2 Calibration and Quality Control Standards Preparation

1. Dissolve stock solutions of DTX, DTX-d5, and DTX-d9 in ACN for calibration and quality control standards.
2. Prepare DTX and DTX-d5 calibration standards in human plasma and protein-free plasma at concentrations ranging from 25 to 25,000 ng/mL. Use DTX-d9 as an internal standard at a concentration of 250 ng/mL (*see* **Note 6**) (Tables 2, 3, 4, 5; Fig. 7).
3. Prepare DTX and DTX-d5 in human plasma and protein-free plasma in duplicate with concentrations of 125, 1000, and

Table 3
Example of DTX calibration curve data in human protein-free plasma. Percent accuracy between the theoretical and actual values is shown along with Quality Control (QC) samples

Theoretical ng/mL	Actual ng/mL	% Accuracy
25	22	89
25	10	42
50	49	98
50	47	95
125	122	97
125	113	90
500	533	107
500	559	112
1,000	1,056	106
1,000	1,193	119
5,000	5,290	106
5,000	5,436	109
10,000	9,957	100
10,000	10,348	104
25,000	23,224	93
25,000	25,567	102
QC		
125	108	86
125	107	85
1,000	1,129	113
1,000	1,167	117
10,000	10,639	106
10,000	10,439	104

10,000 ng/mL DTX as low-, medium-, and high-quality control standards, respectively. The average of the duplicate concentrations would ideally be within 15% of theoretical.

3.4.3 Sample and Calibration Standard Preparation

1. Add 50 μL of sample and calibration standards spiked with 250 ng/mL of DTX-d9 internal standard to a 2 mL eppendorf tube, followed by addition of 200 μL of ice-cold ACN with 0.1% formic acid. Vortex.

Table 4
Example of the DTX-d5 calibration curve in human plasma. Percent accuracy between the theoretical and actual values is shown along with Quality Control (QC) samples

Theoretical ng/mL	Actual ng/mL	% Accuracy
25	22	87
25	24	96
50	47	93
50*	82	163
125	124	99
125	123	98
500	526	105
500	502	101
1,000	1,062	106
1,000	1,021	102
5,000	5,522	110
5,000	5,570	111
10,000	10,569	106
10,000	9,839	98
25,000	25,863	104
25,000	22,540	90
QC		
125	134	107
125	129	103
1,000	1,034	103
1,000	1,069	107
10,000	9,773	98
10,000	10,228	102

*Value omitted from standard curve

2. Place the sample at −80 °C for 10 min and then thaw on ice.
3. Centrifuge the thawed sample at 14,000 × *g* for 20 min at 4 °C to pellet precipitated protein.
4. Transfer the supernatant to a glass tube and dry under nitrogen gas in an evaporator and concentrator workstation at 48 °C.
5. Resuspend the dried residue in 150 μL 30% ACN with 0.1% formic acid.
6. Transfer the extracted sample to a 0.5 mL eppendorf tube and centrifuge at 14,000 × *g* for 5 min at 4 °C.

Table 5
Example of DTX-d5 calibration curve in human protein-free plasma. Percent accuracy between the theoretical and actual values is shown along with Quality Control (QC) samples

Theoretical ng/mL	Actual ng/mL	% Accuracy
25	24	98
25	26	105
50	49	99
50	50	100
125	106	85
125	110	88
500	499	100
500	531	106
1,000	1,006	101
1,000	1,108	111
5,000	5,226	105
5,000	5,343	107
10,000	9,949	100
10,000	10,280	103
25,000	23,596	94
25,000	25,497	102
QC		
125	113	90
125	120	96
1,000	1,029	103
1,000	1,092	109
10,000	10,438	104
10,000	10,471	105

7. Transfer the supernatant to a 1.5 mL amber glass screw top HPLC vial with fixed Teflon insert and cap and place in an HPLC autosampler vial rack.
8. Run matrix sample blank (matrix only), internal standard spiked matrix blank (e.g., plasma spiked with internal standard), and quality control samples with each calibration curve. Follow the LC-MS method in Subheading 3.4.

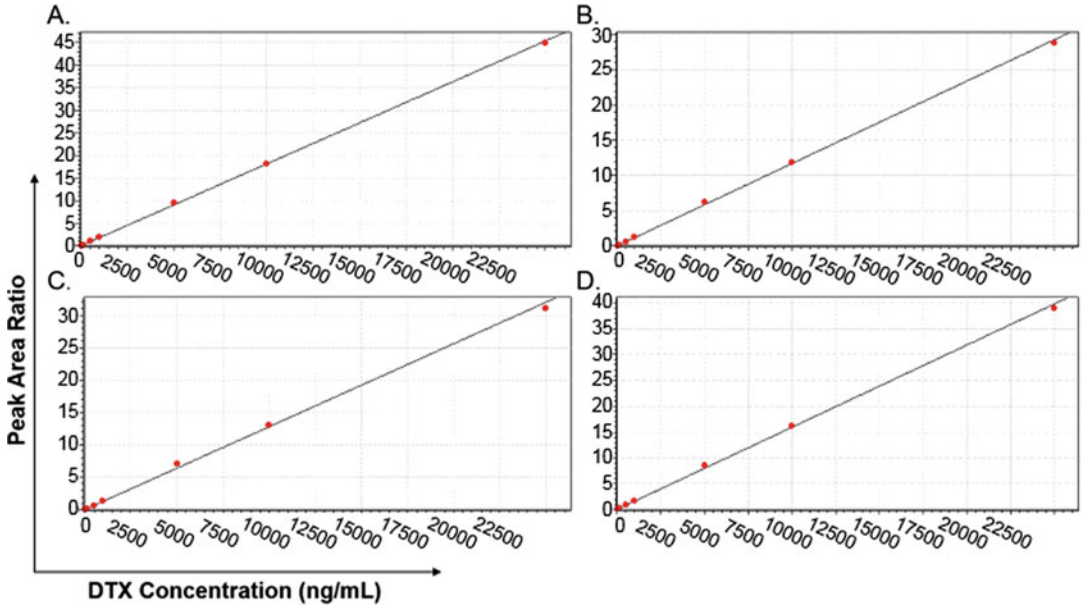

Fig. 7 Example of DTX and DTX-d5 calibration curves. Curves represent peak area ratio of the analyte to the internal standard, DTX-d9, as measured with an LC-MS system vs. the DTX concentration (ng/mL). (**a**) DTX calibration curve in human plasma. Curve data are shown in Table 2. (**b**) DTX calibration curve in human protein-free plasma. Data are shown in Table 3. (**c**) DTX-d5 calibration curve in human plasma. Data are shown in Table 4. (**d**) DTX-d5 calibration curve in human protein-free plasma. Data are shown in Table 5

4 Notes

1. The stable isotope tracer is non-radioactive and generally a deuterated or carbon-13 isotope labeled analog of the normoisotopic drug encapsulated in the nanomedicine formulation. It is important that this isotope is at least 3 amu different from the normoisotopic drug in order to ensure accurate mass separation and quantitation by mass spectrometry.
2. The 500 ng/mL DTX-d5 spike concentration was determined to be the limit of detection for the unbound stable isotope with an unbound concentration of approximately 30 ng/mL (~6% unbound).
3. The ultrafiltration device was determined to have low nonspecific binding to DTX (<20%). Specific binding was determined by incubating 1 μg/mL DTX in protein-free plasma at 37 °C for 30 min, centrifuging, and comparing the filtrate DTX concentration to the reservoir DTX concentration.
4. There is the potential for drug degradation during the ultrafiltration process. The in-apparatus incubation control accounts for this.
5. The concentrations of the nanomedicine chosen should be clinically relevant, based on the actual or expected pharmacokinetic profile.

6. An additional requirement of the method is a second stable isotope that can be used as an internal standard to allow for accurate quantitation of the normoisotopic drug and stable isotope tracer by mass spectrometry. Again, this stable isotope should be at least 3 amu different from both the normoisotopic drug and the stable isotope tracer in order to allow for accurate mass separation and quantitation.

Acknowledgment

This project has been funded in whole or in part with Federal funds from the National Cancer Institute, National Institutes of Health, under Contract No. HHSN261200800001E. The content of this publication does not necessarily reflect the views or policies of the Department of Health and Human Services, nor does mention of trade names, commercial products, or organizations imply endorsement by the U.S. Government.

References

1. Ambardekar VV, Stern ST (2015) NBCD pharmacokinetics and bioanalytical methods to measure drug release. In: Crommelin DJA, de Vlieger JSB (eds) Non-biological complex drugs: the science and the regulatory landscape. Springer International Publishing, Cham, Switzerland, pp 261–287. doi:10.1007/978-3-319-16241-6_8
2. Liu X, Wright M, Hop CECA (2014) Rational use of plasma protein and tissue binding data in drug design. J Med Chem 57(20):8238–8248. doi:10.1021/jm5007935
3. ten Tije AJ, Verweij J, Loos WJ, Sparreboom A (2003) Pharmacological effects of formulation vehicles: implications for cancer chemotherapy. Clin Pharmacokinet 42(7):665–685. doi:10.2165/00003088-200342070-00005
4. Skoczen S, McNeil SE, Stern ST (2015) Stable isotope method to measure drug release from nanomedicines. J Control Release 220(Pt A):169–174. doi:10.1016/j.jconrel.2015.10.042

Chapter 20

Designing an In Vivo Efficacy Study of Nanomedicines for Preclinical Tumor Growth Inhibition

Pavan P. Adiseshaiah and Stephan T. Stern

Abstract

Novel nanoformulated chemotherapeutics and diagnostics require demonstration of efficacy and safety in appropriate animal models prior to conducting early-phase clinical trials. In vivo efficacy experiments are tailored to the tumor model type and route of administration as well as several parameters related to the nanoformulation, like drug loading to determine dosing volume. When designing in vivo efficacy studies for nanomedicines, understanding the relationship between tumor biology and the nanoformulation characteristics is critical to achieving meaningful results, along with applying appropriate drug and nanoformulation controls. In particular, nanoparticles can have multifunctional roles such as targeting and imaging capabilities that require additional considerations when designing in vivo efficacy studies and choosing tumor models. In this chapter, we outline a general study design for a subcutaneously implanted tumor model along with an example of tumor growth inhibition and survival analysis.

Key words Nanoformulation, Tumor model, Subcutaneous, Statistical analysis, Biology

1 Introduction

Drug discovery for cancer involves a significant investment of resources, time, and an interdisciplinary team of scientists (biologists, drug metabolism and pharmacokinetic experts, toxicologists, and formulation chemists) leading up to the development of a clinically viable candidate. One of the cost-prohibitive and key studies prior to clinical translation of a cancer therapeutic is animal studies to examine toxicology and pharmacology of the lead drug candidate. In addition to testing potency of the cancer therapy using numerous in vitro assays, evaluation in tumor-bearing murine models (e.g., syngeneic, xenograft, orthotopic, genetically engineered) allows comparison of the antitumor activity of a novel nanoformulation to that of the FDA-approved standard of care treatment and/or the legacy drug formulation for the specific indication. Drugs formulated in nanoparticles and delivered systemically can have an enhanced in vivo half-life, controlled drug

Scott E. McNeil (ed.), *Characterization of Nanoparticles Intended for Drug Delivery*, Methods in Molecular Biology, Vol. 1682, DOI 10.1007/978-1-4939-7352-1_20,

release profile, as well as altered drug biodistribution, resulting in an optimized dosing regimen that may vary significantly from that of the legacy drug. Therefore, prior to evaluating in vivo efficacy in an animal model, it is imperative to understand the pharmacokinetic profile [1] and maximum tolerated dose [2] of the nanoformulated drug in non-tumor-bearing animal models to determine the appropriate doses, dosing volumes, and dosing regimens. The majority of nanoformulations are designed for intravenous or intraperitoneal delivery; however, certain cancer indications may require specialized routes, like intrathecal administration for glioma or periocular injections for retinoblastoma. An understanding of the physicochemical characteristics of the nanoparticles, the drug release profile, and its pharmacokinetic properties can help design meaningful efficacy studies.

In addition to the nanoformulation properties, another critical aspect to consider when designing in vivo efficacy studies in mouse mouse models is the tumor biology. The presence of wide gaps (nano to micrometer) in the endothelial walls (fenestrations) and dysfunctional lymphatics can enhance nanoparticle accumulation in the tumor interstitium, the phenomenon commonly referred to as enhanced permeation and retention (EPR) [3]. Effective nanoparticle extravasation into the tumor site depends on vessel perfusion, endothelial pore size, and the nanoparticle size [4, 5]. Therefore, having a detailed understanding of the actual clinical tumor microenvironment is very important to guide selection of a relevant tumor model for efficacy studies. Another criterion to consider is at what tumor size should the dose be administered. As tumors grow, the microenvironment must adapt to the increasing size, which can cause changes in the expression levels of a variety of receptors [6]. The changing receptor expression levels can then affect the efficacy of receptor-targeted nanoformulations. For example, VEGF expression is inversely correlated to tumor size in an U87MG tumor-bearing mouse model [6, 7]. The interstitial fluid pressure in a growing tumor can also increase, diminishing the EPR effect and tumor accumulation [8]. Furthermore, certain indications, like pancreatic cancer, have a stromal barrier that can greatly restrict drug accumulation in the tumor. Approaches to reduce the dense fibrotic network in tumors can enhance penetration and efficacy of systemically injected nanomedicines. Jain et al. demonstrated that by inhibiting collagen synthesis in tumors of mouse models, PEGylated liposomal doxorubicin (Doxil) demonstrated improved drug penetration and tumor growth suppression compared to the nanomedicine alone [9]. Overall, the tumor microenvironment in preclinical models can have a significant influence on the clinical relevance of the model, and thus the predictability of the model with regard to the clinical efficacy of nanoformulations under study. Understanding the tumor biology and how the nanoformulation is affected by it can help in the design of relevant and predictive in vivo efficacy studies.

The protocol presented in this chapter serves as a general study design to conduct and analyze in vivo efficacy, using a subcutaneous implanted LS174T xenograft, a human colon cancer tumor model, as an example. Subcutaneously implanted tumor models are commonly used for initial evaluation of drug activity in vivo. LS174T is a good representative tumor model with a vascular pore size ranging between 400 and 600 nm and vascular architecture that is similar to clinical human colon carcinoma [10, 11].

2 Materials

1. Plated LS174T cells, limit to 20 passages.
2. T75 tissue culture flasks.
3. Trypsin/EDTA.
4. Trypan blue exclusion and hemocytometer or automated cell counter.
5. Light microscope.
6. RPMI medium with 10% serum (medium).
7. Hanks' Balanced Salt Solution with Ca^{2+}/Na^{+} Salts (HBSS).
8. 50 mL centrifuge tubes.
9. 6–8-week-old athymic nude mice.
10. Ear tags.
11. 27-G needles.
12. Vernier calipers.

3 Methods

3.1 Cancer Cell Preparation

1. Harvest LS174T cells in T75 flasks when they are in logarithmic growth phase and 70-80% confluent (*see* **Notes 1** and **2**).
2. Aspirate cell culture medium and wash cells with HBSS.
3. Add 2–4 mL of trypsin/EDTA to cells and incubate at 37 °C for 5 min. Gently tap the plate to dislodge the cells and intermittently monitor the cells under the microscope.
4. Add cell culture medium to inactivate trypsin/EDTA and vigorously mix the mixture using a pipette to obtain a single cell suspension.
5. Transfer the single cell suspension to a centrifuge tube and pellet the cells for 10 min at 930 × *g* and 4 °C. Save a 50 μL aliquot of the resulting cell suspension for cell counting.
6. Count the live cells from the aliquot by adding trypan blue solution and use a hemocytometer or automated cell counter.
7. Resuspend cell pellet in HBSS salt solution at 6×10^7 cells/mL.

Table 1
Example of successful animal randomization by tumor volume

Treatment groups	Number of animals	Mean tumor volume (mm^3)*	Standard deviation (mm^3)	Minimum tumor volume (mm^3)	Maximum tumor volume (mm^3)
Vehicle control	10	122.57	40.15	62.51	196.32
Blank nanoformulation	10	121.70	55.06	21.85	212.91
Nanoformulation with API, Dose level #1	10	122.48	60.15	57.02	242.70
Nanoformulation with API, Dose level #2	10	115.05	49.01	53.19	203.19
Clinical formulation of API, Dose level #1	10	160.32	97.26	58.99	366.05
Clinical formulation of API, Dose level #2	10	112.69	29.33	60.37	152.82

*Not significant by ANOVA, $p > 0.05$

3.2 Xenograft Development

1. Anesthetize mice following IACUC approved animal protocol (*see* **Note 3**).
2. Inject 0.1 mL of the cell suspension into one of the mouse flanks subcutaneously using a 27-G needle.
3. Add an ear tag on the animals for identification.
4. Following 4–5 days after cancer cell implantation, measure the length (L) and width (W) of the tumor by calipers to calculate the tumor volume, $V = (L \times W^2)/2$. The width is the smaller of the two measurements (*see* **Note 4**).
5. Once tumors reach the study-desired size, usually 5 mm in the longest diameter, animals are randomized into different treatment groups based on tumor size (*see* **Note 5** and Table 1).

3.3 Tumor Growth Inhibition Study and Ongoing Animal Survival

1. Treatment groups include the drug containing nanoformulation and corresponding control groups like the vehicle, nanoformulation-blank (non-drug loaded), and legacy drug formulation, to evaluate the performance of the nanoformulated drug (*see* **Notes 6–8**). An example of an efficacy study design is shown in Table 2 (*see* **Note 9**).
2. Drug dose and dosing regimens are determined by dose-range finding and pharmacokinetic studies in non-tumor bearing animals (*see* **Note 7**).
3. Most nano formulations for cancer indications are administered by an intravenous route and dosing volume should not exceed 10 mL/kg by bolus and 25 mL/kg by slow-press

Table 2
Example of experimental design for an efficacy study. Treatment groups, drug dose, number of animals, dose volumes, and dose schedule are displayed in the table. Study drugs were administered by intravenous tail vein injection, once every 3 days (q3d), for a total of three doses (q3d × 3)

Treatment groups	Dose (mg API/kg)	Number of animals	Dose volume	Dose schedule/Route of administration
Vehicle control (0.9% saline)	–	10	5 mL/kg	q3d × 3; i.v
Blank nanoformulation	–	10	5 mL/kg	q3d × 3; i.v
Nanoformulation with API (low)	10	10	5 mL/kg	q3d × 3; i.v
Nanoformulation with API (high)	20*	10	5 mL/kg	q3d × 3; i.v
Clinical formulation of API (low)	5	10	5 mL/kg	q3d × 3; i.v
Clinical formulation of API (high)	10*	10	5 mL/kg	q3d × 3; i.v

*Dose at formulation MTD

injection in mice (only in exceptional cases when the relevant drug dose cannot be achieved) (*see* **Note 10**) [12].

4. Tumor and body weights are measured one-three times a week, depending on study duration, to monitor the tumor burden and treatment-induced body weight loss. Animals have to be humanely euthanized if the tumor size reaches 2 cm or if animals experience ≥20% body weight loss.
5. Survival studies can follow tumor growth inhibition studies to track the number of surviving animals over a longer period of time.

3.4 Data Analysis

1. The effect of treatment on tumor size and body weight change can be observed by plotting tumor volume and body weight data as mean ± standard deviation, or as percent change from initial volume/body weight (taken as 100%).
2. Statistical differences in tumor volume and body weight values among treatment groups can be determined using ANOVA, with appropriate post-hoc comparisons.
3. Suggested tumor volume and body weight analysis (Table 3) for study time points which contain **equal numbers** of animals in each group can be analyzed by ANOVA, with post-hoc comparison using either Dunnett's Test for statistical significance in comparison to the control (Table 4) or Duncan's Test for statistical significance between all treatment groups (Table 5).
4. For study time points which contain **unequal numbers** of animals, tumor volume and body weight measurements (Table 3) over the study can be analyzed for statistical significance using ANOVA with suggested post-hoc comparisons by Tukey's HSD Test (Table 6).

Table 3
Example of tumor volume and animal body weight data. Tumor volume and body weight data for all the treatment groups are shown. Statistical analysis was conducted on this dataset. Tables 4, 5, and 6 show statistical outputs

Treatment groups	Number of animals	Tumor volume		Body weight	
		Mean (mm^3)	Standard deviation (mm^3)	Mean (g)	Standard deviation (g)
Vehicle control	10	268	135	21.4	1.9
Blank nanoformulation	10	312	116	22.2	1.0
Nanoformulation with API (low)	10	196	87	21.4	1.9
Nanoformulation with API (high)	10	118	77	21.4	2.1
Clinical formulation of API (low)	10	270	152	20.8	2.1
Clinical formulation of API (high)	10	171	94	20.0	1.5

Table 4
Example of statistical output using Dunnett's test. Significance is presented in comparison to vehicle control group. *MS*, Mean Square value; *df*, degree of freedom

Treatment group	Significance in comparison to vehicle control group (treatment 1)
Probabilities for post hoc tests (2-sided) error: between MS = 13,046, df = 53.000	
Vehicle control	
Blank nanoformulation	0.859688
Nanoformulation with API (low)	0.489476
Nanoformulation with API (high)	0.039806*
Clinical formulation of API (low)	1.000000
Clinical formulation of API (high)	0.214997

*Statistically significant value ($p \leq 0.05$)

5. Unequal sample sizes are often observed in survival studies, or time-to-endpoint studies in which animals are terminated at set neoplasia (tumor diameter reaching $\geq$2 cm or tumor ulceration) or morbidity (loss of $\geq$20% of an initial body weight and or immobility) criteria, as opposed to a set termination day. In this case, the number of animals per treatment group will vary over the course of the study due to differences in animal survival or time to reach neoplasia or morbidity-related endpoints.

Table 5

Example of statistical output using Duncan's test. Significance is presented in comparison to other treatment groups. *Vehicle*, vehicle control; *Blank*, blank nanoformulation; *Nanoformulation*, nanoformulation with API; *Clinical formulation*, clinical formulation with API; *MS*, Mean Square value; *df*, degree of freedom

	Significance in comparison to treatment group					
Treatment group	**Vehicle**	**Blank**	**Nanoformulation (low)**	**Nanoformulation (high)**	**Clinical formulation (low)**	**Clinical formulation (high)**
Approximate probabilities for post hoc tests error: between MS = 12,951, df = 54.000						
Vehicle		0.421745	0.162457	0.007835*	0.968396	0.073933
Blank	0.421745		0.040119*	0.000915*	0.414081	0.013995*
Nanoformulation (low)	0.162457	0.040119*		0.152208	0.175302	0.615460
Nanoformulation (high)	0.007835*	0.000915*	0.152208		0.008196*	0.306157
Clinical formulation (low)	0.968396	0.414081	0.175302	0.008196*		0.077620
Clinical formulation (high)	0.073933	0.013995*	0.615460	0.306157	0.077620	

*Statistically significant value ($p \leq 0.05$)

Table 6

Example of statistical output using Tukey HSD test. Significance is presented in comparison to other treatment groups. *Vehicle*, vehicle control; *Blank*, blank nanoformulation; *Nanoformulation*, nanoformulation with API; *Clinical formulation*, clinical formulation with API; *MS*, Mean Square value; *df*, degree of freedom

	Significance in comparison to treatment group					
Treatment group	**Vehicle**	**Blank**	**Nanoformulation**	**Nanoformulation**	**Clinical formulation**	**Clinical formulation**
Approximate probabilities for post hoc tests error: between MS = 3.9160, df = 54.000						
Vehicle		0.999965	0.613775	0.441642	0.059962	0.001439*
Blank	0.999965		0.732861	0.562889	0.094201	0.002566*
Nanoformulation (low)	0.613775	0.732861		0.999808	0.784073	0.109622
Nanoformulation (high)	0.441642	0.562889	0.999808		0.906406	0.192588
Clinical formulation (low)	0.059962	0.094201	0.784073	0.906406		0.771672
Clinical formulation (high)	0.001439*	0.002566*	0.109622	0.192588	0.771672	

*Statistically significant value ($p \leq 0.05$)

6. Group time-to-endpoint or survival data are commonly analyzed by the Kaplan-Meier analysis, with the log-rank (Mantel-Cox) test to determine statistical significance.
7. Kaplan-Meier analyses of time-to-endpoint and survival data allow for censoring of data. Censoring of non-neoplasia-related endpoints, such as body weight endpoint (loss of $\geq$20% of an initial body weight) data eliminates drug-related endpoints from the analysis of neoplasia-related endpoints (tumor diameter reaching $\geq$2 cm, tumor ulceration, or neoplasia related survival) (Table 7; Fig. 1).

4 Notes

1. All cell culture procedures should follow sterile techniques and be performed in a biological safety cabinet.
2. All cancer cell lines should be tested for human and rodent pathogens (HIV-1, HIV-2, HTLV-1, HTLV-2, Hepatitis B, Hepatitis C, CMV, EBV, JCV, and MoMuLV) prior to use in animal models.
3. Animal study protocols (ASP) should be approved by an Institutional Animal Care and Use Committee (IACUC) prior to initiation of an animal study.
4. Depending on the cancer cell line and mouse strain, the tumor take rate and growth profile can vary significantly. A pilot tumor growth study is recommended to characterize the tumor growth profile and take rate prior to therapeutic evaluation.
5. The randomization process will remove any tumor size bias so the average tumor volume between treatment groups is not significant. The number of animals per treatment group required to achieve the statistical power to detect a significant difference for a given treatment depends on the variability in tumor growth/survival and magnitude of the treatment response [13]. Therefore, it is necessary to perform a pilot study to identify the variability in tumor growth/survival and the anticipated magnitude of the treatment response. Assuming type I error (alpha) and type II error (Beta) are fixed at 5% ($p < 0.05$) and <20%, respectively, then a simplified estimate of sample size for tumor volume data (continuous variable) is given by Eq. 1 [13]:

$$n = 1 + 2C \times (s/d)^2 \quad (1)$$

where s is standard deviation, d is the anticipated difference between control and treatment response, and the constant, C, is 7.85.

Table 7
Example of Kaplan-Meier time-to-endpoint table (body weight endpoint censored). The remission codes are "1" for animals reaching a neoplasia-related endpoint and "0" for censored animals which are euthanized due to drug-related endpoints, and for animals which survived to study termination (study day 80 when remaining animals are euthanized)

Animal number	Time to endpoint (Days)	Endpoint	Remission	Animal number	Time to endpoint (Days)	Endpoint	Remission
Vehicle control				**Nanoformulation with API (20 mg API/kg)**			
2	17	Ulcerated tumor	1	62	22	Body weight loss	0
4	29	Ulcerated tumor	1	64	18	Body weight loss	0
6	20	>2 cm	1	66	18	Animal death	0
8	25	Ulcerated tumor	1	68	67	Tumor ulceration	1
10	29	>2 cm	1	70	80	Survived	0
12	22	Ulcerated tumor	1	72	62	>2 cm	1
14	18	>2 cm	1	74	57	>2 cm	1
16	25	>2 cm	1	76	69	>2 cm	1
18	20	Ulcerated tumor	1	78	48	>2 cm	1
20	25	>2 cm	1	80	69	>2 cm	1
Blank nanoformulation				**Clinical formulation of API (5 mg API/kg)**			
22	17	Tumor ulceration	1	82	27	> 2 cm	1
24	25	>2 cm	1	84	29	> 2 cm	1
26	15	Tumor ulceration	1	86	25	> 2 cm	1
28	29	> 2 cm	1	88	36	> 2 cm	1
30	19	Tumor ulceration	1	90	22	Body weight loss	0
32	19	Tumor ulceration	1	92	34	Tumor ulceration	1
34	29	>2 cm	1	94	17	Body weight loss	0
36	25	>2 cm	1	96	27	>2 cm	1
38	20	>2 cm	1	98	41	Tumor ulceration	1
40	20	> 2 cm	1	100	29	Tumor ulceration	1

(continued)

Table 7
(continued)

Animal number	Time to endpoint (Days)	Endpoint	Remission	Animal number	Time to endpoint (Days)	Endpoint	Remission
Nanoformulation with API (10 mg API/kg)				Clinical formulation of API (10 mg API/kg)			
42	43	>2 cm	1	102	18	Body weight loss	0
44	80	Survived	0	104	48	>2 cm	1
46	51	Tumor ulceration	1	106	18	Body weight loss	0
48	22	Body weight loss	0	108	80	Survived	0
50	43	>2 cm	1	110	48	>2 cm	1
52	36	>2 cm	1	112	22	Body weight loss	0
54	36	Tumor ulceration	1	114	22	Body weight loss	0
56	41	Tumor ulceration	1	116	18	Body weight loss	0
58	36	>2 cm	1	118	51	>2 cm	1
60	22	Body weight loss	0	120	20	Body weight loss	0

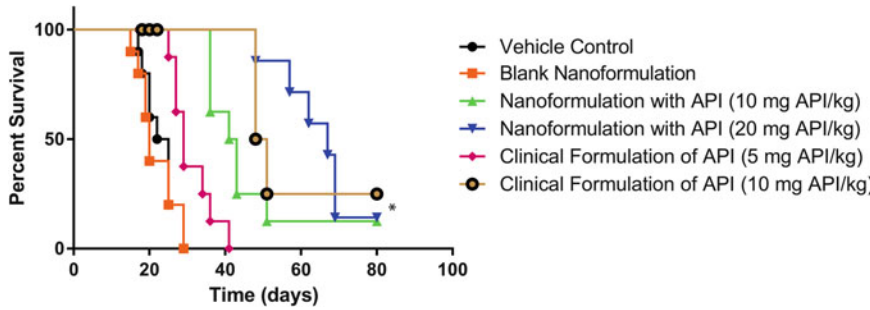

Fig. 1 Example of Kaplan-Meier curve: time to endpoint plots (body weight endpoint censored analysis). *Asterisk* indicates Nanoformulation with API (10 mg API/kg), Nanoformulation with API (20 mg API/kg) and Clinical formulation of API (10 mg API/kg) treatment groups are statistically significant ($p \leq 0.05$, log-rank (Mantel-Cox) test) in comparison to vehicle control. Study day is plotted against the fraction of surviving animals, by treatment group, based on the parameters displayed in Table 7

A simplified estimate of sample size for survival data (dichotomous variable) is given by Eq. 2:

$$N = C \times \left((p_c q_c + p_t p_t)/d^2 \right) + (2/d) + 2 \quad (2)$$

where p_c is the proportion of deaths in the control group, q_c is 1-p_c, p_t is the proportion of deaths in the treatment group, q_t is 1-p_t, d is the anticipated difference between the two groups, and the constant, C, is 7.85.

The sample size based on the above calculations is generally not greater than ten animals for an implanted tumor model with a potent treatment response.

6. Appropriate control agents should be included in the study, such as standard-of-care treatment for a particular cancer type, legacy or conventionally formulated drug control, vehicle (formulation) control, and unloaded nanoparticle control (where applicable). All these agents, along with their doses, intended route of administration, and dosing volume should be included in the ASP and approved by the IACUC.
7. Cytotoxic nanoformulations and comparator treatments should be dosed at equivalent doses and equitoxic maximum tolerated doses (MTDs) (Table 1; MTD defined as dose producing $\geq$20% body weight loss in 10% of animals, i.e., severe toxic dose 10% STD_{10}). Doses should be based on initial dose-range finding studies in non-tumor bearing animals.
8. Nanoformulation appropriate additional controls should be included in the treatment arm. If the nanoformulation has an attached targeting ligand, the inclusion of an untargeted nanoformulation will help identify targeting advantages. If the nanoformulation is a species-specific gene therapy (e.g., siRNA, plasmid DNA, antisense RNA, etc.), utilizing a mouse ortholog of the relevant gene is important to allow assessment of side effects related to manipulation of the gene/protein in off-target tissues.
9. In Table 2, an investigational nanoformulated API at two concentrations is compared with conventional clinical forumulation of API at equitoxic and equivalent doses to evaluate any improvement in the therapeutic index for the nanoformulated API.
10. All preclinical studies should be performed using the intended clinical route of administration to best represent eventual clinical drug exposure and distribution, and related efficacy and toxicities.

Acknowledgment

Frederick National Laboratory is accredited by AAALAC International and follows the Public Health Service Policy for the Care and Use of Laboratory Animals (Health Research Extension Act of 1985, Public Law 99-158, 1986). Animal care is provided in accordance with the procedures outlined in the "Guide for Care and Use of Laboratory Animals" (National Research Council, 1996; National Academy Press, Washington, D.C.). All animal protocols are approved by the FNL Institutional Animal Care and Use Committee (IACUC). Any experiments performed are scientifically justified and are not an unnecessary duplication of previous work by others.

This project has been funded in whole or in part with Federal funds from the National Cancer Institute, National Institutes of Health, under Contract No. HHSN261200800001E. The content of this publication does not necessarily reflect the views or policies of the Department of Health and Human Services, nor does mention of trade names, commercial products, or organizations imply endorsement by the U.S. Government.

References

1. Sparreboom A, Scripture CD, Trieu V, Williams PJ, De T, Yang A, Beals B, Figg WD, Hawkins M, Desai N (2005) Comparative preclinical and clinical pharmacokinetics of a cremophor-free, nanoparticle albumin-bound paclitaxel (ABI-007) and paclitaxel formulated in Cremophor (Taxol). Clin Cancer Res 11 (11):4136–4143. doi:10.1158/1078-0432.ccr-04-2291
2. Desai NP, Trieu V, Hwang LY, Wu R, Soon-Shiong P, Gradishar WJ (2008) Improved effectiveness of nanoparticle albumin-bound (nab) paclitaxel versus polysorbate-based docetaxel in multiple xenografts as a function of HER2 and SPARC status. Anticancer Drugs 19 (9):899–909. doi:10.1097/CAD.0b013e32830f9046
3. Maeda H (2015) Toward a full understanding of the EPR effect in primary and metastatic tumors as well as issues related to its heterogeneity. Adv Drug Deliv Rev 91:3–6. doi:10.1016/j.addr.2015.01.002
4. Hobbs SK, Monsky WL, Yuan F, Roberts WG, Griffith L, Torchilin VP, Jain RK (1998) Regulation of transport pathways in tumor vessels: role of tumor type and microenvironment. Proc Natl Acad Sci U S A 95(8):4607–4612
5. Monsky WL, Fukumura D, Gohongi T, Ancukiewcz M, Weich HA, Torchilin VP, Yuan F, Jain RK (1999) Augmentation of transvascular transport of macromolecules and nanoparticles in tumors using vascular endothelial growth factor. Cancer Res 59(16):4129–4135
6. Adiseshaiah PP, Hall JB, McNeil SE (2010) Nanomaterial standards for efficacy and toxicity assessment. Wiley Interdiscip Rev Nanomed Nanobiotechnol 2(1):99–112. doi:10.1002/wnan.66
7. Cai W, Chen K, Mohamedali KA, Cao Q, Gambhir SS, Rosenblum MG, Chen X (2006) PET of vascular endothelial growth factor receptor expression. J Nucl Med 47(12):2048–2056
8. Heldin C-H, Rubin K, Pietras K, Ostman A (2004) High interstitial fluid pressure [mdash] an obstacle in cancer therapy. Nat Rev Cancer 4(10):806–813
9. Diop-Frimpong B, Chauhan VP, Krane S, Boucher Y, Jain RK (2011) Losartan inhibits collagen I synthesis and improves the distribution and efficacy of nanotherapeutics in tumors. Proc Natl Acad Sci 108(7):2909–2914. doi:10.1073/pnas.1018892108
10. Folarin AA, Konerding MA, Timonen J, Nagl S, Pedley RB (2010) Three-dimensional analysis of tumour vascular corrosion casts using steroimaging and micro-computed tomography. Microvasc Res 80(1):89–98. doi:10.1016/j.mvr.2010.03.007‘

11. Yuan F, Dellian M, Fukumura D, Leunig M, Berk DA, Torchilin VP, Jain RK (1995) Vascular permeability in a human tumor xenograft: molecular size dependence and cutoff size. Cancer Res 55(17):3752–3756
12. Diehl K-H, Hull R, Morton D, Pfister R, Rabemampianina Y, Smith D, Vidal J-M, Vorstenbosch CVD (2001) A good practice guide to the administration of substances and removal of blood, including routes and volumes. J Appl Toxicol 21(1):15–23. doi:10.1002/jat.727
13. Shah H (2011) How to calculate sample size for animal studies? Natl J Physiol Pharm Pharmacol 1(1):35–39

INDEX

Scott E. McNeil (ed.), *Characterization of Nanoparticles Intended for Drug Delivery*, Methods in Molecular Biology, vol. 1682, DOI 10.1007/978-1-4939-7352-1, © Springer Science+Business Media LLC 2018

L

M

N

P

R

S

T

V

W

Y

Z